

Syntheses and structure-activity relationships of novel P2X3 receptor antagonists

Dissertation

zur

Erlangung des Doktorgrades (Dr. rer. nat.)

der

Mathematisch-Naturwissenschaftlichen Fakultät

der

Rheinischen Friedrich-Wilhelms-Universität Bonn

vorgelegt von

Mahmoud Sayed Ahmed Mahmoud Rashed

aus

Kairo, Ägypten

Bonn 2017

Angefertigt mit Genehmigung der Mathematisch-Naturwissenschaftlichen Fakultät der
Rheinischen Friedrich-Wilhelms-Universität Bonn.

1. Gutachter: Prof. Dr. Christa E. Müller

2. Gutachter: Priv.-Doz. Dr. Anke C. Schiedel

Tag der Promotion: 15.01.2018

Erscheinungsjahr: 2018

Die vorliegende Arbeit wurde in der Zeit von November 2013 bis Mai 2017 am Pharmazeutischen Institut der Rheinischen Friedrich-Wilhelms-Universität Bonn unter der Leitung von Frau Prof. Dr. Christa E. Müller durchgeführt.

Mein besonderer Dank gilt Frau Prof. Dr. Christa E. Müller für das interessante Promotionsthema, ihre Unterstützung, ihre Diskussionsbereitschaft und ihre Anregungen, die zum Gelingen dieser Arbeit beigetragen haben.

Ebenso bedanke ich mich an dieser Stelle bei PD Dr. Anke Schiedel für die freundliche Übernahme des Korreferates.

Ich danke der Kulturabteilung und Studienmission der Ägyptischen Botschaft für die finanzielle Unterstützung in Form eines Promotionsstipendiums.

***To My Parents, My Dear Wife
and My Daughter Layan***

1 Table of Contents

Table of Contents 9

1. Introduction..... - 1 -

1.1. Purinergic signaling and purinergic receptors - 1 -

1.1.1. Purinergic signaling - 1 -

1.1.2. Purinergic receptors - 2 -

1.1.2.1. P0, P1 and P2 receptors - 3 -

1.1.3. G protein-coupled receptors (GPCRs)..... - 4 -

1.1.4. P2 receptors (nucleotide receptors)..... - 5 -

1.1.4.1. P2Y receptors..... - 5 -

1.1.4.2. P2X receptors..... - 6 -

1.1.4.2.1. P2X receptor crystal structures - 10 -

1.1.4.2.1.1. P2X4 receptor crystal structure..... - 10 -

1.1.4.2.1.2. P2X3 receptor crystal structure⁴⁹ - 13 -

1.1.4.2.1.3. P2X7 crystal structure..... - 16 -

1.1.5. P2X1, P2X2 and P2X4 receptors..... - 18 -

1.1.5.1. P2X1 receptor subtype - 18 -

1.1.5.2. P2X1 receptor antagonists - 18 -

1.1.5.3. P2X2 receptor subtype - 19 -

1.1.5.4. P2X2 receptor antagonists - 20 -

1.1.5.5. P2X4 receptor subtype - 21 -

1.1.5.6. P2X4 receptor antagonists - 21 -

1.1.5.7. The P2X5 receptor subtype..... - 24 -

1.1.5.8. The P2X6 receptor subtype..... - 25 -

1.1.5.9. The P2X7 receptor subtype..... - 26 -

1.1.5.10. P2X7 receptor antagonists - 26 -

Table of contents

1.1.6. The P2X3 receptor subtype.....	- 27 -
1.1.6.1. Distribution of P2X3 receptors	- 28 -
1.1.6.2. Screening of P2X3 receptors	- 28 -
1.1.6.3. P2X3 receptor antagonists	- 29 -
1.1.7. P2X receptors and pain	- 34 -
1.2. Anthraquinone (AQ) derivatives.....	- 36 -
1.2.1. Anthraquinone derivatives and their applications.....	- 37 -
1.3. Microwave chemistry.....	- 42 -
1.3.1. Microwave-assisted organic synthesis (MAOS).....	- 42 -
1.4. Ullmann reaction.....	- 43 -
1.5. Goldberg condensation reaction	- 44 -
1.6. Triphenylmethanes.....	- 45 -
2. Research objectives.....	- 47 -
2.1. Anthraquinone derivatives	- 47 -
2.2. Bisacodyl-derived compounds.....	- 48 -
3. Results and Discussion.....	- 50 -
3.1. Anthraquinone derivatives	- 50 -
3.1.1. Synthesis of 1-amino-4-(aryl)alkylamino-2-methylantraquinone derivatives.....	- 50 -
3.1.2. Condensation with liquid amines using solvent-free Ullmann reaction	- 50 -
3.1.3. General synthetic procedure (I) used for anthraquinone derivatives 2-17.....	- 52 -
3.1.4. Optimization of the reaction conditions for 1-amino-4-bromo-2-methylantraquinone derivatives	- 56 -
3.1.4.1. Condensation with solid amines	- 56 -
3.1.5. Optimization of the reaction conditions for some 2-substituted anthraquinone derivatives	- 56 -
3.1.5.1. Optimization of the reaction conditions for 1-amino-2,4-dibromoanthraquinone (26)-	- 58 -
3.1.5.2. Optimization of the reaction conditions for 1-amino-2-methylantraquinone (1)	- 59 -

Table of contents

3.1.5.2.1. Optimization of the reaction conditions using ethanol as a solvent.....	- 61 -
3.5.2.1.2. Use of ethyleneglycol as a solvent.....	- 62 -
3.5.2.1.3. Use of methanol as a solvent	- 63 -
3.1.6. Optimization of the reaction conditions using methanol as a solvent	- 65 -
3.1.6.1. Effect of concentration.....	- 65 -
3.1.6.2. Effect of the catalyst	- 66 -
3.1.7. General synthetic procedure (II) used for anthraquinone derivatives 18-25	- 69 -
3.2. Bisacodyl-derived compounds.....	- 71 -
3.2.1. Synthesis of bisacodyl.....	- 71 -
3.2.2. Development of P2X3 receptor antagonists	- 72 -
3.2.3. Alkylation of the <i>bis</i> -phenol metabolite of bisacodyl.....	- 73 -
3.2.4. Preparation of a triarylcarbinol derivative	- 77 -
3.2.4.1. Confirmation of structures	- 78 -
3.2.4.2. Plausible mechanism for the formation of 3-methoxy-10-(4-methoxyphenyl)- pyrido[1,2- <i>a</i>]indole (73)	- 80 -
3.2.5. Miscellaneous modifications	- 85 -
3.2.5.1. Synthesis of <i>N</i> ⁴ -(4-methoxyphenyl)2,4,6-triamino-pyrimidine.....	- 85 -
3.2.5.2. Synthesis of diindolylmethane derivatives	- 86 -
3.2.5.3. Synthesis of 5,5'-(4-(benzyloxy)-1,3-phenylene)-bis-(3-ethyl-1,2,4-oxadiazole) (99) -	87 -
3.2.5.3.1. Deprotection of the methoxy group of compound 97.....	- 88 -
3.2.5.3.2. Proposed mechanism of the formation of the bis-oxadiazole.....	- 89 -
3.3. Pharmacological evaluation	- 90 -
3.3.1. Anthraquinone (AQ) derivatives.....	- 90 -
3.3.1.1. Biological evaluation of anthraquinone derivatives (previous results).....	- 90 -
3.3.1.2. Potency of newly synthesized AQ derivatives on the human P2Y ₄ receptor.....	- 91 -
3.3.1.3. Potency on the human P2X3 receptor.....	- 92 -
3.3.2. Bisacodyl-derived compounds.....	- 96 -

Table of contents

3.3.2.1. Biological evaluation of the synthesized bisacodyl-derived compounds	- 96 -
3.3.2.1.1. Inhibitory potency of bisacodyl-derived compounds on the human P2X3 receptor and study of structure-activity relationships	- 96 -
3.3.2.1.2. Effects of symmetrical substitution of the bisacodyl-derived drug 46 on the inhibitory activity.....	- 99 -
3.3.2.1.3 Effects of asymmetrical substitutions of leads structure 46 on the inhibitory activity.....	- 100 -
3.3.2.1.4. Effects of simplification of the lead structure (46)	- 105 -
3.3.2.1.4.1. Replacement or removal of the pyridine ring	- 105 -
3.3.2.1.5. Miscellaneous modifications	- 106 -
3.3.2.2. Pharmacophore model	- 109 -
3.3.2.2.1. Pharmacophore model features.....	- 110 -
4. Summary.....	- 114 -
4.1. Anthraquinone derivatives	- 114 -
4.1.1. Synthesis and optimization of 1-amino-4-(aryl)alkylamino-2-methylanthraquinone derivatives.....	- 114 -
4.1.2. Biological evaluation of the synthesized anthraquinone derivatives.....	- 115 -
4.2. Bisacodyl-derived compounds.....	- 116 -
4.2.1. Synthesis of Bisacodyl-derived compounds	- 116 -
4.2.2. Inhibitory potency of bisacodyl derivatives on the human P2X3 receptor and study of structure-activity relationships.....	- 117 -
5. Experimental part.....	- 120 -
5.1. General considerations.....	- 120 -
5.2. Pharmacological Assays	- 121 -
5.2.1. Evaluating the pharmacological actions of the compounds at human P2Y ₄ receptors .	- 121 -
5.2.2. Measurement of Ca ²⁺ in transfected 1321N1 astrocytoma cells.....	- 122 -
5.3. Pharmacophore modelling	- 123 -
5.4. Chemistry of anthraquinone derivatives	- 124 -
5.4.1. General synthetic procedure (I) used for anthraquinone derivatives (2-17).....	- 124 -

Table of contents

5.4.2. Characterization of 1-amino-4-(aryl)alkylamino-2-methylanthraquinone derivatives (2-17)	- 125 -
5.4.3. General synthetic procedure (II) used for anthraquinone derivatives (18-25).....	- 136 -
5.4.4. Characterization of 1-amino-4-(aryl)alkylamino-2-methylanthraquinone derivatives (18-25) -	136 -
5.5. Chemistry of bisacodyl-derived compounds	- 142 -
5.5.1. General synthetic procedure (III) (48-66, 68, 69, 72, 78a, 80, 81, 83, 85, and 99)	- 144 -
5.5.2. Characterization of the bisacodyl-derived compounds.....	- 145 -
5.5.3. General synthetic procedure (IV).....	- 161 -
5.5.4. Characterization of compounds 71-74	- 161 -
5.5.5. General synthetic procedure (V) (75-78).....	- 164 -
5.5.6. Characterization of the synthesized derivatives (80, 81, 83, 85, 87 and 88)	- 167 -
5.5.7. General synthetic procedure (VI) used for the synthesized compounds 89, 90 and 95 -	171 -
6. Abbreviation.....	- 178 -
7. References.....	- 180 -

2 1. Introduction

2.1 1.1. Purinergic signaling and purinergic receptors

1.1.1. Purinergic signaling

The extracellular signaling theory of adenosine 5'-triphosphate (ATP), which can bind to receptors and act as a cotransmitter was postulated almost half a century ago.¹ Before that, it was considered for a long time that ATP only plays a role as a universal intracellular source of energy and as a building block for nucleic acid synthesis.² However, ATP can be released into the extracellular space in response to certain physiological or pathological stimuli.³

The extracellular effects of nucleotides such as ATP were originally described by Drury and Szent-Györgyi in 1929, based on the observation that purine nucleotides and nucleosides were effective when applied extracellularly to heart and blood vessels.⁴ Subsequent studies investigated the action of extracellular ATP. Buchthal and Folkow, showed that ganglia are sensitive to extracellular ATP, which results in tetanus-like contractions.⁵ In 1954, this was further corroborated by Holton during mechanical and electrical stimulation of the great sensory nerve of the ear artery in rabbits.⁶ She showed that ATP released from sensory nerves resulted in vasodilatation changing the tone of blood vessels. This observation was an early sign that ATP may be a neurotransmitter in the peripheral nervous system.⁷

It has also been recognized that ATP is co-released with different classical transmitters within the nervous system such as the inhibitory neurotransmitter γ -aminobutyric acid (GABA)⁸ and acetylcholine.⁹ The ATP released into the extracellular space is subject to breakdown to adenosine 5'-diphosphate (ADP) and adenosine 5'-monophosphate (AMP)¹⁰ by different types of ecto-nucleotidases (E-NTPases).^{11,12}

Now, there is plentiful evidence that ATP is an important neurotransmitter in both the central and peripheral nervous system.^{7,13} A strong relation between purinergic signaling and neural transmission, inflammation, malignancy, angiogenesis and diabetes has been observed since then.¹⁴

1.1.2. Purinergic receptors

In 1972, Geoffrey Burnstock proposed the purinergic nerve hypothesis, which supported the existence of non-adrenergic, non-cholinergic autonomic nerves which would be responsible for the neuronal transmission to smooth muscles of the gastrointestinal tract and bladder.¹⁵ ATP, a purine nucleotide, emerged as the most likely neurotransmitter for these neurons and was soon after termed “purinergic” in 1976.¹⁶ Two years later, purinergic receptors were divided into two families, P1 (adenosine sensitive receptors) and P2 (ATP and its analogues sensitive receptors).¹⁷ Burnstock’s theory was not confirmed until the first ATP receptor was cloned from embryonic chick whole brain in 1993.¹⁸ In addition to P1 receptors and P2 receptors P0 receptors, were recently identified in rodents suggesting a third family of purinergic receptors (**Figure 1.1**).¹⁹

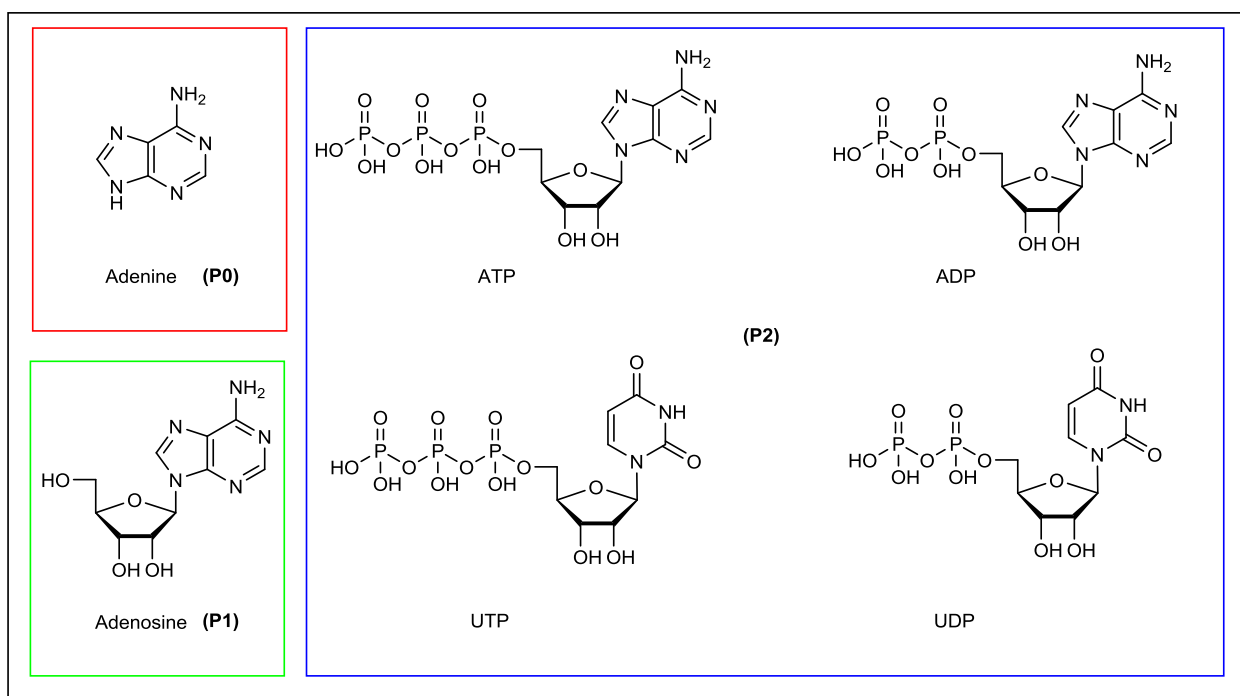


Figure 1.1. Illustration of the structural relationships between the physiological agonists for the three purinergic families. Adenine (red) which is considered as a partial structure of the P1 receptor agonist adenosine (green), which itself is a partial structure of the P2 receptor agonists ATP and ADP (blue).²⁰ UTP: uridine triphosphate; UDP: uridine diphosphate.

1.1.2.1. P0, P1 and P2 receptors

In the following work, these types of purinergic receptor families are classified based on their molecular structure, sensitivity to different agonists and their tissue distribution. Two adenine, four adenosine, eight P2Y and seven P2X receptors have been cloned and characterized.¹⁷ The P0 receptors, known as the adenine receptors (Ade1R and Ade2R), are sensitive to adenine,²¹ the P1 receptors, known as the adenosine receptors (A₁, A_{2A}, A_{2B} and A₃), are sensitive to adenosine²² and the P2 receptors, classified into P2X and P2Y are activated by various nucleotides. The P2Y receptors (P2Y_{1,2,4,6,11-14}) are activated by ATP, ADP, UTP, uridine diphosphate UDP or UDP-glucose.¹⁹ All these receptors are G protein-coupled receptors (GPCRs). The P2X receptors (P2X1-7) are ligand-gated ion channels activated by ATP²² (**Figure 1.2**).

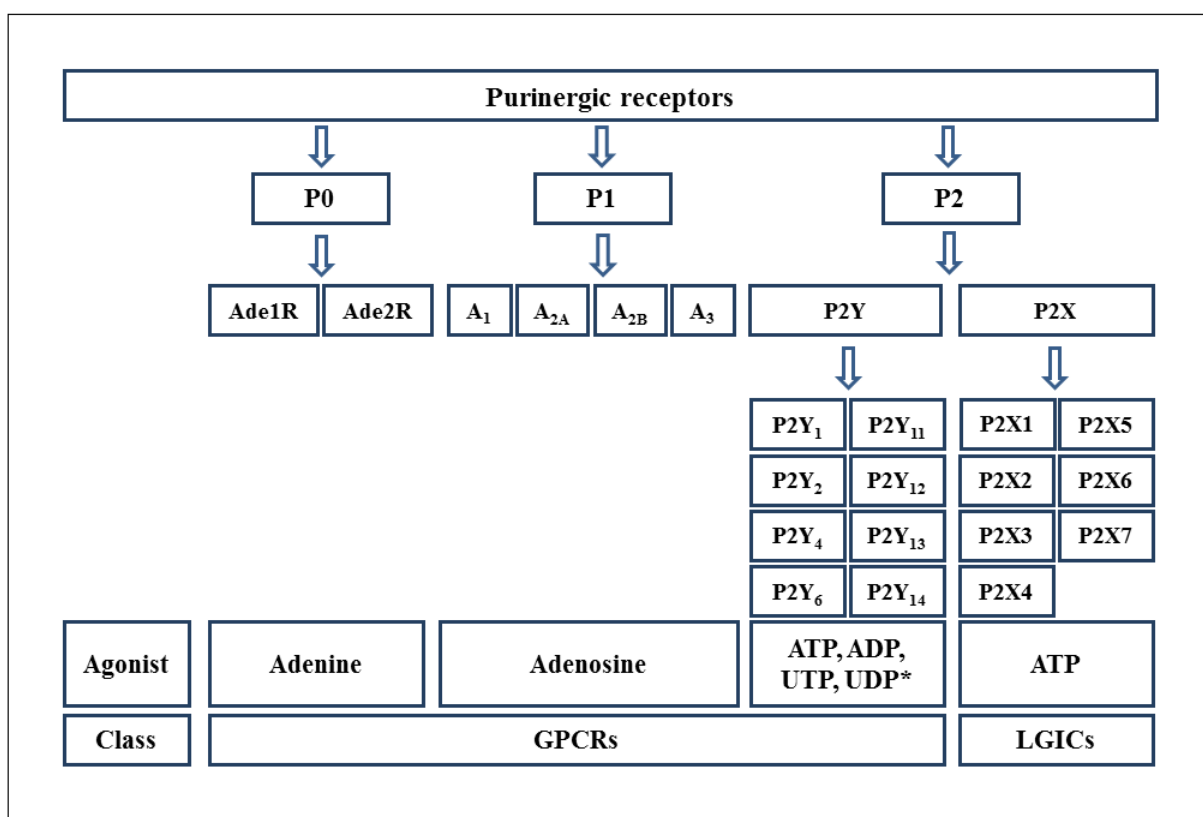


Figure 1.2. Classification of the purinergic receptor family. *ATP (endogenous ligand for P2Y₂ and P2Y₁₁); ADP (endogenous ligand for P2Y₁, P2Y₁₂, and P2Y₁₃); UTP (endogenous ligand for P2Y₂, and P2Y₄); UDP (endogenous ligand for P2Y₆); UDP-glucose (endogenous ligand for P2Y₁₄).¹⁶⁻¹⁸

1.1.3. G protein-coupled receptors (GPCRs)

The name G-protein-coupled receptors was suggested because these receptors primarily act via activation of guanine nucleotide binding proteins (G proteins).²³ GPCRs also commonly referred to as seven transmembrane (TM) receptors (**Figure 1.3**), are a family of integral membrane receptors which play a substantial role in signal transmission in the cells. Information provided by extracellular stimuli is transduced into intracellular second messengers by GPCRs through coupling with G proteins.²⁴ GPCRs have important physiological roles, and the impairment of their function leads to a variety of diseases.²⁵ Different types of ligands can activate GPCRs effectively, such as peptide and non-peptide neurotransmitters, growth factors, hormones, odorant molecules and light.²⁵

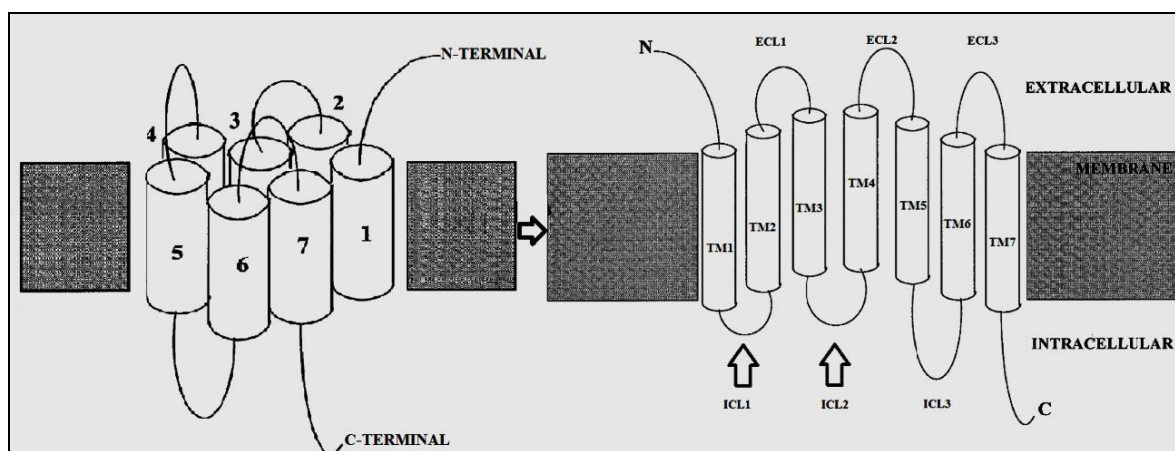


Figure 1.3. Schematic view of basic structural features of GPCRs. Seven transmembrane helices numbered 1-7 are described as cylinders connected by loops which are drawn as lines, while the membrane is shaded. The left part of the diagram demonstrates, in a very simplified style, the three dimensional packing of the seven helices together. The right part of the diagram shows the transmembrane topology of a GPCR (unfolded receptor). The intracellular loops (ICLs) which are formed between transmembrane domains are marked ICL1 to ICL3, and the extracellular loops (ECLs) are marked ECL1 to ECL3.²³

Four families of proteins (ion channels, rhodopsin-like GPCRs, protein kinases, and nuclear hormone receptors) have been described to represent 44% of all human protein drug targets (**Figure 1.4**, left). These privileged families mediate the pharmacological effects of 70% of small-molecule

Introduction

drugs. Rhodopsin-like GPCRs have grown to be one of the leading areas of research. They represent 33% of all drug targets (**Figure 1.4, right**).²⁶

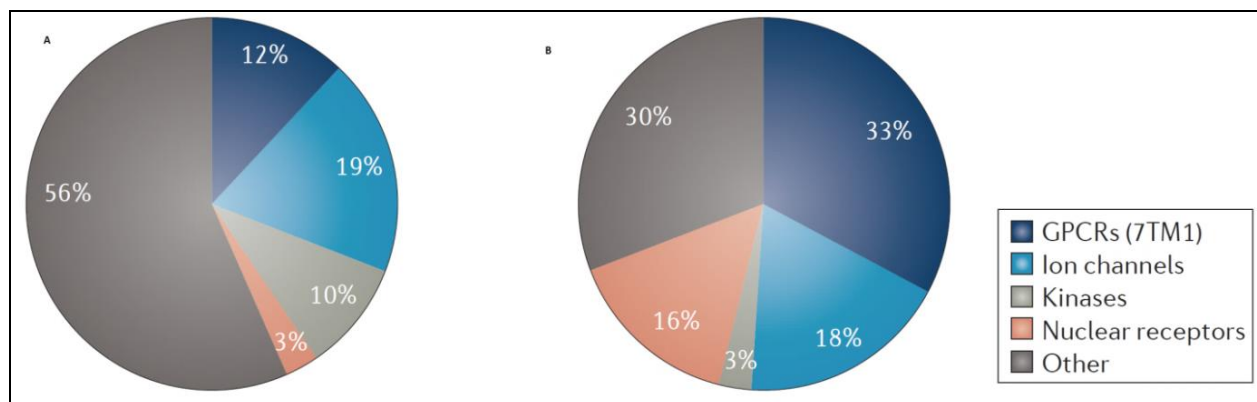


Figure 1.4. Proportions of the main gene families as targets for drugs. **A.** Attribution of human drug targets in the main families. **B.** Attribution of drugs (small-molecules) that target those families.²⁶

1.1.4. P2 receptors (nucleotide receptors)

The current PhD thesis focuses on the P2 receptor family. The P2 receptors are ubiquitously distributed in the body.²⁷ Seven subtypes of ionotropic P2X receptors, which can form homomultimers and heteromultimers, and eight subtypes of metabotropic P2Y receptors are known to exist.

1.1.4.1. P2Y receptors

P2Y receptors are widely distributed and found in various tissues including smooth muscle (vascular and visceral), autonomic, central, enteric and sensory neurons, glia and astrocytes, epithelium and endothelium, heart, as well as soft tissues (kidney, liver, lung, pancreas, prostate and thymus), and bone (**Table 1.1**).^{28,29}

P2Y subtypes can be subdivided into G_q-coupled receptors (P2Y₁, P2Y₂, P2Y₄, P2Y₆, and P2Y₁₁) and G_i-coupled receptors (P2Y₁₂, P2Y₁₃ and P2Y₁₄).³⁰ Based on sequence similarity, P2Y receptors can be grouped into two subfamilies: P2Y_{1,2,4,6,11} and P2Y_{12,13,14}. The percentage of amino acid (AA) sequence identity is relatively low (19-55%). The P2Y₁₂ receptor shows only 19% homology with the other P2Y receptor subtypes.² P2Y receptors are activated by different nucleotides based on the

Introduction

receptor subtype: P2Y_{1,12,13} are activated by ADP; P2Y₂ is activated by UTP and ATP; P2Y₄ is activated by UTP; P2Y₆ is activated by UDP; P2Y₁₁ is activated by ATP; P2Y₁₄ is activated by UDP-glucose.²⁸

Table 1.1. Human P2Y receptors^{19,31}

P2Y Subtype	Main distribution	Agonist	No. of AA
P2Y ₁	Epithelial and endothelial cells, blood platelets, immune cells, osteoclasts, brain	ADP	372
P2Y ₂	Epithelial and endothelial cells, immune cells, renal tubules, osteoblasts	UTP/ATP	376
P2Y ₄	Endothelial cells, spleen, placenta	UTP	365
P2Y ₆	Airway and intestinal epithelial cells, spleen, placenta, thymus	UDP	328
P2Y ₁₁	spleen, intestine, granulocytes	ATP	371
P2Y ₁₂	Platelets, brain (glial cells), microglial cells	ADP	342
P2Y ₁₃	Spleen, brain, erythrocytes lymph nodes, bone marrow	ADP	334
P2Y ₁₄	Placenta, adipose tissue, stomach, intestine, discrete brain regions, mast cells,	UDP-glucose	338

1.1.4.2. P2X receptors

P2X receptors belong to the class of ligand-gated ion channels. Ion channels are a group of membrane proteins which are expressed in virtually every living cell. More than 400 putative ion channels have been recognized in the human genome sequences. Ionotropic channels may be classified on the basis of their regulatory mechanisms into different subclasses. There are mainly two subfamilies. One is the family of voltage-gated ion channels (VGICs), and the other one are the ligand gated ion channels (LGICs). Regulation of the VGIC is controlled by voltage changes, while LGICs are controlled by chemical transmitters.³² LGICs are transmembrane ion channels that convert the binding of a ligand (released from the presynaptic neuron and bound to the postsynaptic neuron), into an ion influx in the postsynaptic membrane. They consist of at least two domains, a transmembrane domain which contains the ion channel and an extracellular domain which

Introduction

comprises the ligand binding site. Upon excitation, the binding of the ligand triggers conformational changes that allow the opening of the ion channel and subsequently the influx of ions across the cell membrane. Besides their prominent role in neurotransmission, they are also found on some nonexcitable cells such as endothelial cells, indicating a wider regulatory role of these receptors outside the nervous system.³³

LGICs are related to membrane proteins which can either form homomeric or heteromeric channels. Homomeric channels are formed by several member of the same subunit, while heteromeric channels occur through the association of different subunits. The composed subunits define both pharmacological properties and functional characteristics of ligand-gated channels.³⁴ Three major superfamilies of LGICs are existing, (i) Cys-loop receptors which are pentameric ion channels, (ii) ionotropic glutamate receptors which are tetrameric ion channels, and (iii) P2X receptors which are trimeric ion channels.³³

Up till now, seven homomeric P2XRs (P2X1-7) and five heteromeric assemblies (P2X1/2, P2X1/5, P2X2/3, P2X2/6 and P2X4/6) have been identified or proposed.²² Recently, it has been reported a P2X2/4/6 heterotrimer as the first P2X receptor containing three different subunits.³⁵ P2XRs have been cloned both from human and rat complementary deoxyribonucleic acid (cDNA) libraries or, mouse and guinea-pig and, in some cases, also from chick and zebrafish libraries.³⁶

Several non-selective antagonists of P2X receptors were discovered. Suramin, 2',3'-*O*-(2,4,6-trinitrophenyl)adenosine 5'-triphosphate (TNP-ATP), Reactive Blue-2 (RB-2), pyridoxalphosphate-6-azophenyl-2'-4'-disulfonic acid (PPADS), and iso-PPADS structures are presented in **Figure 1.5**.³⁷

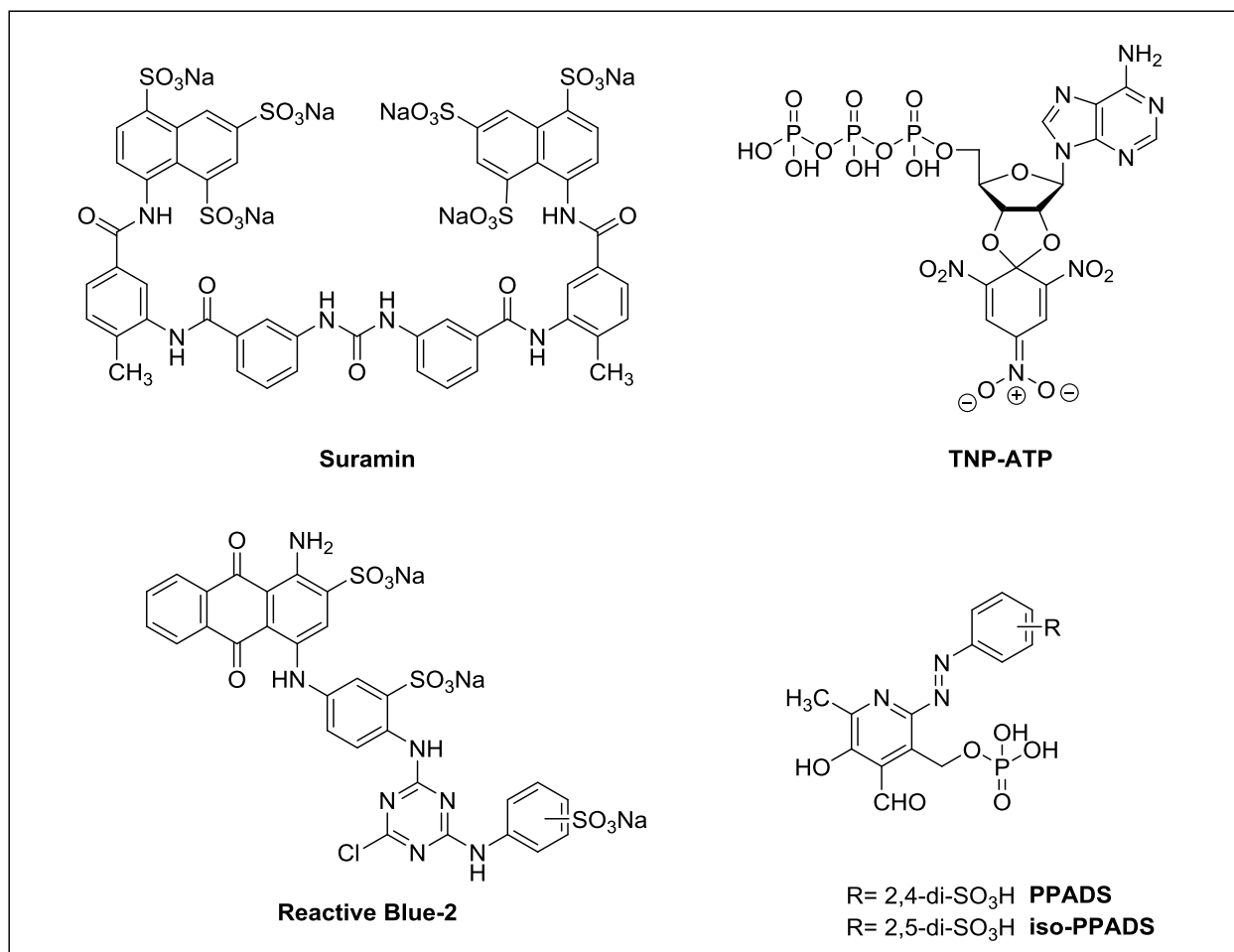


Figure 1.5. Structures of nonselective P2X receptor antagonists.³⁷

Each subunit topology is composed of two hydrophobic transmembrane domains, positioning both N- and C-terminal intracellularly with two transmembrane regions (TM1 and TM2), one of them related to channel opening and closing and the other lining the ion pore; a large extracellular loop, containing ten conserved cysteine residues forming five disulfide bridges and the ATP binding sites. The hydrophobic H5 region near the pore passageway is responsible for the modulation of receptor/channel by various cations including Ca²⁺, Mg²⁺, Zn²⁺ and Cu²⁺, while the ATP-binding site may involve areas related to the extracellular loop (**Figure 1.6**).¹³ Conformational changes happen in response to binding of the agonist ATP, which leads to the opening of the ion channel pore and enables the flow of Ca²⁺, Na⁺ and K⁺ across the membrane.³⁸ Their protein sequence size lies between 384 (P2X4) and 595 (P2X7) amino acids with 30-50% sequence identity.¹³

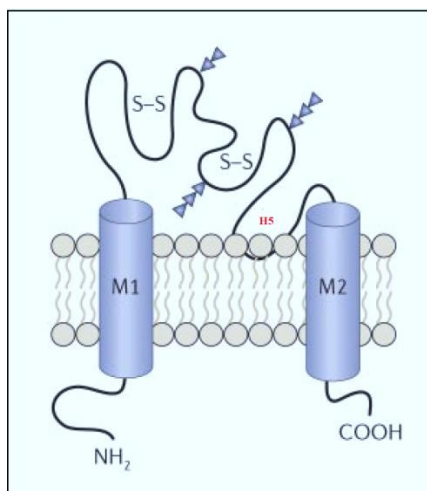


Figure 1.6. The P2X purinoreceptors (NH₂ and COOH termini are located intracellularly; S-S; disulfide bonds; M1 and M2, transmembrane domains).^{13,39}

The P2X receptors are widely expressed in different tissues such as immune cells, platelets, vascular smooth muscle cells and importantly in the peripheral and central nervous system. They are involved in a wide variety of physiological processes, including smooth muscle contraction, cell death, synaptic transmission and presynaptic modulation, cell proliferation, taste, nociception and platelet aggregation (see **Table 1.2**).^{40,41}

Table 1.2. P2X receptor subtypes including distribution and localization^{42,43}

P2X subtype	Main distribution	Desensitization kinetics	No. of amino acids
P2X1	Smooth muscle, sympathetic & parasympathetic ganglia, cerebellum, platelets, pituitary	fast	399
P2X2	Smooth muscle, central and peripheral nervous system, brain, pancreas, retina	slow	472
P2X3	Nociceptive sensory neurons, some sympathetic neurons	fast	397
P2X4	Microglia, testis, colon, endothelial cells	slow	384

P2X subtype	Main distribution	Desensitization kinetics	No. of amino acids
P2X5	Proliferating cells in skin, gut, bladder, thymus, spinal cord, heart, adrenal medulla	slow	417
P2X6	Brain, motor neurons in spinal cord	slow	379
P2X7	Macrophages, mast cells, microglia, pancreas, skin, endocrine organs	slow pore formation	595

1.1.4.2.1. P2X receptor crystal structures

In the following part, crystal structures of P2X receptors will be discussed. The first one is the zebrafish P2X4 receptor (zfP2X4) structure which was discovered in the apo state, later it was co-crystallized with ATP. The second one is the human P2X3 (hP2X3) receptor which has been discovered with different states and it was co-crystallized with ATP and orthosteric inhibitors. The third one is the mammalian P2X7 crystal structure which was co-crystallized with five different allosteric inhibitors.

1.1.4.2.1.1. P2X4 receptor crystal structure

The first crystal structures of a P2X receptor was that of the zebrafish P2X4 receptor (zfP2X4) in the closed and the open state.^{44,45} The crystal structure (zfP2X4) receptor confirmed the trimeric structure of P2X receptors, including the following features: (1) two transmembrane (TM1 and TM2) domains, (2) large extracellular loop containing ATP binding sites, and (3) intracellular N- and C-terminals. It showed that the transmembrane ion channel pore is composed of six α -helices in the extracellular region, two larger helices in the transmembrane region.⁴⁴

The zfP2X4 receptor structure proposed that the TM2 forms the ion pore. The TM2 helices line the central ion channel pore containing the channel gate in the closed resting state. The TM1 was in a peripheral ring to the pore region. The TM domains might exist as the fluke and the upper body domain which is the extracellular region. In the extracellular region the core domain which consist of two β -strands which are connected to each other very tightly with strong interactions. Each

Introduction

subunit showed as a shape of dolphin consisting of the head domain, which contains three β strands and one α -helix, the body domain, the dorsal fin, both right and left flippers (see **Figure 1.7**).

The homomeric zFP2X4 receptor was crystallized by Kawate *et al.* at a 3.1 Å resolution in the closed state with no bound antagonist, and ATP-binding sites were not identified. The zP2X4 receptor is shaped like a chalice with a large extracellular domain about 70 Å above and comparatively smaller transmembrane domains spanning roughly a 28 Å through the membrane.⁴⁶

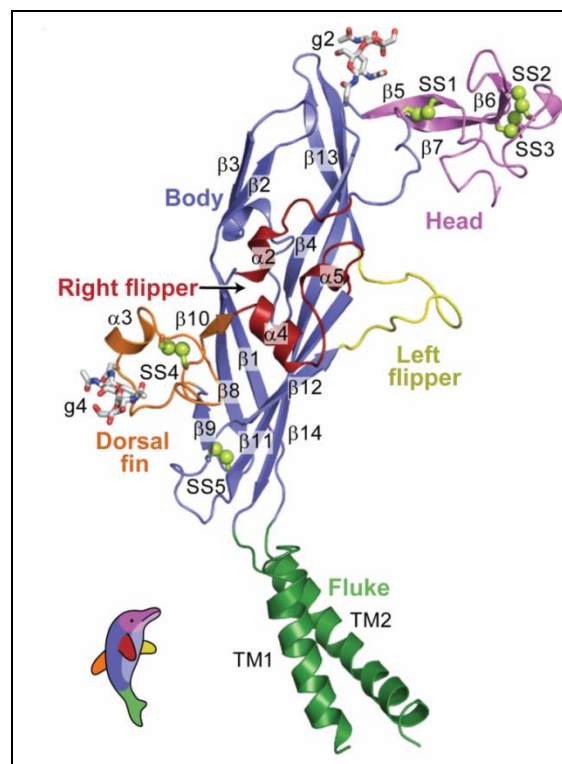


Figure 1.7. Dolphin-like shape of one subunit of the zP2X4 receptor (TM are transmembrane helices, g2 and g4 marks the attached glycans, β 1-14 indicates β -strands, and SS1-5 represents disulfide bonds).⁴⁴

Later in 2012, Hattori *et al.* successfully co-crystallized the zFP2X4 receptor in its open state bound to ATP at a 2.8 Å resolution which confirmed the location of the ATP binding sites. The residues in the zFP2X4 receptor are located at the base of the head region of the receptor, near the predicted ATP binding pocket.⁵⁶ In the ATP-bound open-channel structure (**Figure 1.8, A**) the positively charged amino acid residues K70, K72, K316, N296, and R298 (zFP2X4 numbering) could directly

Introduction

coordinate the binding of the ATP. The α -phosphate group is indirectly coordinate by K193. This interaction occurs through the solvent of crystallization (glycerol), which may be changed by water molecules under physiological conditions (**Figure 1.8, B**). The adenine moiety of ATP is coordinated by T189, L191, and I232 residues, while the ribose ring is recognized by L217. The different structural domains such as hydrophobic and positively charged amino acid residues are able to surround the bound ATP molecule.⁴⁷

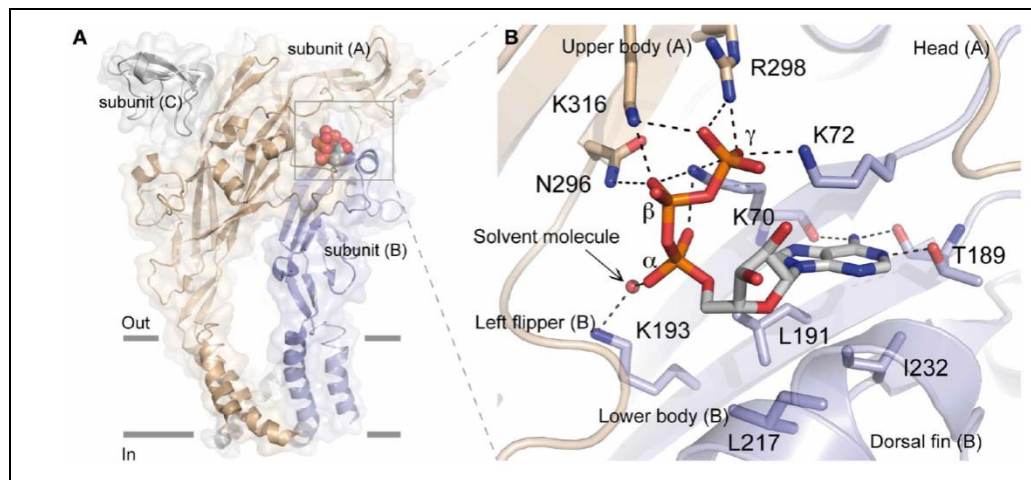


Figure 1.8. A) One ATP molecule which is bound to the trimeric structure of zfp2X4 receptor (lateral view). B) The ATP-binding site (close-up view). Red sphere indicates the oxygen of the glycerol (solvent). Hydrogen bonding is indicated by black dash lines. Due to the subunit of the receptor being similar to a leaping dolphin, the domains are named the upper body and head domain (chain A), and left flipper, lower body and dorsal fin (chain B).⁴⁷

Ion permeability

Conformational change between the subunits of the zfp2X4 receptor, which induced in response to the binding of ATP to the extracellular domain, causes a movement of the TM domains and permits cation influx via the receptor pore. Two pathways were suggested for passage of the ions from the extracellular solution to the transmembrane ion channel. One of the possible pathways of the ion passage is through an area on top of the TM domains. The opening approximately 8 Å in diameter could be big enough to allow the passage of cations such as Na⁺, K⁺ and Ca⁺² to the channel. Another possibility is that the ions access the TM domains through two vestibules rich in acidic

Introduction

residues. Even though in the apo, closed-state structure of the zP2X4 receptor, which shows that it is too narrow (~ 2.3 Å) for hydrated ions to pass through, it is thought that when the agonist binds to the channel, it will expand these constrictions permitting ions to pass through.⁴⁴

Facts about the P2X4 crystal structure

- (1) The crystal structure of zfP2X4 receptor has provided a major advance in the understanding of the molecular architecture of the P2X receptors.
- (2) Compared to other trimeric receptor with each subunit containing two TM domains such as the acid sensing ion channel (ASIC), there is a similarity in pore architecture and the aqueous vestibules.⁴⁸
- (3) Extracellular movements following ATP binding were identified through the comparison between apo and ATP-bound states.⁴⁰
- (4) The ATP-bound structure at 2.8 Å resolution identifies a previously unseen ATP-binding motif and an open pore conformation.

1.1.4.2.1.2. P2X3 receptor crystal structure⁴⁹

The first crystal structure of the human P2X3 receptor was discovered in an apo/resting, agonist-bound/open-pore, agonist-bound/desensitized and antagonist-bound closed states. The ion channel pore in the open state structure is stabilized by an intracellular motif named “cytoplasmic cap” which forms a phospholipid-lined gate for egress of water molecules and ions. The apo/resting state is stabilized by the competitive antagonists TNP-ATP and A-317491. The apo structure of the hP2X3 receptor as a more complete transmembrane domain than that of the P2X receptor. It has different residues defining the pore constriction, and it has a Mg^{2+} ion bound in the head domain.

The extracellular domains and binding pockets of both, the desensitized and the open states of the hP2X3 are similar. There are big differences in the transmembrane domains and at the gates. Both hP2X3 structures (open state and desensitized state) have transmembrane domains with sufficient length to cross a lipid bilayer, and the desensitized state structure has a pore architecture that was

Introduction

not previously observed for any P2X structure. The TM domains of the zfP2X4 structure are short and incomplete compared to the TM domains for the hP2X3 structure.

The cytoplasmic cap anchors the TMs to allow a change in helical axis in TM2 once the channel opened. The cytoplasmic cap undergoes a folding-unfolding transition during channel gating and its stability sets the rate of receptor desensitization. In the closed state, when ATP binds, the signal is transferred and the channels are open. After some time of ATP binding, the signal is not able to be transferred even in the presence of ATP. This state is observed with the P2X3 receptor which is characterized by a fast-desensitizing state. In contrast, the P2X4 receptor is slowly desensitizing. In the fast-desensitizing state, the P2X receptors possess a relatively unstable cap domain, while the slowly and incompletely desensitizing receptors having a more stable cap domain.

The orthosteric ligand-binding site

The binding pocket for the ATP-bound, open state, the TNP-ATP bound, closed state, and the A-317491-bound, closed state of hP2X3 have been characterized (**Figure 1.9**). The open state structure has ATP in the ligand-binding pocket and an open pore, while the desensitized state structure has ATP in the pocket but a closed pore. The orthosteric ligands bind in a cleft at an interface between two protomers. ATP binding residues make interactions with TNP-ATP and A-317491, notably R281, N279, and K65 and T172 (for TNP-ATP) (see **Figure 1.10**).

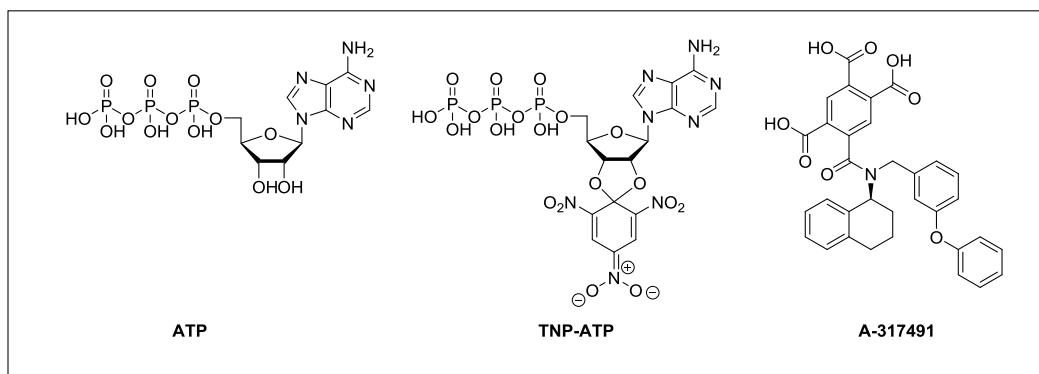


Figure 1.9. Structure of ATP, TNP-ATP and A-317491.³⁷

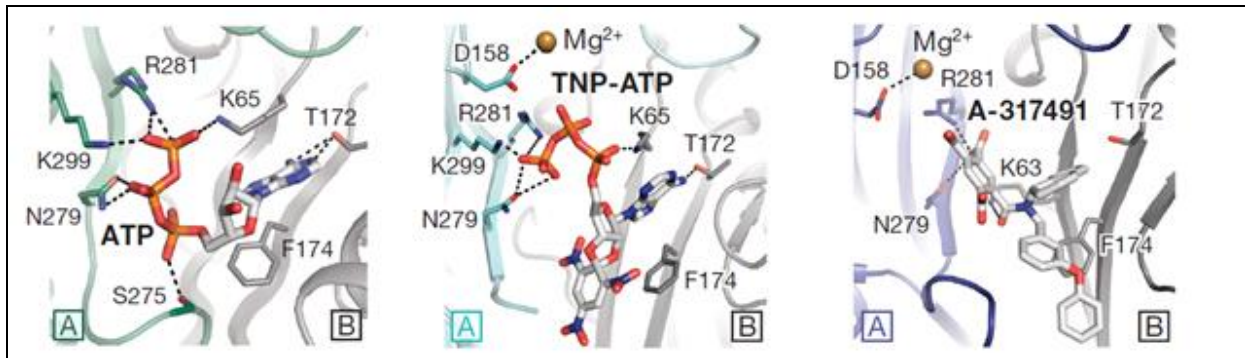


Figure 1.10. The orthosteric ligand-binding site.⁴⁹

Pore-lining surface

The pore radius is a function of distance for the open, apo, and the desensitized state. The extracellular boundary of the gate referred to the amino acid residues I323 and T330, respectively. I323, which considered as the first site of the gate was constructed, and T330 which defines the narrowest region of the pore in the open state. In the desensitized state the pore size and diameter were changed (see **Figure 1.11**).

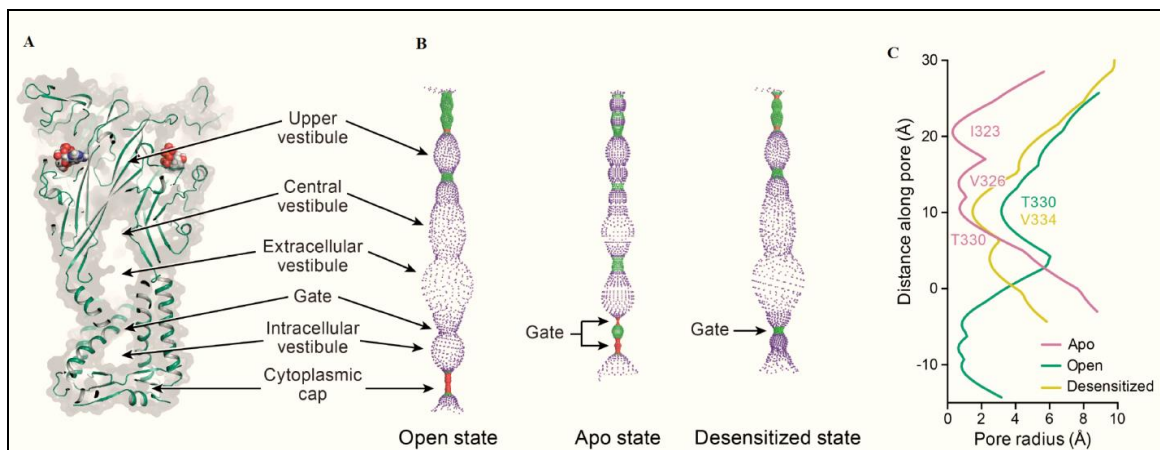


Figure 1.11. The hP2X3 pore-lining surface in the open, apo and desensitized states.⁴⁹

Comparison between hP2X3 and zP2X4 structures emphasizes the longer transmembrane domains and the cytoplasmic domain of hP2X3. In the antagonist-bound state, the competitive antagonists TNP-ATP and A-317491 occupy the orthosteric ligand-binding pocket, and the ion channel pore is closed which is identical to the apo/resting state.

1.1.4.2.1.3. P2X7 crystal structure

Five diverse structures known to be antagonists for P2X7 receptor have been co-crystallized namely, A7400003, A804598, AZ10606120, GW791343, and JNJ47965567 (**Figure 1.12**)^{50,51,52,53,54} using x-ray crystallographic techniques, which showed that these compounds bind in the same binding pocket. Among these five antagonists, three of them namely A740003, A804598, and JNJ47965567 previously have been identified as competitive inhibitors. However, based on the released crystal structures they are predicted as allosteric antagonists. Based on structures diversity, conformation changes of the lower body domain region were occurred. This possibly inhibits indirectly the ATP binding pocket through these allosteric modifications.⁵⁵

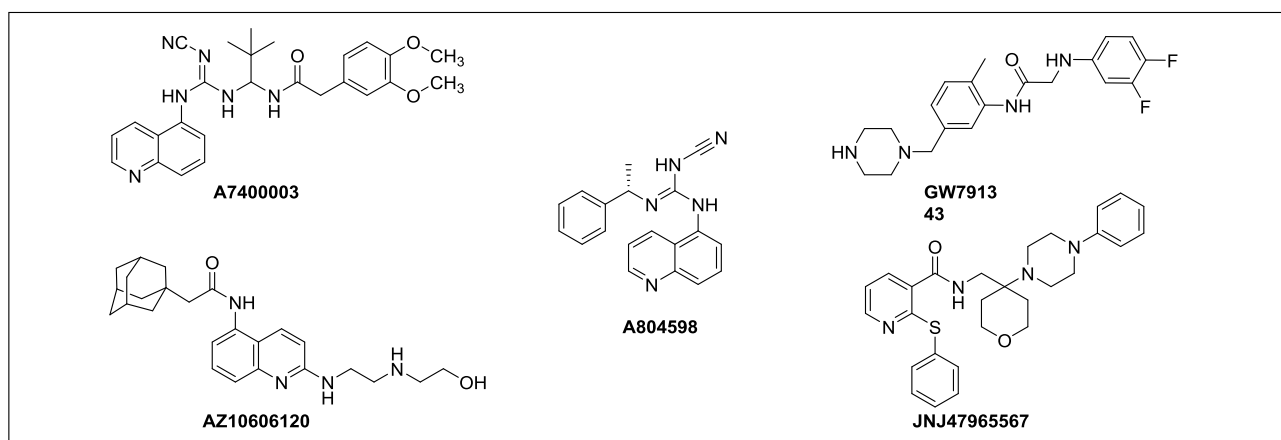


Figure 1.12. Structures of A7400003, AZ10606120, A804598, GW791343, and JNJ47965567.

Allosteric binding pocket

The drug-binding pocket is surrounded by 13 residues which are hydrophobic in nature. Based on the crystal structure information, the known binding pocket is hydrophobic involving F95, F103, M105, F293, and V312 (**Figure 1.13**). Compound A804598 is closer to the binding pocket of ATP. However, the distances and angles between the side-chains and the drugs cannot be precisely evaluated because the resolution of the crystal structure was very low $\sim 3.4 \text{ \AA}$ (**Figure 1.13**).⁵⁵

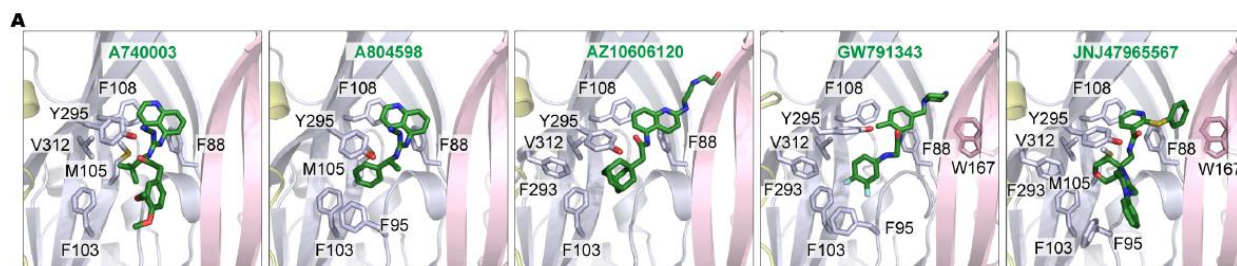


Figure 1.13. The allosteric binding pocket.⁵⁵

In the closed state, the turret was interrupting, the left flipper goes outside down direction, the dorsal fin goes up, and the head body goes down. In the open state the turret has to be slightly moved while the antagonists stopping the turret to move inside (**Figure 1.14**).

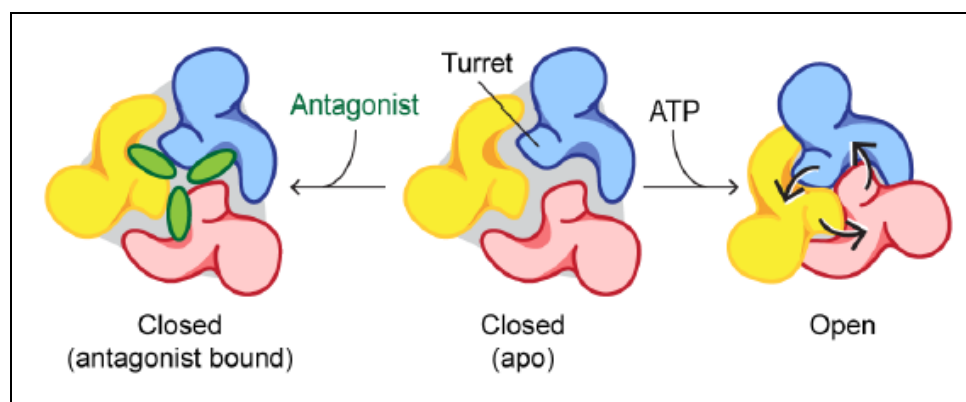


Figure 1.14. Activation and inhibition mechanisms of the P2X7 receptor.⁵⁵

In the beginning the P2X crystal structures were co-crystallized with apo and ATP and later it was with orthosteric inhibitors and further it was extended to allosteric inhibitors.

1.1.5. P2X1, P2X2 and P2X4 receptors

1.1.5.1. P2X1 receptor subtype

P2X1 receptors are widely distributed in smooth muscle cells and platelets, which regulate smooth muscle contractility and prothrombotic functions. P2X1 is similar to the P2X3 receptor in terms of agonist and kinetic properties. However, β,γ -MeATP displays higher potency for P2X1 than for P2X3.⁵⁶

1.1.5.2. P2X1 receptor antagonists

Many P2X1 antagonists have been developed with limitation to increase potency and selectivity, but their drug-likeness is low. Several suramin derivatives were identified with extremely high potency and selectivity for P2X1 receptors. 4,4',4'',4'''-[Carbonyl-bis-(imino-5,1,3-benzenetriyl-bis-(carbonylimino))]tetrakis-1,3-benzene disulfonic acid (NF 449), a potent purinergic receptor antagonist was found to be highly selective for P2X1 (>3,000-fold more potent than suramin at the rat P2X1 receptor).⁵⁷ Certain suramin derivative show a relatively high affinity for P2X1 receptors: 8,8'-[carbonyl-bis-(imino-3,1-phen-ylene-carbonylimino)]bis-1,3,5-naphthalene-trisulfonic acid (NF023) was also identified as a competitive P2X antagonist with IC₅₀ values of 0.21 and 0.24 μ M on rat and human P2X1, respectively. P2X3 receptors have an intermediate sensitivity with IC₅₀ values of 8.5 and 28.9 μ M on rat and human, respectively, while it is less potent at the P2X2 subtype (IC₅₀> 50 μ M), and inactive on P2X4 receptors.⁵⁸ Another suramin derivative with nanomolar inhibitory potency at the P2X1 receptor is 8,8'-[carbonyl-bis-(imino-4,1-phenylene-carbonylimino-4,1-phenylene-carbonyl-imino)]bis-1,3,5 naphthalene trisulfonic acid (NF279), which showed antagonistic activity for P2X1 with an IC₅₀ of 0.050 μ M. Other P2X1 antagonists are derivatives of pyridoxal-5'-phosphate and the 6-azophenyl-2',4'-disulfonate derivative (PPADS), such as MRS2220, which blocks P2X1 at about 10 μ M with no effect on P2X2 or P2X4 receptors or hP2Y₂, hP2Y₄, or rP2Y₆ receptors.⁵⁹ However, none of the previously described antagonists can be considered as an ideal starting point for drug optimization.⁵⁶

RO-0437626 (RO-1), a benzimidazole-2-carboxamide derivative is the only non-acidic small molecule P2X1 antagonist with drug-like properties. RO-1 was discovered through high-throughput

Introduction

screening (HTS) of optimized dipeptide library, which were originally synthesized as potential renin inhibitors, but were shown to be inactive. It showed moderate potency on human P2X1 with an IC_{50} of 3 μ M, and it was the first P2X1 receptor antagonist proven to be > 30-fold selective over other homomeric and heteromeric human P2X receptors (P2X2, P2X3, and P2X2/3, IC_{50} > 100 μ M).⁶⁰ Previously described antagonists are illustrated in **Figure 1.15**.

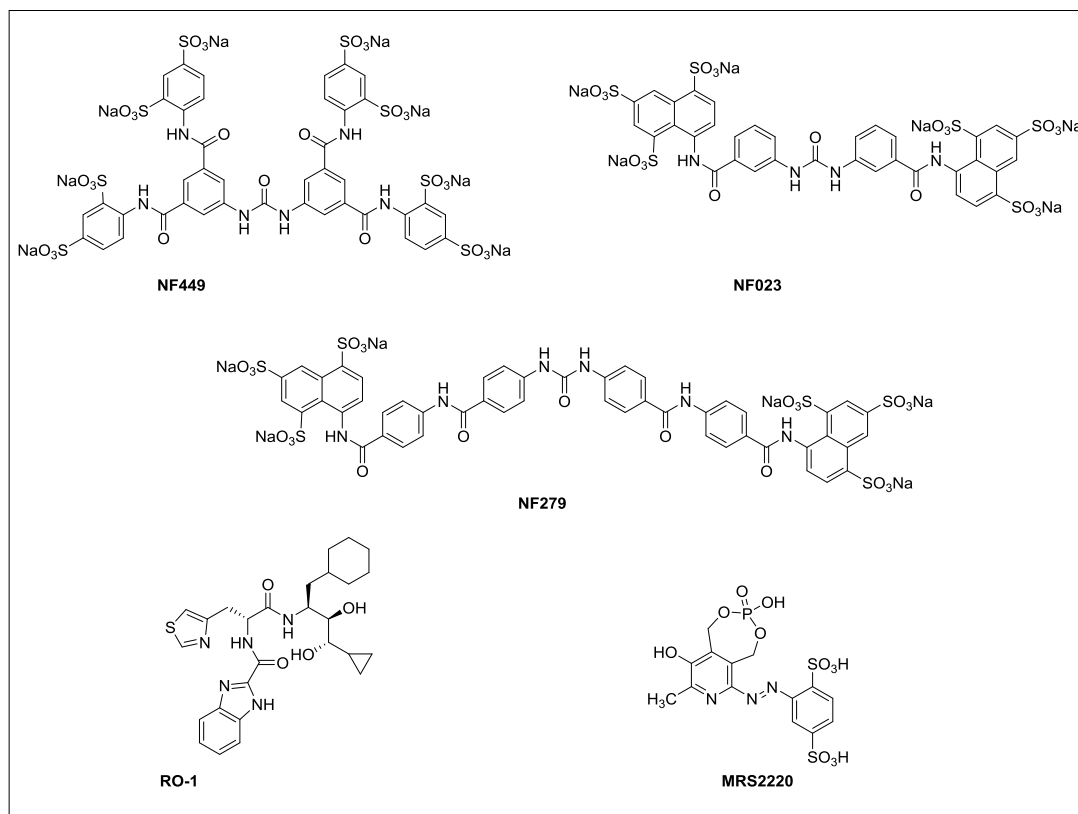


Figure 1.15. Structures of suramin-derived P2X1 antagonists NF449, NF023, NF279, RO-1, and PPADS-derived MRS2220.

1.1.5.3. P2X2 receptor subtype

P2X2 receptors (P2X2R) are distributed within the peripheral and central nervous systems, and on many non-neuronal cell types, where they play a role in ATP-mediated sensory transmission and modulation of synaptic function. Also, P2X2R may possess extended functions in the organization of many central nervous system (CNS) processes, such as memory and learning, motor function,

Introduction

autonomic coordination, and sensory integration. They are similar to P2X4 and P2X5 in agonist activity and slow desensitization kinetics.⁵⁶

P2X2R are established as homomers or heteromers with other receptors. P2X2 subunits may form heteromeric channels in combination with two different partners (P2X3 or P2X6). The P2X2/6 heteromer is composed of two P2X2 monomers and one P2X6 monomer, while the heteromeric P2X2/3 formed by one P2X2 and two P2X3 monomers.⁶¹

The P2X2 receptor activity can be modulated allosterically by transition metals. The most potent metal is copper (Cu^{2+}) which triggered a 25-fold potentiation of the ATP-gated currents. For comparison, zinc (Zn^{2+}), nickel and mercury need 10-fold higher concentration while palladium, cobalt need 12-fold and cadmium needs only 3-fold higher concentrations. Platinum was inactive. The authors concluded after replacing nine alanines with histidines in the extracellular domain of the rat P2X2 receptor that His120, His192, His213 and His245 are residues forming the allosteric metal binding site of the P2X2 receptor. These four mutant histidines and His319 were specifically important for the coordination of (Cu^{2+}), but not (Zn^{2+}).⁶²

1.1.5.4. P2X2 receptor antagonists

Nicardipine is a calcium channel blocker which belongs to the dihydropyridine class. It showed antagonistic activity on recombinant rat P2X2 receptor with an IC_{50} value of 25 μM .⁶³ In 2011, Baqi *et al.* published a series of optimized anthraquinone derivatives related to RB-2, which yielded disodium 1-amino-4-[3-(4,6-dichloro[1,3,5]triazine-2-ylamino)-4-sulfophenylamino]-9,10-dioxo-9,10-dihydroanthracene-2-sulfonate (PSB-1011) and sodium 1-amino-4-[3-(4,6-dichloro[1,3,5]triazine-2-ylamino)phenylamino]-9,10-dioxo-9,10-dihydroanthracene-2-sulfonate (PSB-10211) with IC_{50} of 0.079 μM and 0.086 μM , respectively as the first potent and selective competitive rat P2X2 receptor antagonists (see **Figure 1.16**).⁶⁴

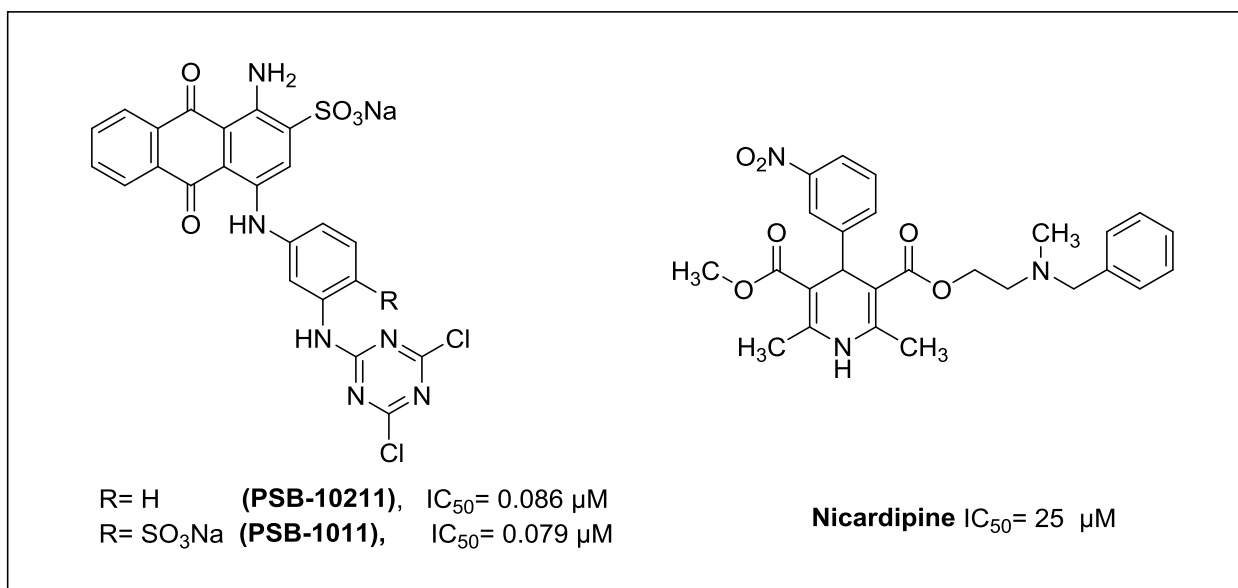


Figure 1.16. Structures of P2X2 receptors antagonists PSB-1011, PSB-10211, and nicardipine.

1.1.5.5. P2X4 receptor subtype

Between the P2X receptors, the P2X4 subtype is prominently distributed through the central and peripheral nervous system including epithelia, smooth muscle cells of the bladder, gastrointestinal tract, kidneys, lungs, uterus, and arteries, uterine endometrium, fat cells, liver, heart, pancreas and activated microglia.^{56,65}

The activation of spinal microglia as a consequence of damage and inflammation in the spinal cord after injury of peripheral nerves leads to an up regulation of P2X4 receptor expression. Stimulation by endogenous ATP results in the formation of brain-derived neurotrophic factor (BDNF).⁶⁶ Therefore, P2X4 receptors are novel targets for the treatment of chronic neuropathic pain.⁶⁷

1.1.5.6. P2X4 receptor antagonists

One of the first selective antagonists of the P2X4 receptor which has been described in literature is the benzodiazepine derivative 5-BDBD (5-(3-bromophenyl)-1,3-dihydro-2H-benzofuro[3,2-e]-1,4-diazepin-2-one). 5-BDBD is moderately potent with an IC_{50} value of $1.6 \mu M$ in human embryonic kidney (HEK)-293 cells expressing human P2X4 receptor.⁶⁸ In 2016, Abdelrahman *et al.*

Introduction

demonstrated that 5-BDBD is a non-competitive antagonist since it does not block [³⁵S] ATP γ S binding. This indicates that it binds allosterically.⁶⁹

Clinically used antidepressant drugs were investigated for their inhibitory effects on human and rat P2X4 receptor. Among these, paroxetine showed inhibition of ATP-mediated calcium influx in 1321N1 astrocytoma cells expressing the P2X4 receptors with an IC₅₀ of 2.45 μ M on human and 1.87 μ M on rat receptors. An antiallodynic effect was seen after intrathecal administration of paroxetine. The authors claimed that the antinociceptive activity of paroxetine as well as other antidepressants used for the therapy of neuropathic pain could be induced at least partially through inhibition of P2X4 receptors.⁷⁰ Radioligand binding assays illustrated that paroxetine is characterized as an allosteric antagonist, because it was unable to displace [³⁵S]ATP γ S from its binding site at the human P2X4 receptor.⁶⁹

Amitriptyline, a tricyclic antidepressant was approved to treat neuropathic pain in humans, but its anti-hyperalgesic mechanism is still unknown. Amitriptyline's inhibitory effect was tested on rat, mouse, and human P2X receptors (P2X2, P2X4, and P2X7). Amitriptyline showed only moderate activity on rat and mouse P2X4 receptor and no activity was found on human P2X4, P2X7 and rat P2X2 receptors. In conclusion, P2X4 receptor blockade is not considered as a contributing factor to amitriptyline's efficacy against neuropathic pain.⁷¹

Recently, Hernandez-Olmos *et al.* reported a series of *N*-substituted phenoxazine derivatives as potent and selective allosteric P2X4 antagonists. Of these derivatives, *N*-(benzyloxycarbonyl)phenoxazine (PSB-12054) is a very potent antagonist on human P2X4 with an IC₅₀ of 0.189 μ M and it has a high selectivity for human P2X4 of over 30-fold as compared to human P2X1, P2X2, P2X3, and P2X7 receptors. In contrast to PSB-12054, the sulfonamide derivative, *N*-(*p*-methylphenylsulfonyl)phenoxazine (PSB-12062) showed lower potency, but was more water-soluble. Interestingly, it has a similar potency in all three species: human, rat and mouse P2X4 receptors with IC₅₀ values of 1.38, 0.928 and 1.76 μ M, respectively. PSB-12062 showed at least a 35-fold selectivity toward P2X4 versus P2X1, P2X2, P2X3, and P2X7 receptors.⁷²

Introduction

More recently, a newly developed series of carbamazepine derivatives was synthesized by Tian *et al.* and the compounds were evaluated as potential P2X4 receptor antagonists. *N,N*-Diisopropyl-5*H*-dibenz[*b,f*]azepine-5-carboxamide was found to be the most potent compound among this series on the human P2X4 receptor with an IC₅₀ value of 3.44 μM, but with lower potency on rat and mouse P2X4 receptors. The compound showed to be fairly selective towards human P2X2 and P2X7 receptors, but no selectivity versus P2X1 and P2X3 receptors was observed.⁷³

In 2015, Ase *et al.* published a new P2X4 receptor-selective phenylurea derived antagonist 1-(2,6-dibromo-4-isopropyl-phenyl)-3-(3-pyridyl)urea (BX430). The compound was identified through an high-throughput screening (HTS) assay and exhibited a non-competitive allosteric mechanism of P2X4 inhibition. BX430 potently inhibited the human P2X4 receptor with an IC₅₀ value of 0.54 μM and effectively antagonized the zebrafish P2X4 receptor but showed little or no effect on the rat and mouse P2X4 orthologues. BX430 is selective for the human P2X4 receptor being ≥ 10-fold more potent than at P2X1, P2X2, P2X3 and 100-fold more potent than P2X7 receptors.⁷⁴

Another successful novel and selective P2X4 antagonist is NP-1815-PX, (5-[3-(5-thioxo-4*H*-[1,2,4]oxadiazol-3-yl)phenyl]-1*H*-naphtho[1,2-*b*][1,4]diazepine-2,4(3*H*,5*H*)-dione) which has been identified as a potent inhibitor of the human P2X4 receptor with an IC₅₀ of 0.26 μM. NP-1815-PX has a high selectivity for the P2X4 receptor compared to other P2XR subtypes. Administration of intrathecal dose of NP-1815-PX produced an antiallodynic effect in a mouse chronic pain model induced by herpes virus without affecting acute nociceptive pain sensitivity.⁷⁵ All the structures of the pervious described compounds are presented in **Figure 1.1.17**.

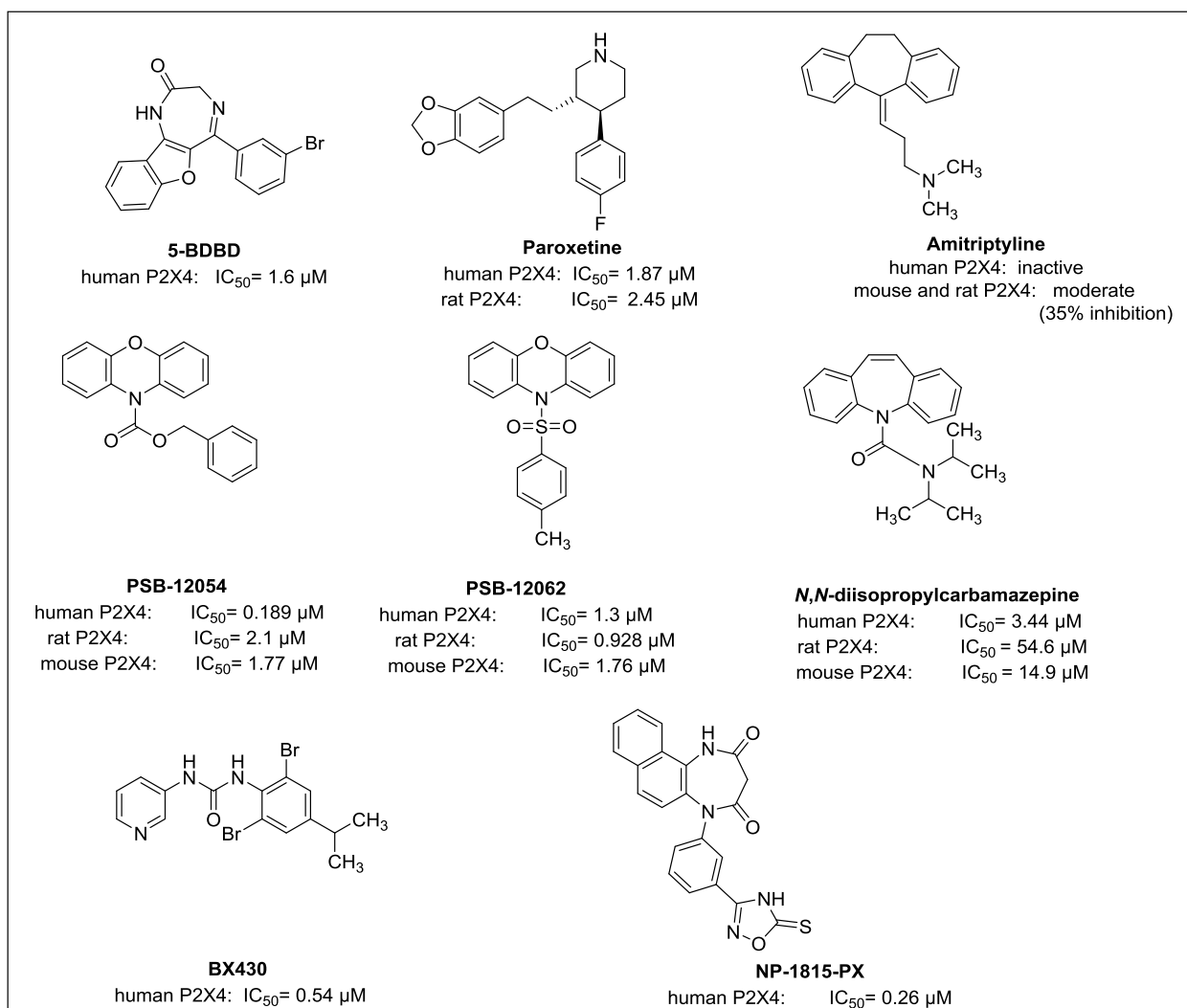


Figure 1.17. Structures and potencies of the P2X4 antagonists 5-BDBD, paroxetine, amitriptyline, PSB-12054, PSB-12062, *N,N*-diisopropylcarbamazepine, BX430, and NP-1815-PX.

1.1.5.7. The P2X5 receptor subtype

In 1996, the cDNA of P2X5 subunit was isolated from rat sympathetic ganglia, and heart.⁷⁶ Compared to the other P2X receptor subtypes, the expression of P2X5 receptors is limited. However, it is expressed in areas such as epithelial cells of the nasal mucosa and may be related to cell differentiation, especially in the skin and skeletal muscles.⁵⁶

P2X5 subunits can probably form heteromeric receptors with P2X1, P2X2, and P2X4 subunits.³⁴ P2X subunits can form hetero-multimers, which are unique from homomeric dimers. For example,

Introduction

hetero-oligomeric P2X1/5 is generated as an association of P2X1 and P2X5 subunits. The resulting hybrid channels display the pharmacological properties of P2X1, and the kinetics of P2X5 receptors. The current of P2X1/5 receptor is characterized by a slow desensitization. The agonist α,β -methylene-adenosine 5'-triphosphate (α,β -meATP) displayed with an EC₅₀ value of 1.1 μ M, and the antagonist TNP-ATP showed an IC₅₀ value of 0.064 μ M which is not observed either with P2X1 or P2X5 alone.⁷⁷

In the plasma membrane, P2X5 subunits can also interact with the P2X2 subunits forming heteromeric receptors with various stoichiometry. It is important to note that the formed P2X2/5 receptors resulted in phosphatidylserine exposure, membrane blebbing, and pore dilatation. Previously, it was thought that these features were related to the P2X7 receptor only. P2X5 subunits can also form heteromeric receptors with P2X1, P2X2, and P2X4 subunits.³⁴

It was reported by Kotnis *et al.* that most humans only express a non-functional isoform of the P2X5 receptor. The non-functional isoform arises from the human P2X5 gene having a single-nucleotide polymorphism (SNP) at the 3' splice of exon 10, which is important for the second transmembrane domain. Therefore, the physiological roles of the P2X5 receptor in humans are difficult to assess.⁷⁸

1.1.5.8. The P2X6 receptor subtype

The P2X6 receptor is expressed throughout the central nervous system (CNS). Homomeric P2X6 channels are formed only after glycosylation. They can be activated by α,β -MeATP and blocked by TNP-ATP. This receptor can easily form heteromeric channels with P2X2 and/or P2X4 and the functional properties of the new heteromer closely resemble those of the P2X2 and P2X4 receptors.⁵⁶

Among the P2X receptors, the P2X6 receptor is the only subtype found to be upregulated selectively during chronic heart failure (CHF). Based on this finding, novel drugs targeting the P2X6 receptor might be used for treating chronic heart failure through the effect on the tumor necrosis factor alpha (TNF α).⁷⁹

1.1.5.9. The P2X7 receptor subtype

The P2X7 receptor (P2X7R) formerly known as P2_Z⁸⁰ has an important role in inflammation and immunity as indicated by recent studies of P2X7R-knockout (KO) mice.⁸¹ The P2X7R has a potential role in regulating survival of cells depending on the extracellular concentrations of ATP. The P2X7R is highly expressed in immune cells such as macrophages and monocytes. It is involved in the potentiation of the release of pro-inflammatory cytokines including IL-1 β and IL-18 from macrophages and microglia.⁸² P2X7R might be drug targets for the treatment of a number of diseases including pain, neurodegeneration, and inflammatory diseases such as rheumatoid arthritis and osteoarthritis.⁸³

1.1.5.10. P2X7 receptor antagonists

Many P2X7 antagonists have been identified with a steady increase since the first patent appeared in 1999. However, no P2X7 antagonist has reached the market yet, even if two compounds made it to clinical trials. The AstraZeneca compound AZD9056, was in phase II clinical trials for several inflammatory indications i.e. rheumatoid arthritis, osteoarthritis, chronic obstructive pulmonary disease, and inflammatory bowel disease. Another clinical trial has been performed by Pfizer. Compound CE-224535 that was indicated for rheumatoid arthritis with twice 500 mg as a daily dose. Due to the lack of efficacy this compound was terminated for osteoarthritic knee pain.⁸⁴ Unfortunately, both compounds failed to give a clear benefits for the patients.³⁷

1-[*N,O*-Bis(5-isoquinolinesulfonyl)-*N*-methyl-L-tyrosyl]-4-phenylpiperazine, an isoquinolinesulfonamide, KN-62, which is a selective antagonist of Ca²⁺/calmodulin-dependent protein kinase II (CaMKII), was the first small molecule to be identified as a P2X7 antagonist. The compound antagonizes the human P2X7R with an IC₅₀ value of 0.100 μ M, while no inhibitory activity on the rat P2X7R was observed.^{85,86} Another potent, selective antagonist is A-740003, which competitively antagonizes P2X7 receptor with IC₅₀ values of 0.018 μ M on rat P2X7 and 0.040 μ M on human P2X7 receptors. A-740003 is selective for P2X7 over different subtypes of P2X and P2Y receptors up to concentrations of 100 μ M. The compound showed notable reduction of nociception in animal models.⁸⁷ Several benzamide derivatives were reported which showed a significant

Introduction

biological effect as inhibitors of the P2X7 receptor with promising results in brain penetration.⁸⁸ The previously stated antagonists of the P2X7 receptor are presented in **Figure 1.18**.

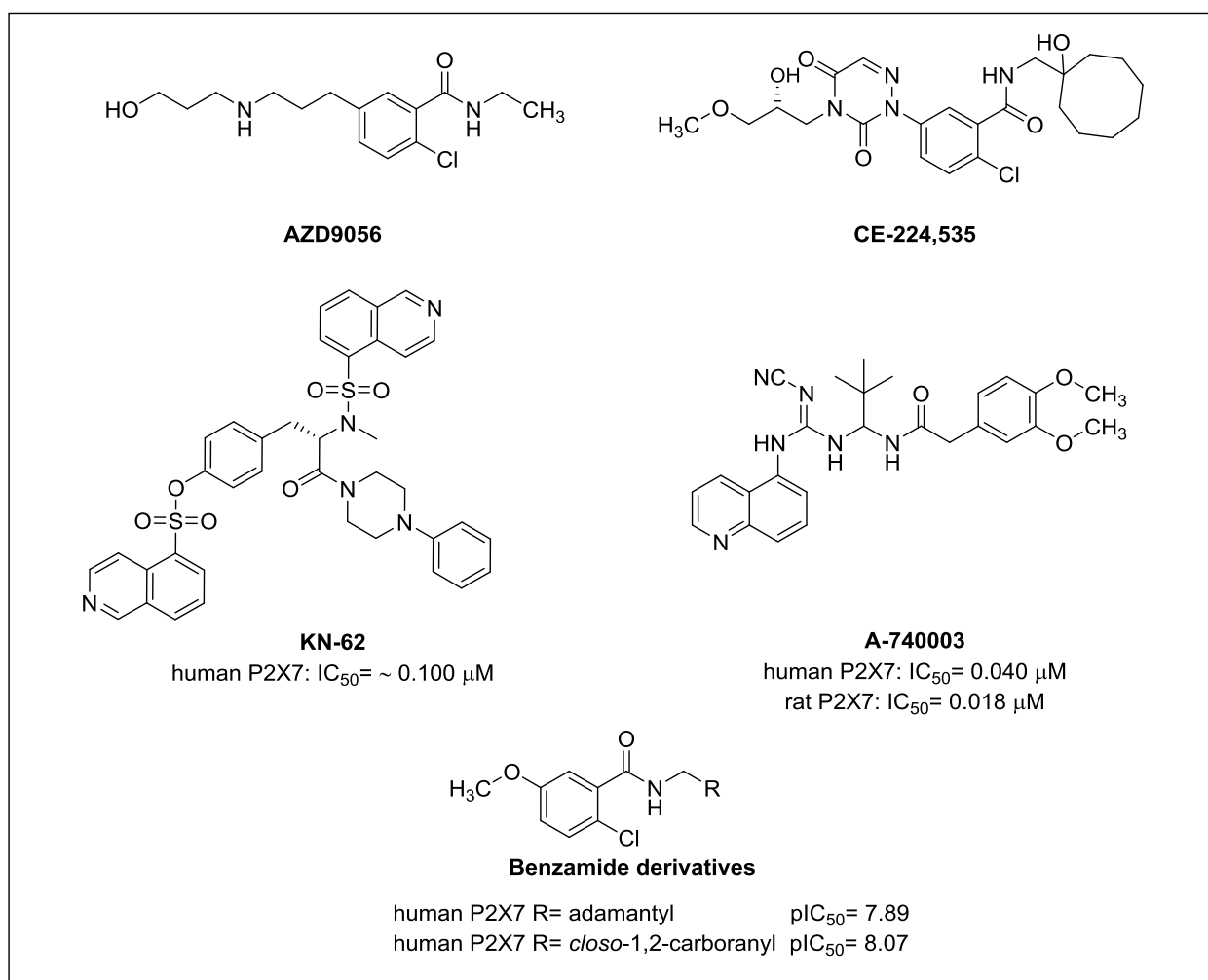


Figure 1.18. Structures of the P2X7 receptor antagonists AZDF9056, CE-224,535, KN-62, A-740003, and two benzamide derivatives.

1.1.6. The P2X3 receptor subtype

In 1995, rat dorsal root ganglion (DRG) sensory neurons were used for cloning the cDNA of the P2X3 receptor.⁸⁹ The P2X3 receptor exists as a homotrimeric channel, but it can also form heteromeric trimers consisting two P2X3 and one P2X2 unit resulting in the P2X2/3 receptor.^{90,91} Among all P2X receptor subtypes, P2X3 is the only receptor which is expressed in a subset of sensory neurons.

1.1.6.1. Distribution of P2X3 receptors

The P2X3 subunit shows a restricted distribution in a subset of sensory neurons including the trigeminal, dorsal root, and inferior ganglion of the vagus nerve. Recently, it was demonstrated to be also expressed in nucleus tractus solitarius and other brain regions. However, the P2X3 receptor is absent from smooth muscle, sympathetic, and enteric neurons.⁴²

Due to the restricted tissue distribution in small to medium C- and A δ -fiber primary afferent neurons, P2X3 receptors have been suggested to be involved in pain-sensing.⁹² Indeed, animal studies revealed that P2X3 knockout animals or P2X3 siRNA- or antisense-treated animals have greatly diminished pain-related behaviors in both inflammatory and neuropathic pain models.⁹³ Moreover, administration of the P2X3 receptor-selective agonist α,β -methylene ATP to the hind paws of rats resulted in exacerbating nociceptive behaviors.⁹⁴

The homomeric P2X3 receptor showed rapid desensitization property (<100 ms) upon prolonged exposure to the physiological agonist ATP, followed by a long regeneration period. On the contrary, the heteromeric P2X2/3 receptor shares the pharmacological profile (α,β -meATP sensitivity) of the homomeric P2X3 receptor and the slow desensitization kinetics of the P2X2 homomer and potentially represents a naturally occurring form of the receptor that is involved in pain perception.^{95,96}

1.1.6.2. Screening of P2X3 receptors

The fast desensitizing of the P2X3 receptor makes the screening by a calcium imaging assay very difficult. The exchange of amino acids, namely P-19, V-21, and I-22, which are located in the cytoplasmic loop before the transmembrane domain for the corresponding amino acids of the P2X2 receptor slowed the desensitization process. Also, it was discovered that replacement of the amino acid serine in position 15 of the native rat P2X3 by valine or another hydrophobic residue showed the strongest effect to slow down the P2X3 receptor desensitization to the level of that of the P2X2 receptor. It was found that the S¹⁵V-rP2X3 mutant allowed the screening of compounds since the signal became detectable.⁹⁷ In the human P2X3 receptor using the same mutation could also result in

Introduction

a reliable alternative for its characterization. Recently, the stable transfection the corresponding construct into 1321N1 astrocytoma cells was successfully achieved by Dr. Aliaa Abdelrahman.

1.1.6.3. P2X3 receptor antagonists

One of the common antagonists is 2',3'-*O*-(2,4,6-trinitrophenyl)adenosine 5'-triphosphate (TNP-ATP), an ATP-derivative. It was the only reported dual P2X3/P2X2/3 antagonist but with limitation of its use to *in vitro* experiments due to its nucleotide nature.⁹⁰

A number of P2X3R antagonists have been developed which are potent, selective and drug-like. These were described in few publications and in several patents. A potent and selective P2X3 P2X2/3R antagonist is the suramin-derived 4,4',4'',4'''-(carbonylbis-(imino-5,1,3- benzenetriylbis-(carbonylimino)))tetrakisbenzenesulfonic acid (NF110), which inhibits P2X3 receptors with low nanomolar potency (**Figure 1.19**).⁹⁸

Homomeric P2X3 and heteromeric P2X2/3 receptors are predominantly present in the pathways of pain signal transmission peripherally and centrally. The first step for the validation of these receptors as chronic pain targets (inflammatory and neuropathic) was the discovery of A-317491, which considered the first non-nucleotide antagonist. It was used to demonstrate the reduction of hyperalgesia and allodynia in a chronic pain animal model.^{99,100}

A-31749 was synthesized at Abbott Laboratories, and has a high affinity with K_i values in the low nanomolar range at human and rat P2X3 and P2X2/3 receptors. Moreover, it is very selective versus other P2 receptors, neurotransmitter receptors, ion channels, and enzymes ($IC_{50} > 10 \mu M$). Furthermore, it binds to the ATP site and is considered as a competitive antagonist like the nucleotide-based antagonist TNP-ATP, which showed a high affinity for P2X1 receptors as well but, more than 100-fold selectivity for P2X3 and P2X2/3 receptors when it was compared to other P2X receptor subtypes. The (*S*)-configured derivative was potent in a chronic pain animal model, while the (*R*)-enantiomer designated A-317344 was completely inactive.^{100,101}

Introduction

MK3901,^{102,103} a compound which is a substituted arylamide derivative (SAAs) with a potency in the low nanomolar range, is a selective CNS-penetrant P2X3 antagonist. MK3901 showed promising results in models of chronic inflammatory and neuropathic pain (see **Figure 1.19**).

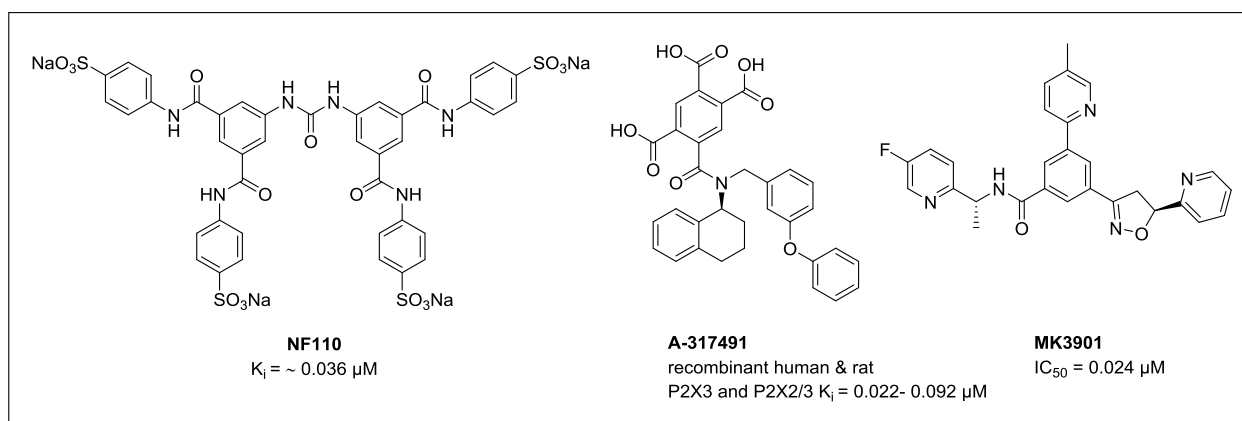
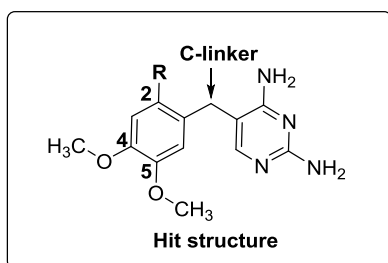


Figure 1.19. Structures and inhibitory potencies of the P2X3 antagonists NF110, A-317491 and MK-3901.

In an effort to discover novel P2X3 or P2X2/3 receptor antagonists with suitable physicochemical and pharmacokinetic properties required for a viable drug candidate, the Roche compound library was subjected to high-throughput screening (HTS), and many hits were obtained. AF-001, a confirmed HTS hit compound with a diaminopyrimidine structure, which had been developed at Hoffmann-La-Roche (Basel) in the early 1970s to investigate the structure-activity relationships of trimethoprim, a bacterial dihydrofolate reductase (DHFR) inhibitor. AF-001, was used as a starting point for the development of P2X3 receptor antagonists. It showed an IC₅₀ value of 1.2 μM. However, the drug trimethoprim itself was completely inactive at 10 μM.¹⁰³ Structures of trimethoprim and AF-001 are shown in **Figure 1.20**.

Optimization of the diaminopyrimidine series



The optimization strategy of the hit structure focused on three main points:

(1) The small alkyl side-chain: R= propyl, *t*-butyl, or methoxy abolished the activity. However, isopropyl substitution led to RO-3 which was 10-fold more potent than AF-001. (2) The linker: reduction of the conformational flexibility by replacing the methylene bridge with an oxygen. (3) The addition of different groups at the 4- and 5- position of the aryl ring to enhance potency and metabolic stability.

The extensive chemical optimization yielded many active and promising analogues. Interestingly, AF-353 (RO-4), an iodoanisoole derivative, was obtained which is a potent and selective P2X3 antagonist with the proper pharmacokinetic profile. The combination of high selectivity for P2X3 and P2X2/3, antagonistic potency, and adequate pharmacokinetic properties made this compound an excellent tool for in vivo studies in animal models. AF-353 (RO-4), is a small drug-like molecule for the potential treatment of pain-related disorders.¹⁰⁴ Another potent and polar antagonist AF-906 (RO-51), which showed an inhibitory potency in the low nanomolar range at both human P2X3 and P2X2/3 receptors (see **Figure 1.20**).³⁷

Introduction

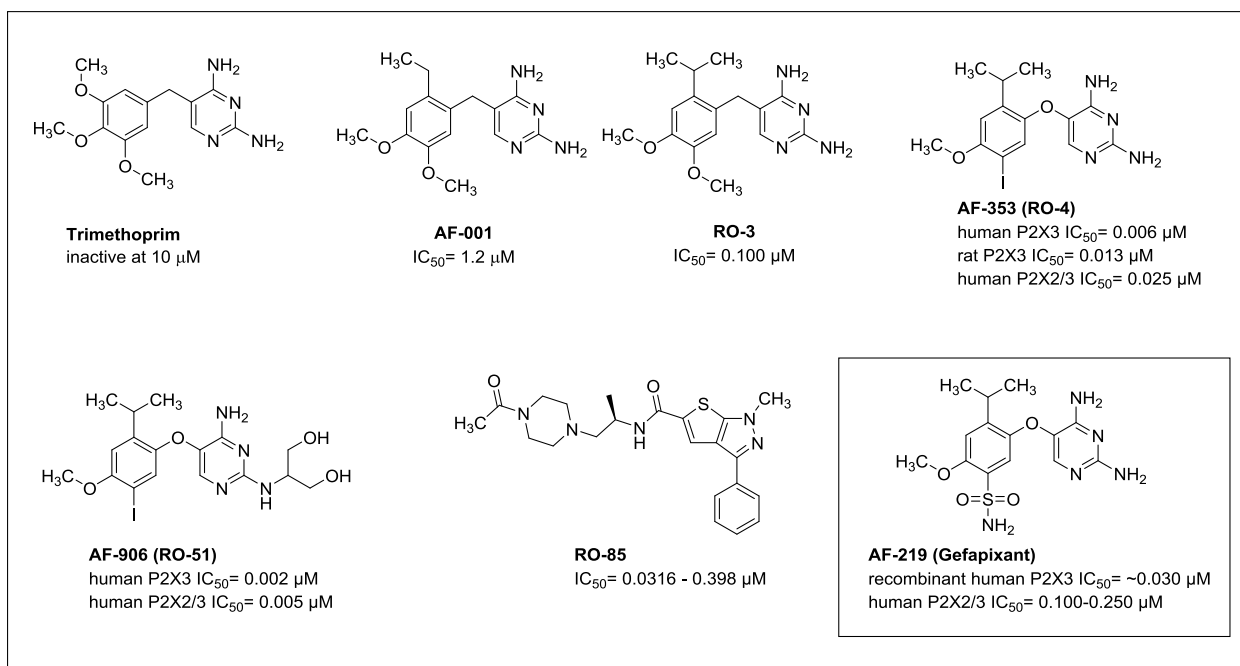


Figure 1.20. Structures and inhibitory potencies of P2X3 antagonists, trimethoprim, AF-001,RO-3, RO-4, RO-51, RO-85 and AF-219 (Gefapixant).

RO-85, 1-methyl-3-phenyl-1*H*-thieno[2,3-*c*]pyrazole-5-carboxylic acid [(*R*)-2-(4-acetyl-piperazin-1-yl)-1-methyl-ethyl]amide, is a thienopyrazole derivative. RO-85 was identified as a potent antagonist on rat and human P2X3 receptors (**Figure 1.20**).¹⁰⁵ RO-85 has a good selectivity profile for the P2X3 receptor, not only over heteromeric P2X2/3 receptors but also versus the other P2X members.¹⁰⁶ RO-85 possesses acceptable pharmacokinetic features including metabolic stability, plasma protein binding, and inhibition of CYP450 isozymes. The compound showed good oral bioavailability when administered orally to rats. The combination of potency, selectivity and pharmacokinetic profile may allow exploration of its therapeutic potential as P2X3 receptor antagonist in *in vivo* studies.¹⁰⁵

AF-219, an aryloxy-diaminopyrimidine, is an orally active small molecule antagonist of the P2X3 receptor with an IC_{50} of $\sim 0.030 \mu\text{M}$ on recombinant human P2X3 homotrimers and $0.100-0.250 \mu\text{M}$ on human P2X2/3 heterotrimeric receptors. It inhibits P2X3 receptors through a non-competitive mechanism. AF-219, showed excellent pharmacokinetic and pharmacodynamic properties and has recently been evaluated in clinical phase II studies for the treatment of osteoarthritic joint pain,

Introduction

interstitial cystitis/bladder pain syndrome, and asthma/chronic cough. A study in patients with chronic refractory cough has been completed and was positive.¹⁰⁷ In 2015, AF-219 was reported by Abdulqawi et al. as a promising new class of antitussive drugs which supports the role of P2X3 receptors in mediation of cough neuronal hypersensitivity (**Figure 1.20**).¹⁰⁸

The physiological heptapeptide spinorphin (**Figure 1.21**), is a highly potent non-competitive antagonist of the human P2X3 receptor expressed in *Xenopus* oocytes. It was reported as the first peptide which selectively antagonizes the P2X3 receptor with an IC₅₀ value of 8.3 pM. The compound showed selectivity for the human P2X3 receptor versus mouse P2X1 and human P2X7 receptors. Honda *et al.* demonstrated antinociceptive and anti-inflammatory activity for spinorphin. However, there are no published data till now on its drug-like features.^{109,110}

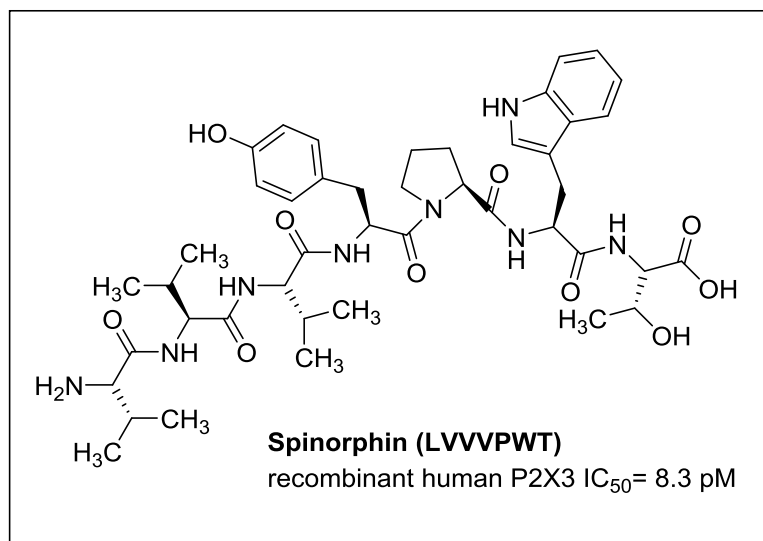


Figure 1.21. Structure of spinorphin.

Two active series of allosteric antagonists derived from either 4-oxo-quinazoline central ring or thia-triaza-tricyclic core were discovered in the HTS of compounds collection obtained from Gedeon Richter Plc, Budapest-Hungary. Interestingly, compound **I** with 4-oxo-quinazoline central ring showed an IC₅₀ value of 0.005 μM which is considered as one of the most potent P2X3 receptor antagonist has been recently published in the literature till now.¹¹¹ Among the reported compounds bearing thia-triaza-tricyclic core, (*S*)-3-(2,5-dimethoxyphenethyl)-*N,N*-dimethyl-4-oxo-3,4,5,6,7,8-hexahydrobenzo[4,5]thieno[2,3-*d*]pyrimidine-7-carboxamide (**II**) was potentially suggested as a

Introduction

candidate for *in vivo* testing. The chiral pure (-) (*S*) enantiomer **IIa**, showed markedly more activity, greater than 30 times in comparison to its stereo-isomer (+) (*R*) **IIb** (IC_{50} = 0.021 μ M, 0.668 μ M, respectively).¹¹²

A novel class of compounds related to pyrrolinone nucleus has been developed and identified as P2X3 receptor antagonists. This class was discovered by Japanese group through a HTS and many potent derivatives were obtained. Isoxazole derivative (**III**) has been described as a potent antagonist with IC_{50} = 0.025 μ M. It is highly selective, no inhibitory effect over 41 receptors and 17 enzymes tested at 10 μ M (data not shown). In addition, the analgesic activity of the compound was evaluated (ED_{50} = 2.6 mg/kg) suggesting that it may be useful as analgesic drug (**Figure 1.22**).¹¹³

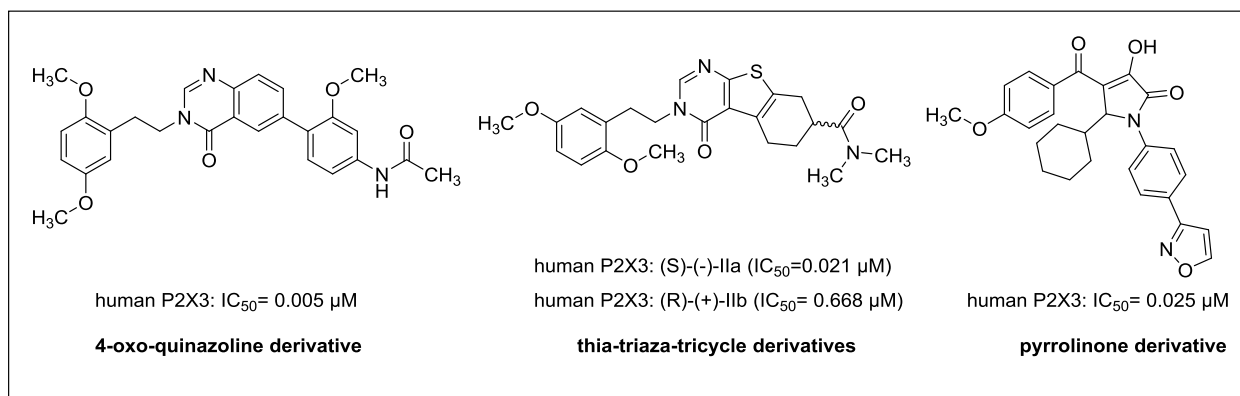


Figure 1.22. Structures and inhibitory potencies of 4-oxo-quinazoline derivative, thia-triaza-tricyclic derivatives, and pyrrolinone derivative.

1.1.7. P2X receptors and pain

Pain is as an unpleasant sensory and emotional experience evoked by noxious stimuli, inflammation, or tissue damage.¹¹⁴ Pain can be classed into nociceptive (physiological) pain, inflammatory pain and neuropathic pain (**Figure 1.23**).¹¹⁵ Nociceptive pain is defined as a response which has developed normally to a noxious stimulus with negligible tissue injury in case of low-intensity, in which medical care is not needed. Noxious stimulus with high-intensity, such as thermal, mechanical or chemical stimulation, lead to activation of specialized sensory neurons mediated by high-threshold unmyelinated (C and A δ) afferents that transfer signals into nociceptive pathways of the CNS to produce pain.¹¹⁶

Introduction

Inflammatory pain is defined as a response to injured tissues and/or inflammatory conditions such as surgery, infection and burns or diseases like arthritis. Primary hyperalgesia is an exaggerated pain which is produced at the site of injury as a result of low-intensity stimulus through activation of high-threshold (C and $A\delta$) afferents (peripheral nociceptors). Allodynia, can be generated by either central sensitization of the dorsal horn of the spinal cord with low-threshold ($A\beta$) afferents or prolonged responses of high-threshold (C and $A\delta$) afferents produced by mild painful stimulus with high-intensity.^{117,115}

Neuropathic pain is a major health problem that affects the quality of life, and it is very difficult to treat.^{118,119} Injury of the nervous system, trauma, diabetes or infection may lead to painful states even with light touching.¹²⁰ The generation of this kind of pain involves both the CNS and the peripheral nervous system (PNS).¹³⁹ It is characterized by an unusual response to stimuli (noxious and non-noxious).¹¹⁵

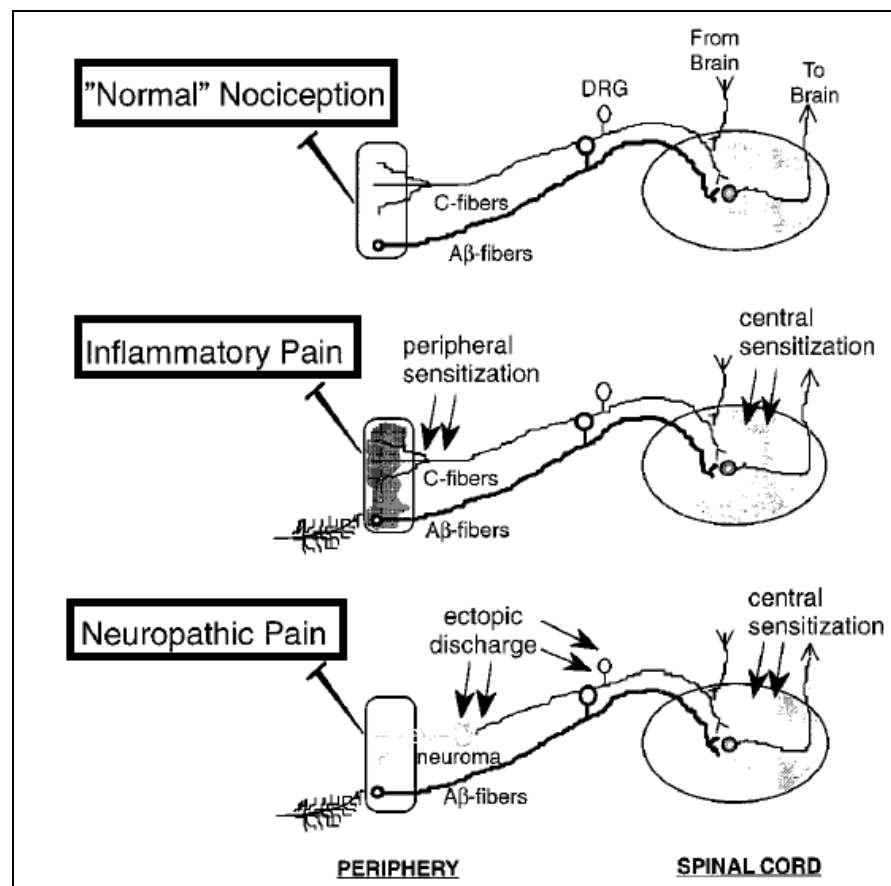


Figure 1.23. Types of pain and sensory processing after peripheral nerve injury.¹¹⁵

Introduction

ATP acting via P2 receptors plays an important role in the changing (modulation or altering) of the sensitivity of nociceptive pain which follows the injury of tissues. Several P2X receptor subtypes, especially P2X3, P2X2/3, P2X4, and P2X7 play a crucial role in pain sensation/transmission as well as the development of neuropathic pain.^{121,122} ATP acting at different purinoceptors directly on neurons in the case of P2X3, P2X2/3 receptors or indirectly through interactions of neural-glia cells in the case of P2X4 and P2X7 receptors is involved.¹²¹

Medicines available for the management of pain include¹²³

- (1) Opioids such as (morphine and fentanyl),
- (2) nonsteroidal anti-inflammatory drugs (NSAIDs) such as aspirin, ibuprofen, celecoxib and rofecoxib.
- (3) Analgesic adjuvant agents such as tricyclic antidepressants (paroxetine and amitriptyline), local anesthetics (e.g. lidocaine), and certain anticonvulsant agents (carbamazepine).

All of these classes of compounds have therapeutic usefulness in different states of pain. However, they have many disadvantages in the clinical use.

The drawbacks of the compounds clinically used for pain management are listed below.

- (1) Tolerance, dependence, respiratory depression, and sedation are major problems with opioids.
- (2) Gastrointestinal disturbances, increasing of the bleeding tendency and low efficacy in severe pain are major drawbacks for NSAIDs.
- (3) CNS and cardiovascular side effects are major problems for analgesic adjuvant agents.

In the present study we have focused on two different classes of compounds that have been identified as P2X receptor antagonists in a screening approach.

1.2. Anthraquinone (AQ) derivatives

Anthraquinones (AQs) also referred to as anthracenediones, are related to the quinone family which is widely distributed in nature as constituents of plants (aloe latex, rhubarb, and senna), microorganisms (fungi and lichens), some insects, and several marine species.¹²⁴ At least 79 AQ

Introduction

derivatives have been demonstrated to be occurring naturally such as emodin, cascarin, physcion, and rhein.¹²⁵

They are polycyclic aromatic compounds, and the parent compound is anthracene, which is formed of three fused phenyl rings (**Figure 1.24**). The parent structure of 9,10-anthracenedione, also called 9,10-dioxoanthracene is made up of tricyclic ring systems in which the central one contains two opposing carbonyl groups at positions 9 and 10.¹²⁶

AQ was synthesized via oxidation of anthracene either with chromic acid or nitric acid (Laurent 1840, and Fritzsche 1868, respectively). However, the compound was of little interest until Graebe and Liebermann in 1868 prepared alizarin (**Figure 1.24**) from anthracene and elucidated the relation between anthracene, anthraquinone, and alizarin. From that time till today, the study of AQ chemistry started to catch the attention of scientists to develop new derivatives related to the AQ scaffold with different pharmacological properties.^{127,128,129,130}

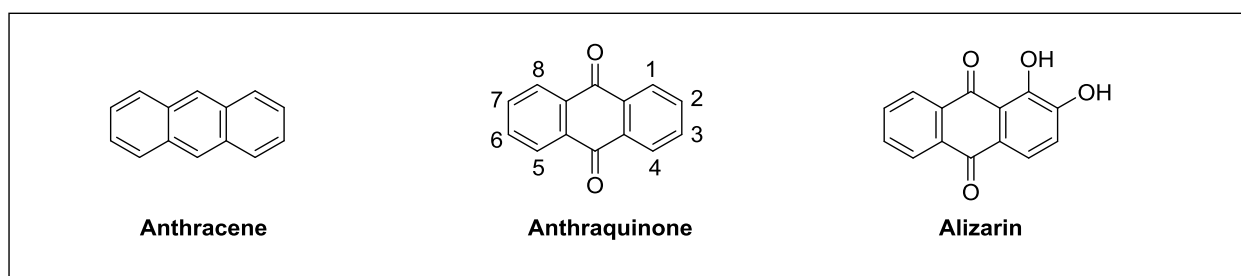


Figure 1.24. Chemical structures of anthracene, anthraquinone, and alizarin.

1.2.1. Anthraquinone derivatives and their applications

AQs and their derivatives constitute a large class with around 700 molecules that were described. Nowadays, their chemical diversity and biological activities are of great interest for industries in many fields such as dyes and pharmaceuticals.¹³¹ AQs and their derivatives are incorporated in a variety of natural and synthetic products which received a great deal of attention.¹³²

Besides their extensive use since decades for the dyeing of natural and synthetic textiles^{133,134}, AQs are of importance for various other applications. They are used in imaging devices, and some AQs are approved for use as colorants in cosmetics, and foods.^{126,135,136} A number of natural and synthetic

Introduction

AQs have shown a wide range of pharmacological activities including antitumor¹³⁷, antiviral¹³⁸, antifungal¹³⁹, anti-inflammatory¹⁴⁰, laxative^{141,142}, antiplatelet^{143,144,145}, and neuroprotective effects.¹⁴⁶ Several AQ drugs are on the market; moreover AQs represent important pharmacological and biochemical tool compounds.

Anthraquinones that are found in plants such as senna, frangula, aloe, cascara, and rhubarb, have been known for their laxative properties for a long time. They have been used in the treatment of constipation, which affects around 14% of the adult population worldwide.¹⁴⁷ Due to side effects observed *in vitro* and in animal studies, the anthranoid laxatives are not recommended for long-term use anymore. However, the use of these anthranoid laxatives for short time is generally safe.¹⁴²

The anticancer activity of AQs was discovered in the mid-1950s.¹⁴⁸ Emodin (1,3,8-trihydroxy-6-methylantraquinone) is a naturally occurring AQ derivative which is distributed widely in Chinese herbs such as *Rheum palmatum*, *Polygonum cuspidatum* and *Polygonum multiflorum*. It has been known and used for more than 2000 years in Chinese medicine and is still used in some herbal preparations. Emodin has a wide range of pharmacological applications such as hepatoprotective, anti-inflammatory, antioxidant and antimicrobial activities. However, there is a limitation to its use, not only does it possess a poor oral bioavailability in rat, but it also triggers hepatotoxicity, kidney toxicity and reproductive toxicity resulting from prolonged use in high doses.¹⁴⁹

Emodin demonstrated anti-cancer activity through inhibition of tumor cell-growth, proliferation, induction of apoptosis, and prevention of metastasis. Many derivatives related to emodin were synthesized and evaluated for their cytotoxic and cytostatic activity; a lot of them were stronger than emodin itself. Among this set of compounds, 4-(*N*-cyclohexylamino)emodin showed promising results, which revealed it as a potential anti-tumor drug (**Figure 1.25**).¹⁵⁰

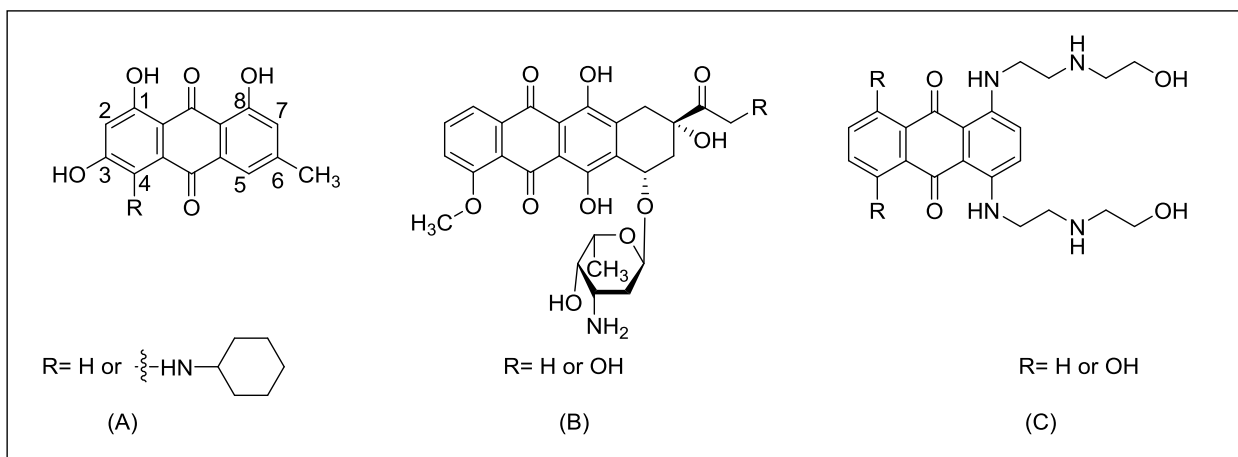


Figure 1.25. (A) The chemical structure of emodine (R= H) and 4-(*N*-cyclohexylamino)emodin (R = *n*-cyclohexylamino). (B) Chemical structure of the anthracyclines daunorubicin (R= H) and doxorubicin (R= OH). (C) Chemical structure of the anthracenediones ametantrone (R= H) and mitoxantrone (R= OH).¹⁵⁰

Daunomycin was originally discovered as a secondary metabolite from *Streptomyces peucetius* in an Italian soil sample. Daunomycin, an anthracycline antibiotic was isolated as a glycoside, formed by an anthracenedione-containing chromophore, which is typically linked to an aminosugar by a glycosidic bond. At the same time, an identical compound was characterized by a French group and named rubidomycin, now termed daunorubicin.^{151,152,153} Daunorubicin was demonstrated to have potent antitumor activity in humans.¹⁵⁴ Daunorubicin (Daunoblastin[®]) and mitoxantrone (Onkotrone[®]), are structurally related. They have strong cytostatic activity against tumor-cell growth via inhibition of topoisomerase II or intercalation into DNA, and DNA strand scission via free radical generation.¹⁵⁵

Ametantrone was reported by Cheng *et al.* It showed a good activity against P-388 leukemia in mice.¹⁵³ Mitoxantrone, an anti-neoplastic agent was modified from the parent 1,4-dehydroxy analogue, ametantrone, and it was proposed to modulate the therapeutic profile of anthracyclines.¹⁵⁶ Mitoxantrone has been applied in the treatment of lymphoma, leukemia, prostate and breast cancer. In 1987, the drug was approved by the food and drug administration (FDA) for the treatment of acute myeloid leukemia (AML). It inhibits the activity of topoisomerase II.¹⁵³ In 1996, it was given

Introduction

FDA approval for symptomatic hormone-refractory prostate cancer treatment.¹⁵⁷ After 4 years, it was also approved for the treatment of multiple sclerosis¹⁵⁸ (**Figure 1.25**).

Beside emodine, the other major rhubarb anthraquinone is rhein (**Figure 1.26**), which possesses protective effects on acute kidney injury (AKI). Rhein can effectively inhibit the progression of endotoxemia-linked AKI with a mechanism akin to the one of its anti-inflammatory action, through suppressing the activity of pro-inflammatory cytokines.¹⁵⁹

Diacerein (**Figure 1.26**), also known as Diacetylrhein, is a prodrug which is formally derived from rhein by acetylation of two hydroxyl groups. Diacerein, is a commercially available drug, used for the treatment of joint diseases such as osteoarthritis of the hips. Its mechanism is different from the ones of the existing NSAIDs.¹⁶⁰ Interestingly, diacerein prevented autoimmune diabetes development in a model of nonobese diabetic mice through the suppression of leukocytes' chemotactic activity to the pancreatic islets.¹²⁵

Danthron (Dantron[®]), also referred to as chrysazin, is a derivative which was developed from anthraquinone (**Figure 1.26**). It has been prescribed as a stimulant laxative in some countries. It was approved for the U.S. market as a laxative until 1999, since then the U.S. FDA ordered the withdrawal of products containing danthron because of the risk of carcinogenesis.¹⁶¹ However, in the United Kingdom, the drug is still allowed but only for the management of constipation in patients with advanced cancer.¹⁶²

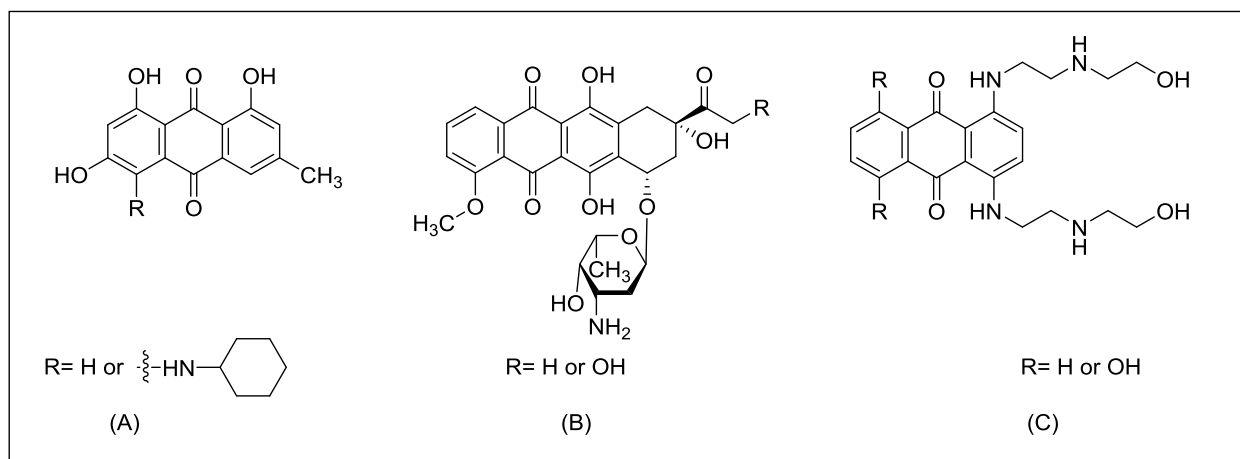


Figure 1.26. Structures of rhein, diacerein, and danthron.

Introduction

Reactive Blue-2 (RB-2) (**Figure 1.27**), a textile dye, which consists of the chromophore anthraquinone linked to mono-chlorotriazine ring.¹⁶³ Previously, such dyes were commonly used in the textile industry. Later they became important as ligands in the purification of enzymes and biopolymers. Since the 1970s these dyes have also been utilized as tools in drug research due to their antagonistic properties at P2-receptors.¹⁶⁴

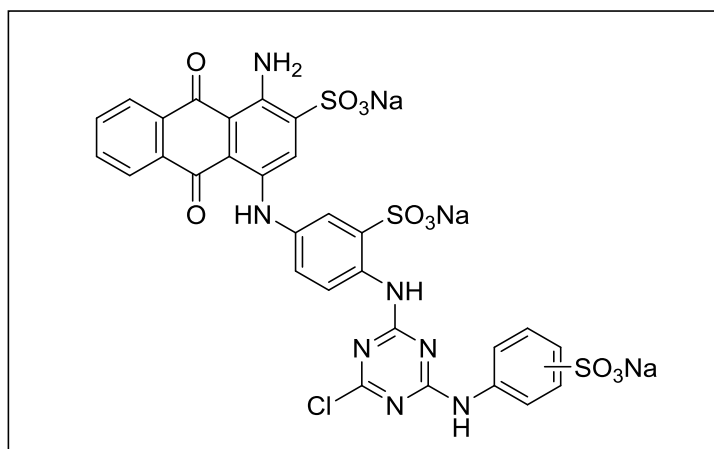


Figure 1.27. Chemical structure of Reactive Blue-2 (RB-2), a mixture of the *meta*- and *para*-sulfonate (35:65).

Due to their importance as drug molecules, a library of AQ derivatives, structurally related to RB-2 has been synthesized and their potencies were tested at a variety of purinergic targets, all of which are characterized by a nucleotide binding site.^{165,166,167,168,64,169,170} Many of the synthesized AQ derivatives bearing a sulfonate group at the 2-position. Since their synthesis starts with the sodium salt of bromaminic acid. However, the effects of other substituents in the AQ 2-position are largely unknown due to the difficulties in preparing the desired compounds. For instance, the method described by Hagen *et al.* for the introduction of a carboxylate group via oxidation of 2-methylantraquinone required harsh reaction conditions using nitric acid in the presence of nitrobenzene and elevated temperatures of the reaction mixture to 200 °C.¹⁷¹ Therefore, the number of anthraquinone derivatives bearing different substituents at the 2-position are small and only very few of them were described in few patents.¹⁷²

Introduction

In our group, a series of anthraquinone derivatives, structurally related to reactive blue 2, was previously synthesized and tested for their antagonistic activity on P2Y₁₂ receptors. Of those derivatives PSB-0739 and PSB-0702 (**Figure 1.28**) were the most active ones with K_i values of 0.025 μM and 0.021 μM respectively.¹⁴⁵ PSB-0801 bearing a 2-methyl group did not affect the response to 2-methylthio-ADP, which was used to activate the P2Y₁₂ receptor.¹⁷³ The two active compounds represent promising lead structures for the development of new antiplatelet drugs.¹⁴⁵

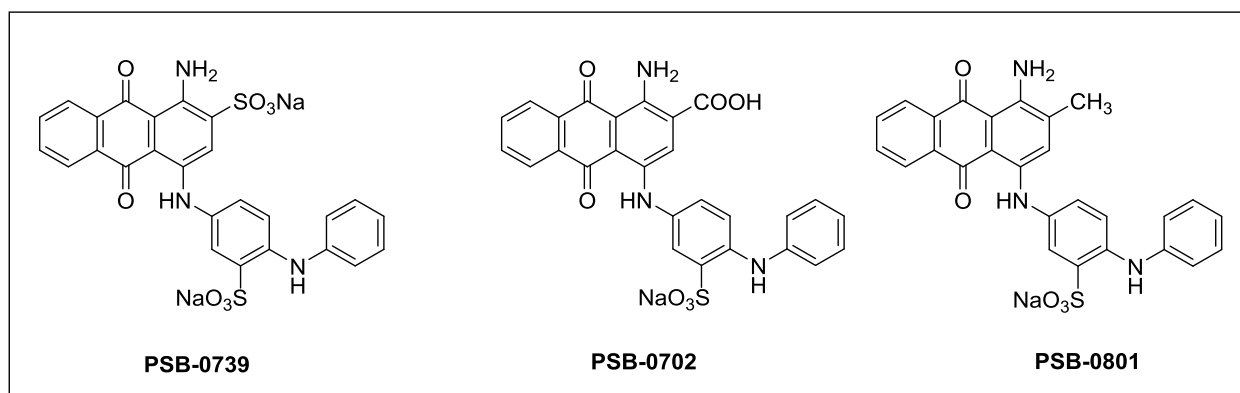


Figure 1.28. Structures anthraquinone derivatives: PSB-0739, PSB-0702, and PSB-0801.

1.3. Microwave chemistry

Chemistry using microwaves has received considerable attention and is very useful for thermal reactions.¹⁷⁴ The synthesis of various organic compounds was successfully realized using microwave irradiation as non-traditional energy source. This concept has become widely accepted as shown by increasing numbers of publications. Microwaves are between the radio and infrared frequencies of the electromagnetic spectrum. Because the radiation wavelength is large, no ionization or bond breaking is observed.¹⁷⁵ In contrast to conventional heating methods, microwave irradiation produces both thermal effects and selective absorption by polar substances.¹⁷⁶

1.3.1. Microwave-assisted organic synthesis (MAOS)

Microwave-assisted organic synthesis can be used as an alternative energy source for many reactions instead of classical heating methods. The reactions performed under microwave conditions show significant enhancement in their rate, and also high chemical yields. Medicinal chemistry

Introduction

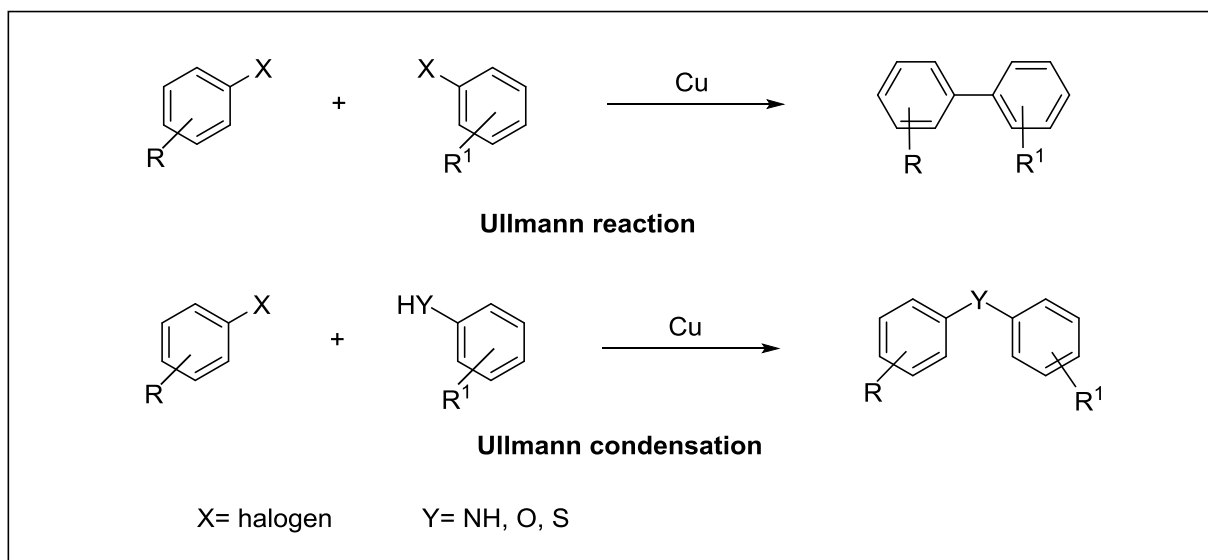
communities apply MAOS especially in cases where speed of the reactions is of considerable value.¹⁷⁷

The advantages of microwave-assisted organic synthesis (MAOS) include:^{178,176}

- (1) Mild conditions which allow comprehensive control of the reactions.
- (2) Reproducibility: high reaction yields can be easily obtained.
- (3) Effectiveness: reaction times become shorter.
- (4) Useful for reactions which cannot be achieved using conventional heating, for example the synthesis of drugs with short half-life (for example, isotopically labelled ones).
- (5) Microwave effect might help to keep the efficacy of the catalysts.
- (6) Assistance in building up combinatorial libraries and rapid parallel synthesis as well.
- (7) Safety concerns: microwave can be used safely (suitable engineering achievable).
- (8) Automatic emergency control can be applied if necessary.

1.4. Ullmann reaction

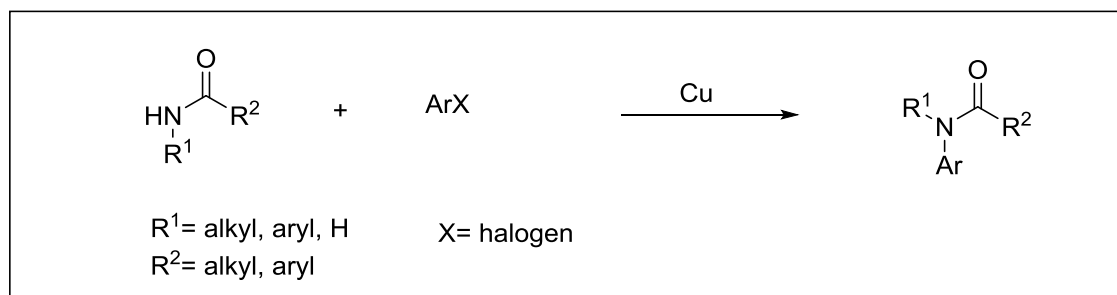
The Ullmann reaction refers to the synthesis of diaryls through condensation of aryl halides and copper.¹⁷⁹ While, the term 'Ullmann condensation reaction' describes the synthesis of aryl -amine, -ether or -thioether from the reaction between an aryl halide with an amine, phenol or thiophenol, respectively.¹⁸⁰ These reactions are mediated by copper (stoichiometric or catalytic). The previous nomenclature is now commonly accepted which depends on the chemical nature of nucleophilic entity (**Scheme 1.1**).¹⁸¹



Scheme 1.1. Schematic representation of Ullmann reaction and Ullmann condensation.

1.5. Goldberg condensation reaction

The synthesis of a new C(aryl)-N bond through condensation between amides and aryl halides catalyzed by copper (**Scheme 1.2**).¹⁸²



Scheme 1.2. Schematic representation of Goldberg condensation reaction.

Ullmann-type reactions usually require harsh conditions, e.g. high reaction temperature, long reaction time and high concentrations of the catalysts were needed. However, modification to conventional Ullmann reaction has recently applied aiming to overcome these drawbacks.¹⁸³ Modified Ullmann reactions are characterized by milder reaction conditions, which facilitate the use of copper-catalyzed reactions.¹⁸¹

1.6. Triphenylmethanes

Triarylmethanes (TRAMs) constitute a valuable class of compounds which have an importance in medicinal chemistry. TRAMs can have a wide range of pharmacological activities including laxative, antitumor, antiviral, antifungal, anti-inflammatory, antituberculosis, antioxidant and anti-diabetic effects.^{184,185,186,187,188} Furthermore, some TRAMs are applied as dyes,¹⁸⁹ even as food colorants.¹⁹⁰ The chemical structures of selected TRAMs and their activities are presented in **Figure 1.29**.

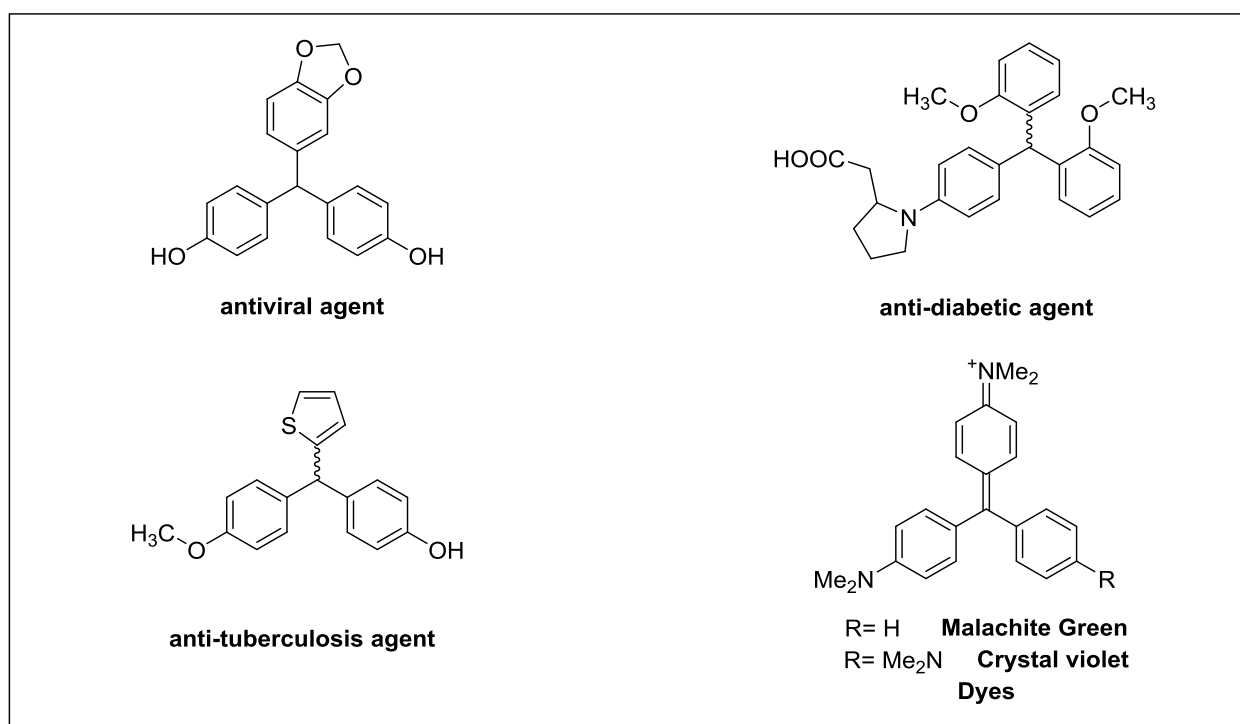


Figure 1.29. Representative examples of biologically active triarylmethane derivatives.

The drug bisacodyl is structurally related to the [triphenylmethane](#) derivatives with similarity to [phenolphthalein](#). It is used as a laxative drug throughout the world for the treatment of constipation.¹⁹¹ The hydrolyzed diphenol, bis-(*p*-hydroxyphenyl)-pyridyl-2-methane, termed BHPM (**Figure 1.30**), is the active metabolite of bisacodyl and responsible for the intestinal stimulating effect through direct action on the colon.¹⁹² Bisacodyl is known as a non-toxic drug in humans. Moreover, it may have potential as anti-cancer agent in combination with other chemotherapeutic

Introduction

drugs. It is considered as the first known compound which is targeting glioblastoma tumor stem-like cells.¹⁹³

Development of new drugs is considered to be not an easy task and is associated with a lot of challenges. Among the promising ways to generate drugs is finding new clinical indications or pharmacological targets for already existing drugs that have been approved by the FDA. This is referred to as drug repurposing.¹⁹⁴

Screening of 440 approved drugs for their inhibitory potency has been done in our group by Dr. Claudia Spanier at different P2X receptor subtypes aimed to find new lead structures which could be used for the development of selective agonists and antagonists. Bisacodyl has been identified as a potent antagonist of the P2X3 receptor. Based on this scaffold, a small library of nine compounds was synthesized by M. Sc. The-Hung Vu. The most potent P2X3 antagonist was BHPM.¹⁹⁵

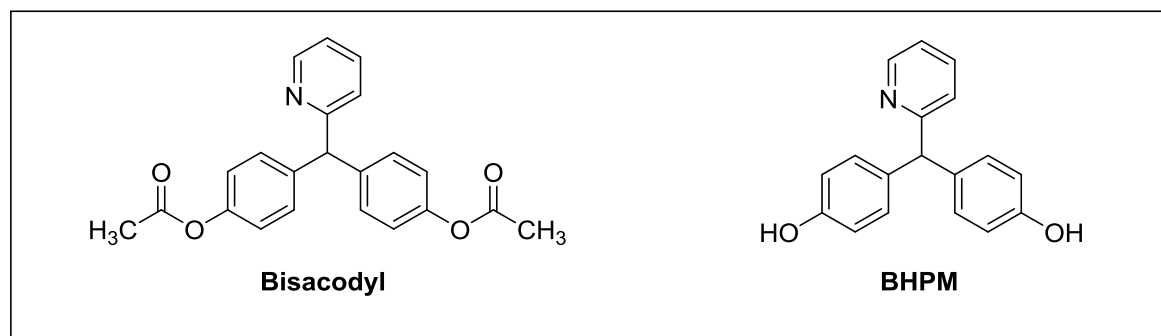


Figure 1.30. Structure of bisacodyl and its active metabolite BHPM.

3 2. Research objectives

3.1 2.1. Anthraquinone derivatives

Many of the synthesized anthraquinone (AQ) derivatives, which have been developed as selective and potent antagonists for different P2 receptors as well as ectonucleotidase inhibitors contain a sulfonate group (SO_3^-) at the 2-position. The AQ derivatives RB-2 and Acid Blue 25 (AB-25) served as lead structures (**Figure 2.1**). The negative charge on the sulfonate group renders the molecules highly polar and prevents oral bioavailability. Therefore, we aimed in this study to improve the physicochemical properties of the molecules by replacing the sulfonate group with other substituents such as a methyl group. The effect of other substituents has not been well investigated due to difficulties and limitations in preparing the desired compounds.¹⁷²

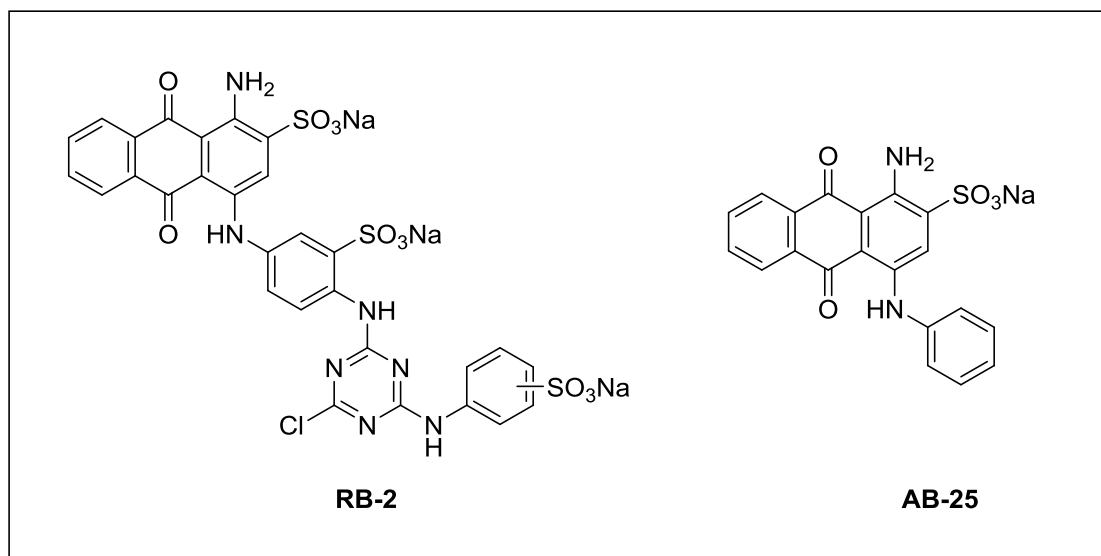


Figure 2.1. Structures of RB-2 and AB-25, lead structures for the development of ligands for purinergic targets.¹⁷²

It is important to mention that the method previously used for synthesizing AQ derivatives with acidic moieties at the 2-position, namely the Ullmann condensation¹⁶⁵ of 4-bromo-AQ derivatives with solid amines, was not successful for the preparation of AQ derivatives having a methyl group at the 2-position. The goal of the present study was to develop a synthetic access to such target compounds. This would require exploration and optimization of reaction conditions for a

model compound to establish the optimum conditions for the reaction. This method could later be used to synthesize 1-amino-4-(aryl)alkylamino-2-methylantraquinone derivatives as depicted in the **Figure 2.2**. The new method may also be applied to the synthesis of other AQ derivative bearing different substituents at the 2-position.

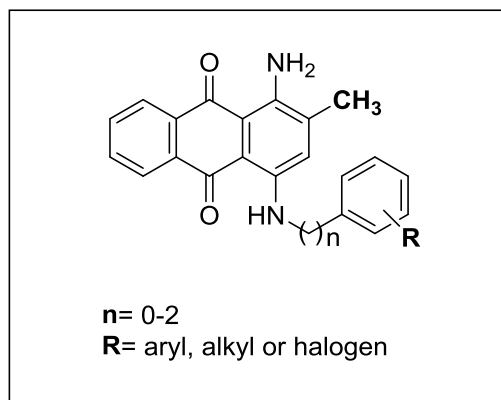


Figure 2.2. 1-Amino-4-(aryl)alkylamino-2-methylantraquinone derivatives.

Additionally, this study aims to (i) evaluate the synthesized anthraquinone derivatives on different targets, and (ii) to investigate the structure-activity relationships (SARs) of the synthesized anthraquinone derivatives to obtain information regarding the 2-position of the AQ core structure.

3.2 2.2. *Bisacodyl-derived compounds*

Sir James Black, a Nobel Laureate of 1988 in Physiology and Medicine stated that “The most fruitful basis for the discovery of a new drug is to start with an old drug”. Millions of people are suffering from different kinds of pain like acute, chronic, and neuropathic pain.¹⁹⁶ Neuropathic pain can develop due to surgical nerve injury, trauma, diabetes or infection.¹²⁰ While many medications are currently approved for the management of acute pain, unfortunately none of these drugs is sufficiently effective in the treatment of chronic, neuropathic pain.

From a long time, the role of ATP in sensory functions has been well established before its discovery as an extracellular neurotransmitter. Purinergic receptors regulate ATP modulatory functions in the sensory pathways. ATP can activate many primary afferent neurons, especially

Research objectives

C-fibers through P2X3 receptors. P2X3 receptors expressed by dorsal root ganglionic (DRG) neurons may have key roles in the inflammatory cascade and in the development of neuropathic pain.¹⁹⁷ The extensive activation of such receptors is believed to be involved in many chronic conditions including neuropathic pain and migraine. Since these conditions are frequently resistant to treatment, new molecules targeting P2X3 receptors may be useful to achieve pain control.¹⁹⁸

While targeting of P2X3 receptors already has a long historical background, it has only recently become obvious that it will probably have a promising future. However, there are still only very few P2X3 antagonists known which possess suitable properties for brain penetration.

One of our goals in this study was to develop potent, selective P2X3 receptor antagonists, which may be further developed to have properties for peroral application and potential for brain penetration. Based on the identification of bisacodyl as a potent P2X3 receptor antagonist which was reported in a study conducted by our group, we sought to further characterize the structure-activity relationships of bisacodyl by synthesizing a variety of derivatives. The proposed modifications are depicted in **Figure 2.3**.

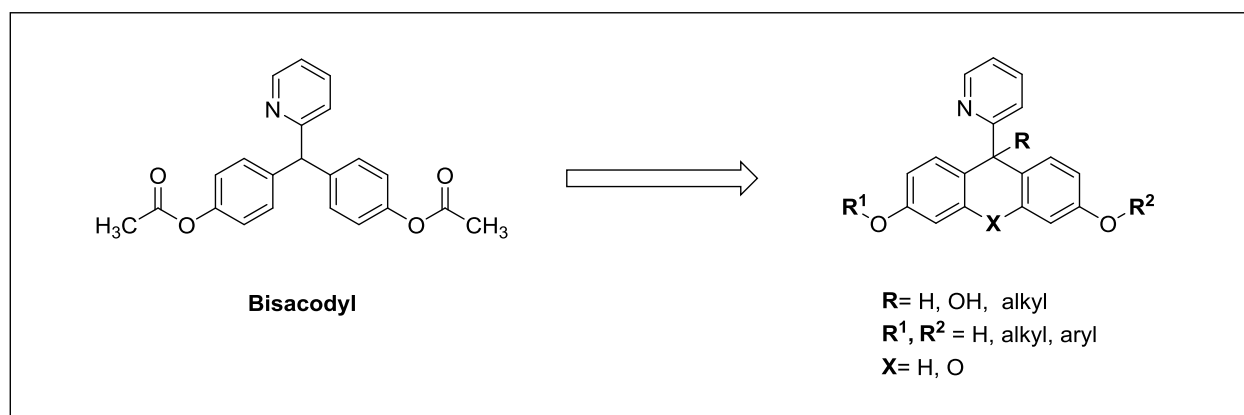


Figure 2.3. General proposed modifications for the drug bisacodyl.

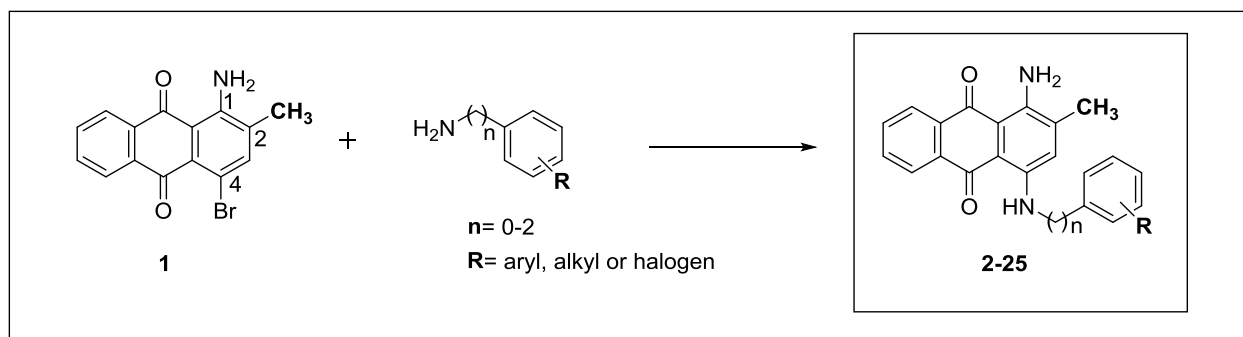
This study might lead to more potent P2X3 receptor antagonist that may - in contrast to bisacodyl - display systemic effects, and in particular penetrate into the central nervous system (CNS).

4 3. Results and Discussion

4.1 3.1. Anthraquinone derivatives

3.1.1. Synthesis of 1-amino-4-(aryl)alkylamino-2-methylanthraquinone derivatives

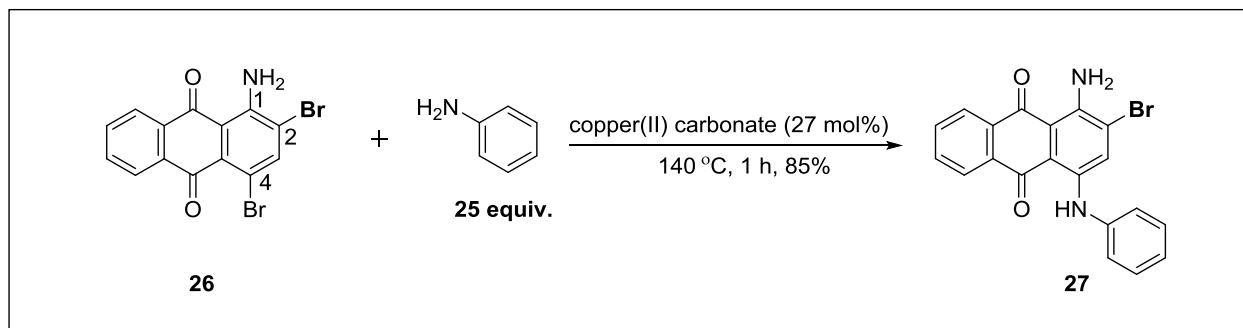
The synthesis of aryl(alkyl)amino-2-methylanthraquinone derivatives was implemented by the Ullmann coupling reaction using two different synthetic protocols (conventional heating protocol or microwave heating protocol) starting with commercially available 1-amino-4-bromo-2-methylanthracene-9,10-dione (2-methyl-AQ, **1**) which was condensed with different liquid or solid amines (**Scheme 3.1**). According to the physical nature of the amine used, the coupling method was selected. For liquid amines, the Ullmann coupling was performed using the conventional heating protocol (solvent-free reaction). For solid amine reactions in which a solvent was needed, the Ullmann coupling was done using a microwave heating protocol which will be discussed later in more detail.



Scheme 3.1. General scheme for Ullmann reaction of 1-amino-4-bromo-2-methylanthracene-9,10-dione with amines.

3.1.2. Condensation with liquid amines using solvent-free Ullmann reaction

The solvent-free method described by Ukponmwan *et al.*¹⁹⁹ was previously employed by Malik *et al.* for condensation of 1-amino-2,4-dibromoanthracene-9,10-dione (**26**) with aniline to give 1-amino-2-bromo-4-phenylaminoanthraquinone (**27**) (**Scheme 3.2**). Though the reaction time was 1 h and it produced a high yield (85%), it must be considered that the method required 25 equiv. of aniline used as a reagent and solvent, which is not favorable.²⁰⁰



Scheme 3.2. Synthesis of 1-amino-2-bromo-4-phenylaminoanthraquinone using the method of Ukponmwan *et al.*¹⁹⁹

The synthesis of the targeted 2-methylantraquinone derivatives was conducted using solvent-free reaction conditions according to the procedure described by Harris *et al.*²⁰¹ This method was also used by Baqi *et al.* for the condensation of 2-methyl-AQ (**1**) with aniline. The reaction was performed using 15 equiv. of aniline in the presence of potassium acetate and copper(I) acetate (10 mol%) under an argon atmosphere at 110 °C, affording 1-amino-2-methyl-4-(phenylamino)anthracene-9,10-dione (**2**) in a good yield of 64%.²⁰² This method was optimized with respect to the aniline amount. The condensation of 2-methyl-AQ (**1**) was finally conducted using three equivalents of aniline (3, 6, or 10). However, with lower concentrations, additional side-products were formed. The AQ dimers **28** and **29**, which were obtained as new side-products, (**Figure 3.1**) could be identified by liquid chromatography-mass spectroscopy (LC-MS) analysis. Thus, an aniline excess of 15 equiv. was fixed for subsequent condensation reactions to avoid dimerization reactions. This phenomenon may occur because of the electron-donating effect of the 2-methyl group causing the 1-amino group of the anthraquinone derivative to be relatively nucleophilic in nature.²⁰⁰

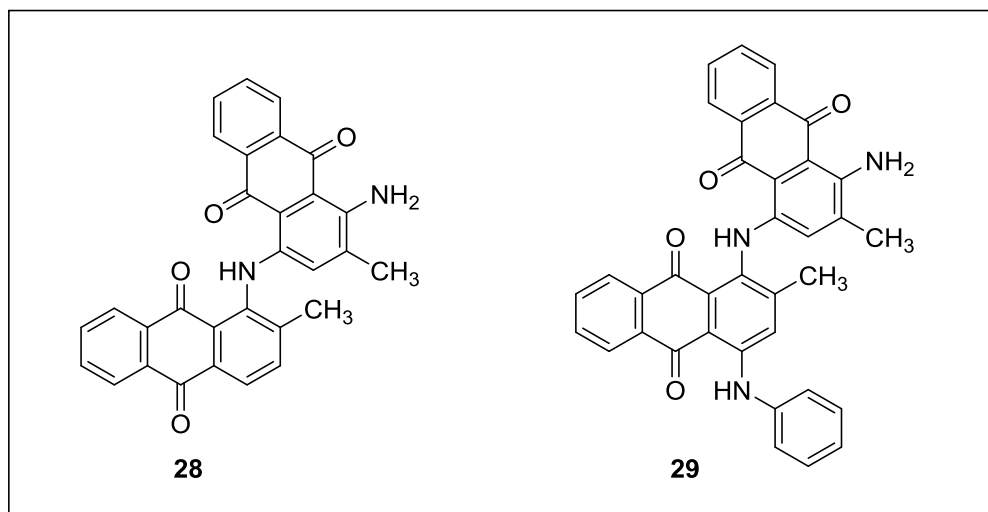
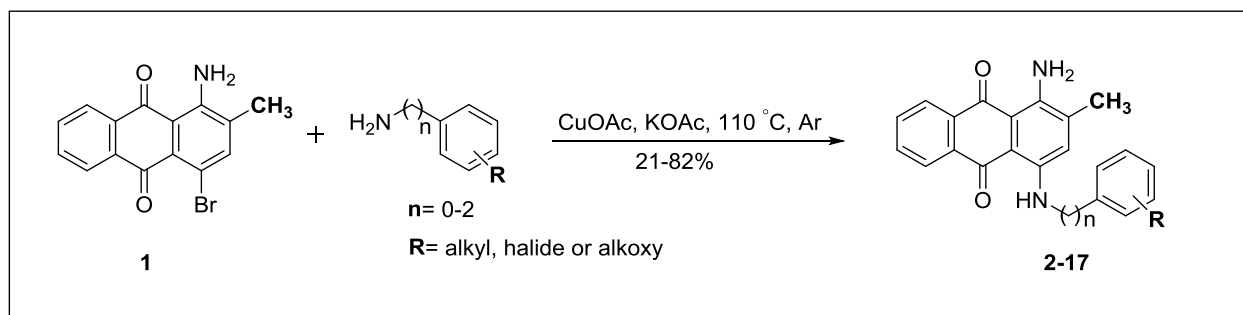


Figure 3.1. Proposed structures of side-products (dimerized anthraquinones).²⁰⁰

3.1.3. General synthetic procedure (I) used for anthraquinone derivatives 2-17

The method of Baqi *et al.* will be used for the condensation of other amines which are liquid in nature as outlined in **Scheme 3.3**.²⁰²

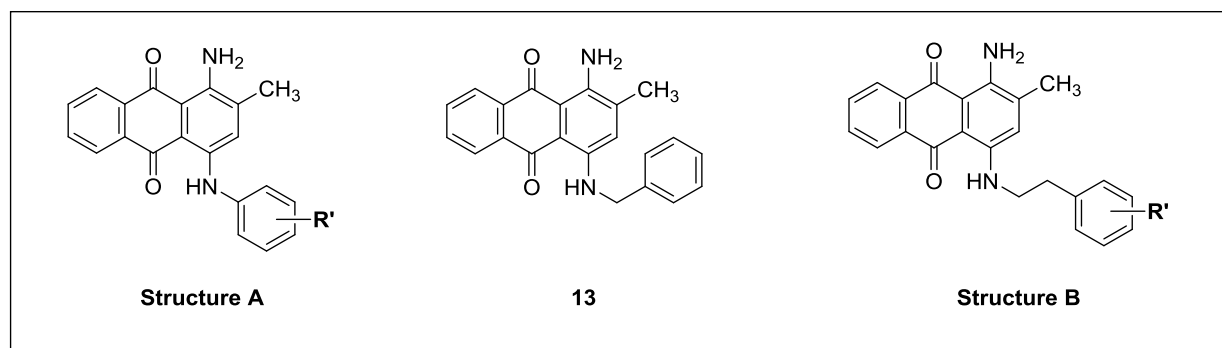


Scheme 3.3. Ullmann reaction of 1-amino-4-bromo-2-methylanthracene-9,10-dione with amines using a conventional heating method.²⁰²

The solvent-free method was successfully applied for the preparation of the AQs **2-17** (**Table 3.1**). The reactions progressed smoothly with variable rates and yields.

Results and Discussion

Table 3.1. Reaction times, HRMS, UV absorption, melting points, yields, and purity of the synthesized anthraquinone derivatives **2-17** obtained from liquid amines^a



Cmpd	R'	Reaction time (h:min)	HRMS (g/mol) ^b m/z: [M+H] ⁺		λ_{\max} (nm)	m.p. (°C)	Yield % ^c	Purity (%) ^d
			Calcd.	Found				

Structure A

2	H	01:50	329.1264	329.1265	570, 608	251-253	76	96
3	2-C ₂ H ₅	13:00	357.1598	357.1583	608	178-180	58	96
4	3-C ₂ H ₅	01:50	357.1598	357.1582	606	229-230	82	98
5	4-C ₂ H ₅	00:30	357.1598	357.1573	608	230-232	74	96
6	2-CH ₃	2:30	343.1441	343.1421	606	207-209	44	95
7	2-Cl	77:00	363.0895	363.0860	602	188-189	21	95
8	3-Cl	18:00	363.0895	363.0832	566, 606	280-281	66	97
9	4-Cl	18:00	363.0895	363.0841	604	293-294	72	98
10	2-OCH ₃	02:40	359.1390	359.1377	602	170-172	66	96
11	3-OCH ₃	02:30	359.1390	359.1385	570, 608	231-233	78	95
12	4-OCH ₃	02:00	359.1390	359.1372	574, 608	217-219	49	97
13	see structure above	01:50	343.1441	343.1431	610	215-216	51	97

Results and Discussion

Cmpd	R'	Reaction time (h:min)	HRMS (g/mol) ^b m/z: [M+H] ⁺		λ_{\max} (nm)	m.p. (°C)	Yield % ^c	Purity (%) ^d
			Calcd.	Found				

Structure B

14	2-Cl	18:00	391.1208	391.1192	568, 610	225-226	56	97
15	3-Cl	01:20	391.1208	391.1191	610	192-194	55	98
16	4-Cl	02:00	391.1208	391.1195	610	224-225	69	96
17	3-F	01:15	375.1503	375.1494	568, 610	257-258	70	97

^aReaction conditions: 2-methyl-AQ, amine (15 equiv.), potassium acetate (2.25 equiv.), copper(I) acetate (10 mol%), 110 °C, argon. ^bHRMS recorded on a micrOTOF-Q, HPLC coupled-mass spectrometer (Bruker). ^cIsolated yield. ^dPurity determined by LC-MS coupled to a diode array UV detector (220-700 nm).

Compound **2** was previously synthesized under solvent-free conditions. Condensation of 2-methyl-AQ **1** was carried out using 15 equiv. of aniline in the presence of potassium acetate and copper(I) acetate (10 mol%) at 110 °C afforded compound **2** after 300 min with 64% yield.²⁰² It is noteworthy that when copper(II) acetate (10 mol%) was utilized instead of the copper(I) acetate (10 mol%), the reaction became faster (110 min) with much higher yield (76%).

Reactions were completed smoothly within 30-150 min for ethyl- or methyl-substituted aniline derivatives (**5**, **4** and **6**) with one exception: *ortho*-ethyl derivative **3** imposed a negative effect on the reaction rate which proceeded to completion within 13 h. This may be explained in part by steric hindrance due to the *ortho*-ethyl substituent.

Although the isolated yields were good in case of *ortho*-methyl substitution (44%), the outcome was much better for the *ortho*-, *meta*- and *para*-ethyl substitutions with 58%, 82%, and 74%, respectively. The formation of a copper complex with the nucleophile (amine) prior to activation of the aryl halide (4-bromo-AQ derivatives) has been proposed for Ullmann condensation

Results and Discussion

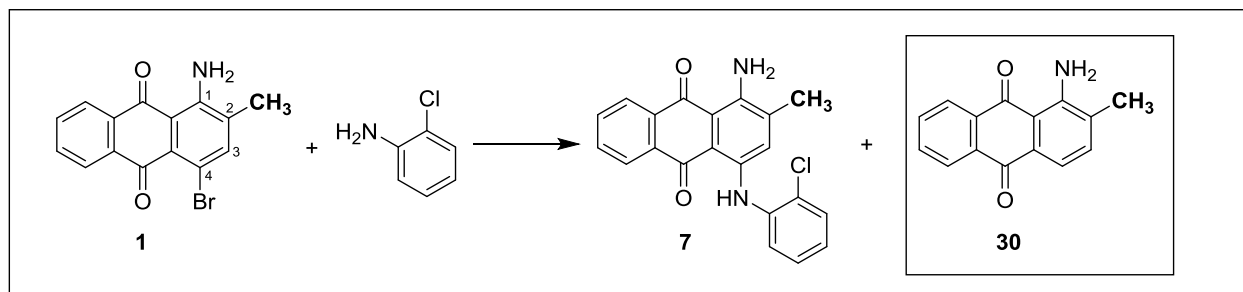
reactions.²⁰⁰ Thus, coordination of *o*-ethylaniline to the copper catalyst may result in hindrance of the subsequent coordination of the 4-bromo-AQ derivative.¹⁸¹

The same procedure was applied to the condensation of **1** with *ortho*-, *meta*- and *para*-chloro-substituted aniline derivatives (**7**, **8** and **9**, Table 3.1). A low yield was obtained in case of the *ortho*-chloro substitution, while relatively high yields were obtained for *meta*- and *para*-chloro substituents (21%, 66% and 72%, respectively). The reactions were progressed at a slower rate than in the case of non-substituted aniline, requiring 77 h (**7**) and 18 h (**8** and **9**) to completion, compared to only 110 min required for the synthesis of 1-amino-2-methyl-4-(phenylamino)anthracene-9,10-dione (**2**). This may be due to the electron-withdrawing effect of the chlorine atom, which deactivates the aromatic ring and reduces the nucleophilicity of the amine. Moreover, steric hindrance imposed by the size of the chlorine atom in case of an *ortho*-chloro substituent may provide a probable explanation for the long reaction time (77 h).

In contrast to the chloro substitutions, the presence of an *ortho*-, *meta*- or *para*-methoxy residue on the aniline had a similar effect as the non-substituted aniline, affording products **10**, **11** and **12** within 160, 150, 120 min respectively. This is potentially due to the electron-donating effect of methoxy group, which activates the aromatic ring and increases the nucleophilicity of the amine.

The reaction of 3-chlorophenethylamine, 4-chlorophenethylamine or 3-fluorophenethylamine with 2-methyl-AQ proceeded equally as that with aniline, and products **15**, **16** and **17** were obtained within 80 min, 120 min and 75 min, respectively. The reaction of 2-chlorophenethylamine required 18 h to be completed.

In conclusion, the applied solvent-free procedure provided the targeted products **2-17** in good to excellent yields (44-82%), with the exception of 1-amino-4-(2-chlorophenylamino)-2-methylantraquinone (**7**), which was the only product obtained in low yield (21 %). A major side-reaction was the reductive debromination of 2-methyl-AQ. Product **7** was difficult to isolate from the debromo-AQ side-product (**30**, Scheme 3.4) requiring multiple purification runs by column chromatography, and therefore resulted in a reduced isolated yield.



Scheme 3.4. Formation of the debromo-AQ derivative as a side-product of the Ullmann amination reaction of 2-methyl-AQ.

3.1.4. Optimization of the reaction conditions for 1-amino-4-bromo-2-methylantraquinone derivatives

3.1.4.1. Condensation with solid amines

The solvent-free method was successful to obtain the target compounds **2-17**, however a major problem with this kind of reaction procedure is its limitation to liquid amines or to solid amines with low melting point (e.g. 1-naphthylamine).²⁰⁰ Condensation with solid amines with a high melting point necessitated the use of a solvent as a reaction medium. In the present study we focused on the optimization of the reaction conditions for 2-methylantraquinone derivatives.

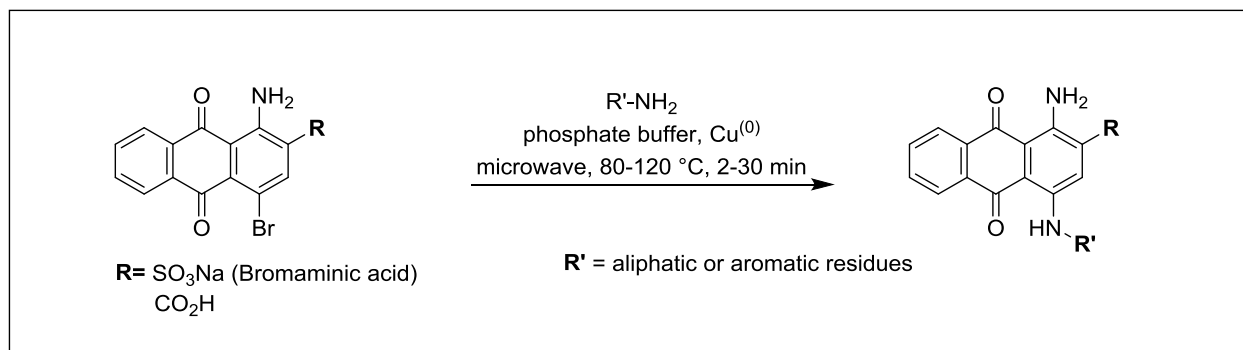
3.1.5. Optimization of the reaction conditions for some 2-substituted anthraquinone derivatives

Recently, Malik *et al.* developed methods for the synthesis of bromaminic acid analogues bearing different substituents at the 2-position of the anthraquinone moiety. The reaction started with the synthesis of 2-hydroxymethylantraquinone from 1-aminoanthraquinone followed by conversion to its corresponding carbaldehyde, carboxylic acid, and nitrile derivatives. The latter was then converted to its bioisostere tetrazole.²⁰²

Baqi *et al.* reported a modification of the Ullmann coupling reaction. Cu^0 was used as a catalyst in aqueous phosphate buffer (pH 6-7) under microwave irradiation which afforded a series of anthraquinone derivatives structurally related to RB-2. The anthraquinone derivatives bearing an acidic functionality at the 2-position were easily accessible through this method. Successful examples of this method were **PSB-0739**, which is bearing a sulfonate group at the 2-position,

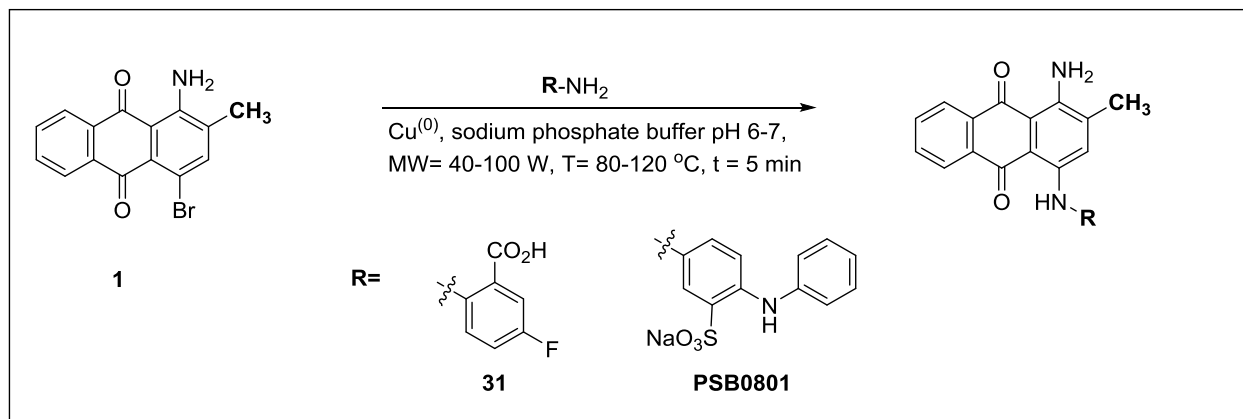
Results and Discussion

and **PSB-0702**, which bears a carboxylic group at the same position. Reactions of bromaminic acid (sodium 1-amino-4-bromoanthraquinone-2-sulfonic acid) or 1-amino-4-bromoanthraquinone-2-carboxylic acid with different amines are shown in **Scheme 3.5**.^{165,166}



Scheme 3.5. Synthetic procedure for anthraquinone derivatives with acidic groups at the 2-position.^{165,166}

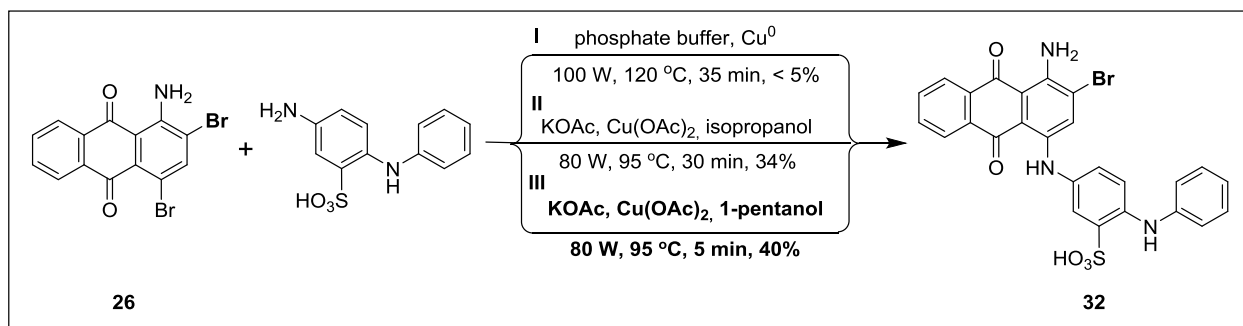
The previously described synthetic procedure, which has been proven as an efficient method for obtaining anthraquinone derivatives bearing acidic groups at the 2-position was applied for non-acidic functionalities such as 2-methylantraquinone derivatives, starting with 1-amino-4-bromo-2-methylantraquinone (0.1 and 0.2 mmol) yielding **31** or **PSB-0801**. The reaction was carried out using 2-amino-5-fluorobenzoic acid (0.2 mmol) in the case of **31** and 4-aminodiphenylamine-2-sulfonic acid (0.4 mmol) in the case of **PSB-0801**, in the presence of a buffer solution of Na₂HPO₄ (pH 9.6, 4.5 mL) and NaH₂PO₄ (pH 4.2, 0.5 mL) and finely powdered elemental copper (0.002-0.003 g, 5-10 mol%), under microwave irradiation (100 W, 120 °C), see **Scheme 3.6**. The reactions were completed within 5 min, affording 1-amino-4-(2-carboxy-4-fluorophenylamino)-2-methylantracene-9,10-dione (**31**) and 1-amino-2-methyl-4-(4-phenylamino-3-sulfophenylamino)anthracene-9,10-dione (**PSB-0801**). The yield of both compounds was low (21%).^{166,203}



Scheme 3.6. Synthetic procedure for anthraquinone derivatives with non-acidic functional groups at the 2-position of the anthraquinone core.

3.1.5.1. Optimization of the reaction conditions for 1-amino-2,4-dibromoanthraquinone (**26**)

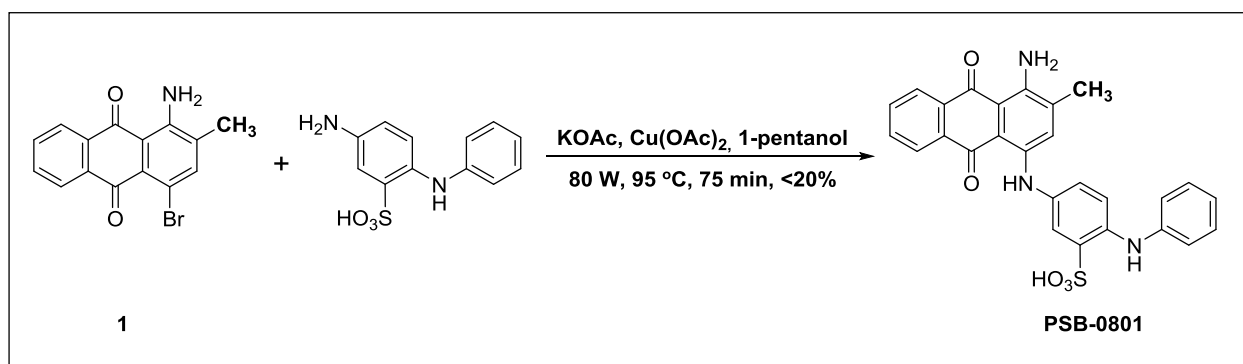
In previous work, our laboratory sought the optimal reaction conditions for different 2-substituted AQ derivatives. Several systematic trials were conducted with the goal to optimize the reaction conditions for non-acidic functionalities at the 2-position of the AQ scaffold using MW heating. Initially, the method of Baqi *et al.*^{166,165} was applied for the condensation of 2-bromo-AQ (**26**) with 4-aminodiphenylamine-2-sulfonic acid. However, only less than 5% of the product was obtained (entry **I**, **Scheme 3.7**). Different solvents including non-polar (toluene, diglyme), slightly polar (1,4-dioxane, dichloromethane, and tetrahydrofuran (THF)), polar aprotic (e.g. *N,N*-dimethylformamide (DMF), acetonitrile, dimethylsulfoxide (DMSO), and *N*-methyl-2-pyrrolidone (NMP)) and polar protic ones (water, ethanol, 2-ethoxyethanol, isopropanol, *t*-butanol and 1-pentanol) were tried. Isopropanol and 1-pentanol were found to be superior solvents resulting in product **32** with yields of 34% and 40%, respectively (entry **II** and **III**, **Scheme 3.7**). It is worth mentioning that the highest conversion rate of 2-bromo-AQ (**26**) was achieved with 1-pentanol (87%). Besides, different reactions were performed using different catalysts including copper (0) and copper(II) acetate. As a result of investigating a variety of conditions, it was concluded that 1-pentanol as a solvent and copper(II) acetate as a catalyst were critical components for the synthesis of various compounds by reaction of 2-bromo-AQ (**26**) with different solid amines.²⁰⁰



Scheme 3.7. Synthetic procedure for 2-bromoanthraquinone derivative **32** using different reaction conditions.²⁰⁰

3.1.5.2. Optimization of the reaction conditions for 1-amino-2-methylanthraquinone (**1**)

Since the optimum reaction conditions for 2-bromo-AQ were 1-pentanol (4 mL), potassium acetate (5 equiv.), and copper(II) acetate, (5 mol%), we tried the same conditions for 2-methyl-AQ (**1**) with solid amines. The condensation of **1** (0.1 or 0.25 equiv.) with 4-aminodiphenylamine-2-sulfonic acid (0.3 or 0.75 equiv.) only afforded less than 20% of **PSB-0801** (**Scheme 3.8**). No improvement in the yield was achieved under the conditions summarized in **Scheme 3.8** in comparison to the previous conditions applied for acidic anthraquinones summarized in **Scheme 3.6**.

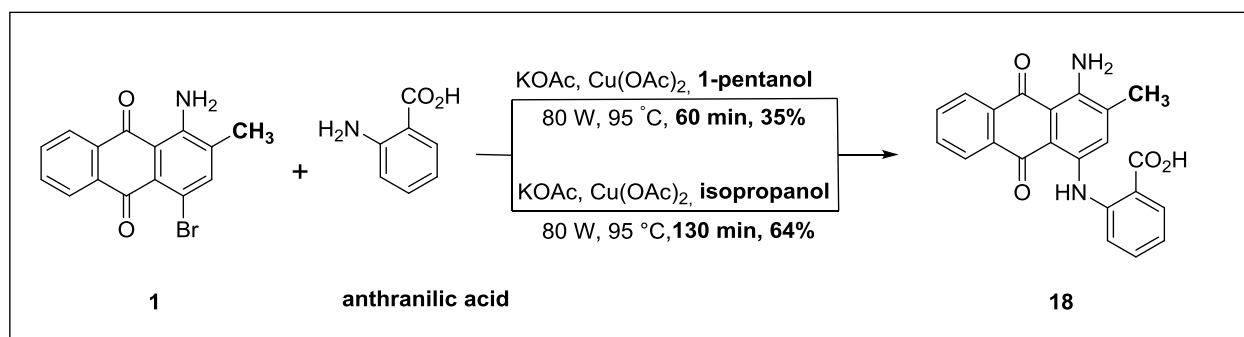


Scheme 3.8. Synthetic procedure for **PSB-0801** using the optimized conditions for 2-bromoanthraquinone derivatives.

When 1-pentanol was tested with other solid amines such as 2-aminobenzoic acid (anthranilic acid) under the previous microwave (MW) conditions (**Scheme 3.9**), it afforded only 35% of product **18** (entry **1**, **Table 3.2**). The reaction stopped after 60 min and no further progress was

Results and Discussion

observed after that time. The produced yield was very low compared to > 90% yield achieved with the corresponding 2-bromo- and the 2-cyano-AQ derivatives.²⁰⁰ Interestingly, when isopropanol was used as a solvent, the time needed for maximum conversion was doubled while the yield also increased to 64% (entry 2, Table 3.2).



Scheme 3.9. Synthetic procedure for the synthesis of compound **18** using different solvents.

According to the result of LC-MS, the condensation between compound **1** and 1-pentanol or isopropanol was also observed. While the reaction in case of 1-pentanol resulted in 6% of the condensed product **33** with 10% remaining starting material, the condensed product **34** was 5% and the unreacted starting material was 24% when the reaction was performed in isopropanol (**Figure 3.2**).

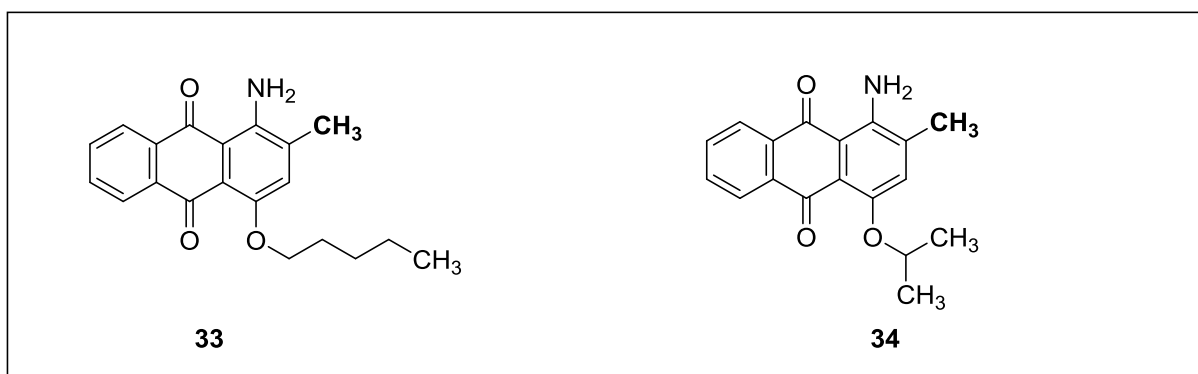


Figure 3.2. Condensation products resulting from 1-pentanol and isopropanol.

Condensation of 2-methyl-AQ with anthranilic acid in 1-pentanol took 60 min. In case of isopropanol, the reaction stopped after 130 min and the conversion process was incomplete.

Table 3.2. Reactions using 1-pentanol or isopropanol as solvents

Entry	Solvent	Reaction time (min)	Yield%		
			Compound 18	2-methyl-AQ (1)	Alkoxy side-products
1	1-pentanol	60	35	10	6 ^a
2	isopropanol	130	64	24	5 ^b

^aCompound **33**, 1-amino-2-methyl-4-(pentyloxy)anthracene-9,10-dione and ^bcompound **34**, 1-amino-4-isopropoxy-2-methylanthracene-9,10-dione.

Comparing both solvents, isopropanol showed a much better yield than 1-pentanol, however it was still not satisfactory. Thus, we decided to use other solvents such as ethanol or mixtures of ethanol and water.

4.1.1.1 3.1.5.2.1. Optimization of the reaction conditions using ethanol as a solvent

Reaction of 2-methyl-AQ (**1**) with anthranilic acid in ethanol was completed within 95 min, after which no further improvement of the produced yield was observed. The yield of the target compound was 80%, and 7% of condensation product with ethanol as a side product was obtained. When water (12.5% v/v) was added to ethanol, the reaction time had to be extended for an extra 35 minutes to achieve almost the same yield of the target compound without having any condensation with ethanol. At the same reaction time, this observation was also noticed with 25% v/v water with negligible change in the yield. But in the case of 50% v/v water, the yield was significantly decreased to 27%. A higher percentage of 2-methyl-AQ (**1**) was obtained using water/ethanol 50% v/v, and the lowest yield was obtained in water/ethanol 12.5% v/v. Therefore, we concluded that water addition prevents the condensation of the 2-methyl-AQ (**1**) with ethanol, but it affects the yield in a negative manner (**Table 3.3**).

Table 3.3. Reactions using ethanol and water/ethanol mixtures as solvents

Entry	Solvent	Reaction time (min)	Yield%		
			Compound 18	2-methyl-AQ (1)	Ethoxy side-product*
1	ethanol	95	80	13	7
2	water /ethanol (12.5% v/v)	130	76	-	-
3	water /ethanol (25% v/v)	130	71	7	-
4	water /ethanol (50% v/v)	130	27	46	-

*1-Amino-4-ethoxy-2-methylanthracene-9,10-dione (**35**, **Figure 3.3**).

Upon using ethanol alone as a solvent, the reaction proceeded in a straightforward way compared to 1-pentanol or isopropanol. The yield was also doubled when compared to 1-pentanol, and increased by 15% when compared to isopropanol. These results show that the presence of water may act negatively on the yield and the more water is in the reaction medium, the lower is the yield.

To further investigate the impact of solvents on the reaction, we tried several solvents without changing the reaction conditions. In this context, the reaction mixture consisted of 2-methyl-AQ (**1**, 0.1 mmol), anthranilic acid (0.3 mmol, 3 equiv.), potassium acetate (5 equiv.), and copper(II) acetate (5 mol%) in addition to various solvents (4 mL).

3.5.2.1.2. Use of ethyleneglycol as a solvent

Condensation of 2-methyl-AQ with anthranilic acid in ethyleneglycol as a solvent (entry **1**, **Table 3.4**) resulted in a reduction of the yield (43%) when compared to ethanol. The ethyleneglycol-condensed side-product (**36**, **Figure 3.3**) was obtained in 7% yield, while the *debromo* derivative **30** was the main contaminant amounting to 10%. The reaction was completed within 95 min (**Table 3.4**).

3.5.2.1.3. Use of methanol as a solvent

When methanol was used as a solvent (entry **2**, **Table 3.4**), the reaction time was 15 minutes longer than in case of ethanol (110 min). The yield of the desired product **18** jumped to 90%. The methoxy-condensed side-product, 1-amino-4-methoxy-2-methylantracene-9,10-dione (compound **37**, **Figure 3.3**), was formed in 8% yield. When phosphate buffer, which was previously used for substituted anthraquinones with acidic groups at the 2-position, was added to methanol (12.5% v/v, 0.5 mL), the yield was decreased to 17% (entry **3**, **Table 3.4**). This indicates that the phosphate buffer is not efficient for compounds with non-acidic substituents at the 2-position.

Table 3.4. Reactions using ethyleneglycol, methanol and phosphate buffer/methanol as solvents

Entry	Solvent	Reaction time (min)	Yield%		
			Compound 18	2-methyl-AQ (1)	Alkoxy side-products
1	ethyleneglycol	95	44	-	7 ^a
2	methanol	110	90	2	8
3	phosphate buffer /methanol (12.5% v/v)	110	17	79	-

^a1-Amino-4-(2-hydroxyethoxy)-2-methylantracene-9,10-dione (compound **36**, **Figure 3.3**).

According to the result of LC-MS, the condensation between compound **1** and ethanol, ethyleneglycol or methanol was also observed (**Figure 3.3**).

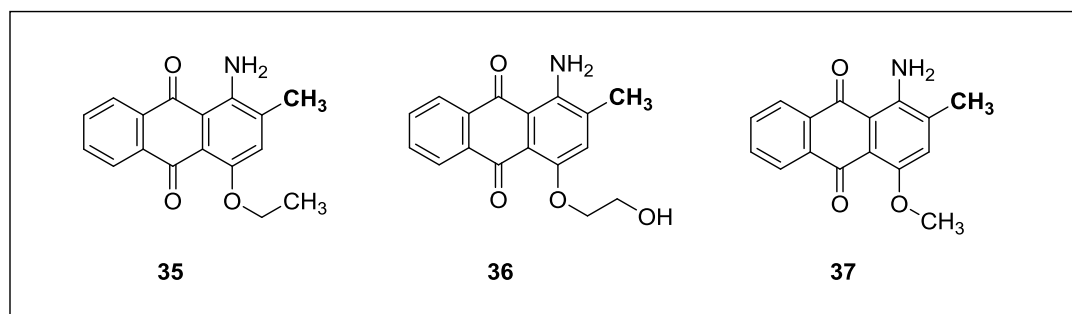


Figure 3.3. Condensation products resulting from ethanol, ethyleneglycol, and methanol.

Results and Discussion

In conclusion, different solvents were employed to select the most proper one for reactions of solid amines. Upon changing 1-pentanol to isopropanol the yield was improved to 64 %, but the conversion was still incomplete. A further improved yield (80%) was observed when ethanol served as a solvent. When the polarity of the medium was increased by using a mixture of water and ethanol, this was not favorable, and the yield decreased with increasing water concentration, with only 27% yield in 50% aqueous ethanol. However, an excellent yield of 90% was obtained in methanol, while the yield dropped to 44 % and 17% in case of ethyleneglycol, or a mixture of phosphate buffer and methanol (12.5% v/v), respectively (**Figure 3.4**).

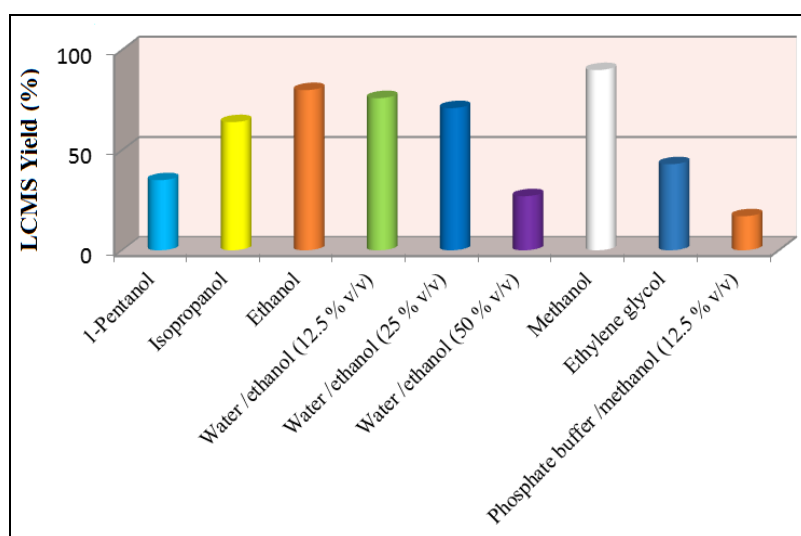
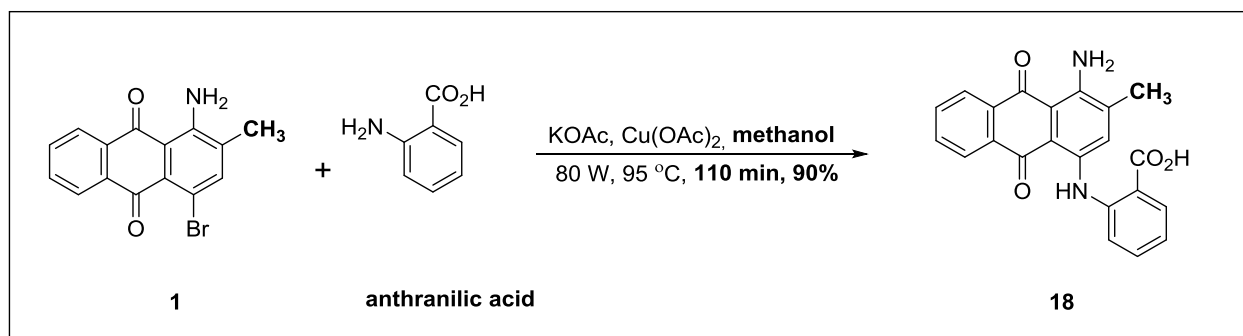


Figure 3.4. Optimization of the reaction of 1-amino-4-bromo-2-methylantraquinone (**1**) with anthranilic acid with regard to the solvent. Reaction conditions: 2-methyl-AQ (**1**, 0.1 mmol.), anthranilic acid (3 equiv.), potassium acetate (5 equiv.), copper(II) acetate (5 mol%), 4 mL of solvent, 95 °C, microwave 80 W.

Since methanol was one of the solvents under trial which produced a high yield, it was selected for further reactions. The condensation reaction conditions are depicted in **Scheme 3.10**.



Scheme 3.10. Synthetic procedure for compound **18** using methanol as a solvent.

3.1.6. Optimization of the reaction conditions using methanol as a solvent

3.1.6.1. Effect of concentration

To our surprise when the reaction was conducted using a higher amount (0.25 mmol) of 2-methyl-AQ (**1**) than initially used during the optimization process (0.1 mmol, entry **1**, **Table 3.5**), the yield dropped to 64% and the unreacted components were 8% (entry **2**, **Table 3.5**), while the main side-product was the debrominated product **30**.

Table 3.5. Optimization using methanol as a solvent with a higher concentration of 2-methyl-AQ^a.

Entry	Amount of 2-methyl-AQ (1) (mmol)	Solvent (4 mL)	Reaction time (min)	Yield% ^b		
				Compound 18	2-methyl-AQ (1)	Methoxy side-product
1	0.1	methanol	110	90	2	8
2	0.25			64	8	8

^aReaction conditions: 2-methyl-AQ (**1**, 0.1 or 0.25 mmol.), anthranilic acid (0.3 or 0.75 mmol, 3 equiv.), potassium acetate (5 equiv.), copper(II) acetate (5 mol%), 95 °C microwave 80 W.

^bYield% according to the result of LCMS.

Based on these findings, we preferred to keep 0.1 mmol as a standard amount for further reactions.

3.1.6.2. Effect of the catalyst

To investigate the effect of the catalyst on the reaction, we employed different copper catalysts. The reaction of 2-methyl-AQ with anthranilic acid using copper(II) acetate monohydrate (5 mol%) instead of copper(II) acetate resulted in a significant reduction in the yield from 90% to 40 % which may indicate that the presence of water in the crystal was detrimental for the reaction (entry **2**, **Table 3.6**). As previously described, elemental copper (copper(0)) was advantageous for Ullmann condensation reactions of AQs bearing acidic functional groups at the 2-position. Thus, we conducted the reactions with different concentrations of copper(0). Upon shifting to elemental copper (5 mol%) instead of copper(II) acetate monohydrate, the yield unfavorably dropped to 80% without any improvement in reaction time (80 min). When the concentration of copper(0) was increased to 10 mol%, there was a further drop in the yield (63%) with the same reaction time (entries **3** and **4**, **Table 3.6**).

We had expected that copper(0) might improve the reaction rate, so we conducted the reaction using a combination of copper(0) and copper(II) acetate (5 mol% each). Indeed the reaction rate slightly improved compared to copper(II) acetate alone (entry **5**, **Table 3.6**). To our surprise, using a mixture of copper(II) acetate monohydrate and copper(0) (5 mol% each) significantly improved both the yield (93%) and the reaction time (60 min) (entry **6**, **Table 3.6**) when compared to copper(II) acetate monohydrate alone.

Since the addition of copper (0) significantly improved the reaction outcome, we carried out multiple reactions using higher concentrations of copper (0) (10% or 15%). While the reaction time markedly improved as expected (45 min, and 25 min), the yields were reduced (64 % and 61 %, respectively) (entries **7** and **8**, **Table 3.6**).

Table 3.6. Optimization of the reaction of 2-methyl-AQ (**1**) with anthranilic acid with regard to the catalyst^a

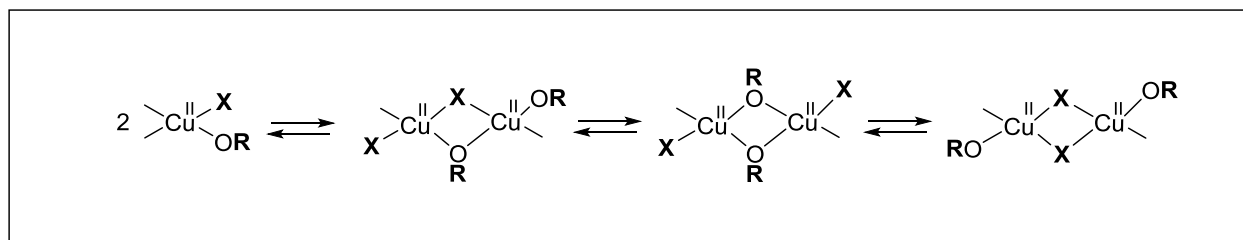
Entry	Catalyst (5 mol%) ^b	Time (min)	Isolated Yield (%)
1	Cu(OAc) ₂	110	90
2	Cu(OAc) ₂ ·H ₂ O	110	40

Results and Discussion

Entry	Catalyst (5 mol%) ^b	Time (min)	Isolated Yield (%)
3	Cu ⁰	80	80
4	Cu ^{0c}	80	63
5	Cu(OAc) ₂ /Cu ⁰	80	70
6	Cu(OAc) ₂ ·H ₂ O/Cu ⁰	60	93
7	Cu(OAc) ₂ ·H ₂ O/Cu ^{0d}	45	64
8	Cu(OAc) ₂ ·H ₂ O/Cu ^{0e}	25	61

^aReaction conditions: 2-methyl-AQ (**1**, 0.1 mmol), anthranilic acid (3 equiv.), potassium acetate (5 equiv.), 4 mL of methanol, 95 °C, microwave 80 W. ^bIn case of using a mixture, 5 mol % of each component was employed. ^c10 mol%, ^d10 mol% each. ^e15 mol% each.

Till now, the mechanism of Ullmann-type reactions has not been fully understood.^{204,205} In general, the progress or inhibition of the reactions mediated by copper is influenced by many parameters such as reaction medium which may explain the variability of reaction rates.^{200,206} In the present study, different attempts were made towards the optimization of the reaction conditions. The solvent played a fundamental effect on the reaction rate and yield which is supported by our results. Polar protic solvents, namely ethanol and methanol, were favorable for condensation of 2-methyl-AQ (**1**) with different amines. These findings could be explained by the fact that solvents having free hydroxyl group may also act as ligands. The study by Tuong, Arai and Hida has reported a series of mechanistic investigations on Ullmann condensations of haloanthraquinones with variable chemical structures such as amines, ligands and catalysts. The authors concluded that the reaction was enhanced by the presence of free hydroxyl-containing compounds such as alcohols. The free hydroxyl group of the alcohol can form a complex with the catalyst which shows much higher catalytic activity than the original copper species (**Scheme 3.11**).^{207,208,209}



Scheme 3.11. Reported alkoxy-Cu^{II} complexes by Arai *et al.*²⁰⁸ X= Cu counter anion e.g. halide.

There is a strong correlation between the lipophilicity of the AQ derivatives and the polarity of the solvent. Ideally, the more lipophilic the AQ derivative is, the less polar the solvent has to be. Since, 2-methyl-AQ (**1**) is lipophilic, it required solvents such as ethanol and methanol, instead of water as was the case of acidic AQ derivatives.²⁰⁰

Among the catalysts applied in the presence of methanol, both copper (0), copper(II) acetate and a mixture of copper(0) and copper(II) acetate monohydrate were acceptable (**Figure 3.5**).

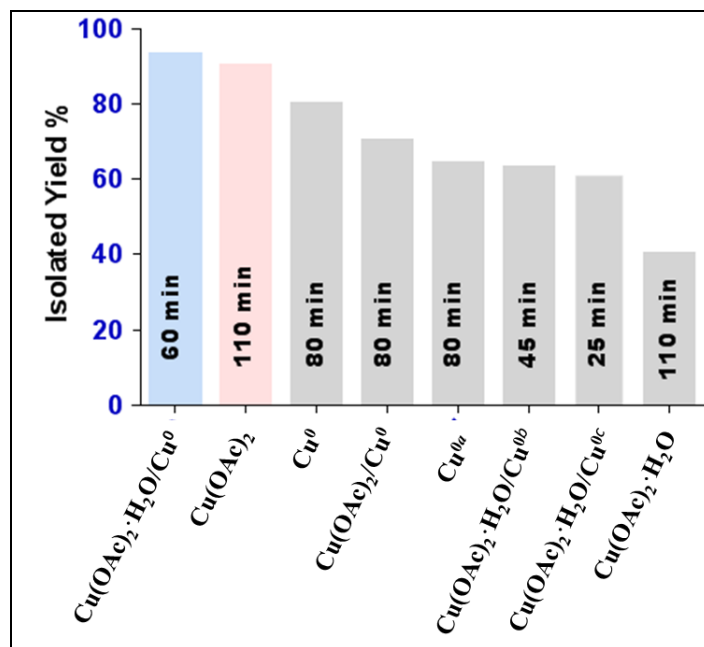
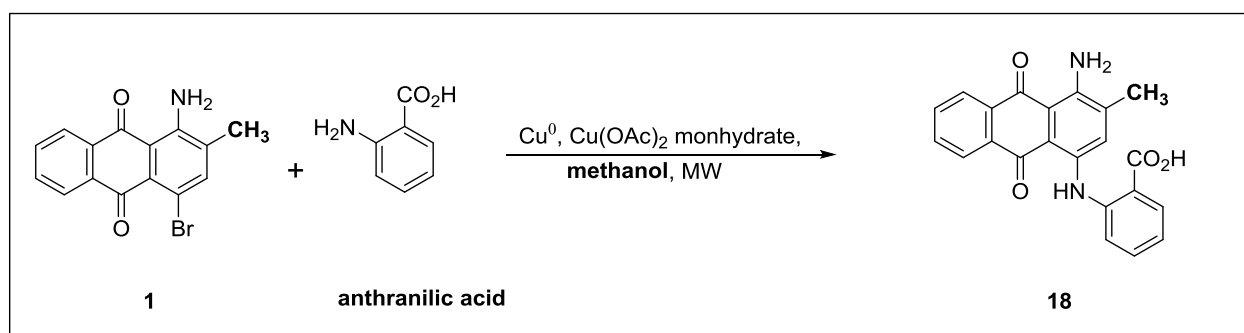


Figure 3.5. Effects of different catalysts on the reaction of 2-methyl-AQ (**1**) in methanol. ^a10 mol%, ^b10 mol% each, and ^c15 mol% each.

3.1.7. General synthetic procedure (II) used for anthraquinone derivatives 18-25

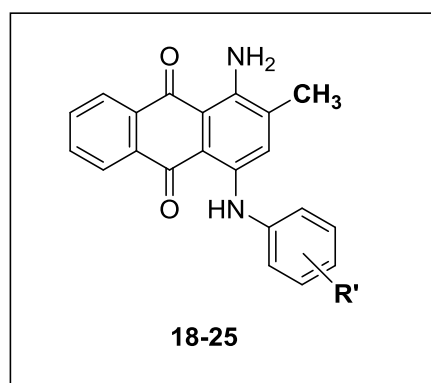
The optimized reaction conditions for 2-methyl-AQ were methanol (4 mL) as a solvent, potassium acetate (5 equiv.), and a mixture of copper(0), and copper(II) acetate monohydrate (5 mol% each) as catalysts (**Scheme 3.12**).



Scheme 3.12. Ullmann reaction of 2-methyl-AQ (**1**) with amino derivatives using microwave heating.

The above described method was successful for the synthesis of the 2-methyl-substituted AQ derivatives **18-25** (**Table 3.7**).

Table 3.7. Reaction times, HRMS, UV absorption, melting points, yields, and purity of the synthesized anthraquinone derivatives **18-25** obtained from solid amines^a



Cmpd	R'	Reaction time (min)	HRMS (g/mol) ^b <i>m/z</i> : [M-H] ⁻		λ_{max} (nm)	m.p. (°C)	Yield % ^c	Purity (%) ^d
			Calcd	Found				
18	2-CO ₂ H	70	371.1037	371.1036	616	>300	93	99

Results and Discussion

19	3-CO ₂ H	55	371.1037	371.1039	608	>300	36	96
20	4-CO ₂ H	65	371.1037	371.1033	612	>300	40	99
21	2-CO ₂ H-4-F	70	389.0938	389.0943 ^e	612	>300	44	95
22	3-SO ₃ H-4-NHC ₆ H ₅	40	500.1280	500.1266 ^e	608	>300	42	96
23	4-NHC ₆ H ₅	35	n.d.*		608	n.d.*	48	85
24	3-OH	70	343,1088	343,1087	616	285-286	43	93
25	4-OH	45	n.d.*		610	225-226	45	91

^aReaction conditions: 2-methyl-AQ (**1**, 0.1 mmol, 1 equiv.), amine (3 equiv.), potassium acetate (5 equiv.), copper(II) acetate (5 mol%), 4 mL of methanol, microwave 80 W, 95 °C, ^bHRMS was recorded on a micrOTOF-Q, HPLC coupled-mass spectrometer (Bruker). ^cIsolated yield. ^dPurity was determined by LC-MS coupled to a diode array UV detector (220-700 nm), ^e*m/z*: [M+H]⁺. n.d.*: not determined.

Regarding the position of the carboxyl group, the reaction with 3-aminobenzoic acid (**19**) requires 55 min until no further progress was observed with marked decrease in the yield 36%. However, condensation of 2-methyl-AQ (**1**) with 4-aminobenzoic acid (**20**) using the same conditions, the reaction time nearly the same compared to compound **18**, but the yield was dropped 2-fold decrease.

Introduction of fluorine atom at the *para*-position (**21**) had a negative impact on the yield 44% compared to compound **18**. After 70 min, there is no progress was noticed and the condensation side-product was increased instead of compound **21**. Compound **22** was previously prepared by reaction in phosphate buffer in only 21% yield.

In conclusion, the new, optimized method provided the targeted products **18-25** in acceptable to excellent yields (36-93%).

4.2 3.2. Bisacodyl-derived compounds

Bisacodyl (4,4'-diacetoxy-diphenyl)-(pyridyl-2)-methane is a member of the TRAM family. Bisacodyl was identified by our group to be a moderately potent P2X3 receptor antagonist and was selected for further characterization.¹⁹⁵

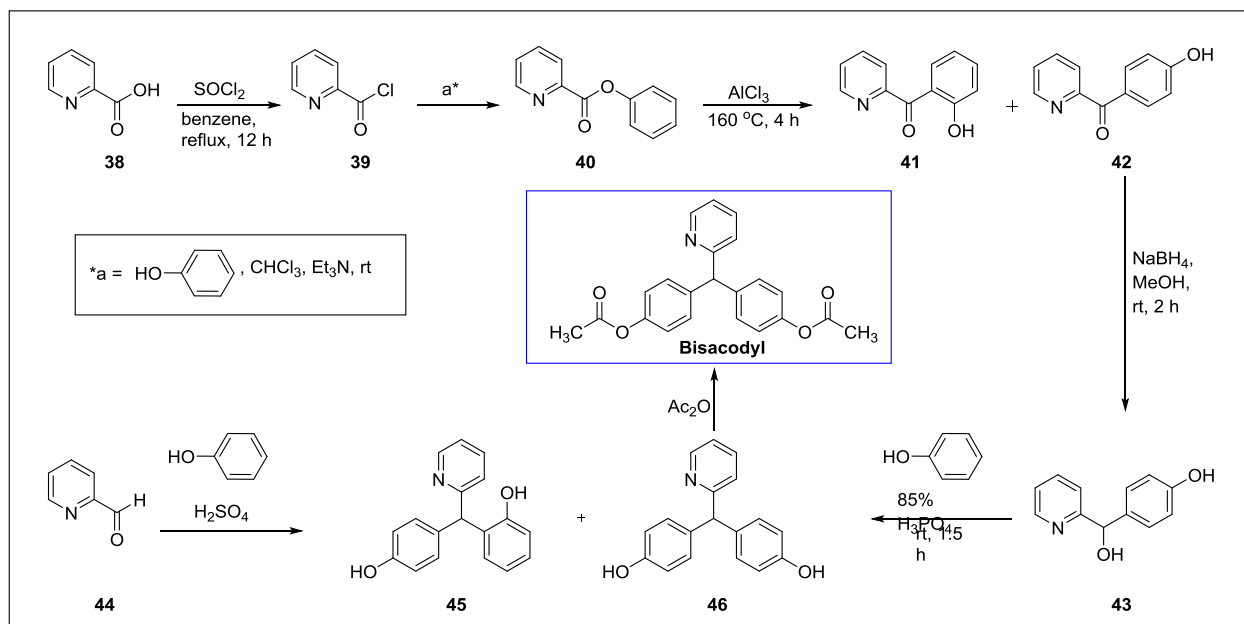
3.2.1. Synthesis of bisacodyl

Bisacodyl is composed of a tricyclic structure, where an *ortho*-pyridyl ring is attached to a central carbon atom in addition to two phenyl residues which bear acetate moieties at the *para*- positions. Bisacodyl was synthesized by acetylation of the precursor bis-(*p*-hydroxyphenyl)-pyridyl-2-methane **46** according to literature.^{210,211,212} This precursor can be prepared by two different pathways as follows:

1. Starting with pyridine-2-carboxylic acid (**38**), which is converted to the corresponding acid chloride **39** with thionyl chloride. Compound **39** is subsequently reacted with phenol to give pyridine 2-carboxylic acid phenyl ester (phenyl picolinate) **40**. Fries rearrangement is the key step of this method which allows the transfer of the 2-pyridylacetyl group of **40** forming the isomers 2-hydroxyphenyl-2-pyridyl-ketone (*ortho*-, **41**) and 4-hydroxyphenyl-2-pyridyl-ketone (*para*-, **42**) (1 : 2), which can be easily separated by column chromatography on silica gel using cyclohexane/ethyl acetate (70 : 30) as eluent system. The reduction of the key intermediate 4-hydroxyphenyl-2-pyridyl-ketone (*para*-, **42**) results in the formation of the alcohol derivative (**43**), which is then condensed with phenol in the presence of phosphoric acid to afford the key precursor **46**.²¹¹ However, there are some limitations associated with the application of this method including its being a multi-step synthetic process.

2. Condensation reaction between 2-pyridinecarboxaldehyde (**44**) and phenol catalyzed by sulfuric acid. The reaction yields the *ortho*- and *para*- isomers, namely 2-((4-hydroxyphenyl)(pyridin-2-yl)methyl)phenol (**45**) and the key precursor **46**. The remarkable advantage of this method is the improvement in the production process in addition to being an inexpensive pathway for saving resources.²¹² Since the condensation is the most efficient method to prepare triarylmethanes, it will be used in the next chapter for the synthesis of derivatives and analogs.

Bisacodyl was obtained by acetylation of the key precursor **46** with acetic anhydride in the presence of 4-dimethylaminopyridine (DMAP) or pyridine (**Scheme 3.13**).



Scheme 3.13. Synthetic procedures for bisacodyl.

3.2.2. Development of P2X3 receptor antagonists

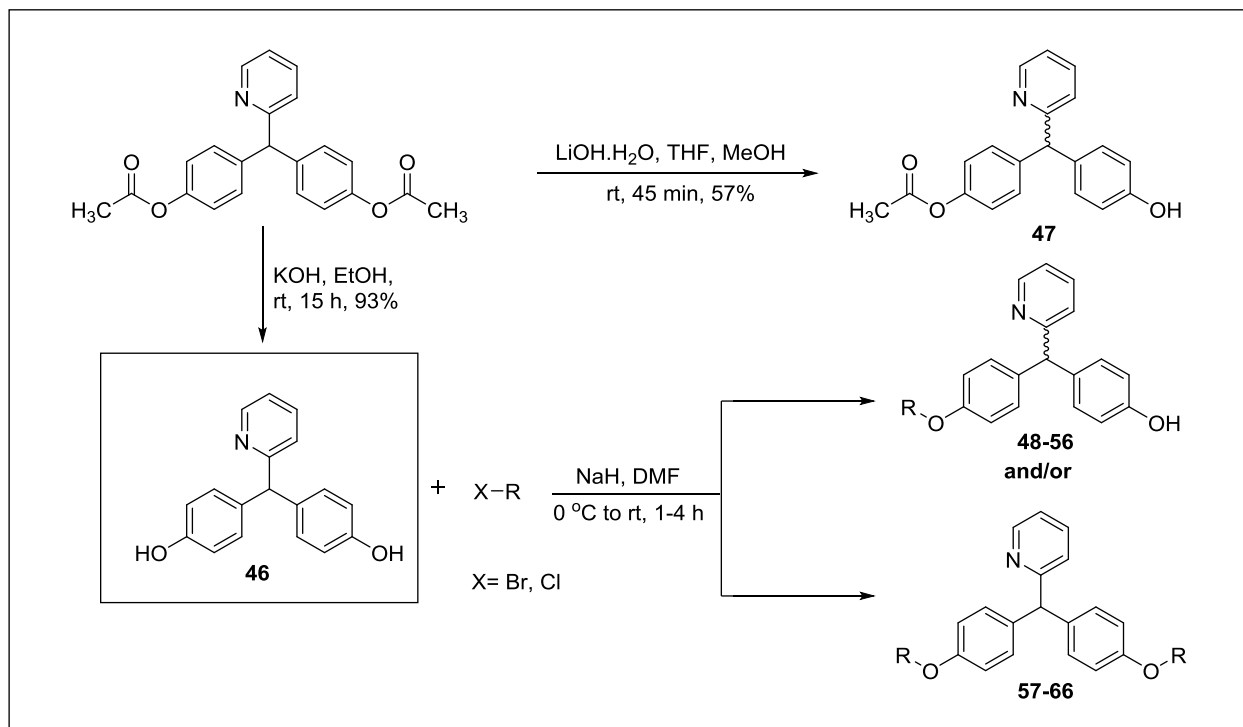
Bisacodyl is a moderately potent P2X3 receptor antagonist, which was selected for further optimization. The previous analysis of nine bisacodyl derivatives showed that the di-hydroxy metabolite was the most potent compound among the synthesized series (work by The-Hung Vu and Claudia Spanier). In order to investigate the structure-activity relationships and to elucidate the effects of different residues on the activity, a series of bisacodyl derivatives was synthesized and evaluated at the human P2X3 receptor for antagonistic activity.

Following a reported procedure, commercially obtained bisacodyl was subjected to hydrolysis of the di-acetyl ester groups using a solution of potassium hydroxide/10% aqueous (aq.) ethanol affording the *bis*-phenol derivative **46** in an excellent yield.²¹³ It should be noted that this high yield cannot be reached when using a mixture of methanol : water (4 : 1) as a solvent instead of ethanol : water (1 : 9). The removal of only one-acetyl ester group of bisacodyl can be achieved using lithium hydroxide monohydrate as a base in a mixture of tetrahydrofuran (THF) and methanol (MeOH) to form the monohydroxyl derivative **47** as described in **Scheme 1.14**.

3.2.3. Alkylation of the *bis*-phenol metabolite of bisacodyl

The *bis*-phenol **46** can be converted to aryl ethers through alkylation using alkylating agents in the presence of potassium carbonate as a base and dry acetone as a solvent under reflux conditions. However, there is a major drawback with using this method due to the long time required for completion of the reaction (22 h).²¹⁴ In most cases the mono-alkylated compounds were required, and this method may not be ideal for the preparation of such compounds.

In the present study, *bis*-phenol **46** was subjected to alkylation using different alkylating agents in the presence of sodium hydride (NaH) as a base, in *N,N*-dimethylformamide (DMF) as a solvent.²¹³ All reactions proceeded smoothly, starting at 0 °C and allowing the reaction mixtures to warm up to room temperature. Reactions were completed within 1-4 h affording a series of derivatives with different substituents at the 4,4'-positions (**48-66**) in moderate to high yields (**Scheme 1.14** and **Table 3.8**).



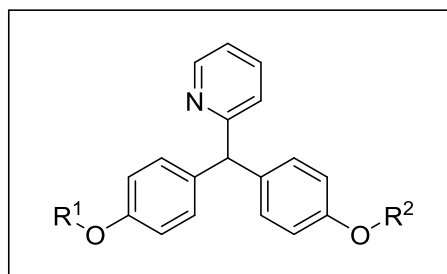
Scheme 1.14. Synthesis of compounds **46**, **47** and 4,4'-substituted derivatives.

Since it was easy to obtain the *bis*-phenol **46** on a gram scale, most reactions were conducted with 1 mmol. While the reactions involving different alkyl chains (linear, unsaturated, branched,

Results and Discussion

and aromatic) proceeded smoothly without any problem, differences in the rates and yields of the reactions were observed (**Table 3.8**).

Table 3.8. Reaction times, HRMS, melting points, yields, and purity of the synthesized bisacodyl-derived compounds **48-66** obtained by etherification of compound **46**^a



Cmpd	R ¹	R ²	Reaction time (h)	HRMS (g/mol) ^b m/z: [M+H] ⁺		m.p. (°C) (or n _D ²⁰)	Yield % ^c	Purity (%) ^d
				Calcd.	Found			
48	H		1	332.1656	332.1657 ^e	145-146	31	97
49	H		1.5	332.1656	332.1682 ^e	160-162	44	99
50	H		2	382.0448	382.0444 ^e	155-157	42	96
51	H		1	n.d.*	n.d.*	n.d.*	46	98
52	H		2	334.1449	334.1454 ^e	100-102	43	95
53	H		3	n.d.*	n.d.*	112-114	32	97
54	H		3	410.1398	410.1415 ^e	195-197	13	99
55	H		1	366.1500	366.1498 ^e	160-161	20	98
56	H		1	380.1656	380.1653	135-136	9	95
57			2	390.2428	390.2397	(1.5310)	94	95

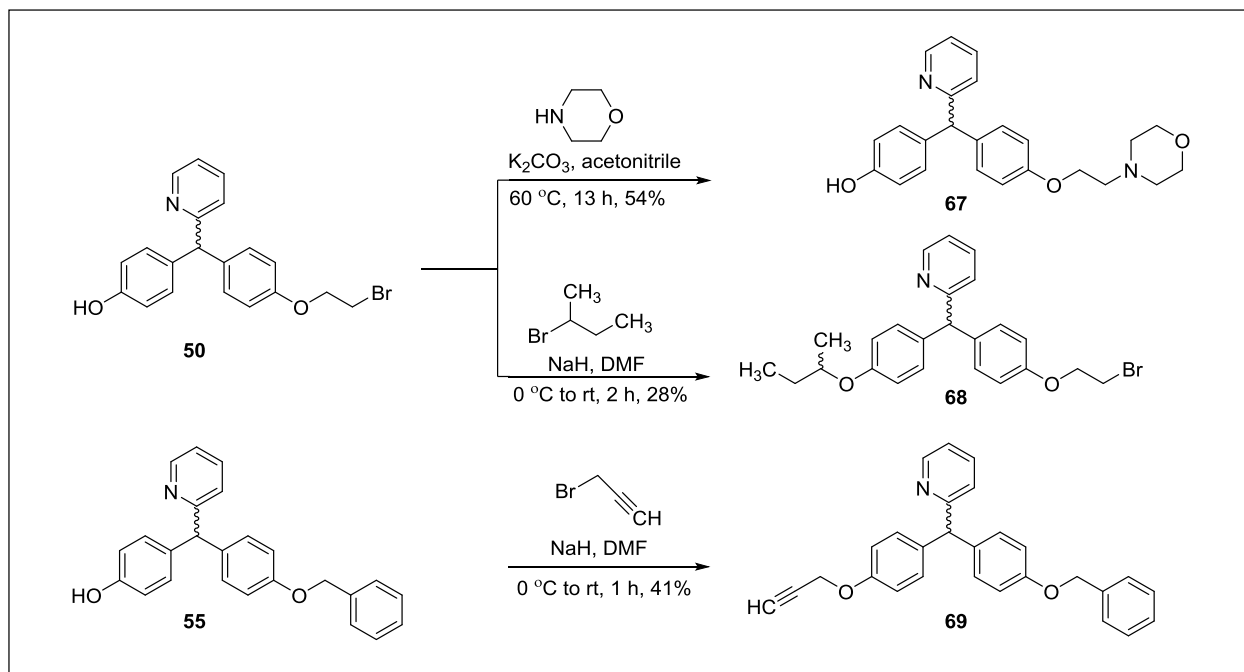
Results and Discussion

Cmpd	R ¹	R ²	Reaction time (h)	HRMS (g/mol) ^b m/z: [M+H] ⁺		m.p. (°C) (or n_D^{20})	Yield % ^c	Purity (%) ^d
				Calcd.	Found			
58			4	394.2013	394.1983	(1.5817)	79	96
59			2	450.1911	450.1871	75-77	77	95
60			3	410.2115	410.2085	(1.5940)	66	99
61			1.5	390.2428	390.2358	(1.4480)	31	96
62			3	502.3680	502.3701	60-62	55	96
63			3	546.1911	546.1877	170-172	68	100
64			2	518.2326	518.2312	122-124	29	99
65			1	458.2115	458.2079	113-115	39	96
66			1	486.2428	486.2398	(1.5693)	33	97

^aReaction conditions: *bis*-phenol (**46**, 1-3 equiv.), sodium hydride (2.2-6.6 equiv.), alkylating agent (2.2-6.6 equiv.), 10 mL of *N,N*-dimethylformamide for each equiv. of **46**, 0 °C to rt.

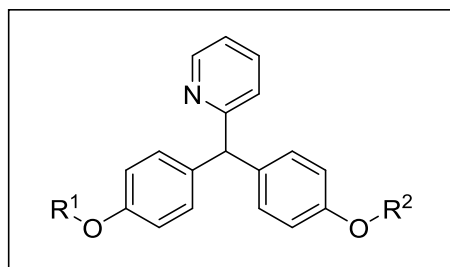
^bHRMS was recorded on a micrOTOF-Q, HPLC coupled-mass spectrometer (Bruker). ^cIsolated yield. ^dPurity was determined by LC-MS coupled to a diode array UV detector (220-700 nm), ^em/z: [M-H]⁻. n.d. *: not determined. (n_D^{20}): Refractive index.

Moreover, we aimed to replace the bromine atom on the side chain of compound **50**. Thus the morpholine derivative **67** was synthesized through reaction of compound **50** with morpholine in the presence of potassium carbonate as a base in acetonitrile at 60 °C as shown in **Scheme 3.15**.²¹⁵ Compounds **50** and **55** were subjected to further alkylation as described in **Scheme 3.15** affording the di-alkylated derivatives **68** and **69**, with two different alkyl groups in an acceptable yields (see **Table 3.9**).



Scheme 3.15. Synthesis of the morpholine derivative **67** and di-alkylated derivatives **68** and **69**.

Table 3.9. Reaction times, HRMS, melting points, yields, and purity of the synthesized derivatives **67-69**



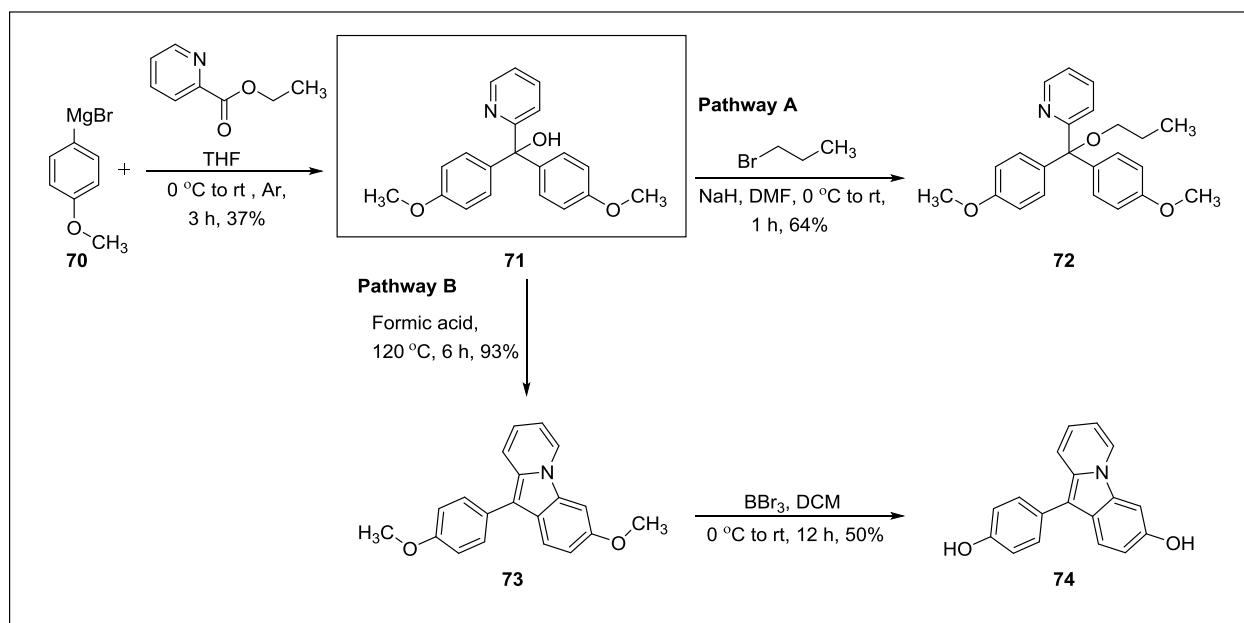
Cmpd	R ¹	R ²	Reaction time (h)	HRMS (g/mol) <i>m/z</i> : [M+H] ⁺		m.p. (°C) (or <i>n</i> _D ²⁰)	Yield (%)	Purity (%)
				Calcd.	Found			
67		H	13	389.1871	389.1886 ^a	140-142	54	99
68			2	440.1220	440.1167	Semi-solid	28	97
69			1	406.1802	406.1791	(1.5431)	41	95

^a[M-H]⁻. (*n*_D²⁰): Refractive index.

3.2.4. Preparation of a triarylcarbinol derivative

We aimed to study the structure-activity relationships of the hit structure **46** to determine which position would be critical for the enhancement of the activity. Therefore, the hydrogen atom attached to the central carbon atom in the hit structure **46** was replaced by a hydroxyl group to form the corresponding carbinol derivative. This was conducted by reaction of the commercial 4-methoxyphenylmagnesium bromide with ethyl 2-picolinate under an argon atmosphere followed by quenching the reaction with aqueous ammonium chloride (NH₄Cl).²¹⁶ Subsequently, the carbinol derivative **71** was reacted with the alkylating agent 1-bromopropane (**Scheme 3.16, Pathway A**) to afford the corresponding propyl derivative **72** in a good isolated yield (64%) (**Table 3.10**).

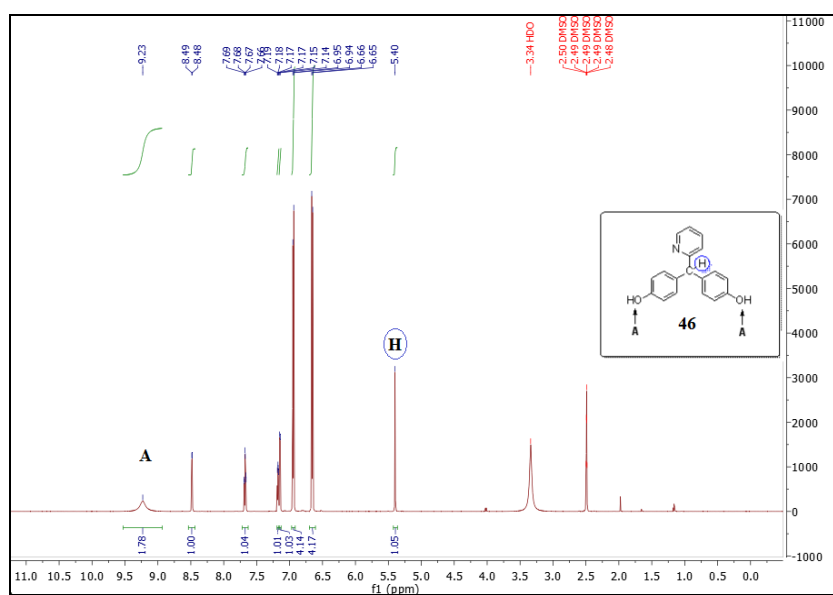
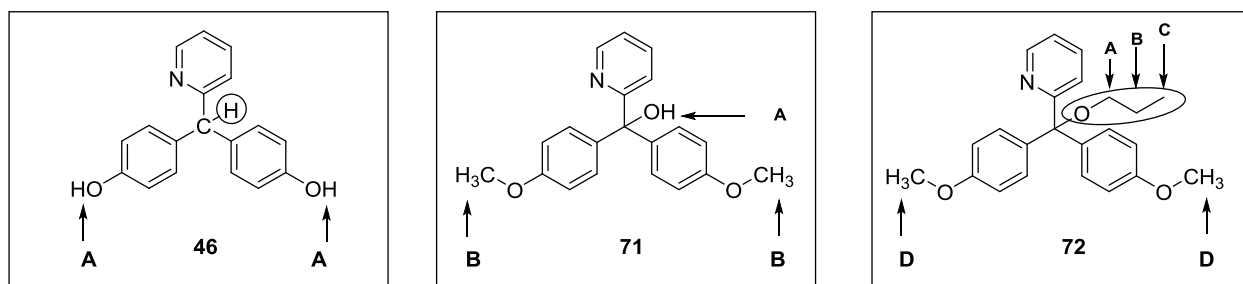
The pyrido[1,2-*a*]indole derivative **73** (**Pathway B**), which constitutes the cyclized form of carbinol **71**, was obtained by an adapted procedure reported by Karthikeyan *et al.*²¹⁷ The reaction was carried out in a pressure tube in the presence of formic acid at 120 °C and compound **73** was obtained in an excellent yield of 93% (**Table 3.10**). The corresponding hydroxy derivative **74** was synthesized through *O*-demethylation of the cyclized pyrido[1,2-*a*]indole **73**, by boron tribromide to afford product **74** in 50% yield (**Scheme 3.16, Table 3.10**).



Scheme 3.16. Synthetic pathways to compounds **71-74**.

3.2.4.1. Confirmation of structures

The structures of the synthesized carbinol **71** and its propyl derivative **72** were confirmed by ^1H and ^{13}C NMR spectroscopy (Figure 3.6). However, the molecular ion peak was not detected by (LC/ESI-MS) since both structures were not ionized during measurement under positive or negative mode.



Results and Discussion

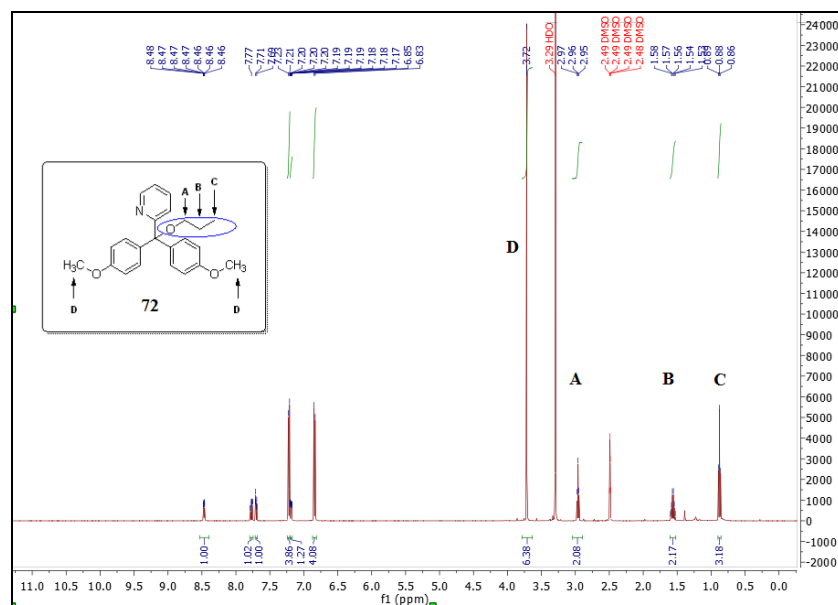
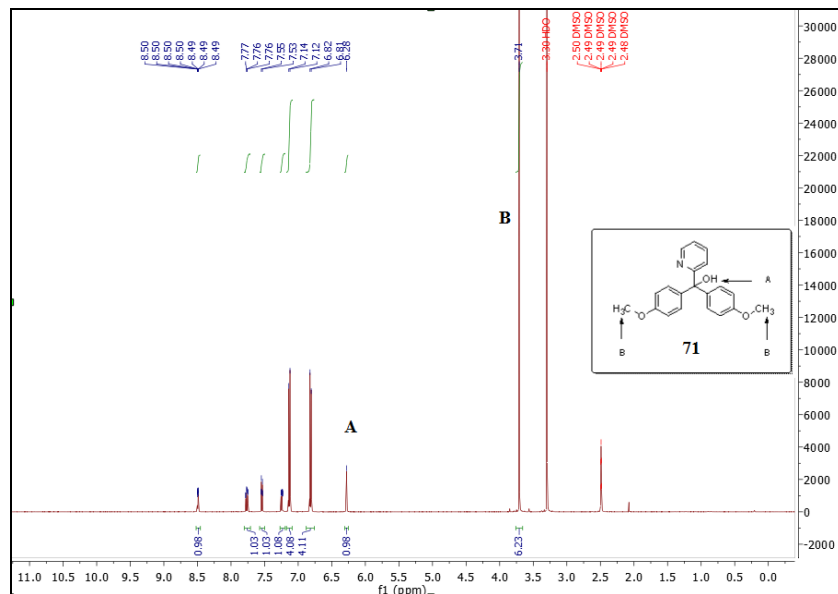
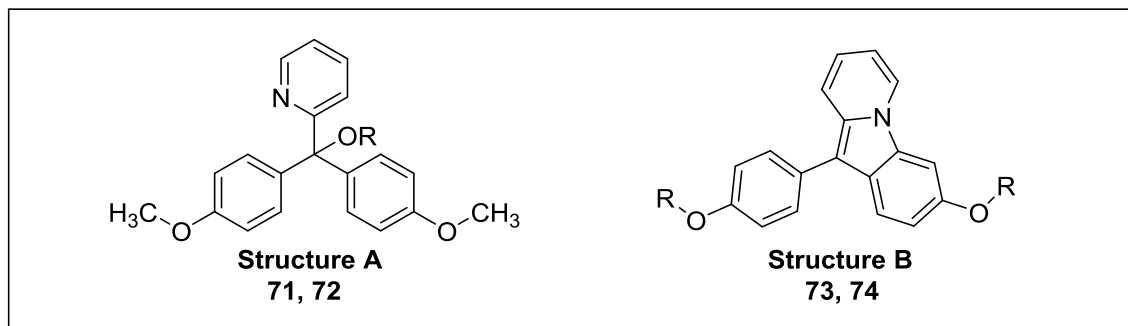


Figure 3.6. Comparison of the three ^1H NMR spectra for structures **46**, **71** and **72**. ^1H NMR spectral data were collected on a Bruker Avance NMR spectrometer at 600 MHz in case of compound **46** and at 500 MHz in case of compounds **71** and **72**. DMSO- d_6 was used as a solvent.

Based on the NMR spectra, we can conclude that the carbinol derivative **71** was formed (signal at 5.40 ppm in case of compound **46** and 6.28 for **71**). The formation of the propyl derivative **72**

was confirmed by the presence of signals for the propyl group in the aliphatic region instead of the alcoholic hydroxyl group of the carbinol derivative.

Table 3.11. Reaction times, melting points, and yields of the synthesized derivatives **71-74**



Cmpd	R	Reaction time (h)	m.p. (°C)	Yield %
------	---	-------------------	-----------	---------

Structure A

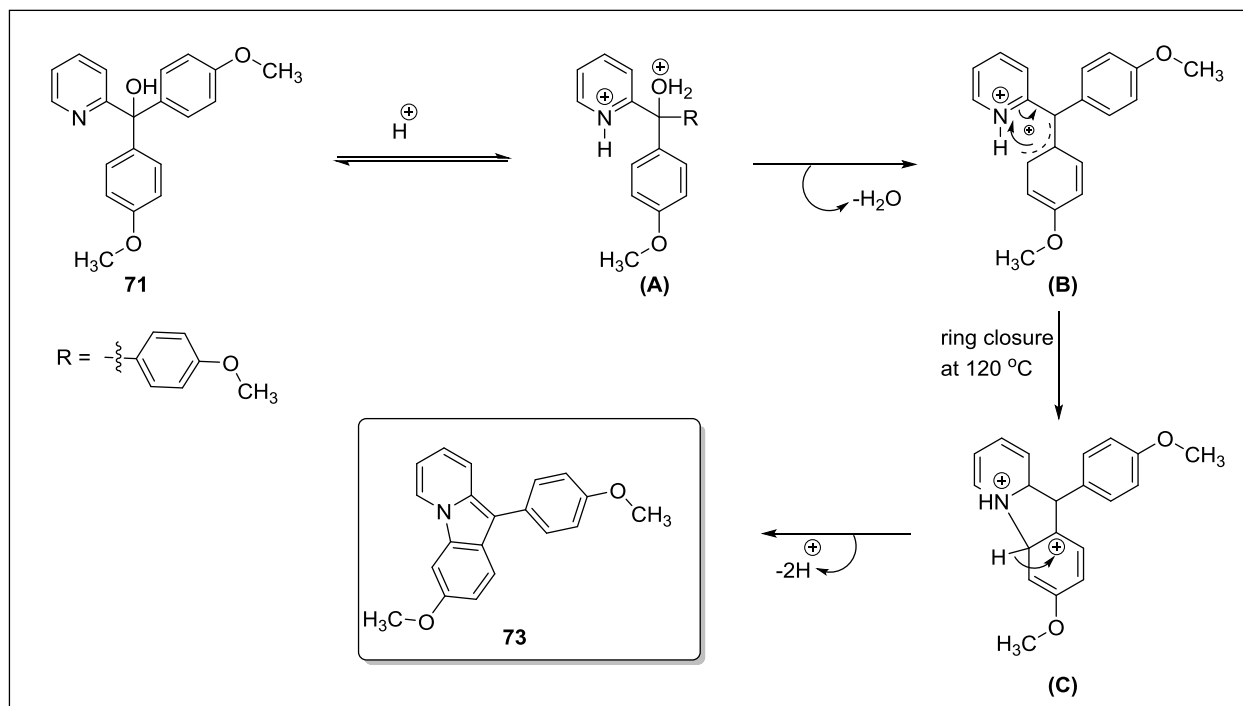
71	H	3	88-89	37
72	propyl	1	100-102	64

Structure B

73	CH ₃	6	156-158	93
74	H	12	94-96	50

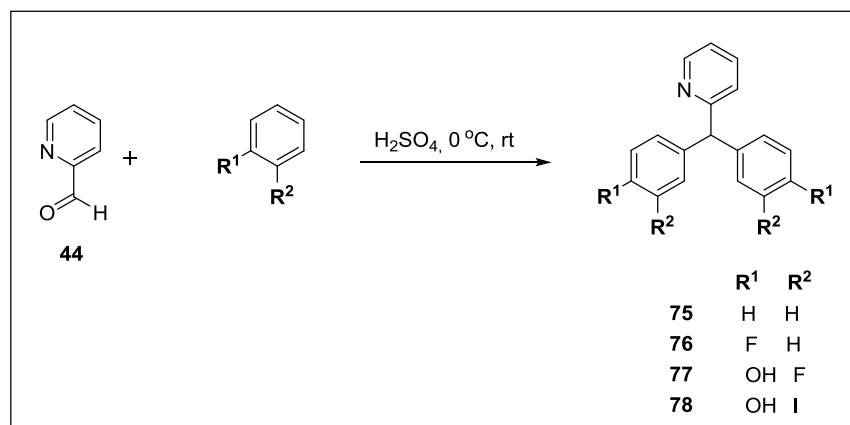
3.2.4.2. Plausible mechanism for the formation of 3-methoxy-10-(4-methoxyphenyl)-pyrido[1,2-*a*]indole (**73**)

The aza-Nazarov-type cyclized product was successfully obtained through intramolecular C-H amination mediated by formic acid, and the mechanism may be proposed as follows.²¹⁷ The carbinol derivative **71** is converted into its protonated form in the acidic medium (formic acid) affording intermediate **A**. Subsequently the tertiary carbocation **B** is formed when a water molecule is dissociated. At 120 °C, this carbocation is subjected to an electrocyclic ring closure reaction which leads to the formation of intermediate **C**. Then, deprotonation and re-aromatization takes place and the desired cyclized derivative **73** is formed (**Scheme 3.17**).



Scheme 3.17. Proposed mechanism for the intramolecular reaction producing pyrido[1,2-*a*]indole **73**.²¹⁷

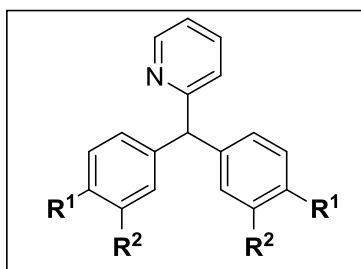
In the beginning we focused on the derivatives with disubstituted hydroxyl groups at the 4- and 4'-positions. Then, we tried to determine the effect of the lacking of both hydroxyl groups on the activity **75**. We also tried to replace the hydroxyl groups with electro-negative fluorine atoms **76**. While we showed that substitution in the 4- and 4'-positions is advantageous, we also aimed to study substitution of the 3,3'-positions. We aimed to introduce electro-negative atoms beside the hydroxyl groups, namely a small fluorine atom (**77**) or a larger iodine atom (**78**). Among the different approaches for the preparation of such compounds we used a procedure which is outlined in **Scheme 3.18** Condensation reaction of 2-pyridinecarboxaldehyde with different moieties (fluorobenzene, 2-fluorophenol and 2-iodophenol) was performed in the presence of concentrated sulfuric acid at 0 °C.²¹⁸



Scheme 3.18. Synthetic pathway for obtaining compounds **75-78**.

Replacement of the hydroxyl groups of compound **78** with methoxy residues for (**78a**) was conducted using the same procedure which had been used for alkylation of *bis*-phenol (**Table 3.12**).

Table 3.12. Reaction times, HRMS, melting points, yields, and purity of the synthesized derivatives **75-78a**



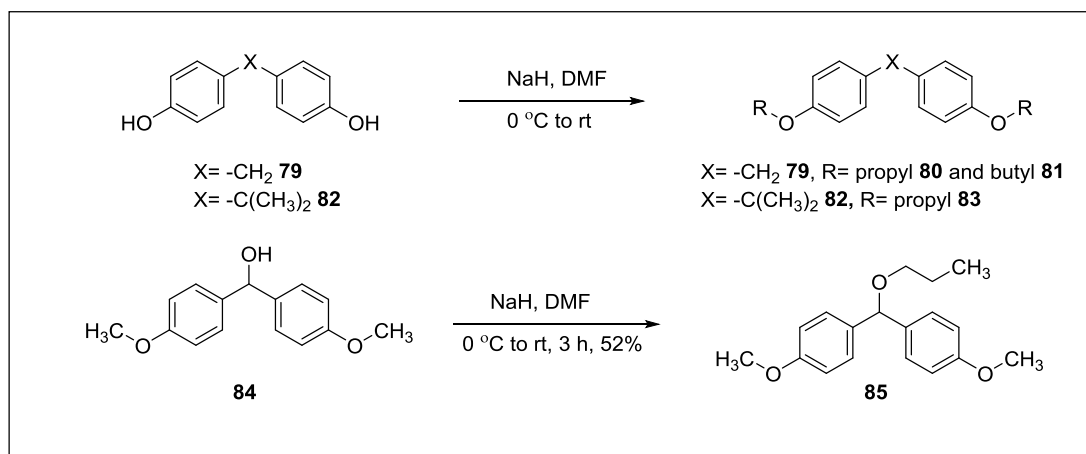
Cmpd	R ¹	R ²	Reaction time (h)	HRMS (g/mol) <i>m/z</i> : [M-H] ⁻		m.p. (°C)	Yield (%)	Purity (%)
				Calcd.	Found			
75	H		13	246.1277	246.1275 ^a	62-64	61	96
76	F		13	282.1089	282.1083 ^a	n.d.*	25	97
77	OH	F	9	312.0842	312.085	246-248	60	97
78	OH	I	14	527.8963	527.8960	186-187	24	97
78a	OCH ₃	I	0.5	555.9276	555.9265	68-70	83	98

^a[M+H]⁺. n.d.*: not determined.

Results and Discussion

The next part of this study was dedicated to the simplification of structure **46**. We specifically aimed to remove or replace the pyridine ring by other substituents while maintaining the other features (two aryl rings) and to accordingly assess its importance for the activity.

To achieve that, direct alkylation was performed on compound **79** with 1-bromopropane or 1-bromobutane in the presence of sodium hydride as a base in DMF, thereby producing the propyl and butyl derivatives **80** and **81**. Similarly, the treatment of compounds **82** and **84** with 1-bromopropane generated the propyl derivatives **83** and **85** (Scheme 3.19).²¹⁹



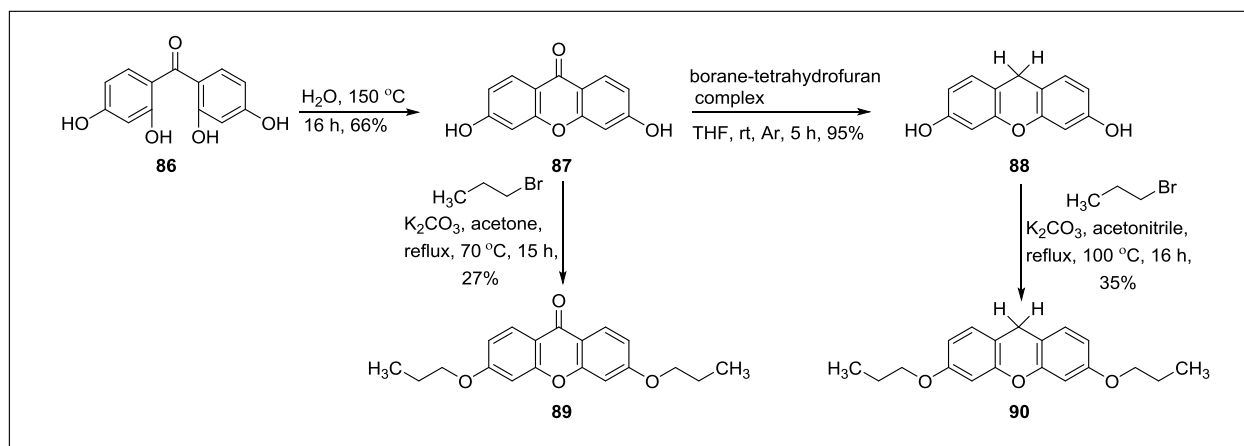
Scheme 3.19. Synthesis of the alkylated derivatives **80**, **81**, **83** and **85**.

The synthetic strategy to obtain compounds **89** and **90** relied mainly on the alkylation of the key intermediates **87** and **88**, as described in **Scheme 3.20**. The 3,6-dihydroxy-9*H*-xanthen-9-one (xanthone scaffold) containing two hydroxyl groups (**87**) was generated in a pressure tube through dehydration of commercially available 2,2',4,4'-tetrahydroxybenzophenone **86**. The reaction was only accomplished under high pressure and elevated temperature. Temperature is the key element in this dehydration reaction. In fact, the high temperature is necessary to evaporate the water by generating steam. The latter creates the pressure essential to produce the xanthone compounds.^{220,221} The higher the temperature, the greater the pressure and the faster the reaction will proceed.

In the second step, compound **87** was subjected to reduction using borane-tetrahydrofuran complex (1.0 M in THF). The reaction proceeded smoothly at room temperature under argon affording 9*H*-xanthene-3,6-diol (**88**) in an excellent yield (**Scheme 3.20**, **Table 3.13**).²²² Then, the

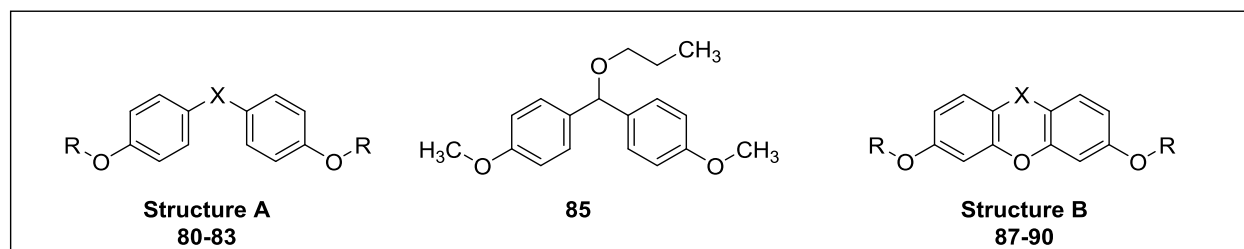
Results and Discussion

propyl side chains were introduced on the two hydroxyl groups in the presence of potassium carbonate as a base in solvents such as acetone or acetonitrile, to give compounds **89** and **90** (Scheme 3.20).²²³



Scheme 3.20. Synthesis of xanthone and xanthene derivatives **89** and **90**.

Table 3.13. Reaction times, HRMS, melting points, yields, and purity of the synthesized derivatives **80**, **81**, **83**, **85** and **87-90**.



Cmpd	R	X	Reaction time (h)	HRMS (g/mol) ^a <i>m/z</i> : [M+H] ⁺		m.p. (°C) (or <i>n</i> _D ²⁰)	Yield % ^b	Purity (%) ^c
				Calcd.	Found			

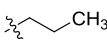
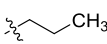
Structure A

80		CH ₂	4	285.1849	285.1853	(1.534)	35	95
81		CH ₂	3	313.2162	313.2158	46-48	64	99
83		C(CH ₃) ₂	4	313.2162	313.2165	(1.3282)	75	98
85	See structure above		3	n.d.*		(1.4480)	52	n.d.*

Results and Discussion

Cmpd	R	X	Reaction time (h)	HRMS (g/mol) ^a <i>m/z</i> : [M+H] ⁺		m.p. (°C) (or <i>n</i> _D ²⁰)	Yield % ^b	Purity (%) ^c
				Calcd.	Found			

Structure B

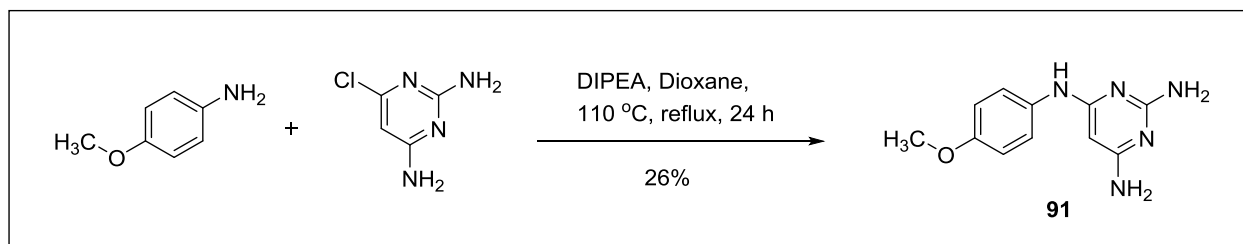
87	-H	C=O	16	227.0350	227.0374 ^d	> 300	66	99
88	-H	CH ₂	5	213.0557	213.0577 ^d	215-217	95	95
89		C=O	16	313.1434	313.1439	115-117	35	99
90		CH ₂	15	299.1642	299.1648	83-84	27	94

^aHRMS was recorded on a micrOTOF-Q mass spectrometer (Bruker) coupled with an HPLC instrument. ^bIsolated yield. ^cPurity was determined by LC-MS coupled to UV detector, ^d*m/z*: [M-H]⁻. n.d.*: not determined. (*n*_D²⁰): Refractive index.

3.2.5. Miscellaneous modifications

3.2.5.1. Synthesis of *N*⁴-(4-methoxyphenyl)2,4,6-triamino-pyrimidine

The protocols reported for the synthesis of arylaminopyrimidines seem to be quite similar.²²⁴ Elena *et al.* reported a convenient synthetic procedure to generate the pyrimidine derivatives. We used the same strategy to synthesize the title compound. *N*⁴-substituted pyrimidine derivative **91** prepared from 6-chloro-2,4-pyrimidinediamine by a nucleophilic aromatic substitution with *para*-methoxyaniline in the presence of *N,N*-diisopropylethylamine (DIPEA) as a base using dioxane as a solvent as outlined in **Scheme 3.21**.²²⁵ The purification of the product was relatively difficult due to poor separation on silica gel, even when different eluent systems were utilized. Thus, the compound required multiple purification procedures using flash chromatography. This may explain the low isolated yield (26%).



Scheme 3.21. Synthesis of *N*⁴-(4-methoxyphenyl)pyrimidine-2,4,6-triamine

3.2.5.2. Synthesis of diindolylmethane derivatives

Indole-containing compounds are privileged structures in medicinal chemistry²²⁶ endowed with many biological activities such as anti-inflammatory, cytotoxic, antitumour, antiviral, and antimicrobial effects. Indole is an important precursor which is widely used in the synthesis of many drugs, such as indomethacin (**Figure 3.7**). Diindolylmethanes (DIMs), are composed of two indole molecules and display a wide spectrum of pharmacological activities including antibacterial (**Figure 3.7**) and antioxidant activities in addition to being inducers of apoptosis in human cancer cells.^{227,228}

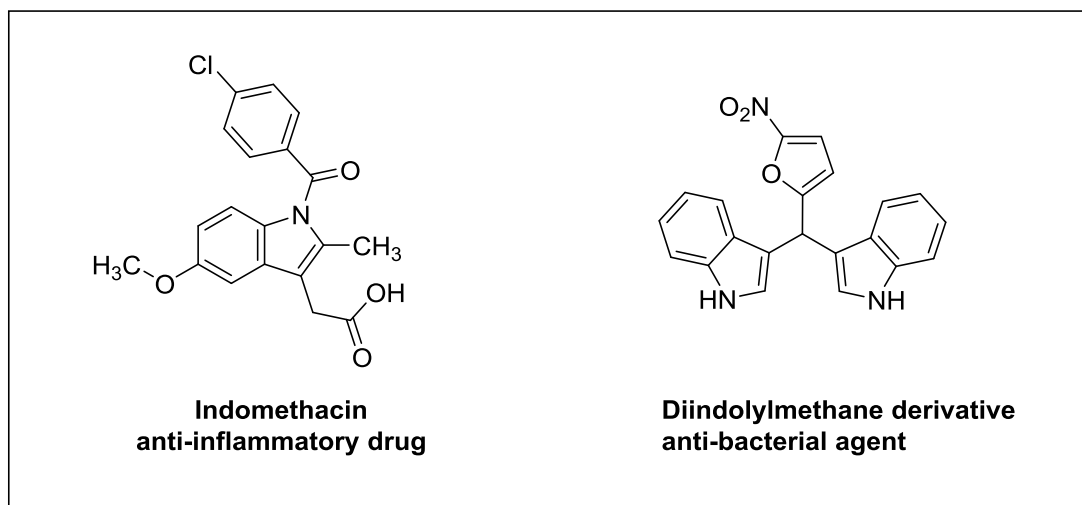
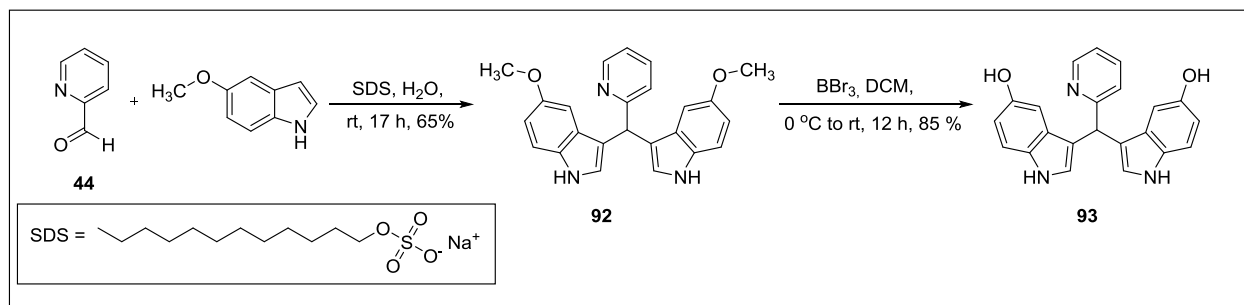


Figure 3.7. Chemical structures of indomethacin and nitrofuryl-diindolylmethane.

For these reasons, we sought to replace the phenol scaffolds of **46** with indole moieties as shown in **Scheme 3.22**. Several studies including that reported by Kobayashi *et al.* demonstrated that surfactants besides Lewis and Brønsted acid catalysis showed positive impact on the formation of the carbon-carbon bond in water. However, many reports suggested the de-activation of Lewis

Results and Discussion

acid catalysts by the nitrogen atom of indole.²²⁹ In the present study, condensation of 5-methoxyindole and 2-pyridinecarbaldehyde (**44**) was done using sodium dodecylsulfate (SDS) as a surfactant in aqueous medium to give the key intermediate diindolylmethane **92** in a good yield.²³⁰ The major advantage of this approach is the use of a green chemistry procedure, in which toxic catalysts and solvents can be avoided. The target compound **93** was prepared in a very good yield through deprotection of the two methoxy groups using boron tribromide in dichloromethane, as outlined in **Scheme 3.22**.



Scheme 3.22. Synthesis of diindolylmethanes **92** and **93**. SDS: sodium dodecylsulfate

Oxadiazole moieties were shown to constitute bioisosteres of urea in the development of β_3 adrenergic receptor agonists.²³¹ They were also demonstrated as bioisosteres for esters and amides. 1,2,4-Oxadiazole-containing molecules are an important class of compounds which possess a wide range of pharmacological applications. Some oxadiazole derivatives are classified as potent antitumor agents, coronary artery dilators, anthelmintic and muscle relaxants,²³² and some oxadiazole derivatives were shown to display antitussive, antiallergic, anti-inflammatory, antiplatelet activity *in vitro*, while others were active as glycogen phosphorylase (GP) inhibitors.²³³ The 1,2,4-oxadiazole ring was selected for its key role in many pharmacologically active compounds. Thus, we aimed to synthesize compounds containing the oxadiazole moiety.

3.2.5.3. Synthesis of 5,5'-(4-(benzyloxy)-1,3-phenylene)-bis-(3-ethyl-1,2,4-oxadiazole) (**99**)

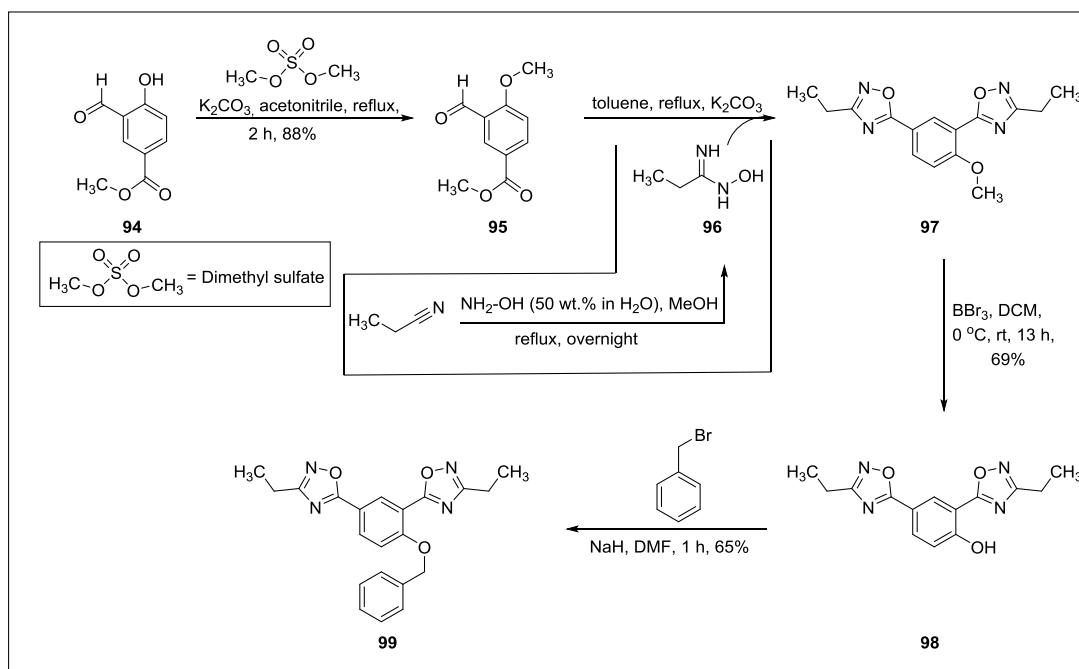
As outlined in **Scheme 3.23**, the synthesis of compound **95** was done by treatment of the commercially available methyl 3-formyl-4-hydroxybenzoate **94** with the alkylating agent dimethyl sulfate in the presence of potassium carbonate as a base using acetonitrile as a solvent. The reaction was performed under reflux and was completed after 2 h affording the corresponding methoxy derivative in 88% yield.²²³ In the next step, the replacement of the ester

Results and Discussion

and aldehyde groups by 1,2,4-oxadiazole rings (**97**) was achieved through the reaction of propionamidoxime (**96**) with compound **95**.²³⁴ Propionamidoxime²³⁵ was synthesized through reaction of propionitrile with hydroxylamine (**Scheme 3.23**).

4.2.1.1.1 3.2.5.3.1. Deprotection of the methoxy group of compound 97

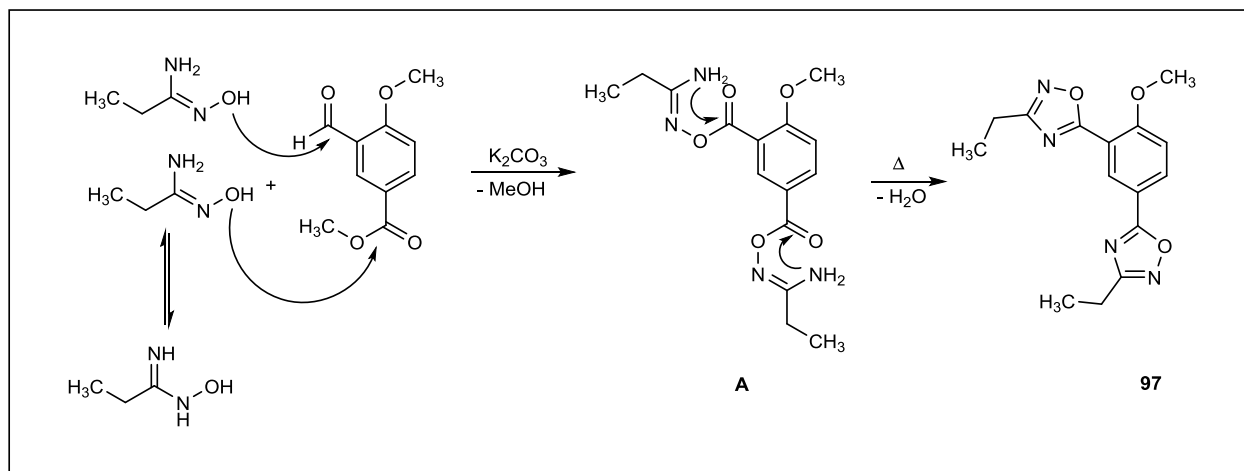
Many deprotecting agents have been demonstrated as efficient tools for removal of methoxy groups to access the corresponding hydroxyl groups. This includes aluminum chloride, lithium chloride and boron tribromide.^{236,237,238} In our study, we tried the *O*-demethylation of compound **97** using boron tribromide in dichloromethane under an argon atmosphere. The reaction started at 0 °C which then reached room temperature. The corresponding hydroxyl derivative **98** was obtained in a good isolated yield without use of any complicated purification procedures. Then, alkylation of the hydroxyl group was performed using benzyl bromide as an alkylating agent and sodium hydride as a base in DMF, and the desired product **99** was obtained in a good yield (**Scheme 3.23**).



Scheme 3.23. Synthesis of 5,5'-(4-(benzyloxy)-1,3-phenylene)-bis-(3-ethyl-1,2,4-oxadiazole) (**99**).

4.2.1.1.2 3.2.5.3.2. Proposed mechanism of the formation of the bis-oxadiazole

Synthesis of *bis*-oxadiazoles can be achieved in two consecutive steps utilizing a base to catalyze the reaction between the propionamidoxime and the carbonyl-containing compound. The cyclization (intramolecular reaction) of the intermediate **A** was achieved at elevated temperature, a process known as thermal cyclization (**Scheme 3.24**).²³⁹



Scheme 3.24. Proposed mechanism of the formation of the *bis*-oxadiazole.²³⁹

5 3.3. Pharmacological evaluation

5.1 3.3.1. Anthraquinone (AQ) derivatives

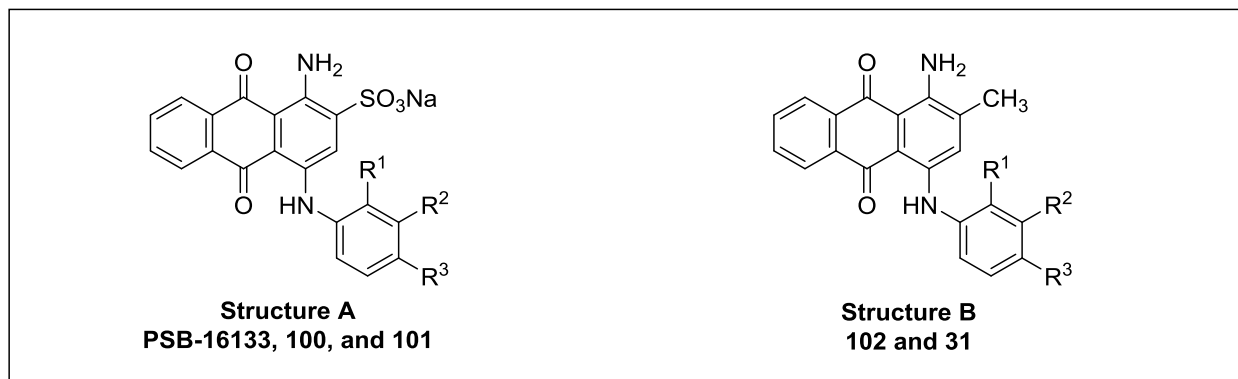
3.3.1.1. Biological evaluation of anthraquinone derivatives (previous results)

Our group has previously studied a number of AQ derivatives as antagonists of different P2 purine receptors. A series of AQ derivatives, structurally related to Reactive Blue 2 (RB-2) and Acid Blue 25 (AB-25) have been synthesized and tested for their antagonistic activity on different P2Y receptors, e.g. P2Y₁₂. Some of these derivatives were bearing a sulfonate group at the 2-position, e.g. **PSB-0739**, while others bear a carboxylic acid group, e.g. **PSB-0702 (Figure 1.28)**. These two derivatives have shown the best affinity for the P2Y₁₂ receptor so far with K_i values of 0.025 μ M and 0.021 μ M, respectively.¹⁴⁵

Because of the success of these compounds, a library of AQ derivatives was synthesized in order to develop potent anthraquinones (AQs) for other target receptors. The activity of AQs has been studied at several P2Y receptor subtypes. **PSB-16133**, sodium 1-amino-4-[4-(2,4-dimethylphenylthio)phenylamino]-9,10-dioxo-9,10-dihydroanthracene-2-sulfonate, was found to be a potent antagonist at the human P2Y₄ receptor with an IC_{50} = 0.233 μ M. Compound **100** showed a lower potency (IC_{50} = 1.70 μ M) that was completely abolished when the 2-sulfonate group was replaced with a methyl group (**102**). In comparison to compound **101** bearing a sulfonate at the 2-position, which was inactive at 100 μ M, there was no improvement in the activity upon replacement of the acidic group with a methyl residue (**31**) (**Table 3.14**).²⁴⁰

Results and Discussion

Table 3.14. Inhibitory potencies of selected AQ derivatives on the human P2Y₄ receptor²⁴⁰



compd	R ¹	R ²	R ³	IC ₅₀ ± SEM (μM) ^a (or % inhibition at indicated concentration)
-------	----------------	----------------	----------------	---

Structure A

PSB-16133	H	H		0.233 ± 0.079
100	H	OMe	H	1.70 ± 0.28
101	CO ₂ H	H	F	>100 (17%) ^b

Structure B

102	H	OMe	H	>30 (38%) ^c
31	CO ₂ H	H	F	≈100 (57%) ^b

^aPotency to inhibit calcium mobilization induced by receptor activation with UTP in 1321N1 astrocytoma cells stably transfected with the human P2Y₄ receptor. ^bPercent inhibition at 100 μM. ^cPercent inhibition at 30 μM.²⁴⁰

3.3.1.2. Potency of newly synthesized AQ derivatives on the human P2Y₄ receptor

The AQ derivatives synthesized as part of this project were assessed for antagonistic potency on the human P2Y₄ receptor in Ca²⁺ mobilization assays using stably transfected 1321N1 astrocytoma cells. A monoclonal human P2Y₄ cell line was created and Ca²⁺ measurements on the P2Y₄ receptor were performed by Dr. Muhammad Rafehi according to a previously published procedure.²⁴⁰ Poor solubility of the compounds in aqueous buffer was noted during the screening

Results and Discussion

process due to the lipophilicity of the derivatives. To overcome this challenge and to avoid precipitation during the assay, all compounds were screened at a micromolar concentration level. Unfortunately, all of the synthesized AQ derivatives having a methyl group at the 2-position were found inactive when the screening was conducted at 1 μM . Thus it appears that the acidic function in this position is required for the activity. Based on a homology model previously established by our group, it seems that the lack of the sulfonate group at the 2-position is responsible for the loss of the activity of these 2-methyl-AQ derivatives. We believe that the acidic functionality is essential for strong electrostatic and hydrogen bonding interactions with amino acids Lys179 and Arg272 of the human P2Y₄ receptor.²⁴⁰

AQs may also be antagonists at P2X receptor subtypes. A series of AQ derivatives structurally related to RB-2 yielded **PSB-1011** and **PSB-10211** as P2X₂ antagonists with IC₅₀ values of 0.079 μM , and 0.086 μM , respectively. These two derivatives represented the first potent and selective competitive P2X₂ receptor antagonists. Based on the success of these compounds, we aimed to find superior potent and selective AQ derivatives with enhanced potency for other P2X receptors.⁶⁴

3.3.1.3. Potency on the human P2X₃ receptor

A monoclonal human P2X₃ cell line was created and Ca²⁺ measurements on P2X₃ were done by Dr. Aliaa Abdelrahman. P2X₃ receptor blockade was determined by measuring agonist-mediated increases in cytosolic Ca²⁺ concentration.

The synthesized 1-amino-2-methyl-4-substituted AQ derivatives were investigated for their activity on the human P2X₃ receptor using Ca²⁺ mobilization assay. In **Figure 3.8**, examples of concentration-inhibition curves of the two active AQ derivatives **6** and **22** are depicted.

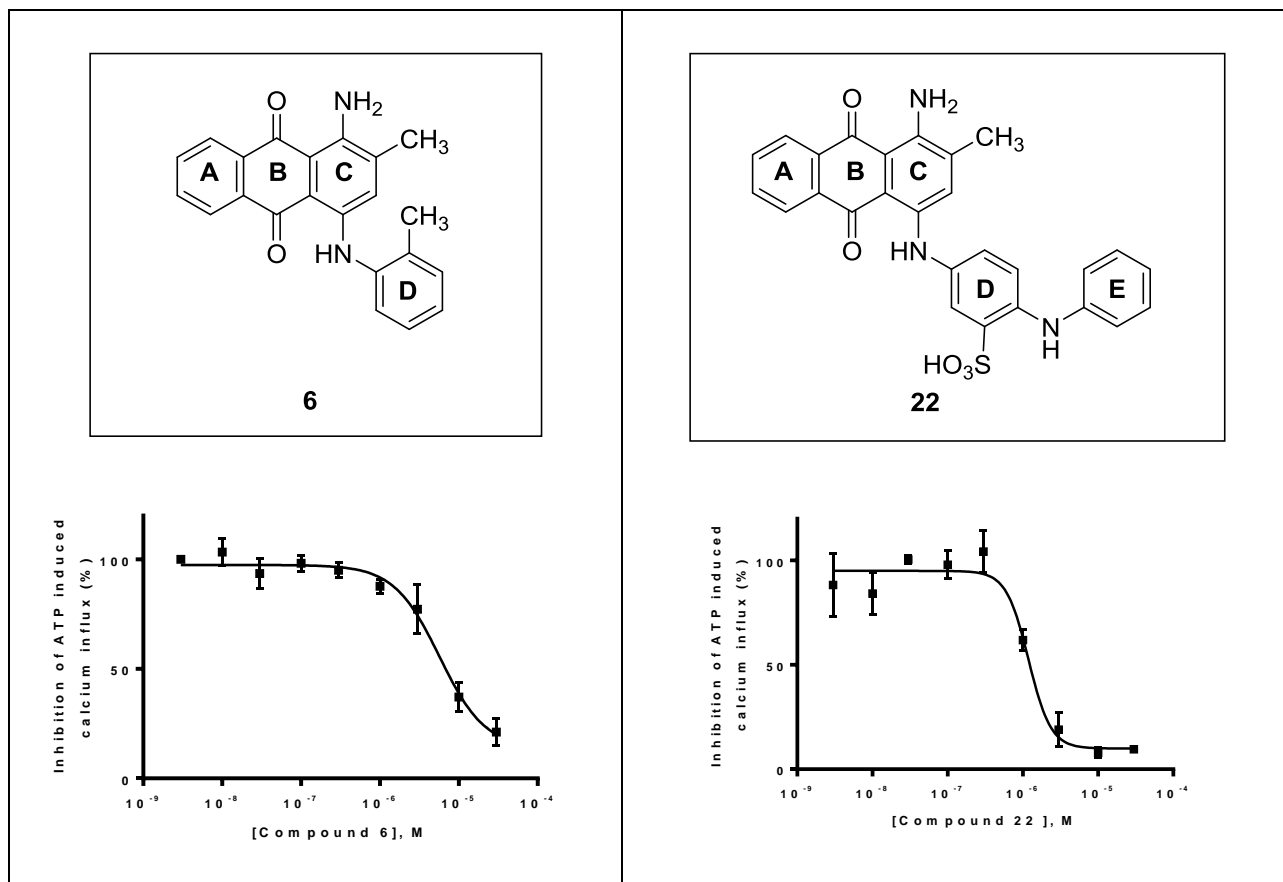
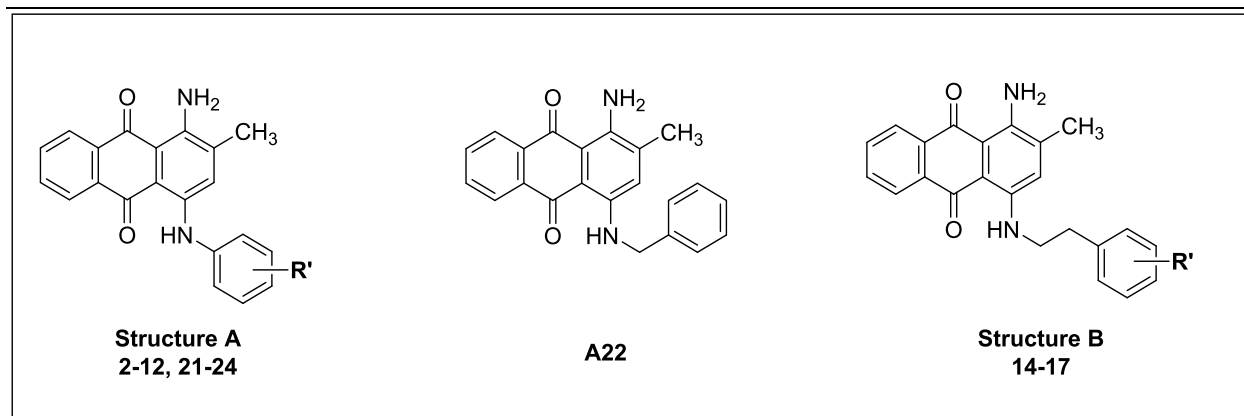


Figure 3.8. Concentration-inhibition curves of the two active AQ derivatives **6** and **22** on the human P2X3 receptor. IC₅₀ values (μM): **6**, 7.46 ± 1.25; **22**, 3.07 ± 1.14.

All AQ derivatives bearing a methyl group at the 2-position were inactive at the P2X3 receptor at 10 μM except for compounds **6** and **22** (Table 3.15). Compound **23** was found inactive although it shows the same pattern of rings as **22** but without the sulfonate group at the C-3' position in ring D. Electrostatic interactions are likely to be generated between the negatively charged sulfonate group and positively charged amino acids of the P2X3 receptor. Interestingly, compound **6** (IC₅₀ = 7.46 μM) which was anticipated to completely lose the activity as a result of lacking E ring was found active with only 2-fold lower potency when compared to compound **22**.

Table 3.15. Potencies of AQ derivatives on the human P2X3 receptor



Cmpd	R'	IC ₅₀ ± SEM [μM] (% Inhibition at 10 μM)	Cmpd	R'	IC ₅₀ ± SEM [μM] (% Inhibition at 10 μM)
2	H	>10 (16 ± 7)	18	2-CO ₂ H	>10 (20 ± 8)
			19	3-CO ₂ H	>10 (32 ± 2)
3	2-C ₂ H ₅	>10 (22 ± 4)	20	4-CO ₂ H	>>10 (10 ± 5)
4	3-C ₂ H ₅	>10 (1 ± 3)	21	2-CO ₂ H- 4-F	>10 (21 ± 9)
5	4-C ₂ H ₅	>10 (23 ± 4)	22	3-SO ₃ H- 4-NHC ₆ H ₅	3.07 ± 1.14
6	2-CH ₃	7.46 ± 1.25	23	4-NHC ₆ H ₅	>10 (25 ± 11)
7	2-Cl	>10 (30 ± 5)	24	3-OH	>>10 (-3 ± 8)
8	3-Cl	>10 (5 ± 5)	Structure B		
9	4-Cl	>10 (17 ± 7)	14	2-Cl	>>10 (13 ± 2)
10	2-OCH ₃	≥10 (51 ± 9)	15	3-Cl	>>10 (2 ± 3)
11	3-OCH ₃	n.d.*	16	4-Cl	>10 (18 ± 18)
12	4-OCH ₃	>10 (14 ± 3)	17	3-F	>>10 (3 ± 1)
13	see structure above	>>10 (2 ± 2)			

n.d.* not determined

Results and Discussion

In conclusion, a small library of 22 AQ derivatives bearing a methyl group at the 2-position were evaluated for their inhibitory activity on the human P2X3 receptor. Compound **22** having an ABCDE ring system with a sulfonate group at the C-3' position in ring D showed a promising result. Moreover, the small compound **6** displayed some P2X3-inhibitory activity. Our results indicate that the AQ derivatives may have different binding modes depending on the substitution patterns.

Possible approaches for enhancing the activity of AQ derivatives on the human P2X3 receptor.

- (1) Synthesis of analogues of compound **22** with variations of substituents on ring D while keeping the acidic functionality (SO₃H or COOH) in addition to having NH as a linker, or replacing the NH linker by oxygen or sulfur.
- (2) Introduction of substituents to ring E to determine the optimal residue which may enhance the activity (**Figure 3.9**).

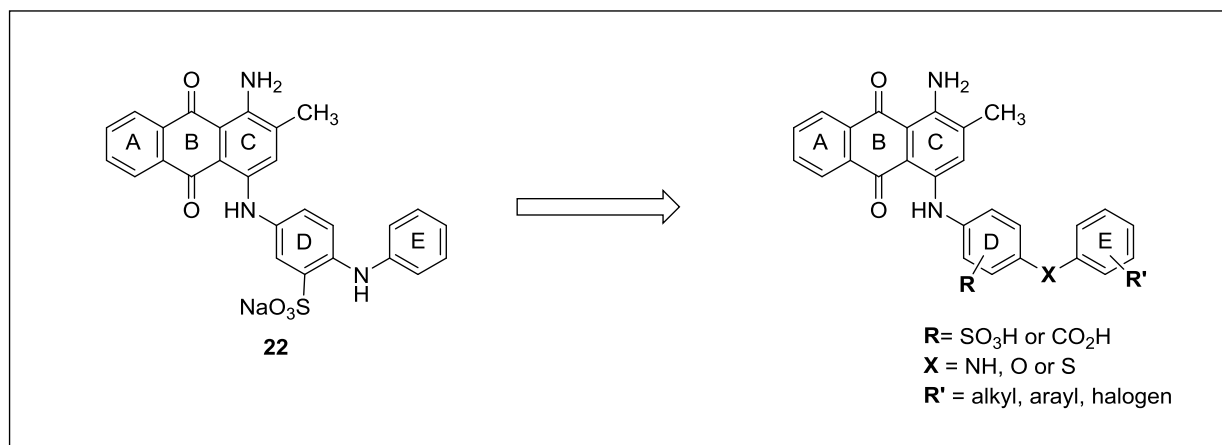


Figure 3.9. Proposed modifications of AQ **22** for potential enhancement of the inhibitory activity at the human P2X3 receptor.

5.2 3.3.2. *Bisacodyl-derived compounds*

3.3.2.1. Biological evaluation of the synthesized bisacodyl-derived compounds

The bisacodyl-related compounds synthesized in the present study were investigated for their inhibitory potency on the P2X₃ receptor. Initially, the compounds were screened at four different concentrations (0.01 μ M, 0.10 μ M, 1 μ M, and 10 μ M). Compounds which showed an inhibition of $\geq 50\%$ at 10 μ M were further characterized and concentration-inhibition curves were generated from which IC₅₀ values could be determined. The results of the synthesized compounds will be discussed, however for comparison purposes, examples of other bisacodyl derivatives or compounds from the literature will be included.

3.3.2.1.1. Inhibitory potency of bisacodyl-derived compounds on the human P2X₃ receptor and study of structure-activity relationships

The synthesized bisacodyl-derived compounds were biologically evaluated on the human P2X₃ receptor. The evaluation of the hit compound and all the derivatives were done using calcium mobilization assays in transfected 1321N1 astrocytoma cell lines. Examples of concentration-inhibition curves of the most potent bisacodyl-derived compounds are depicted in **Figure 3.10**.

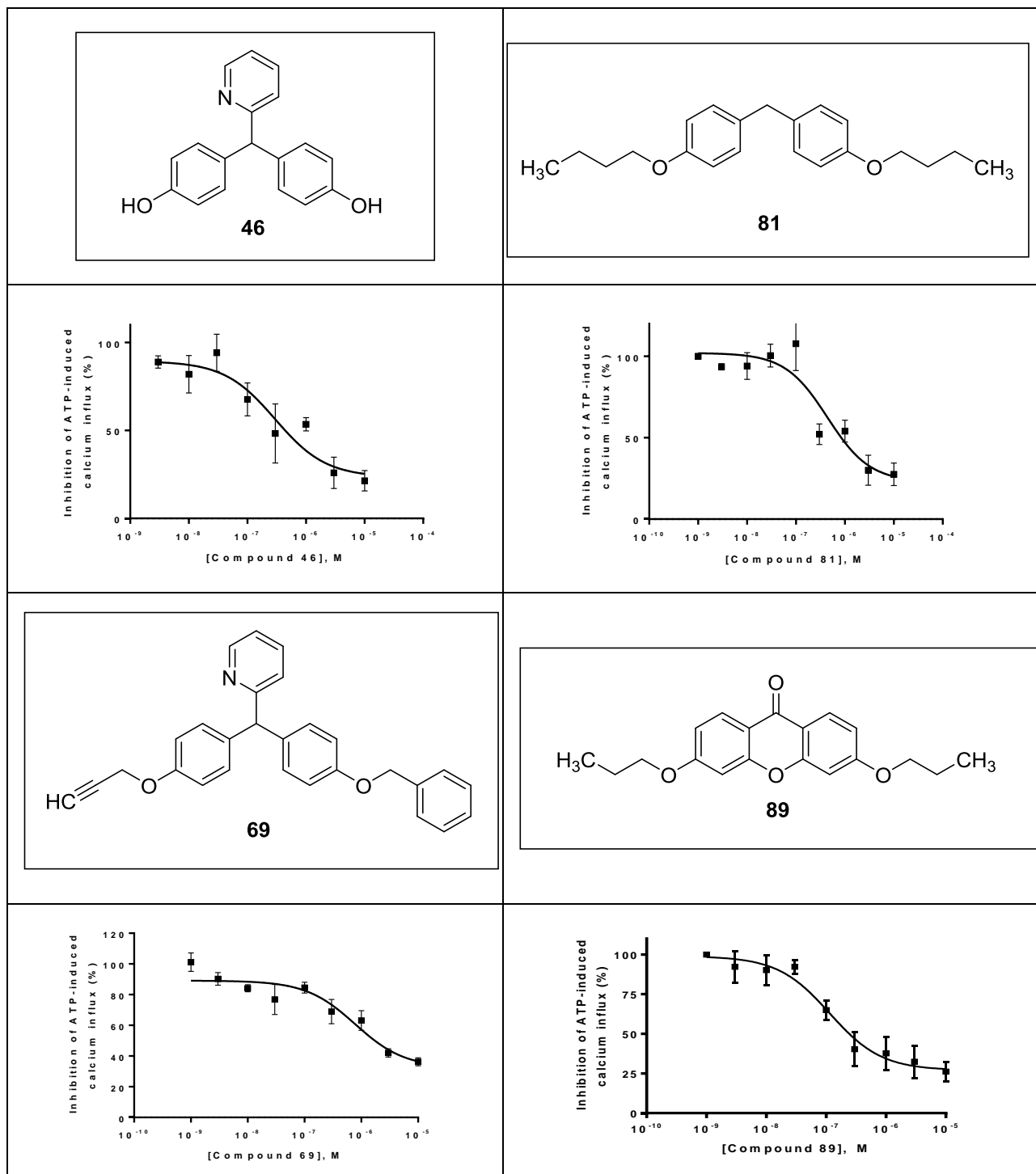
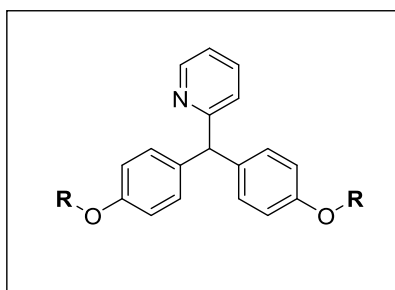


Figure 3.10. Concentration-inhibition curves of selected bisacodyl-derived compounds on the human P2X3 receptor. IC₅₀ values (μM): **46**, 0.421 ± 0.196; **81**, 0.493 ± 0.115; **69**, 0.645 ± 0.144; and **89**, 0.121 ± 0.012.

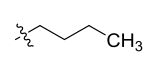
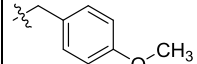
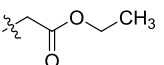
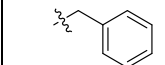
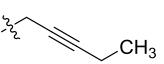
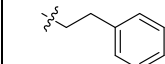
Results and Discussion

The evaluation was aimed to investigate the effects of substituents at different positions on the inhibitory activity of compounds at the P2X3 receptor. Our studies demonstrated that bisacodyl was identified as a potent antagonist on the human P2X3 receptor with an IC_{50} value of 1.59 μ M. Interestingly, the hydrolyzed product, diphenol **46**, which was obtained via removal of the di-acetyl residues, was found to be more active with an IC_{50} value of 0.421 μ M. This compound was chosen as a lead structure. We were interested to test the effects of other substituents in place of the di-hydroxyl groups at the 4,4'-positions on the activity. Thus, a total of 22 derivatives were obtained via etherification of the phenolic hydroxyl groups with either aliphatic or aromatic residues (different lengths, linear, unsaturated, or branched chains). On the other hand, we were interested in testing the effect of modifying the position of the hydroxyl groups and of simplification of the hit structure on the inhibitory activity at P2X3 receptors. The analysis of the structure-activity relationships of the synthesized derivatives of these series could give more insights in possible interactions between bisacodyl-derived ligands and the P2X3 receptor. **Table 3.16** and **Table 3.17** list the IC_{50} values of selected derivatives.

Table 3.16. Inhibitory potency of symmetrical bisacodyl derivatives on the human P2X3 receptor



Cmpd	R	$IC_{50} \pm SEM$ (μM) (% inhibition at 10 μ M)	Cmpd	R	$IC_{50} \pm SEM$ (μM) (% inhibition at 10 μ M)
Bisacodyl	COCH ₃	1.59 \pm 1.37 (79 \pm 3)*	46	H	0.421 \pm 0.196 (81 \pm 6)*
58		≥ 10 (46 \pm 5)	49		1.08 \pm 0.22 (58 \pm 2)*
62		> 10 (32 \pm 23)	63		> 10 (19 \pm 8)

Cmpd	R	IC ₅₀ ± SEM (μM) (% inhibition at 10 μM)	Cmpd	R	IC ₅₀ ± SEM (μM) (% inhibition at 10 μM)
57		2.72 ± 0.53 (71 ± 15)*	64		>>10 (20 ± 20)
59		2.48 ± 0.67 (92 ± 2)*	65		>10 (37 ± 8)
60		1.65 ± 0.55 (63 ± 3)*	66		>10 (44 ± 5)

*Maximal inhibition observed.

3.3.2.1.2. Effects of symmetrical substitution of the bisacodyl-derived drug 46 on the inhibitory activity

Symmetrical substitution of the di-hydroxyl groups either with aliphatic residues, methoxyethyl **58**, octyl **62**, or with aromatic residues, e.g. *para*-methoxybenzoyl **63**, *para*-methoxybenzyl **64**, benzyl **65**, or phenethyl **66** abolished the activity (**Table 3.16**). The symmetric benzyl derivative **65** showed only 37% inhibition when tested at 10 μM. The introduction of a methoxy group in the *para*-position of the benzyl moiety (**64**) increased the lipophilicity of the compound but had no impact on the inhibitory activity. No enhancement of the activity was observed when the length of the carbon chain between the phenyl ring and the oxygen atom was increased to two methylene units (**66**) instead of one (**65**). This observation indicates that the symmetric substitution with bulky residues on both sides completely abolishes the activity.

In order to investigate the impact of aliphatic side chains on the inhibitory activity, many derivatives with various residues were prepared. Previously, the effect of aliphatic substitutions had been limited to the methoxy, ethoxy and propoxy derivatives which were synthesized in our group by M. Sc. The-Hung Vu. The preliminary results revealed that the elongation of the attached aliphatic side chains did not improve the affinity towards the P2X3 receptor as compared to the hydrolyzed diphenol **46**. However, it was shown by our group that the di-substituted propoxy derivative is more potent than the ethoxy derivative which is also more potent than the methoxy derivative. To have a broader picture about the elongation of this carbon

Results and Discussion

chain, we additionally synthesized the butyl and octyl derivatives. We also modified the carbon chains to branched and unsaturated ones.

The introduction of symmetrical aliphatic chains with different residues led, as shown in **Table 3.16**, to a lower activity compared to the hydrolyzed diphenol compound **46**. For instance, the butyl derivative **57** and the *sec*-butyl derivative **49**, showed almost identical IC₅₀ values of 2.72 and 1.08 μM, respectively. The symmetrical 2-pentyne derivative **60** was found to be almost 4-fold less potent than the hydrolyzed diphenol **46**. No improvement in the potency was observed upon introducing the symmetrical ethyl acetate residues in compound **59**, resulting in an IC₅₀ value of 2.48 μM.

Comparing the biological activity of bisacodyl derivatives with different substituents, it was noticed that the introduction of symmetrical substitutions with aromatic moieties at the 4,4'-positions completely abolished the activity, whereas symmetrical substitutions with aliphatic moieties at the same positions were tolerated, but less favorable as compared to the lead structure **46**. A long aliphatic residue such as an octyl chain completely abolished the activity.

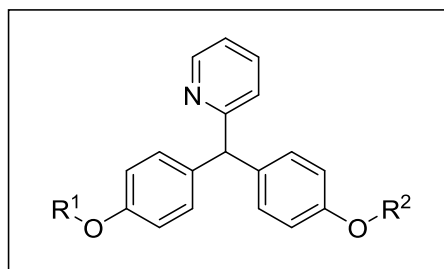
5.2.1.1.1 3.3.2.1.3 Effects of asymmetrical substitutions of leads structure 46 on the inhibitory activity

Compound **47** that was obtained by cleavage of only one acetyl group of bisacodyl showed only 46% inhibition of ATP-induced P2X₃ activation when screened at 10 μM. A surprising finding was that when one hydroxyl group of **46** was substituted with an aliphatic residue e.g. butan-1-ol (**52**), the activity was completely lost (**Table 3.17**). The asymmetric butyl derivative **48** was found to be slightly less active than its symmetric analog **57**. In contrast, the asymmetric octyl derivative **53** showed an increase in the inhibitory activity in comparison to the symmetric octyl derivative **62**. The presence of a long side chain such as an octyl residue leads to an increase in the lipophilicity and positively effects on the activity. Replacement of bromine in the asymmetric derivative **50** by a morpholine moiety led to an increase in the bulkiness in the case of **67**, which may explain the slight increase in potency. The combination of a bromine containing side chain with a *sec*-butyl moiety, in the case of **68**, resulted in an insignificant, 2-fold increase in the activity with an IC₅₀ value of 1.69 μM compared to **50**.

Results and Discussion

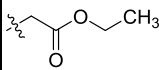
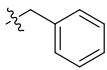
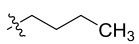
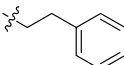
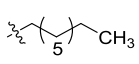
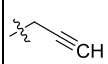
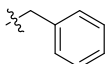
The antagonistic potency of asymmetric benzyl-containing derivative **55** was demonstrated with an IC_{50} value of $3.70 \mu\text{M}$, while the presence of two benzyl residues in **65** led to no inhibitory activity when screened at $10 \mu\text{M}$. The activity was dramatically increased to the nanomolar range when the hydroxyl group of **55** was substituted with a propargyl residue (**69**), resulting in a more than 5-fold potency increase with an IC_{50} of $0.645 \mu\text{M}$ as compared to **55**. In comparison to **55**, the asymmetric *para*-methoxybenzoyl derivative **54** led to a slight increase in potency with an IC_{50} of $1.17 \mu\text{M}$, while the symmetric compound **63** did not show any potency when tested at $10 \mu\text{M}$. Compound **56** differs from **55** by the presence of one methylene group more in the bridge between the phenyl ring and the oxygen atom. This difference increased the lipophilicity and led to a 2-fold insignificant increase in potency. These results suggest that combination between a propargyl residue in (**69**) and a phenethyl group of (in **56**) may enhance the inhibitory potency to the low nanomolar range. However, it has to be noted that the inhibition, especially by the more lipophilic compounds, was only partial (see **Figure 3.10**).

Table 3.17. Inhibitory potency of some bisacodyl derivatives with asymmetrical substitution on the human P2X3 receptor



Cmpd	R ¹	R ²	IC ₅₀ ± SEM (μM) (% inhibition at 10 μM)	Cmpd	R ¹	R ²	IC ₅₀ ± SEM (μM) (% inhibition at 10 μM)
47	H	-COCH ₃	>10 (46 ± 3)	52	H		>10 (35 ± 10)
50	H		3.35 ± 1.01 (86 ± 4)*	68			1.69 ± 0.35 (81 ± 5)*
67	H		2.26 ± 1.07 (75 ± 7)*	54	H		1.17 ± 0.58 (76 ± 8)*

Results and Discussion

Cmpd	R ¹	R ²	IC ₅₀ ± SEM (μM) (% inhibition at 10 μM)	Cmpd	R ¹	R ²	IC ₅₀ ± SEM (μM) (% inhibition at 10 μM)
51	H		3.97 ± 0.72 (81 ± 5)*	55	H		3.70 ± 1.12 (64 ± 6)*
48	H		3.66 ± 0.98 (101 ± 4)*	56	H		1.47 ± 0.30 (92 ± 3)*
53	H		1.58 ± 0.44 (85 ± 4)*	69			0.645 ± 0.144 (64 ± 3)*

*Maximal inhibition observed.

These findings demonstrate that the inhibitory activity associated with symmetrical and unsymmetrical substitution by aliphatic side chains is not satisfactory. The symmetrical substitution with aromatic side chains led to complete loss of activity, while the combination of different residues in unsymmetrically substituted compounds retained some inhibitory activity. It can be concluded that the most potent compounds among the bisacodyl derivatives are **46** and **69** with IC₅₀ values of 0.421 and 0.645 μM, respectively. The binding mode of **69** may be as follows: The propargyl residue may interact through hydrophobic interactions. The second residue may interact through π-π interactions. Both interactions probably increase the inhibitory activity. On the other hand, the hydrolyzed diphenol **46** may display a different binding mode.

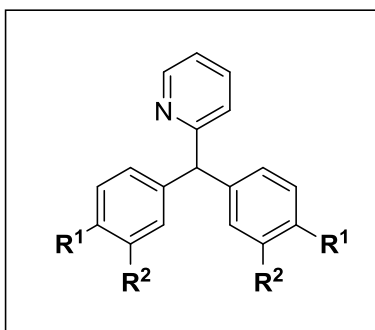
In order to elucidate the impact of the position of the residues, several modifications were carried out. For example, as seen in **Table 3.18**, we completely removed the hydroxyl functionalities in **75** or introduced fluorine atoms instead of the hydroxyl groups in **76**. We also combined fluorine and hydroxyl groups in **77** or replaced the fluorine atoms by other halogen atoms such as iodine in **78**. In addition, we also alkylated the hydroxyl groups of **78** resulting in **78a**.

The importance of the hydroxyl groups at the 4,4'-positions of hit structure **46** was evaluated either by their removal in case of compound **75** or by replacing them with fluorine atoms (**76**). The activity in both cases dropped by 13-fold as compared to the hit structure **46**. The combination of fluorine atoms with hydroxyl groups was not tolerated in the case of **77**. When the fluorine atom was replaced with another bigger halogen atom such as iodine, the activity was restored **78**. In contrast, replacing the hydroxyl groups of compound **78** with methoxy residues in

Results and Discussion

78a, increased the lipophilicity of the phenyl rings but had a negative impact on the inhibitory activity (**Table 3.18**).

Table 3.18. Inhibitory potencies of selected bisacodyl-derived compounds **75-78a** on the human P2X3



Cmpd	R ¹	R ²	IC ₅₀ ± SEM (μM) (% inhibition at 10 μM)	Cmpd	R ¹	R ²	IC ₅₀ ± SEM (μM) (% inhibition at 10 μM)
75	H		5.67 ± 0.68 (68 ± 4)*	78	-OH	I	1.63 ± 0.21 (98 ± 3)*
76	F	H	5.83 ± 1.25 (64 ± 8)*	78a	-OCH ₃	I	>>10 (5 ± 12)
77	OH	F	>10 (32 ± 7)				

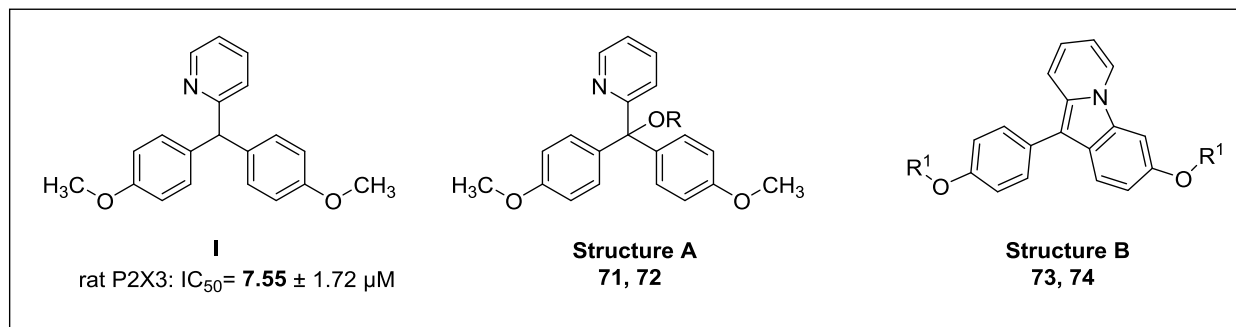
*Maximal inhibition observed.

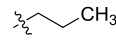
As a next step, we investigated the effects of substituents at the central carbon atom (**Table 3.19, structure A**). The introduction of a hydroxyl group resulted in a loss of the inhibitory potency (**71**) in comparison with the same structure without the alcoholic functionality, which had been previously synthesized by M.Sc. The-Hung Vu and was tested on rat P2X3 receptor with an IC₅₀ value of 7.55 μM (**I, Table 3.19**).¹⁹⁵ In contrast, the alkylation of the alcoholic hydroxyl group with a propyl residue in compound **72** unexpectedly led to an increase in activity yielding an IC₅₀ value of 1.62 μM. There might be species differences between rat and human P2X3 receptors and the direct comparison may be not be accurate, since previous studies were performed at the rat P2X3 receptor but we can conclude that the propyl ether substitution at that position might be

Results and Discussion

profitable. Concerning the alcoholic functionality, the removal of this hydroxyl group via cyclization (**73**) abolished activity. Methyl ether **73** was less potent than bisphenol (**74**, Table 3.19, structure B).

Table 3.19. Inhibitory potencies of carbinol derivative **71**, its propyl derivative **72**, cyclized form of carbinol **73** and its hydroxylated derivative **74**



Cmpd	R	IC ₅₀ ± SEM (μM) (% inhibition at 10 μM)	Cmpd	R ¹	IC ₅₀ ± SEM (μM) (% inhibition at 10 μM)
Structure A			Structure B		
71	H	≥10 (44 ± 7)	73	CH ₃	≥10 (52 ± 7)
72		1.62 ± 0.61 (75 ± 8)*	74	H	4.53 ± 1.13 (78 ± 13)*

*Maximal inhibition observed.

There seems to be a negative effect due to by the presence of an alcoholic hydroxyl group instead of a hydrogen atom on the central carbon. We noticed an improvement upon replacing it with a propyl ether group.

3.3.2.1.4. Effects of simplification of the lead structure (46)

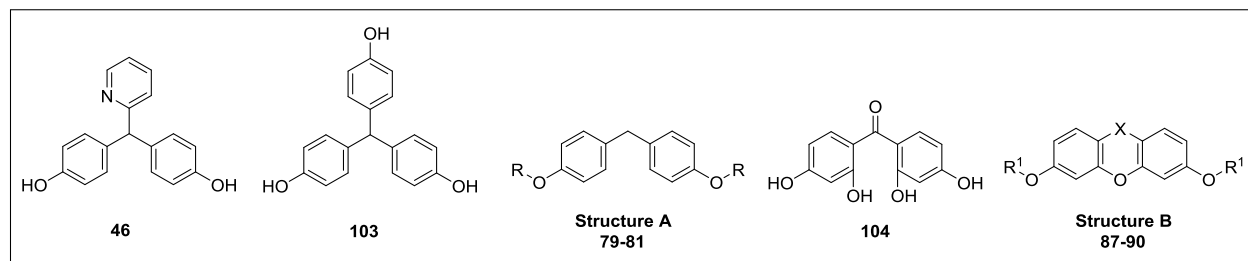
5.2.1.1.2 3.3.2.1.4.1. Replacement or removal of the pyridine ring

Replacement of the pyridine ring by a phenol moiety in case of the commercially available compound **103** (tris-(4-hydroxyphenyl)methane) resulted in a loss of the activity. The attempt to completely remove the pyridine ring in (**79**), resulted in a 3-fold decrease in the activity compared to the compound with the pyridine ring (**46**). Introduction of propyl ether residues instead of the di-hydroxyl groups of **79** (**80**, **Table 3.20**) had no change in the activity compared to compound **79**. Surprisingly, the introduction of a hydrophobic butyl group in case of **81**, which increases the lipophilicity, had a positive impact on the inhibitory activity with a 5-fold increase in the potency, resulting in an IC_{50} value of 0.493 μ M in comparison with (**57**, **Table 3.16**, IC_{50} = 2.72 μ M). This compound is equipotent to **46** (IC_{50} = 0.421 μ M).

Initially, we were aiming to form the xanthone scaffold in order to see the effect of the molecule's planarity on its activity. Commercially available compound **104** was completely inactive. Unfortunately, the xanthone compound **87** did not show any significant activity, with only 22% inhibition at 10 μ M. We then removed the carbonyl group by reduction, thus obtaining the xanthene compound **88**. However, the activity of the compound was not determined because the compound interfered with the dye used for biological testing. Interestingly, changing the hydroxyl groups of xanthene **88** with propyl residues **90**, had no pronounced effect on the inhibitory activity. Surprisingly, the propyl derivative of the xanthone (**89**) was found to be the most potent compound of the present series, with an IC_{50} value of 0.121 μ M on the human P2X3 receptor. The presence of a carbonyl group on the xanthone resulted in a higher potency (34-fold) in comparison to **90**. Compound **89** was found to be 3-fold more potent than the hit compound **46**. This result demonstrates that the pyridine ring can be replaced by a carbonyl group in the presence of hydrophobic groups such as propyl which may interact through hydrophobic interactions.

Results and Discussion

Table 3.20. Inhibitory potencies of selected compounds related to bisacodyl on the human P2X3 receptor



Cmpd	R	IC ₅₀ ± SEM (μM) (% inhibition at 10 μM)	Cmpd	R ¹	X	IC ₅₀ ± SEM (μM) (% inhibition at 10 μM)
103	See structure above	>>10 (10 ± 5)	104	See structure above		>>10 (-13 ± 4)
Structure A			Structure B			
79	H	1.26 ± 0.11 (75 ± 8)*	87	H	COCH ₂	>>10 (22 ± 12)
80		1.10 ± 0.36 (73 ± 3)*	88	H	CH ₂	Interferes with the experiment
81		0.493 ± 0.115 (71 ± 9)*	89		COCH ₂	0.121 ± 0.012 (74 ± 6)*
			90		CH ₂	4.11 ± 0.87 (92 ± 4)*

*Maximal inhibition observed.

3.3.2.1.5. Miscellaneous modifications

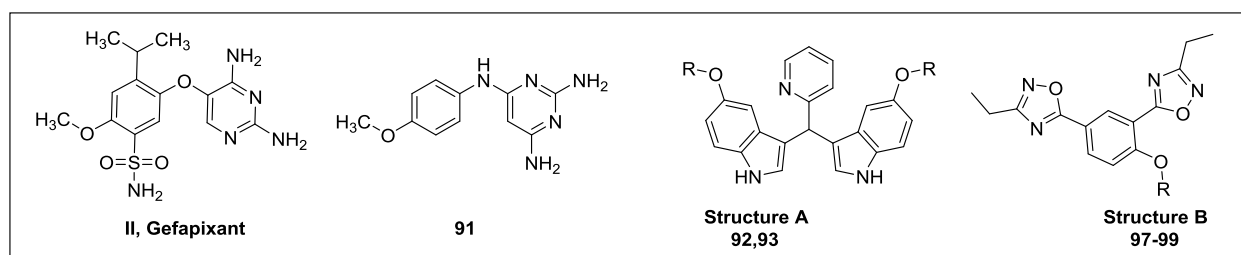
The diaminopyrimidine class of compounds comprises a lot of potent P2X3 antagonists such as **Gefapixant (II, Table 3.21)**, which has been evaluated in a phase II clinical trial and the result was positive in patients with chronic refractory cough. In our case, the introduction of a diaminopyrimidine moiety (**91**) did not result in any inhibitory activity. The positions of the amino groups may be inadequate.

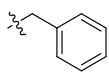
Results and Discussion

Then, we tried to explore structures with an indole moiety. Replacement of the *bis*-phenol moieties by symmetrical 5-methoxy indoles (**92**) or the corresponding hydroxyl derivative (**93**, **Table 3.21**, **structure A**), had a negative impact on the inhibitory activity.

We decided to explore structures with *bis*-oxadiazole moieties on the phenyl ring. Compound **97** and **98** were inactive at 10 μ M. The introduction of a benzyl group in **99** showed a slight increase in the potency with an IC_{50} value in the micromolar range (**Table 3.21**, **structure B**).

Table 3.21. Inhibitory potencies of compounds **91-93** and compounds **97-99**



Cmpd	R	$IC_{50} \pm SEM$ (μ M) (% inhibition at 10 μ M)	Cmpd	R	$IC_{50} \pm SEM$ (μ M) (% inhibition at 10 μ M)
Structure A			Structure B		
91	See structure above	$\gg 10$ (12 ± 7)	97	CH ₃	>10 (37 ± 10)
92	CH ₃	$\gg 10$ (27 ± 7)	98	H	>10 (21 ± 3)
93	H	$\gg 10$ (21 ± 9)	99		5.44 \pm 1.12 (96 \pm 5)*

*Maximal inhibition observed.

For further confirmation of our data, different concentrations of bisacodyl, compounds **46**, **81** and **89** were tested for inhibition of ATP-induced calcium influx in 1321N1 astrocytoma cells stably transfected with the human P2X3 receptor. We found that all compound attenuated ATP-induced calcium influx in a dose-dependent manner. Notably, higher concentrations of compounds **81** and **89** almost completely inhibited ATP-induced calcium influx (**Figure 3.11**).

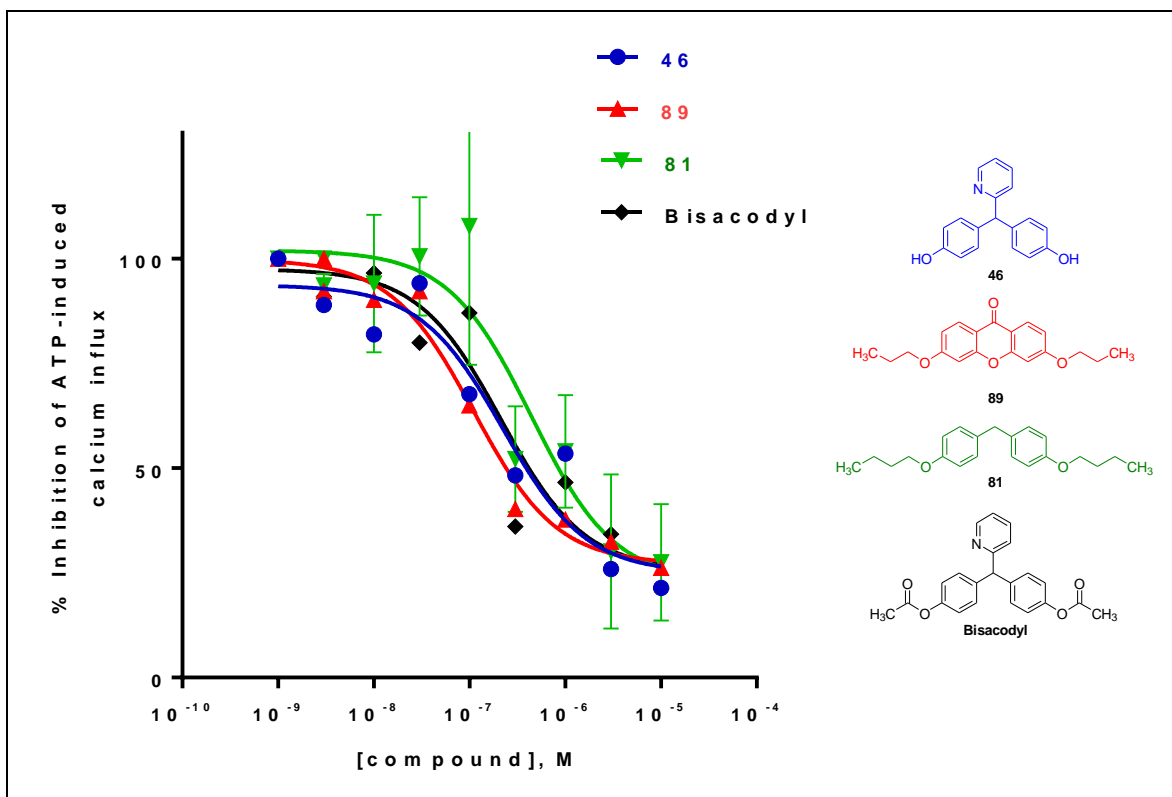


Figure 3.11. Concentration-inhibition curves of the most potent bisacodyl-derived compounds on the human P2X3 receptor.

Detailed structure-activity relationships of selected bisacodyl-derived compounds are summarized in **Figure 3.12** and **Figure 3.13**. These findings might help in the development of new potent and selective compounds for the human P2X3 receptor to fully understand their structure-activity relationships.

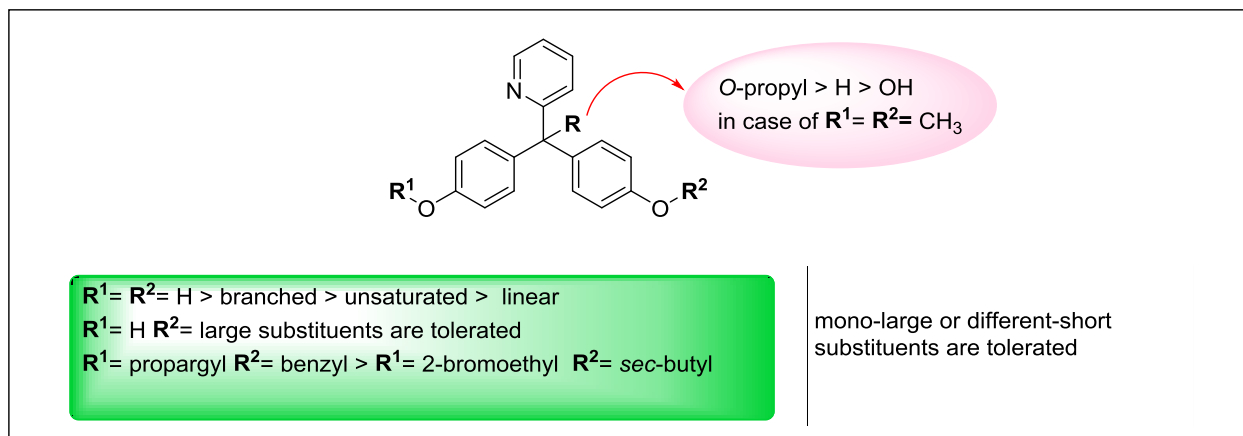


Figure 3.12. Structure-activity relationships of selected bisacodyl-derived compounds (**46**, **48-56**, **57-66**, **71** and **72**) on the human P2X3 receptor.

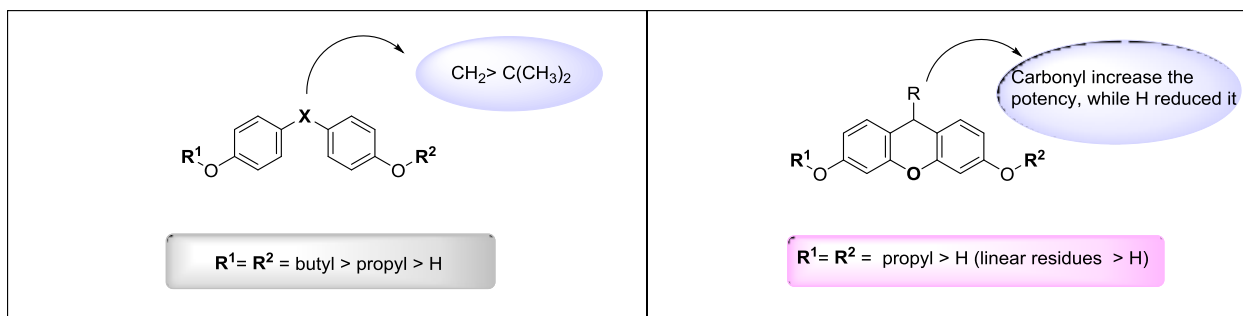


Figure 3.13. Structure-activity relationships of selected bisacodyl-derived compounds (**80**, **81**, and **87-90**) on the human P2X3 receptor.

3.3.2.2. Pharmacophore model

In order to understand and rationalize important structural features of human P2X3 receptor antagonists, we generated a pharmacophore model based on a very potent compound which possesses a 4-oxo-quinazoline as a central ring, namely *N*-(4-(3-(2,5-dimethoxyphenethyl)-4-oxo-3,4-dihydroquinazolin-6-yl)-3-methoxyphenyl)acetamide showing an IC_{50} value of 0.005 μM (**Figure 3.14**). The pharmacophore model may rationalize the observed structure-activity relationships between the potent antagonist and the newly synthesized molecules described in the previous section. Furthermore, the model possibly helps to design new potent compounds.

3.3.2.2.1. Pharmacophore model features

The pharmacophore model revealed two hydrophobic pockets, one constituted by the phenyl ring which is attached to the quinazoline moiety at the 6-position (**F1**), and the other hydrophobic pocket is represented by the phenyl ring of the quinazolin-4-one moiety (**F2**). The latter feature has to be an aromatic ring. Additionally, a hydrogen bond acceptor, the nitrogen atom (N^1) of the quinazolin-4-one scaffold (**F3**), was identified as an important pharmacophore feature. The pharmacophore features identified from the potent antagonist are shown in **Figure 3.14**.

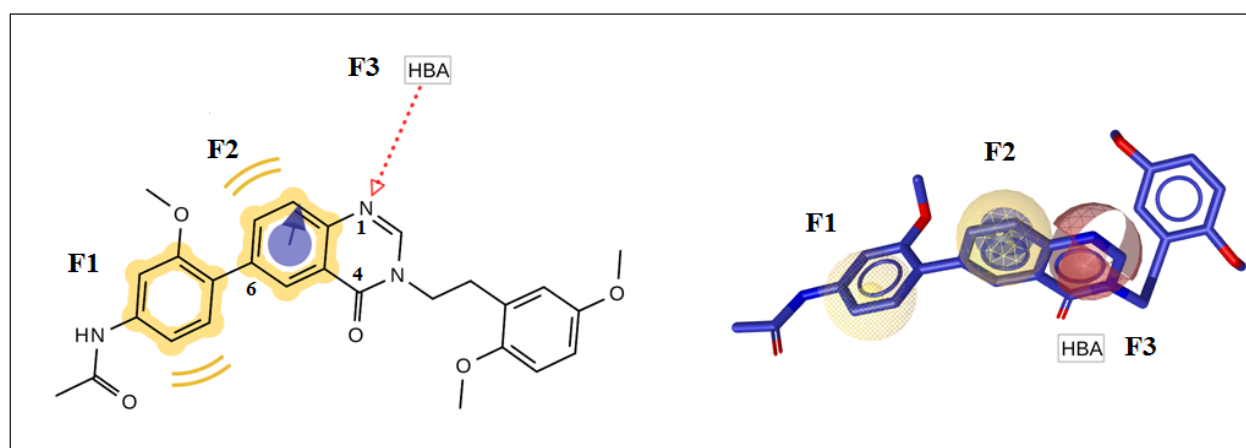


Figure 3.14. The pharmacophore features of a very potent P2X3 receptor antagonist described in literature.¹¹¹

In comparison, our lead compound **46** possesses two hydrophobic pockets and two hydroxyl groups (**Figure 3.15**). Among these two hydroxyl groups, only one hydroxyl group acts as a hydrogen bond acceptor, which is definitely needed, but the requirement of the second one was not confirmed. Based on the pharmacophore model, one of the two hydroxyl groups may be matching feature **F3**.

To further rationalize the results identified for the synthesized compounds, we mapped these data obtained from the pharmacophore model with the determined biological activities. If the hydroxyl groups were substituted with shorter chains such as butyl (**57**, $IC_{50} = 2.72 \mu M$) significantly decreases the activity, and a longer chain such as octyl (**62**, $IC_{50} > 10 \mu M$) or *para*-methoxybenzyl (**64**, $IC_{50} \gg 10 \mu M$) abolishes the activity (**Table 3.16**). However, it was found that substitutions with longer length are acceptable and the compounds were active. For example, in compounds **53**

Results and Discussion

and **54** one of the hydroxyl groups is substituted with octyl or *para*-methoxybenzoyl moieties, respectively, and the activity was slightly decreased with IC₅₀ values of 1.58 μM and 1.17 μM, respectively (Table 3.17). This shows that one of the hydroxyl groups of compound **46** may be comparable with the N¹ of the quinazolin-4-one ring of the potent antagonist and confirms that there is a need of a hydrogen bond acceptor at this position. Furthermore, substitution of the hydroxyl groups with shorter chains on one side and large hydrophobic groups on the other side is also tolerated. For example, compound **69** with propargyl and benzyl substitutions showed an IC₅₀ value of 0.645 μM (Table 3.17).

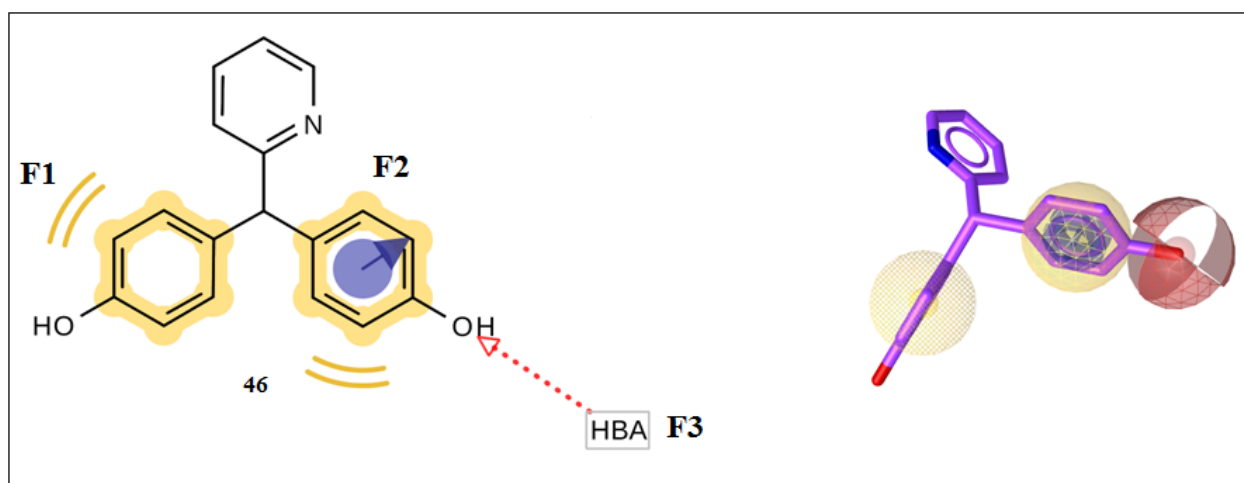


Figure 3.15. The pharmacophore features of compound **46**.

The analysis of the pharmacophore model showed that there is no feature matching with the pyridine ring of compound **46**. There is no need for that pyridine to keep the activity. This was confirmed with compound **89**, in which the pyridine ring is replaced with a carbonyl group leading to improved activity by 3-fold in comparison to lead structure **46** with an IC₅₀ value of 0.121 μM for **89**. The alignment of the features **F1-F3** with compound **89** is shown in **Figure 3.16**. However, this has to be confirmed with additional molecules to be synthesized and tested.

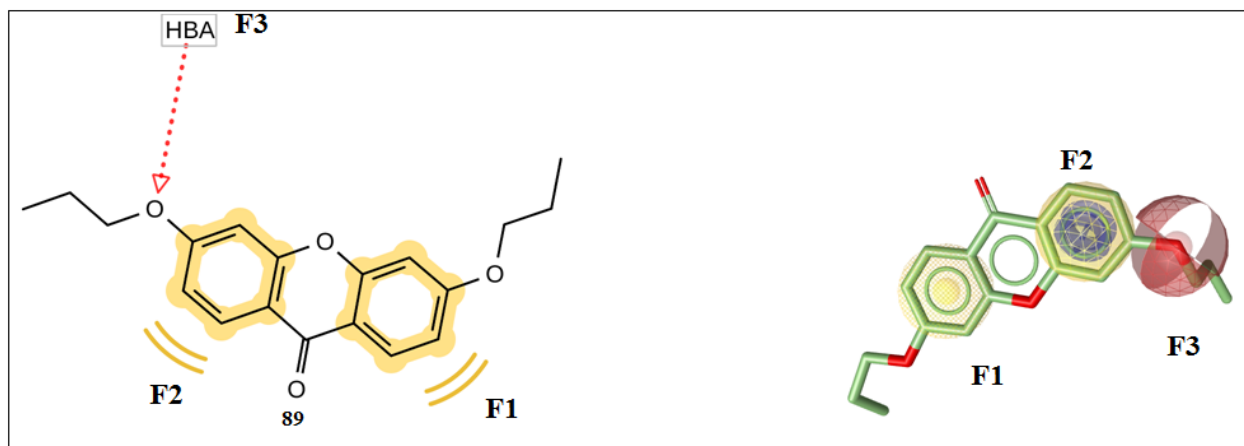


Figure 3.16. The pharmacophore features of compound **89**.

Finally, we compared the structural features of the potent quinazoline antagonist (**Figure 3.14**) with the best synthesized compound **89** as shown in **Figure 3.17**. This further confirms that one of the hydroxyl groups may be replaced with a shorter alkoxy chain and substituting the pyridine ring with a carbonyl group leads to improvement of the activity.

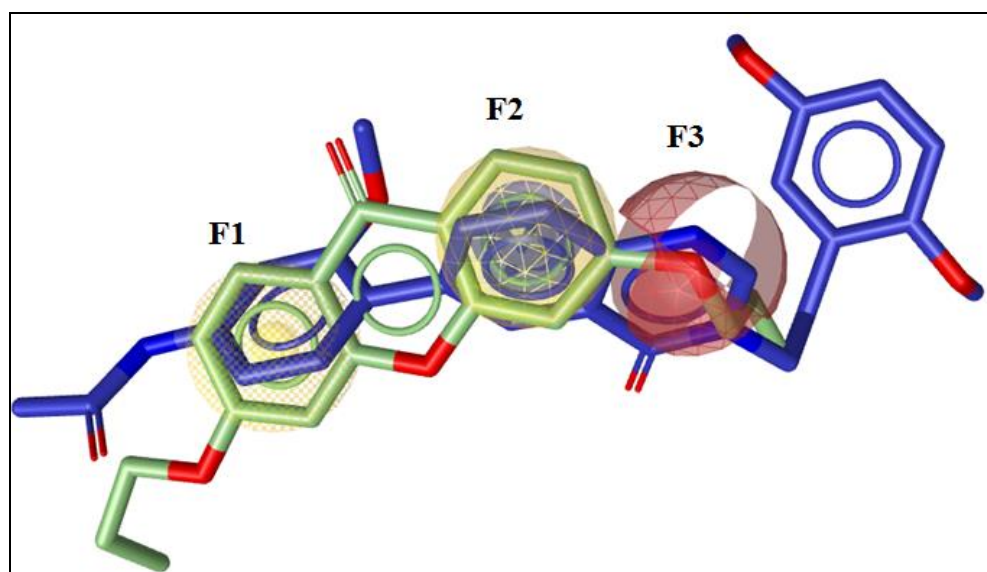


Figure 3.17. Comparison of the potent P2X3 antagonist, a 4-quinazoline derivative (blue) and compound **89** (green) showing the pharmacophore model features **F1-F3**.

Results and Discussion

A summary of the main findings and of the principal issues and suggestions which have arisen in this discussion are provided in **Figure 3.18**. Based on the pharmacophore modelling results, bisacodyl core is suggested to have better interactions with the P2X3 receptor.

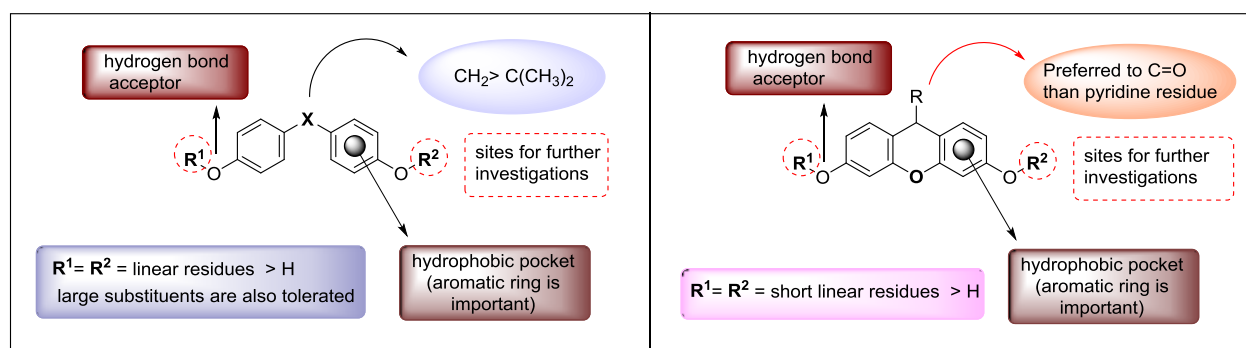


Figure 3.18. Structure-activity relationships of bisacodyl-derived compounds on the human P2X3 receptor.

Outlook

Following the pharmacophore model, the synthesis of derivatives of compound **89** with various substitutions introducing hydrophobic groups only on one side (on one phenolic group), might further improve potency (**Figure 3.19**).

The compounds' selectivity versus the different P2X receptor subtypes will have to be determined in future studies.

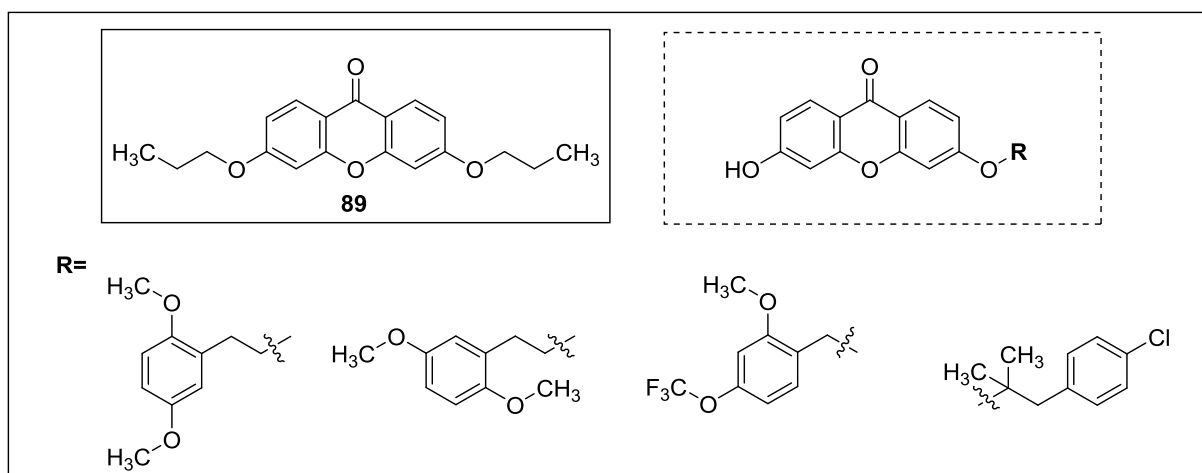


Figure 3.19. Proposed hydrophobic groups for potential enhancement of P2X3 receptor-blocking activity.

6 4. Summary

P2X3 receptors are ligand-gated ion channels activated by extracellular ATP. Their activation is associated with the pro-nociceptive effects of ATP. P2X3 receptor antagonists are promising drugs for the treatment of inflammatory pain. This project has focused on the synthesis of novel classes of P2X3 receptor antagonists.

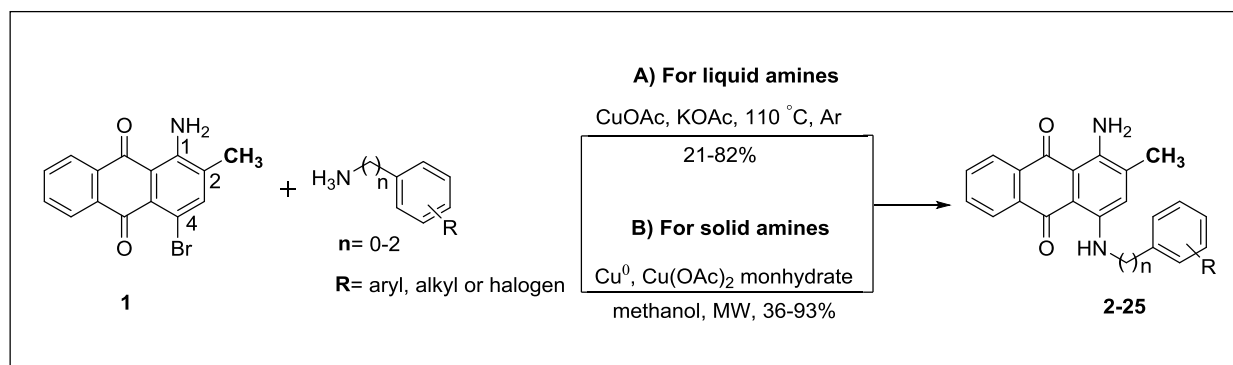
6.1 4.1. Anthraquinone derivatives

4.1.1. Synthesis and optimization of 1-amino-4-(aryl)alkylamino-2-methylantraquinone derivatives

Anthraquinone (AQ) derivatives related to Reactive Blue 2 have previously been described to block P2Y as well as P2X receptors. An acidic group in the 2-position (sulfonate or bioisoster) was found to be essential for interaction with P2Y receptors, but was expected to potentially be less important for inhibition P2X receptors. In order to study AQ derivatives with a non-acidic group in the 2-position, we had to optimize the reaction conditions of the Ullmann coupling reactions employed to prepare the desired 4-aryl-, alkyl- or arylalkyl-aminouracil derivatives (**Scheme 4.1**).

Ullmann condensation reactions had previously been successfully applied for amines which are liquid in nature (**Scheme 4.1, A**). In the present study the reaction conditions for employing solid amines were carefully optimized. While 1-pentanol was established as the best solvent for AQs bearing a bromine atom at the 2-position, methanol was found as the optimal solvent for condensation of solid amines with the 2-methyl-substituted AQ derivative, 1-amino-4-bromo-2-methylantraquinone (**1**). It was also suitable for reactions of 2-hydroxymethyl-AQ derivatives with the addition of a small percentage of water (2.5% v/v) to initiate the reaction. The use of a mixture of copper(0), and copper(II) acetate monohydrate as a catalyst was required for 2-methyl-substituted AQ derivatives (**Scheme 4.1, B**). This mixture of catalysts was also superior to copper(II) acetate alone which had previously been used in case of 2-bromo- and 2-hydroxymethyl-AQ derivatives. Our results show that copper-catalyzed reactions are highly variable depending on the AQ derivative present in the medium. Yields (21-82% in case of the solvent-free synthetic procedure) and reaction rates (30 min to 77 h) in case of the solvent-free

synthetic procedure) were highly variable. They also depended on the catalysts and the nature of the employed amines.



Scheme 4.1. General scheme for successful Ullmann coupling reactions of 1-amino-4-bromo-2-methylantraquinone-9,10-dione with amines.

4.1.2. Biological evaluation of the synthesized anthraquinone derivatives

A series of 24 1-amino-4-(aryl)alkylamino-2-methylantraquinone derivatives has been synthesized and fully characterized, 18 of these being novel derivatives not previously described in literature. The synthesized derivatives were biologically assessed on the human P2X3 receptor as well as other P2 receptor subtypes.

While at P2Y receptors the sulfonate group at the 2-position was essential for activity, this was not the case for the P2X3 receptor. Compound **22** was the most potent P2X3 antagonist of the present series with an IC_{50} value of $3.07\ \mu\text{M}$ (see **Figure 4.1**). Interestingly, compound **6** ($\text{IC}_{50} = 7.46\ \mu\text{M}$) which lacks ring E and is not acidic at all anymore was found to display an only 2-fold lower potency compared to compound **22** (**Figure 4.1**).

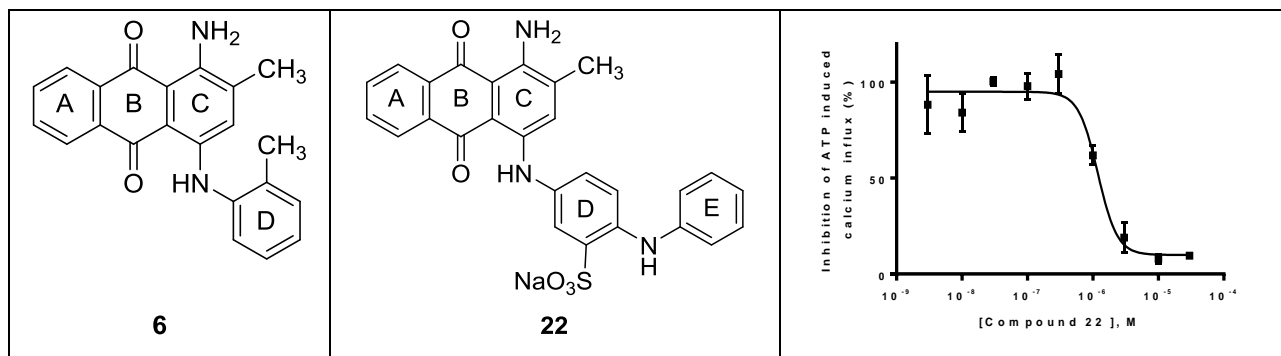


Figure 4.1. Structures of selected anthraquinone derivatives which act as antagonists at the human P2X3 receptor.

Thus, anthraquinone derivatives bearing an uncharged group such as methyl at the 2-position, which showed no activity on P2Y receptors, represent new lead structures for optimization as P2X3 receptor antagonists.

6.2 4.2. Bisacodyl-derived compounds

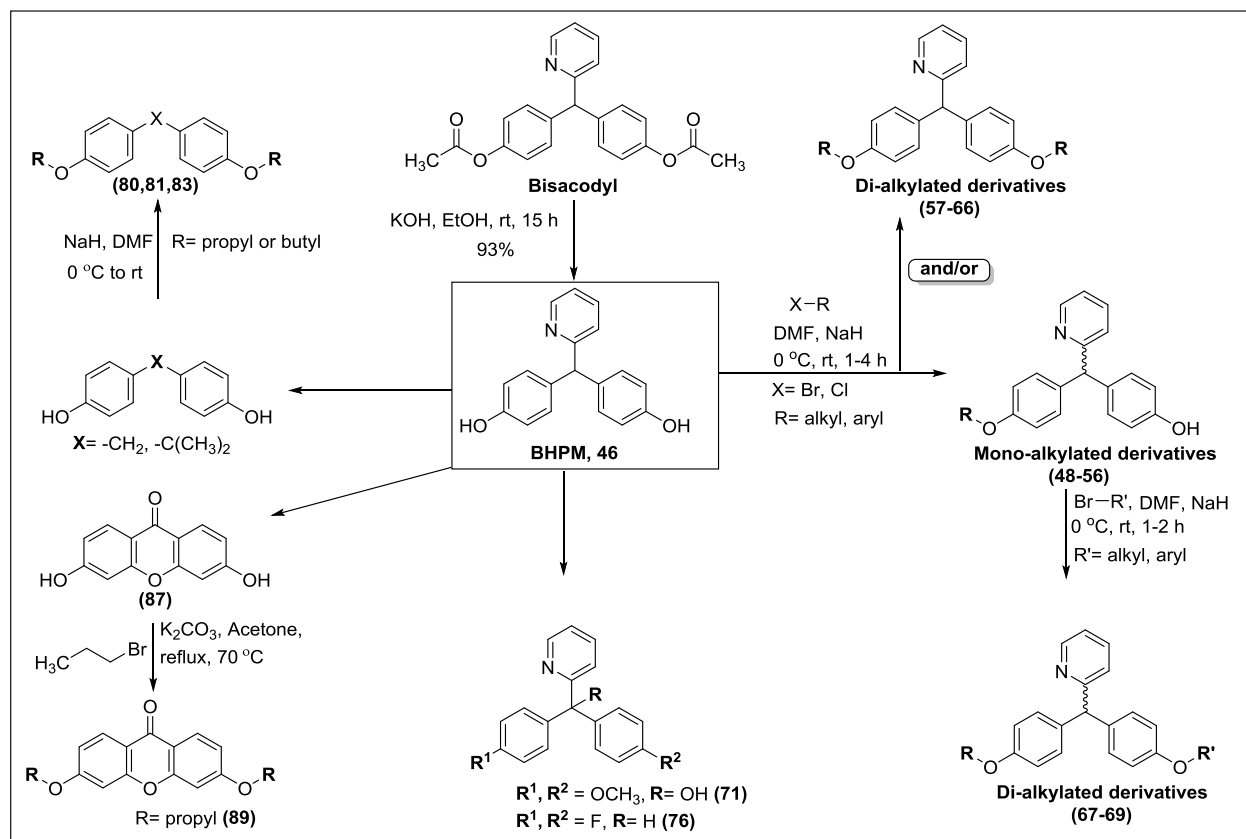
4.2.1. Synthesis of Bisacodyl-derived compounds

The prodrug bisacodyl, which is employed as a laxative therapeutic, and its pharmacologically active metabolite *bis*-(*p*-hydroxyphenyl)pyridyl-2-methane (**46**), were recently found in our laboratory to block P2X3 receptors. The laxative drug **46** was found to be significantly more potent than its prodrug bisacodyl. In the present study, structure-activity relationships were extensively explored by synthesizing derivatives and analogs of **46**.

To this end the prodrug bisacodyl was hydrolyzed to obtain the *bis*-phenol **46**, which was subsequently alkylated to obtain a variety of mono- (**48-56**) and di- (**57-66**) alkylated derivatives. Some of the mono-alkylated compounds were further alkylated to obtain unsymmetrically substituted compounds (**67-69**). In order to study the role of the phenolic OH groups they were replaced by bioisosteric fluorine atoms, which can, however, not act as hydrogen bond donors in contrast to hydroxy groups (**76**).

Moreover, we prepared related hydroxylated triphenylmethane derivative (**71**). Finally, we simplified the structure of **46** by removing the pyridine ring (**80, 81, and 83**) or by replacing it by

a carbonyl function (**87** and **89**) while maintaining the other features (two phenol rings) (**Scheme 4.2**).



Scheme 4.2. Synthetic scheme for some bisacodyl-derived compounds.

4.2.2. Inhibitory potency of bisacodyl derivatives on the human P2X3 receptor and study of structure-activity relationships

The synthesized bisacodyl derivatives and analogs were investigated as P2X3 receptor antagonists by measuring their potency to inhibit ATP-induced calcium influx in 1321N1 astrocytoma cells stably transfected with the human P2X3 receptor (**Figure 4.2**). A total of 56 compounds were synthesized and tested for biological activity, 36 of which are novel compounds. The prodrug bisacodyl exhibited P2X3-antagonistic potency with an IC_{50} value of 1.59 μ M at the human receptor. The biologically active laxative drug **46** that is formed from bisacodyl by ester hydrolysis is significantly more potent than the prodrug with an IC_{50} value of 0.421 μ M at the human P2X3 receptor. An even higher potency had been determined for the rat P2X3 receptor (IC_{50} = 0.0194 μ M).¹⁹⁵ Deletion of the pyridine ring led to potent compounds (**81**

and **89**). Compound **81** had an IC_{50} value of $0.493 \mu\text{M}$ and was nearly equipotent to the lead structure **46**. The cyclized analog **89**, a dibenzo-pyranone derivative was found to be the most potent P2X3 receptor antagonist of the present series with an IC_{50} value of $0.121 \mu\text{M}$ at the human receptor, being 3-fold more potent than the lead structure **46** (see **Figure 4.2** and **Figure 4.3**).

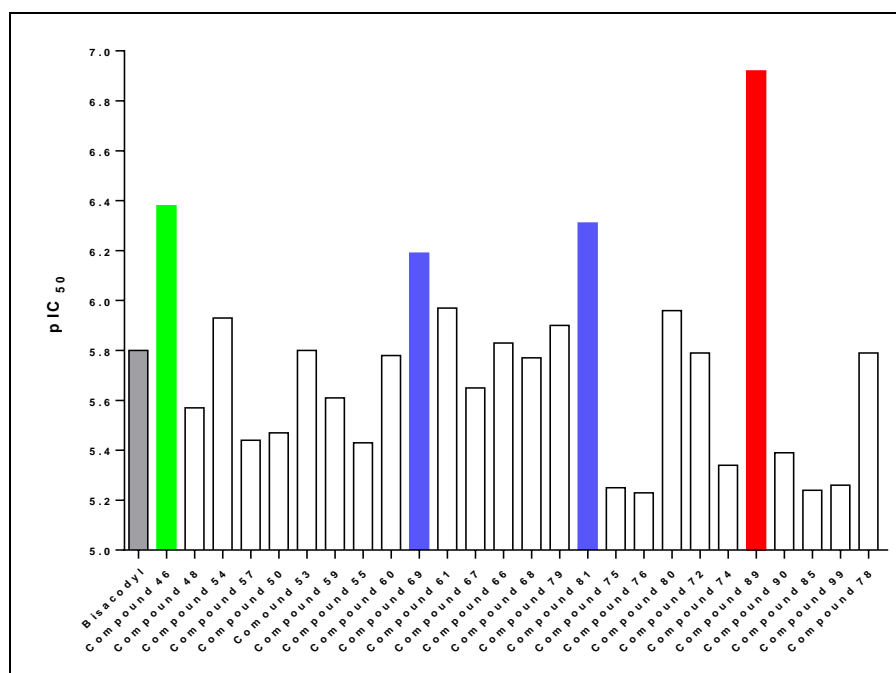


Figure 4.2. Inhibitory potencies of selected bisacodyl-derived compounds

The structures of most potent compounds within this series are shown in **Figure 4.3**.

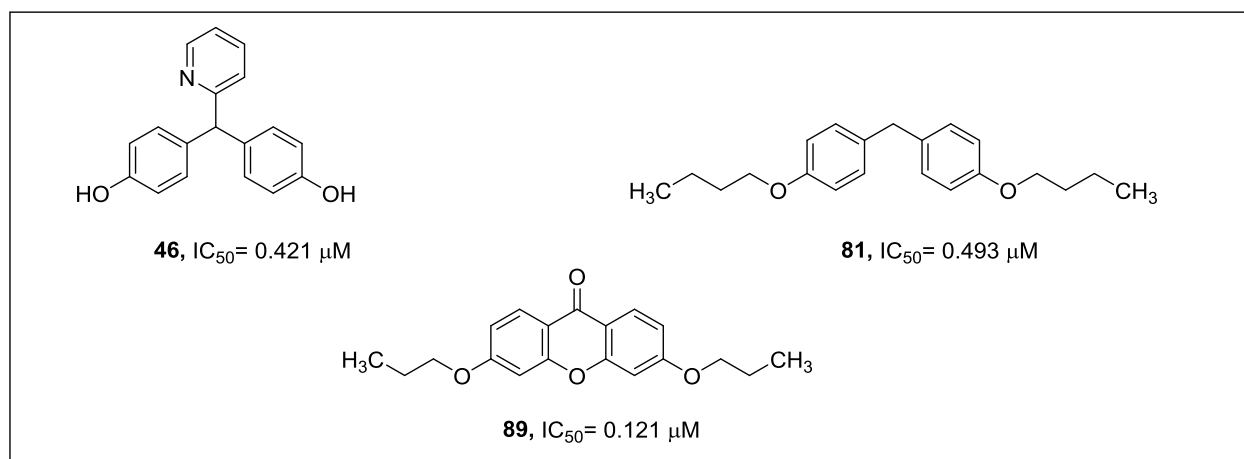


Figure 4.3. Structures of the most potent bisacodyl-derived P2X3 receptor antagonists.

Summary

In conclusion, the synthesis and structure-activity relationship analysis of bisacodyl-derived compounds resulted in potent – presumably allosteric - antagonists for the human P2X3 receptor. A pharmacophore model was subsequently developed which provides a basis for further improvement. These new P2X3 receptor antagonists represent a promising class of novel therapeutics for inflammatory diseases.

7 5. Experimental part

7.1 5.1. General considerations

All commercially available materials were obtained from different sources (ABCR, Alfa Aesar, Acros, Merck, Grüssing, Sigma Aldrich, and Fluka, Germany) and TCI (Belgium) and used as received unless otherwise revealed. Solvents used for both extraction and purification purposes were of technical grade and some of them were subjected to additional distillation before use.

Reactions were controlled by thin layer chromatography (TLC) performed on pre-coated aluminum-packed silica gel 60 sheets with fluorescent indicator UV254 or pre-coated aluminum-packed sheets RP silica gel C18 with fluorescent indicator UV254 (Merck, Darmstadt, Germany).

Silica gel 60 (0.040-0.063 mm, Merck) was used for column chromatography. Flash chromatography was performed on a Büchi apparatus using silica gel RP-18 (Macherey-Nagel, Germany) or silica gel 60 (0.060-0.200 mm, Acros).

Compounds were visualized under UV light (254 nm), but the colored compounds were visible at daylight. All melting points determined by on a Büchi-545 melting point apparatus were uncorrected. Refractive index (n_D^{20}) was measured on refractometer, Carl Zeiss, Germany.

Microwave (MW) experiments were conducted with a CEM Focused™ Microwave Synthesis type Discover apparatus in 10 mL sealed reaction tubes. Lyophilization of compounds was done using a freeze dryer (CHRIST ALPHA 1-4 LSC).

Mass spectra of isolated compounds were determined on an API 2000 (Applied Biosystems) mass spectrometer (turbo ion spray ion source) coupled with an Agilent 1100 HPLC system (Agilent, Böblingen, Germany). The following procedure was used: the sample was dissolved at a concentration of 1.0 mg/mL in methanol, acetonitrile, water, or a mixture of two of them. Sample solution (8 µL) was injected into the HPLC column (Macherey-Nagel EC50/2Nucleodur C18 Gravity 3 µm). HPLC was started with 90% water : 10% methanol (containing 2mM ammonium acetate). After 1 min, the gradient immediately started at a flow rate of 300 µL/min to

Experimental Part

reach 100% methanol in 9 min followed by washing with 100% methanol for another 10 min. The ultra violet (UV) absorption was detected at 190 to 900 nm using a diode array detector (DAD). The purity of the compounds was determined at 200-700 nm and proved to be $\geq 95\%$ (except **23-25** and **90**).

^1H - and ^{13}C -NMR spectral data were performed at room temperature on either a Bruker AV-500 MHz spectrometer (^1H), and 126 MHz (^{13}C) or on a Bruker AV-600 MHz spectrometer (^1H), and 151 MHz (^{13}C). Sample measurement of pure compounds was done using chloroform-*d*, DMSO-*d*₆, or acetone-*d*₆, as solvents. Data were expressed as chemical shifts (δ) in parts per million (ppm) related to residual deuterated solvent, i.e. chloroform, (^1H : δ 7.26; ^{13}C : 77.36); DMSO, (^1H : δ 2.49; ^{13}C : 39.7); methanol, (^1H : δ 3.31, 4.87; ^{13}C : 49.00) and tetramethylsilane (TMS) used as internal standard on the δ scale. ^1H coupling constants *J* were given in Hz and multiplicities of the spin were given as s (singlet), d (doublet), t (triplet), q (quartet), dd (doublet of doublets), td (triplet of doublets), m (multiplet), br (broad) and qt (quartet of triplet).

High-resolution mass spectral (HRMS) data were recorded on a Q-TOF micro mass spectrometer (Bruker) with electrospray ionization (ESI)-source and coupled with an HPLC Dionex Ultimate 3000 system (Thermo Scientific). The temperature of the HPLC column (Macherey-Nagel EC50/2 Nucleodur C18 Gravity 3 μm) was 25 °C, and a flow rate of 0.3 mL/min was applied. Then, 1 μL of a 0.6 mg/mL from the sample solution in acetonitrile was injected into the previously described column and HPLC separation was started with 10% acetonitrile and 90% water containing 2 mM ammonium acetate. After 1 min, the gradient was started reaching 100% acetonitrile within 9 min and then flushed with the same concentration for another 5 min. With these conditions, positive or negative full scan MS were observed from 50-1000 *m/z*.

7.2 5.2. Pharmacological Assays

5.2.1. Evaluating the pharmacological actions of the compounds at human P2Y₄ receptors

The whole set of experiments were conducted by Dr. Muhammad Rafehi (Pharmaceutical Institute, University of Bonn) on P2Y₄-R-expressing 1321N1 human brain astrocytoma cells. Prior to the assays, the 1321N1 human astrocytoma cells were transfected with a plasmid encoding the

Experimental Part

sequence for the human P2Y₄ receptors according to the procedure described previously²⁴¹ and monoclonal antibodies selected. The cells were grown in Dulbecco's Modified Eagle's Medium (DMEM) completed with 10% fetal calf serum (FCS), 1% of a penicillin/streptomycin, and 200 µg/mL of Geneticin in T175 culture flasks (175 cm² surface area). The DMEM and other supplements were provided by Invitrogen (Life Technologies GmbH, Darmstadt, Germany). The cells were then incubated at 37 °C in 10% CO₂ humidified air. Cells were maintained in the exponential growth phase throughout the experiment and closely monitored for any potential mycoplasma contamination.

Calcium-mobilization assay. This assay was done as previously reported.⁷² Briefly, the DMEM medium was removed and cells were gently rinsed with sterile phosphate-buffered saline (PBS) and detached by trypsin/ EDTA (0.05%/ 0.6 mM) solution. The cells were then re-suspended in complete DMEM and cultured into sterile flat bottom 96-well polystyrene coated microplates (Corning[®] 3340) at concentration of 50,000 cells/ well then incubated at 37 °C in 10% CO₂ humidified air for 24 hours till cells become adherent to the wells. The compounds were then tested for their inhibitory activity on the P2Y₄ receptor -mediated intracellular calcium mobilization using a FlexStation 3[®] plate reader (Molecular Devices GmbH, Biberach an der Riss, Germany). Briefly, the adherent cells were loaded with fluo-4 acetoxymethyl ester (Life Technologies GmbH, Darmstadt, Germany) for 60 minutes. The excess dye was removed and Hank's balanced salt solution (HBSS) buffer was added to the cells. The cells were pre-incubated with the test compound for 30 min and the physiological ligand uridine 5'-triphosphate was injected at a final concentration of 500 nM, which corresponds to its EC₈₀ at a final volume of 200 µl per well. The produced fluorescence was measured at 525 nm following excitation at 488 nm. Each experiment was conducted in triplicates using 2 independent sets. The IC₅₀ values were calculated by non-linear regression equation using GraphPad Prism[®] 5.0 software (San Diego, CA, USA).²⁴² *Experiments were performed by Dr. Muhammad Rafehi.*

5.2.2. Measurement of Ca²⁺ in transfected 1321N1 astrocytoma cells

A monoclonal human P2X₃ cell line was created and Ca²⁺ measurements on P2X₃ were done in our group. Human P2X₃ receptor function was determined on the basis of agonist-mediated increases in cytosolic Ca²⁺ concentration. The calcium 5 assay kit was used as an indicator of the relative levels of intracellular Ca²⁺ in a 96-well format using a fluorescence imaging plate reader

(Novostar, BMG, Germany). Cells were grown to confluence in 96-well black-walled tissue culture plates and loaded calcium 5 dye in Hank's balanced salt solution (HBSS, containing 10 mM HEPES, pH 7.3) for 1 h at 37 °C. Compound solutions were prepared in DMSO depending. The final DMSO concentration in the assays did not exceed 0.5%. Fluorescence intensity was measured at 510 nm for 30 s at 0.4 s intervals. Buffer or test compounds were injected sequentially into separate wells using the automatic pipetting device. At least three independent experiments were performed in duplicate. Antagonists were added 30 min before the addition of agonists (agonist concentration ~ EC₈₀). The assays were performed in a final volume of 200 µl. Compounds were tested at 7-8 different concentrations spanning three orders of magnitude of concentrations. *Experiments were performed by Dr. Aliaa Abdelrahman.*

7.3 5.3. Pharmacophore modelling

Based on the conformations for each compound, LigandScout 4.1 was used to construct possible pharmacophore models.²⁴³ For this, approximately 200 conformations were generated by iCon with the best settings option for compounds belong to the training set.²⁴⁴ Ten pharmacophore models were generated with different scores using LigandScout4.1 package which showed different feature patterns and pharmacophore-fit values of each compound. The pharmacophore model with the highest score was considered as the best model. In a shared feature pharmacophore model generation, LigandScout generates pharmacophore models from the chemical functionalities of the training compounds and aligns the molecules according to their pharmacophores.²⁴⁵ The features present in all the training molecules are further considered for model building. The shared pharmacophore features are created and assembled together comprising the final pharmacophore model to get the best alignment. These pharmacophore models contain only the chemical features present in all the training molecules. The number of frequent chemical features decreases by increasing the number of the training molecules, particularly when diverse structures are used. In our current study with the known P2X3 antagonists and newly synthesized compounds, we started with a large number of training sets and finally find the best model with two molecules. The shared feature pharmacophore generation uses these values to determine which molecules should be considered when building the pharmacophore space and which molecules should map to all or some of the features in the

final pharmacophores.²⁴⁶ We would like to thank Inte:Ligand GmbH for providing the evaluation license of LigandScout 4.1. *This study was performed by Dr. Vigneshwaran Namasivayam.*

7.4 5.4. Chemistry of anthraquinone derivatives

5.4.1. General synthetic procedure (I) used for anthraquinone derivatives (2-17)

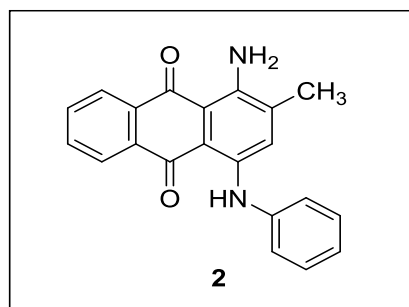
To a mixture consisting of 1-amino-4-bromo-2-methylanthracene-9,10-dione (**1**, 1 equiv.) and copper(I) acetate (10 mol%) in the presence of potassium acetate (2.25 equiv.) the corresponding amine (15 equiv.) was added. The reaction mixture was heated at 110 °C under an argon atmosphere, and the progress of the reaction was controlled by TLC. The formed mixture was then allowed to cool to room temperature and work-up was done according to procedure **A** or **B** as described below.

Work-up procedure A. Using a vacuum pump, the obtained blue precipitate after addition of 1-5 mL of ethanol was filtered off, washed successively with ethanol, 0.1 M HCl, and water (ca. 5-25 mL each) and then dried at 70 °C in an oven overnight. Purification of the crude product was done using column chromatography on silica gel providing the desired products in high purities. For some compounds, the latter step of column chromatography was repeated 2-3 times to gain a purity of $\geq 95\%$ as determined by LCMS.

Work-up procedure B. The reaction mixture was dissolved in ca. 30-50 mL dichloromethane, and then washed with ca. 20 mL of conc. HCl whereby a color change from blue to violet was clearly observed. Extraction was done using dichloromethane and water (ca. 75-100 mL each), upon which the still remaining amine was transferred to the aqueous layer whereas the blue color containing the product was transferred to the organic layer. The acid addition and extraction process were repeated until the amine was completely transferred into the aqueous layer (as monitored by TLC). The organic layers obtained were washed with 30 mL of brine, dried over anhydrous MgSO₄ and then evaporated under reduced pressure. Column chromatography of the crude product on silica gel provided the products in high purities. For some compounds, the previous step of column chromatography was repeated 2-3 times to achieve purity of $\geq 95\%$ as determined by LCMS.

5.4.2. Characterization of 1-amino-4-(aryl)alkylamino-2-methylanthraquinone derivatives (2-17)

1-Amino-2-methyl-4-(phenylamino)anthracene-9,10-dione (2)⁶⁴



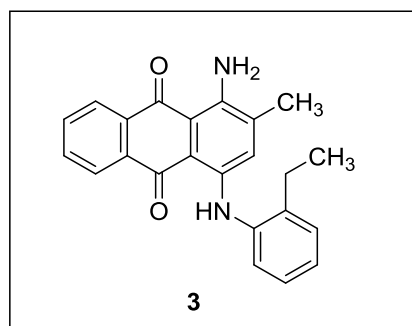
The compound was synthesized according to general procedure (I). 1-Amino-4-bromo-2-methylanthracene-9,10-dione (1) (316.2 mg, 1 mmol, 1 equiv.), copper(I) acetate (13.2 mg, 10 mol%), potassium acetate (220.5 mg, 2.25 mmol, 2.25 equiv.) and aniline (1.4 mL, 1400 mg, 15 mmol, 15 equiv.).

Reaction time: 110 min. **Work up procedure A.** Purification

was done by column chromatography on silica gel using cyclohexane/dichloromethane (10:90).

Appearance: blue powder. **Yield:** 248 mg (76%); **m.p.** 251-253 °C. **Solubility:** The compound is soluble in acetone, chloroform and DMSO, but insoluble in water. **Analytical data:** ¹H-NMR (DMSO-*d*₆, 500 MHz) δ (ppm) = 2.26 (s, 3H, CH₃); 7.18 (t, *J* = 7.34 Hz, 1H, 4'-H); 7.31 (d, *J* = 7.79 Hz, 2H, 2'-H, 6'-H); 7.41-7.43 (m, 2H, 3'-H, 5'-H); 7.44 (s, 1H, 3-H); 7.81-7.84 (m, 2H, 6-H, 7-H); 8.25-8.28 (m, 2H, 5-H, 8-H); 12.25 (s, 1H, 4-NH); (1-NH₂ not detectable). ¹³C-NMR (DMSO, 126 MHz) δ (ppm) = 18.67 (-CH₃), 108.07, 109.61 (C-4a, C-9a), 123.17, 124.41, 124.50 (C-3), 125.99, 126.12 (C-5, C-8), 129.81, 132.81(C-6), 133.01 (C-7), 133.95, 134.10 (C-8a, C-10a), 137.53 (C-2), 139.38, 142.00 (C-4), 147.21 (C-1), 181.95, 182.02 (C-9, C-10). Purity by HPLC-UV (254 nm) ESI-MS: 96%. HRMS (ESI-TOF) *m/z*: [M+H]⁺ Calcd. for C₂₁H₁₇N₂O₂ 329.1264, Found 329.1265.

1-Amino-4-((2-ethylphenyl)amino)-2-methylanthracene-9,10-dione (3)

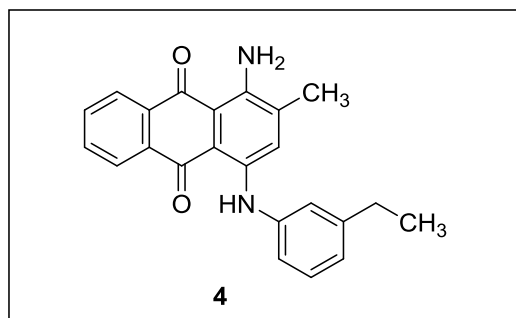


The compound was synthesized according to general procedure (I). 1-Amino-4-bromo-2-methylanthracene-9,10-dione (1) (316.2 mg, 1 mmol, 1 equiv.), copper(I) acetate (13.2 mg, 10 mol%), potassium acetate (220.5 mg, 2.25 mmol, 2.5 equiv.) and 2-ethylaniline (1.8 mL, 1818 mg, 15 mmol, 15

Experimental Part

equiv.). **Reaction time:** 13 h. **Work up procedure A.** Purification was done by column chromatography on silica gel using cyclohexane/dichloromethane (50:50). **Appearance:** blue powder. **Yield:** 208 mg (58%); **m.p.** 178-180 °C. **Solubility:** The compound is soluble in acetone, dichloromethane and DMSO, but insoluble in water. **Analytical data:** $^1\text{H-NMR}$ (Chloroform-*d*, 500 MHz) δ (ppm) = 1.25 (t, $J = 7.50$ Hz, 3H, $-\text{CH}_2-\text{CH}_3$); 2.27 (s, 3H, CH_3); 2.72 (q, $J = 7.49$ Hz, 2H, $-\text{CH}_2-\text{CH}_3$); 7.11 (s, 1H, 3-H); 7.22 (d, $J = 7.77$ Hz, 1H, 3'-H); 7.26 (m, 2H, 4'-H, 5'-H); 7.35 (d, $J = 7.27$ Hz, 1H, 6'-H); 7.70-7.75 (m, 2H, 6-H, 7-H); 8.34-8.37 (m, 2H, 5-H, 8-H); 12.05 (s, 1H, 4-NH); (1-NH₂ not detectable). $^{13}\text{C-NMR}$ (CDCl₃, 126 MHz) δ (ppm) = 14.55 ($-\text{CH}_2-\text{CH}_3$), 18.39 ($-\text{CH}_3$), 24.83 ($-\text{CH}_2-\text{CH}_3$), 110.09, 111.55 (C-4a, C-9a), 124.32, 125.87, 125.93 (C-3), 126.25, 129.30, 126.45 (C-5, C-8), 126.65, 129.52, 132.46 (C-6, C-7), 134.17, 134.61 (C-8a, C-10a), 136.19 (C-2), 137.14, 139.63, 142.99 (C-4), 144.96 (C-1), 183.01, 184.32 (C-9, C-10). Purity by **HPLC-UV (220-700 nm):** 96%. **HRMS (ESI-TOF) m/z :** $[\text{M}+\text{H}]^+$ Calcd. for C₂₃H₂₁N₂O₂ 357.1598, Found 357.1583.

1-Amino-4-((3-ethylphenyl)amino)-2-methylanthracene-9,10-dione (4)

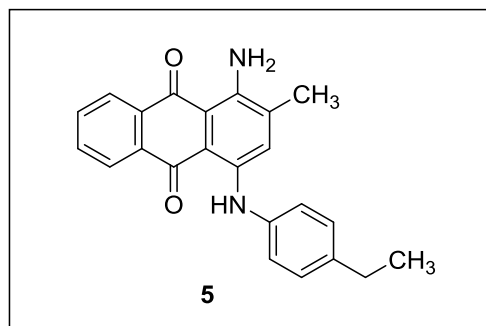


The compound was synthesized according to general procedure (I). 1-Amino-4-bromo-2-methylanthracene-9,10-dione (1) (316.2 mg, 1 mmol, 1 equiv.), copper(I) acetate (13.2 mg, 10 mol%), potassium acetate (220.5 mg, 2.25 mmol, 2.25 equiv.) and 3-ethylaniline (1.8 mL, 1818 mg, 15 mmol, 15 equiv.). **Reaction time:**

110 min. **Work up procedure A.** Purification was done by column chromatography on silica gel using cyclohexane/dichloromethane (50:50). **Appearance:** blue powder. **Yield:** 293 mg (82%); **m.p.** 229-230 °C. **Solubility:** The compound is soluble in acetone, dichloromethane and DMSO, but insoluble in water. **Analytical data:** $^1\text{H-NMR}$ (DMSO-*d*₆, 500 MHz) δ (ppm) = 1.21 (t, $J = 7.57$ Hz, 3H, $-\text{CH}_2-\text{CH}_3$); 2.25 (s, 3H, CH_3); 2.63 (q, $J = 7.58$ Hz, 2H, $-\text{CH}_2-\text{CH}_3$); 7.03 (d, $J = 7.54$ Hz, 1H, 2'-H); 7.10-7.16 (m, 2H, 4'-H, 5'-H); 7.32 (d, $J = 7.66$ Hz, 1H, 6'-H); 7.44 (s, 1H, 3-H); 7.80-7.84 (m, 2H, 6-H, 7-H); 8.25-8.28 (m, 2H, 5-H, 8-H); 12.26 (s, 1H, 4-NH); (1-NH₂ not detectable). $^{13}\text{C-NMR}$ (DMSO, 126 MHz) δ (ppm) = 15.49 ($-\text{CH}_2-\text{CH}_3$), 18.23 ($-\text{CH}_3$), 28.17 ($-\text{CH}_2-\text{CH}_3$), 108.04, 109.47 (C-4a, C-9a), 120.47, 122.64, 124.03 (C-3), 124.60, 125.97, 126.11 (C-5, C-8), 129.63, 132.78, 132.96 (C-6, C-7), 133.97, 134.10 (C-8a, C-10a), 137.50 (C-2),

139.29, 142.16, 145.68 (C-4), 147.18 (C-1), 181.82, 181.98 (C-9, C-10). Purity by **HPLC-UV (220-650 nm)**: 98%. **HRMS (ESI-TOF) m/z** : $[M+H]^+$ Calcd. for $C_{23}H_{21}N_2O_2$ 357.1598, Found 357.1582.

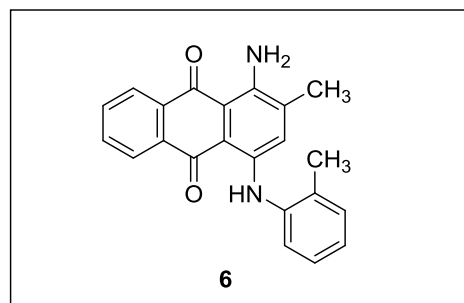
1-Amino-4-((4-ethylphenyl)amino)-2-methylanthracene-9,10-dione (5)



The compound was synthesized according to general procedure (I). 1-Amino-4-bromo-2-methylanthracene-9,10-dione (**1**) (316.2 mg, 1 mmol, 1 equiv.), copper(I) acetate (13.2 mg, 10 mol%), potassium acetate (220.5 mg, 2.25 mmol, 2.25 equiv.) and 4-ethylaniline (1.8 mL, 1818 mg, 15 mmol, 15 equiv.). **Reaction time**: 30 min.

Work up procedure A. Purification was done by column chromatography on silica gel using cyclohexane/dichloromethane (30:70). **Appearance**: blue powder. **Yield**: 262 mg (74%); **m.p.** 230-232 °C. **Solubility**: The compound is soluble in acetone, dichloromethane and DMSO, but insoluble in water. **Analytical data**: **1H -NMR (Chloroform- d , 600 MHz) δ (ppm)** = 1.28 (t, J = 7.62 Hz, 3H, $-CH_2-CH_3$); 2.23 (s, 3H, CH_3); 2.68 (q, J = 7.62 Hz, 2H, $-CH_2-CH_3$); 7.18 (d, J = 8.28 Hz, 2H, 2'-H, 6'-H); 7.23 (d, J = 8.21 Hz, 2H, 3'-H, 5'-H); 7.36 (s, 1H, 3-H); 7.70-7.73 (m, 2H, 6-H, 7-H); 8.33-8.35 (m, 2H, 5-H, 8-H); 12.14 (s, 1H, 4-NH); (1-NH₂ not detectable). **^{13}C -NMR (CDCl₃, 151 MHz) δ (ppm)** = 15.54 ($-CH_2-CH_3$), 18.21 ($-CH_3$), 28.36 ($-CH_2-CH_3$), 110.23, 110.33 (C-4a, C-9a), 124.27, 124.56, 126.18 (C-3), 126.36, 128.86 (C-5, C-8), 132.49, 132.34 (C-6, C-7), 134.39, 134.69 (C-8a, C-10a), 135.31 (C-2), 137.23, 140.84, 143.68 (C-4), 145.23 (C-1), 182.87, 183.95 (C-9, C-10). Purity by **HPLC-UV (220-700 nm)**: 96%. **HRMS (ESI-TOF) m/z** : $[M+H]^+$ Calcd. for $C_{23}H_{21}N_2O_2$ 357.1598, Found 357.1573.

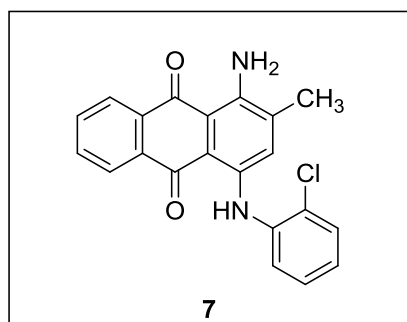
1-Amino-2-methyl-4-(*o*-tolylamino)anthracene-9,10-dione (6)



The compound was synthesized according to general procedure (I). 1-Amino-4-bromo-2-methylanthracene-9,10-dione (**1**) (316.2 mg, 1 mmol, 1 equiv.), copper(I) acetate (13.2 mg, 10 mol%), potassium acetate (220.5 mg,

2.25 mmol, 2.5 equiv.) and *o*-toluidine (1.6 mL, 1607 mg, 15 mmol, 15 equiv.). **Reaction time:** 150 min. **Work up procedure A.** Purification was done by column chromatography on silica gel using cyclohexane/dichloromethane (20:80). **Appearance:** blue powder. **Yield:** 150 mg (44%); **m.p.** 207-209 °C. **Solubility:** The compound is soluble in acetone, ethanol and DMSO, but insoluble in water. **Analytical data:** ¹H-NMR (Chloroform-*d*, 600 MHz) δ (ppm) = 2.20 (s, 3H, 2-CH₃); 2.33 (s, 3H, 2'-CH₃); 7.10-7.14 (m, 2H, 3'-H, 6'-H); 7.21-7.25 (m, 2H, 4'-H, 5'-H); 7.29 (d, *J* = 7.48 Hz, 3-H); 7.69-7.71 (m, 2H, 6-H, 7-H); 8.33-8.35 (m, 2H, 5-H, 8-H); 12.02 (s, 1H, 4-NH); (1-NH₂ not detectable). ¹³C-NMR (CDCl₃, 151 MHz) δ (ppm) = 18.18 (2-CH₃, 2'-CH₃), 110.14, 110.31 (C-4a, C-9a), 124.47 (C-3), 125.24, 125.35, 126.18, 126.37, 126.67 (C-5, C-8), 131.18 (C-2), 132.37, 132.48 (C-8a, C-10a), 134.43, 134.68 (C-6, C-7), 135.43, 138.24, 143.99 (C-4), 150.52 (C-1), 183.04, 182.98 (C-9, C-10). Purity by HPLC-UV (220-700 nm): 95%. **HRMS (ESI-TOF) *m/z*:** [M+H]⁺ Calcd. for C₂₂H₁₉N₂O₂ 343.1441, Found 343.1421.

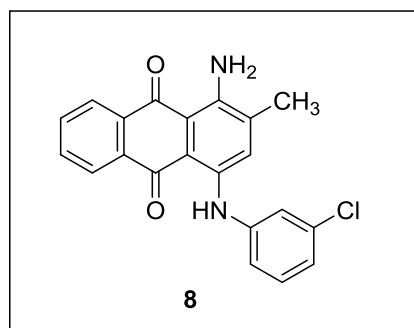
1-Amino-4-((2-chlorophenyl)amino)-2-methylanthracene-9,10-dione (7)



The compound was synthesized according to general procedure (I). 1-Amino-4-bromo-2-methylanthracene-9,10-dione (1) (316.2 mg, 1 mmol, 1 equiv.), copper(I) acetate (13.2 mg, 10 mol%), potassium acetate (220.5 mg, 2.25 mmol, 2.25 equiv.) and 2-chloroaniline (1.6 mL, 1913 mg, 15 mmol, 15 equiv.). **Reaction time:** 77 h. **Work up procedure A.** Purification was done by column chromatography on silica gel using cyclohexane/dichloromethane (30:70) and then purified by HPLC. **Appearance:** blue powder. **Yield:** 83 mg (21%); **m.p.** 188-189 °C. **Solubility:** The compound is soluble in acetone, dichloromethane, DMSO, but insoluble in water. **Analytical data:** ¹H-NMR (DMSO-*d*₆, 500 MHz) δ (ppm) = 2.26 (s, 3H, CH₃); 7.15-7.19 (m, 7.73 Hz, 1H, 4'-H); 7.39 (s, 1H, 3-H); 7.37 (dd, *J* = 1.27, 7.94 Hz, 1H, 6'-H); 7.52 (dd, *J* = 1.50, 8.15 Hz, 1H, 5'-H); 7.60 (dd, *J* = 1.49, 8.10 Hz, 1H, 3'-H); 7.81-7.87 (m, 2H, 6-H, 7-H); 8.25-8.28 (m, 2H, 5-H, 8-H); 12.16 (s, 1H, 4-NH); (1-NH₂ not detectable). ¹³C-NMR (DMSO, 126 MHz) δ (ppm) = 18.60 (-CH₃), 108.28, 110.93 (C-4a, C-9a), 123.72 (C-3), 124.79, 125.15, 126.13 (C-5), 126.16 (C-8), 128.28, 130.34, 132.69 (C6), 132.95 (C7), 133.34, 134.76 (C-8a, C-10a), 134.12 (C-2), 136.81, 137.30, 140.34 (C-4),

147.42 (C-1), 182.27, 182.83 (C-9, C-10). Purity by **HPLC-UV (254 nm)**: 95%. **HRMS (ESI-TOF) m/z** : $[M+H]^+$ Calcd. for $C_{21}H_{16}ClN_2O_2$ 363.0895, Found 363.0860.

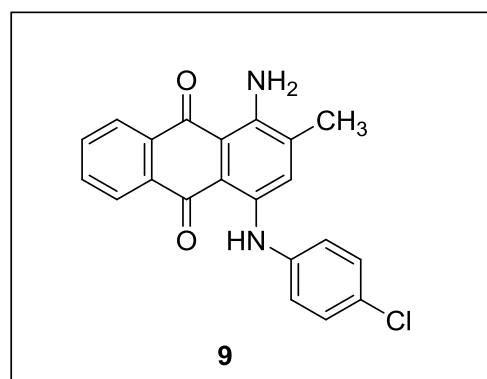
1-Amino-4-((3-chlorophenyl)amino)-2-methylantracene-9,10-dione (8)



The compound was synthesized according to general procedure (I). 1-Amino-4-bromo-2-methylantracene-9,10-dione (**1**) (316.2 mg, 1 mmol, 1 equiv.), copper(I) acetate (13.2 mg, 10 mol%), potassium acetate (220.5 mg, 2.25 mmol, 2.25 equiv.) and 3-chloroaniline (1.6 mL, 1913 mg, 15 mmol, 15 equiv.). **Reaction time**: 18 h. **Work up procedure A**. Purification was done by column chromatography on silica gel

using cyclohexane/dichloromethane (30:70). **Appearance**: blue powder. **Yield**: 240 mg (66%); **m.p.** 280-281 °C. **Solubility**: The compound is soluble in acetone, dichloromethane and DMSO, but insoluble in water. **Analytical data**: $^1\text{H-NMR}$ (DMSO- d_6 , 500 MHz) δ (ppm) = 2.28 (s, 3H, CH_3); 7.17-7.19 (m, 1H, 5'-H); 7.27 (dd, $J = 2.07, 7.95$ Hz, 1H, 2'-H); 7.37 (t, $J = 2.14$ Hz, 1H, 6'-H); 7.41 (t, $J = 8.03$ Hz, 1H, 4'-H); 7.48 (s, 1H, 3-H); 7.83-7.86 (m, 2H, 6-H, 7-H); 8.24-8.28 (m, 2H, 5-H, 8-H); 12.03 (s, 1H, 4-NH); (1-NH $_2$ not detectable). $^{13}\text{C-NMR}$ (DMSO- d_6 , 126 MHz) δ (ppm) = 18.62 ($-CH_3$), 108.24, 110.54 (C-4a, C-9a), 121.06, 122.12, 123.66 (C-3), 124.97, 126.06, 126.17 (C-5, C-8), 131.24, 132.96 (C-2), 133.30, 133.80 (C-8a, C-10a), 134.09, 134.11, (C-6, C-7), 137.38, 140.64, 141.52 (C-4), 147.52 (C-1), 182.25, 182.60 (C-9, C-10). Purity by **HPLC-UV (200-650 nm)**: 97%. **HRMS (ESI-TOF) m/z** : $[M+H]^+$ Calcd. for $C_{21}H_{16}ClN_2O_2$ 363.0895, Found 363.0832.

1-Amino-4-((4-chlorophenyl)amino)-2-methylantracene-9,10-dione (9)

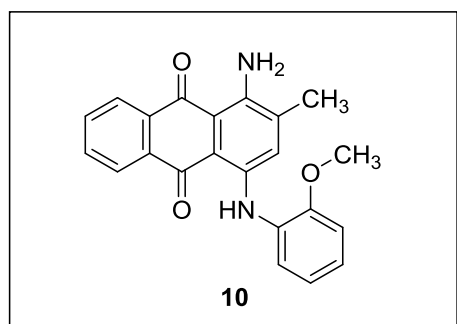


The compound was synthesized according to general procedure (I). 1-Amino-4-bromo-2-methylantracene-

Experimental Part

9,10-dione (**1**) (316.2 mg, 1 mmol, 1 equiv.), copper(I) acetate (13.2 mg, 10 mol%), potassium acetate (220.5 mg, 2.25 mmol, 2.25 equiv.) and 4-chloroaniline (1.6 mL, 1913 mg, 15 mmol, 15 equiv.). **Reaction time:** 18 h. **Work up procedure A.** Purification was done by column chromatography on silica gel using cyclohexane/dichloromethane (30:70). **Appearance:** blue powder. **Yield:** 260 mg (72%); **m.p.** 293-294 °C. **Solubility:** The compound is soluble in acetone, dichloromethane and DMSO, but insoluble in water. **Analytical data:** $^1\text{H-NMR}$ (DMSO- d_6 , 500 MHz) δ (ppm) = 2.30 (s, 3H, CH_3); 7.32-7.34 (m, 2H, 2'-H, 6'-H); 7.44-7.47 (m, 3H, 3'-H, 5'-H, 3-H); 7.80-7.85 (m, 2H, 6-H, 7-H); 8.24-8.27 (m, 2H, 5-H, 8-H); 12.15 (s, 1H, 4-NH); (1-NH₂ not detectable). $^{13}\text{C-NMR}$ (DMSO- d_6 , 126 MHz) δ (ppm) = 18.62 (-CH₃), 108.24, 110.54 (C-4a, C-9a), 124.57 (C-3), 124.62, 127.96, 129.63, 126.02 (C-5), 126.15 (C-8), 132.85, 132.89 (C-8a, C-10a), 133.18 (C-2), 133.85, 134.10 (C-6, C-7), 137.51, 138.61, 141.29 (C-4), 147.33 (C-1), 182.14, 182.30 (C-9, C-10). Purity by HPLC-UV (220-650 nm): 98%. **HRMS (ESI-TOF) m/z :** [M+H]⁺ Calcd. for C₂₁H₁₆ClN₂O₂ 363.0895, Found 363.0841.

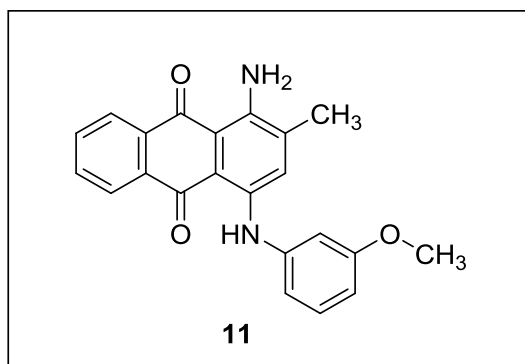
1-Amino-4-((2-methoxyphenyl)amino)-2-methylantracene-9,10-dione (**10**)



The compound was synthesized according to general procedure (I). 1-Amino-4-bromo-2-methylantracene-9,10-dione (**1**) (316.2 mg, 1 mmol, 1 equiv.), copper(I) acetate (13.2 mg, 10 mol%), potassium acetate (220.5 mg, 2.25 mmol, 2.25 equiv.) and 2-methoxyaniline (1.7 mL, 1847 mg, 15 mmol, 15 equiv.). **Reaction time:** 160 min. **Work up procedure A.** Purification was done by column chromatography on silica gel using cyclohexane/dichloromethane (10:90). **Appearance:** blue powder. **Yield:** 235 mg (66%); **m.p.** 170-172 °C. **Solubility:** The compound is soluble in acetone, dichloromethane and DMSO, but insoluble in water. **Analytical data:** $^1\text{H-NMR}$ (Chloroform- d , 600 MHz) δ (ppm) = 2.24 (s, 3H, CH_3); 3.91 (s, 3H, -OCH₃); 6.97 (dd, J = 1.34, 7.60 Hz, 1H, 6'-H); 6.99-7.00 (m, 1H, 5'-H); 7.12-7.15 (m, 1H, 4'-H); 7.33 (dd, J = 1.58, 7.69 Hz, 1H, 3'-H); 7.39 (s, 1H, 3-H); 7.69-7.73 (m, 2H, 6-H, 7-H); 8.33-8.37 (m, 2H, 5-H, 8-H); 11.97 (s, 1H, 4-NH); (1-NH₂ not detectable). $^{13}\text{C-NMR}$ (CDCl₃, 151 MHz) δ (ppm) = 18.30 (-CH₃), 55.79 (-OCH₃), 110.81, 111.06 (C-4a, C-9a), 111.51, 120.59, 123.26 (C-3), 124.84, 124.92, 126.28, 126.33 (C-5, C-8), 128.75 (C-2), 132.38, 132.56 (C-6, C-7), 134.27, 134.66 (C-8a, C-10a); 135.14, 142.76,

144.67 (C-4), 152.49 (C-1), 183.03, 184.12 (C-9, C-10). Purity by **HPLC-UV (220-400 nm)**: 96%. **HRMS (ESI-TOF) m/z** : $[M+H]^+$ Calcd. for $C_{22}H_{19}N_2O_3$ 359.1390, Found 359.1377.

1-Amino-4-((3-methoxyphenyl)amino)-2-methylanthracene-9,10-dione (11)²⁴⁰

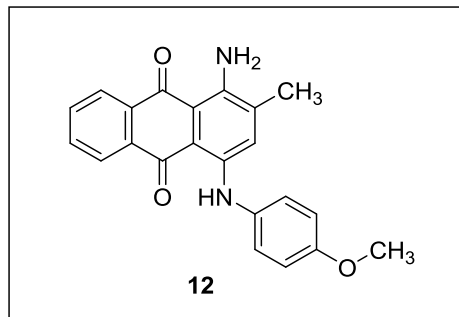


The compound was synthesized according to general procedure (I). 1-Amino-4-bromo-2-methylanthracene-9,10-dione (**1**) (316.2 mg, 1 mmol, 1 equiv.), copper(I) acetate (13.2 mg, 10 mol%), potassium acetate (220.5 mg, 2.25 mmol, 2.5 equiv.) and 3-methoxyaniline (1.7 mL, 1847 mg, 15 mmol, 15 equiv.). **Reaction time**: 150 min. **Work up**

procedure A. Purification was done by column chromatography on silica gel using cyclohexane/dichloromethane (25:75). **Appearance**: blue powder. **Yield**: 281 mg (78%); **m.p.** 231-233 °C. **Solubility**: The compound is soluble in acetone, dichloromethane and DMSO, but insoluble in water. **Analytical data**: **1H -NMR (Chloroform-*d*, 500 MHz) δ (ppm)** = 2.26 (s, 3H, CH_3); 3.78 (s, 3H, $-OCH_3$); 6.75 (d, $J = 8.10$ Hz, 1H, 2'-H); 6.86-6.89 (m, 2H, 4'-H, 6'-H); 7.32 (t, $J = 7.97$ Hz, 1H, 5'-H); 7.48 (s, 1H, 3-H); 7.81-7.83 (m, 2H, 6-H, 7-H); 8.24-8.27 (m, 2H, 5-H, 8-H); 12.19 (s, 1H, 4-NH); (1-NH₂ not detectable). **^{13}C -NMR (CDCl₃, 126 MHz) δ (ppm)** = 18.64 ($-CH_3$), 55.33 ($-OCH_3$), 108.07, 108.51 (C-4a, C-9a), 109.76, 110.23, 115.19, 124.83 (C-3), 125.98, 126.10 (C-5, C-8), 130.48 (C-2), 132.80, 133.02 (C-6, C-7), 133.91, 134.09 (C-8a, C-10a), 137.42, 140.68, 141.77, 147.22 (C-4), 160.50 (C-1), 182.00, 182.02 (C-9, C-10). Purity by **HPLC-UV (200-650 nm)**: 95%. **HRMS (ESI-TOF) m/z** : $[M+H]^+$ Calcd. for $C_{22}H_{19}N_2O_3$ 359.1390, Found 359.1385.

1-Amino-4-((4-methoxyphenyl)amino)-2-methylanthracene-9,10-dione (12)

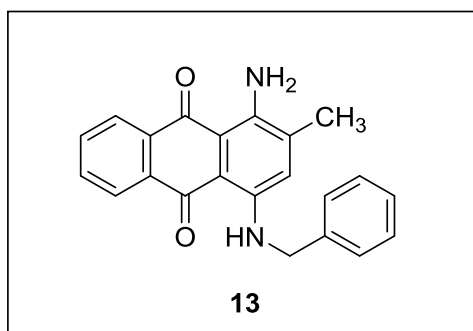
Experimental Part



The compound was synthesized according to general procedure (I). 1-Amino-4-bromo-2-methylantracene-9,10-dione (**1**) (316.2 mg, 1 mmol, 1 equiv.), copper(I) acetate (13.2 mg, 10 mol%), potassium acetate (220.5 mg, 2.25 mmol, 2.25 equiv.) and 4-methoxyaniline (1.7 mL, 1847 mg, 15 mmol, 15 equiv.). **Reaction time:** 120 min.

Work up procedure B. Purification was done by column chromatography on silica gel using cyclohexane/dichloromethane (15:85). **Appearance:** blue powder. **Yield:** 175 mg (49%); **m.p.** 217-219 °C. **Solubility:** The compound is soluble in acetone, dichloromethane and DMSO, but insoluble in water. **Analytical data:** $^1\text{H-NMR}$ (Chloroform-*d*, 600 MHz) δ (ppm) = 2.24 (s, 3H, CH_3); 3.85 (s, 3H, $-\text{OCH}_3$); 6.95 (d, $J = 8.93$ Hz, 2H, 3'-H, 5'-H); 7.19 (d, $J = 8.88$ Hz, 3H, 2'-H, 6'-H, 3-H); 7.69-7.73 (m, 2H, 6-H, 7-H); 8.34-8.35 (m, 2H, 5-H, 8-H); 12.06 (s, 1H, 4-NH); (1-NH₂ not detectable). $^{13}\text{C-NMR}$ (CDCl_3 , 151 MHz) δ (ppm) = 18.24 ($-\text{CH}_3$), 55.73 ($-\text{OCH}_3$), 109.78, 110.43 (C-4a, C-9a), 114.77, 124.27 (C-3), 126.13, 132.25, 126.35, 126.47 (C-5, C-8), 132.28, 132.36 (C-6, C-7), 132.50 (C-2), 134.34, 134.56 (C-8a, C-10a), 134.56, 135.58, 144.65 (C-4), 157.25 (C-1), 182.69, 183.97 (C-9, C-10). Purity by **HPLC-UV (220-700 nm):** 97%. **HRMS (ESI-TOF) m/z :** $[\text{M}+\text{H}]^+$ Calcd. for $\text{C}_{22}\text{H}_{19}\text{N}_2\text{O}_3$ 359.1390, Found 359.1372.

1-Amino-4-(benzylamino)-2-methylantracene-9,10-dione (**13**)



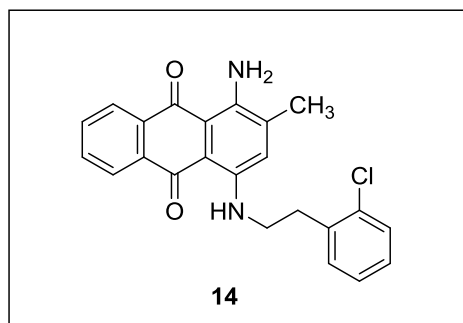
The compound was synthesized according to general procedure (I). 1-Amino-4-bromo-2-methylantracene-9,10-dione (**1**) (316.2 mg, 1 mmol, 1 equiv.), copper(I) acetate (13.2 mg, 10 mol%), potassium acetate (220.5 mg, 2.25 mmol, 2.5 equiv.) and phenylmethanamine (1.6 mL, 1607 mg, 15 mmol, 15 equiv.). **Reaction time:** 110 min.

Work up procedure B. Purification was done by column chromatography on silica gel using cyclohexane/dichloromethane (10:90). **Appearance:** blue powder. **Yield:** 175 mg (51%); **m.p.** 215-216 °C. **Solubility:** The compound is soluble in acetone, dichloromethane and DMSO, but insoluble in water. **Analytical data:** $^1\text{H-NMR}$ (Chloroform-*d*, 600 MHz) δ (ppm) = 2.29 (s, 3H, CH_3); 4.61 (s, 2H, 4-NH CH_2 -); 7.10 (s, 1H, 3-H); 7.28-7.40

Experimental Part

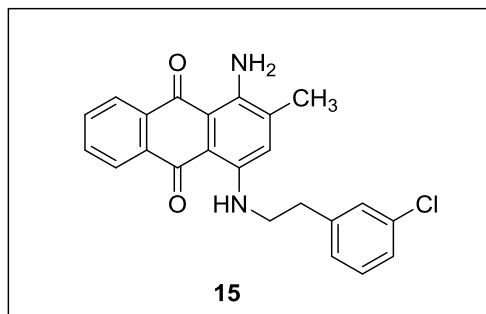
(m, 5H, 2'-H, 3'-H, 4'-H, 5'-H, 6'-H); 7.68-7.73 (m, 2H, 6-H, 7-H); 8.26-8.32 (m, 2H, 5-H, 8-H); (1-NH₂ not detectable). ¹³C-NMR (CDCl₃, 151 MHz) δ (ppm) = 18.69 (CH₃), 48.11 (-CH₂-), 111.11, 111.39 (C-4a, C-9a), 123.86, 126.27, 126.45, 127.48, 127.72, 128.88 (C-5, C-8), 130.93 (C-3), 132.63, 132.80 (C-6, C-7), 134.07, 134.41 (C-8a, C-10a), 136.27 (C-2), 137.28, 143.72 (C-4), 144.07 (C-1), 183.21, 184.34 (C-9, C-10). Purity by HPLC-UV (220-650 nm): 97%. HRMS (ESI-TOF) *m/z*: [M+H]⁺ Calcd. for C₂₂H₁₉N₂O₂ 343.1441, Found 343.1431.

1-Amino-4-((2-chlorophenethyl)amino)-2-methylanthracene-9,10-dione (14)



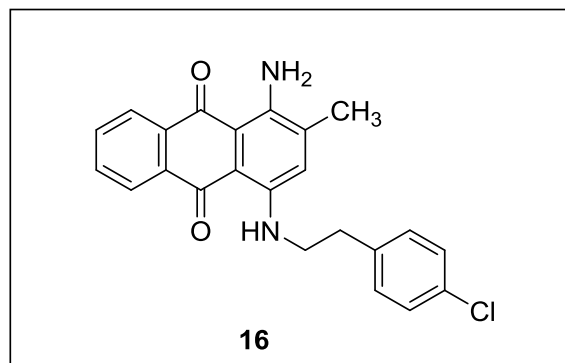
The compound was synthesized according to general procedure (I). 1-Amino-4-bromo-2-methylanthracene-9,10-dione (**1**) (316.2 mg, 1 mmol, 1 equiv.), copper(I) acetate (13.2 mg, 10 mol%), potassium acetate (220.5 mg, 2.25 mmol, 2.25 equiv.) and 2-(2-chlorophenyl)ethanamine (2 mL, 2334 mg, 15 mmol, 15 equiv.). **Reaction time:** 18 h. **Work up procedure A.**

Purification was done by column chromatography on silica gel using ethyl acetate/cyclohexane (30:70). **Appearance:** blue powder. **Yield:** 220 mg (56%); **m.p.** 225-226 °C. **Solubility:** The compound is soluble in acetone, soluble in DMSO and ethanol, but insoluble in water. **Analytical data:** ¹H-NMR (DMSO-*d*₆, 500 MHz) δ (ppm) = 2.31 (s, 3H, CH₃); 3.11 (t, *J* = 7.32 Hz, 2H, -NHCH₂-CH₂-Ph); 3.71 (m, 2H, -NHCH₂-CH₂-Ph); 7.28-7.32 (m, 2H, 3'-H, 4'-H); 7.35 (s, 1H, 3-H); 7.46-7.49 (m, 2H, 5'-H, 6'-H); 7.78-7.81 (m, 2H, 6-H, 7-H); 8.24-8.27 (m, 2H, 5-H, 8-H); 10.87 (s, 1H, 4-NH); (1-NH₂ not detectable). ¹³C-NMR (DMSO, 126 MHz) δ (ppm) = 19.38 (-CH₃), 35.73 (-CH₂-CH₂-), 44.77 (-CH₂-CH₂-), 108.08, 108.81 (C-4a, C-9a), 123.97, 126.49, 126.69 (C-3), 128.21, 129.30, 130.14 (C-5, C-8), 132.25, 132.99, 133.24 (C-6, C-7), 134.06, 134.69 (C-8a, C-10a), 135.08 (C-2), 137.19, 138.77, 146.68 (C-4), 147.00 (C-1), 180.97, 182.52 (C-9, C-10). Purity by HPLC-UV (200-700 nm): 97%. HRMS (ESI-TOF) *m/z*: [M+H]⁺ Calcd. for C₂₃H₂₀ClN₂O₂ 391.1208, Found 391.1192.

1-Amino-4-((3-chlorophenethyl)amino)-2-methylanthracene-9,10-dione (15)

The compound was synthesized according to general procedure (I). 1-Amino-4-bromo-2-methylanthracene-9,10-dione (**1**) (316.2 mg, 1 mmol, 1 equiv.), copper(I) acetate (13.2 mg, 10 mol%), potassium acetate (220.5 mg, 2.25 mmol, 2.25 equiv.) and 2-(3-chlorophenyl)ethanamine (2 mL, 2334 mg, 15 mmol, 15 equiv.). **Reaction time:** 80 min. **Work up procedure A.**

Purification was done by column chromatography on silica gel using cyclohexane/dichloromethane (10:90). **Appearance:** blue powder. **Yield:** 215 mg (55%); **m.p.** 192-194 °C. **Solubility:** The compound is soluble in acetone, dichloromethane and DMSO, but insoluble in water. **Analytical data:** ¹H-NMR (Chloroform-*d*, 600 MHz) δ (ppm) = 2.25 (s, 3H, CH₃); 3.02 (t, *J* = 7.11 Hz, 2H, -NHCH₂-CH₂-Ph); 3.57 (t, *J* = 7.15 Hz, 2H, -NHCH₂-CH₂-Ph); 6.96 (s, 1H, 2'-H); 7.16 (d, *J* = 7.02 Hz, 1H, 6'-H); 7.21 (m, 1H, 5'-H); 7.24 (d, *J* = 5.06 Hz, 1H, 4'-H); 7.26 (s, 1H, 3-H); 7.67-7.71 (m, 2H, 6-H, 7-H); 8.29-8.32 (m, 2H, 5-H, 8-H), (4-NH and 1-NH₂ not detectable). ¹³C-NMR (CDCl₃, 151 MHz) δ (ppm) = 18.46 (CH₃), 35.73 (-CH₂-CH₂-), 44.77 (-CH₂-CH₂-), 109.68, 110.54 (C-4a, C-9a), 122.72, 126.09, 126.28 (C-3), 126.86, 127.08, 128.87 (C-5, C-8), 129.89, 132.18, 132.46 (C-6, C-7), 134.19, 134.41 (C-8a, C-10a), 134.68 (C-2), 135.93, 140.74, 144.38 (C-4), 145.15 (C-1), 182.50, 184.01 (C-9, C-10). Purity by **HPLC-UV (200-650 nm):** 98%. **HRMS (ESI-TOF) *m/z*:** [M+H]⁺ Calcd. for C₂₃H₂₀ClN₂O₂ 391.1208, Found 391.1191.

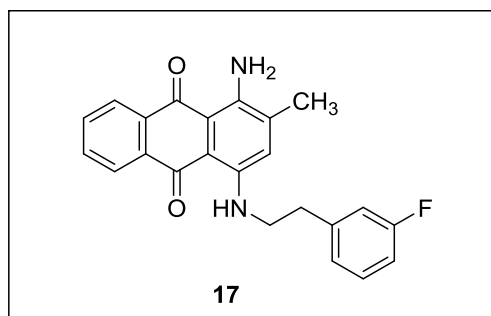
1-Amino-4-((4-chlorophenethyl)amino)-2-methylanthracene-9,10-dione (16)

The compound was synthesized according to general procedure (I). 1-Amino-4-bromo-2-methylanthracene-9,10-dione (**1**) (316.2 mg, 1 mmol, 1 equiv.), copper(I) acetate (13.2 mg, 10 mol%), potassium acetate (220.5 mg, 2.25 mmol, 2.25 equiv.) and 2-(4-chlorophenyl)ethanamine (2 mL, 2334 mg, 15 mmol, 15 equiv.). **Reaction**

time: 120 min. **Work up procedure A.** Purification was done by column chromatography on

silica gel using ethyl acetate/cyclohexane (30:70). **Appearance:** blue powder. **Yield:** 271 mg (69%); **m.p.** 224-225 °C. **Solubility:** The compound is soluble in acetone, dichloromethane and DMSO, but insoluble in water. **Analytical data:** $^1\text{H-NMR}$ (Chloroform-*d*, 600 MHz) δ (ppm) = 2.29 (s, 3H, CH_3); 2.96 (t, $J = 7.13$ Hz, 2H, $-\text{NHCH}_2\text{-CH}_2\text{-Ph}$); 3.67 (q, $J = 6.73$ Hz, 2H, $\text{NHCH}_2\text{-CH}_2\text{-Ph}$); 7.30 (s, 1H, 3-H); 7.36 (m, 4H, 2'-H, 3'-H, 5'-H, 6'-H); 7.29 (d, $J = 7.89$ Hz, 2H, 3'-H, 5'-H); 7.74-7.78 (m, 2H, 6-H, 7-H); 8.19-8.24 (m, 2H, 5-H, 8-H); 10.82 (s, 1H, 4-NH); (1-NH₂ not detectable). $^{13}\text{C-NMR}$ (DMSO, 126 MHz) δ (ppm) = 18.55 (CH_3), 34.81 ($-\text{CH}_2\text{-CH}_2-$), 43.46 ($-\text{CH}_2\text{-CH}_2-$), 107.15, 108.01 (C-4a, C-9a), 123.31; 125.72, 125.90 (C-3), 128.37, 130.85 (C-5, C-8), 131.09, 132.16 (C-6, C-7), 132.43, 133.92 (C-8a, C-10a), 134.34 (C-2), 138.03, 138.23, 145.92 (C-4); 146.30 (C-1), 180.11, 181.72 (C-9, C-10). Purity by **HPLC-UV (200-650 nm)**: 96%. **HRMS (ESI-TOF) m/z :** $[\text{M}+\text{H}]^+$ Calcd. for $\text{C}_{23}\text{H}_{20}\text{ClN}_2\text{O}_2$ 391.1208, Found 391.1195.

1-Amino-4-((3-fluorophenethyl)amino)-2-methylantracene-9,10-dione (17)



The compound was synthesized according to general procedure (I). 1-Amino-4-bromo-2-methylantracene-9,10-dione (1) (316.2 mg, 1 mmol), copper(I) acetate (13.2 mg, 10 mol%), potassium acetate (220.5 mg, 2.25 mmol, 2.25 equiv.) and 2-(3-fluorophenyl)ethanamine (2 mL, 2100 mg, 15 mmol, 15 equiv.). **Reaction time:**

75 min. **Work up procedure A.** Purification was done by column chromatography on silica gel using cyclohexane/dichloromethane (10:90). **Appearance:** blue powder. **Yield:** 260 mg (70%); **m.p.** 257-258 °C. **Solubility:** The compound is soluble in acetone, dichloromethane and DMSO, but insoluble in water. **Analytical data:** $^1\text{H-NMR}$ (Chloroform-*d*, 600 MHz) δ (ppm) = 2.32 (s, 3H, CH_3); 3.11 (t, $J = 7.36$ Hz, 2H, $-\text{NHCH}_2\text{-CH}_2\text{-Ph}$); 3.62 (t, $J = 7.39$ Hz, 2H, $-\text{NHCH}_2\text{-CH}_2\text{-Ph}$); 6.94-6.97 (m, 1H, 5'-H); 7.00 (d, $J = 9.63$ Hz, 1H, 2'-H); 7.09 (d, $J = 7.48$ Hz, 1H, 6'-H); 7.16 (s, 1H, 3-H); 7.29-7.31 (m, 1H, 4'-H); 7.71-7.72 (m, 2H, 6-H, 7-H); 8.27-8.32 (m, 2H, 5-H, 8-H); (1-NH₂ not detectable). $^{13}\text{C-NMR}$ (CDCl_3 , 151 MHz) δ (ppm) = 18.50 (CH_3), 35.35 ($-\text{CH}_2\text{-CH}_2-$), 45.98 ($-\text{CH}_2\text{-CH}_2-$), 113.65, 113.79 (C-4a, C-9a), 115.61, 115.75, 124.58 (C-3), 126.28, 128.44 (C-5, C-8), 130.18, 130.23, 132.71, 132.76 (C-6, C-7), 134.14, 134.33 (C-8a, C-10a), 135.93 (C-2), 140.78, 140.82, 162.19 (C-4), 163.82 (C-1), 183.19, 184.17 (C-9, C-10).

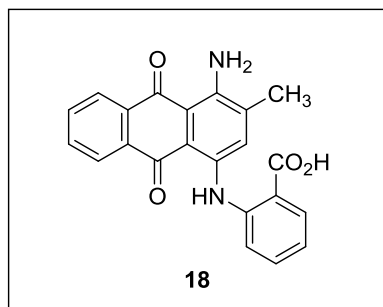
Purity by HPLC-UV (200-650 nm): 97%. HRMS (ESI-TOF) m/z : $[M+H]^+$ Calcd. for $C_{23}H_{20}FN_2O_2$ 375.1503, Found 375.1494.

5.4.3. General synthetic procedure (II) used for anthraquinone derivatives (18-25)

1-Amino-4-bromo-2-methylantracene-9,10-dione (**1**), a mixture of copper metal and copper(II) acetate monohydrate (5 mol% each) as a catalyst, potassium acetate (5 equiv.), the appropriate amine derivative (1.5 or 3 equiv.), and 3.0-4.0 mL of the solvent (methanol, 2.5% v/v) were placed into a 10 mL microwave vial equipped with a magnetic stirrer. The reaction mixture vial was capped and irradiated in a microwave oven using different conditions until complete reaction (as monitored by TLC). The vessel was then allowed to cool to room temperature, the formed mixture was dissolved in water (ca. 250 mL) and the aqueous mixture was extracted with dichloromethane (3×150 mL) until the organic layer became colorless. In cases where a portion of the product was dissolved in dichloromethane layer, the combined organic layers were washed with 0.1 N NaOH solution until the pH reached ca. 7.5-8. The previous basic washing step was repeated until the transfer of the product to the aqueous layer was completed. Using the rotary evaporator, the volume of the combined aqueous extracts was then reduced to approximately 20-100 mL; based on the solubility of each compound in water. After that, purification of the solution was achieved by either using normal column chromatography on silica gel or flash column chromatography on reversed-phase C-18 material using a gradient of acetone in water at concentrations of (5%, 20%, 40%, 60%, and up to 100%) as needed. The collected blue fractions containing the product were concentrated in order to reduce the volume of water and remove acetone. Finally, the remaining water was removed by lyophilization on a freeze dryer, and the desired products were afforded as blue solids.

5.4.4. Characterization of 1-amino-4-(aryl)alkylamino-2-methylantraquinone derivatives (18-25)

1-Amino-4-(2-carboxyphenylamino)-2-methylantracene-9,10-dione (**18**)

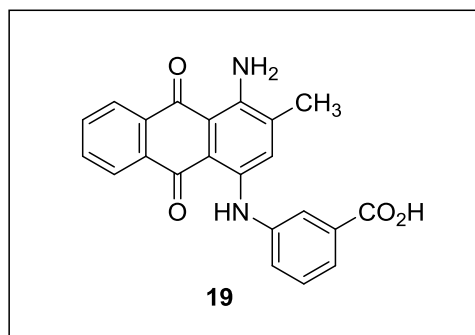


The compound was synthesized according to general procedure (II). 1-Amino-4-bromo-2-methylantracene-9,10-dione (**1**) (79 mg, 0.25 mmol, 1 equiv.), copper(II) acetate monohydrate (2.5

Experimental Part

mg, 5 mol%), copper metal (ca. 0.8 mg, 5 mol%), potassium acetate (122.5 mg, 1.25 mmol, 5 equiv.), 2-aminobenzoic acid (103 mg, 0.75 mmol, 3 equiv.), methanol (2.5% v/v, 4.0 mL), MW condition: 80 W, 95 °C; pressure up to 10 bar. **Reaction time:** 70 min. **Work up.** Purification was done by flash column chromatography on reversed-phase C18 material using gradient of acetone in water 5%, 10%, 20%, then 40%). **Appearance:** blue powder. **Yield:** 87 mg (93%); **m.p.** > 300 °C. **Solubility:** The compound is soluble in acetone, ethanol, DMSO and water. **Analytical data:** ¹H-NMR (DMSO-*d*₆, 500 MHz) δ (ppm) = 2.21 (s, 3H, CH₃); 7.02-7.05 (m, 1H, 4'-H or 5'-H); 7.35 (d, *J* = 8.11 Hz, 1H, 6'-H); 7.43-7.46 (m, 1H, 4'-H or 5'-H); 7.56 (s, 1H, 3-H); 7.79-7.85 (m, 2H, 6-H, 7-H); 7.92 (d, *J* = 7.77 Hz, 1H, 3'-H); 8.20-8.26 (m, 2H, 5-H, 8-H); 12.43 (s, 1H, 4-NH); (1-NH₂ not detectable). ¹³C-NMR (DMSO, 126 MHz) δ (ppm) = 18.59 (-CH₃); 108.95, 112.42 (C-4a, C-9a), 119.86, 120.95 (C-3), 125.87, 126.26 (C-5), 126.96 (C-8), 128.64, 131.30, 132.55 (C-6), 132.60 (C-7), 134.04, 134.38 (C-8a, C-10a), 135.19, 139.15, 140.03 (C-4), 147.33 (C-1), 170.24 (-COOH), 180.54, 182.42 (C-9, C-10). Purity by HPLC-UV (200-700 nm): 99%. HRMS (ESI-TOF) *m/z*: [M-H]⁻ Calcd. for C₂₂H₁₅N₂O₄ 371.1037, Found 371.1036.

1-Amino-4-(3-carboxyphenylamino)-2-methylanthracene-9,10-dione (19)

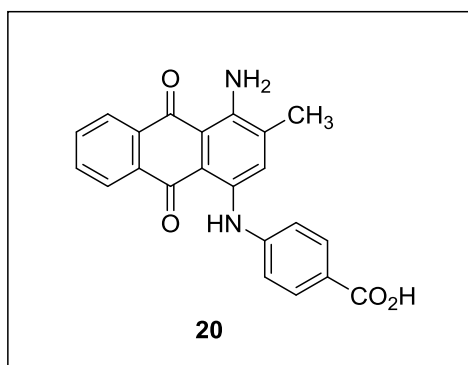


The compound was synthesized according to general procedure (II). 1-Amino-4-bromo-2-methylanthracene-9,10-dione (1) (79 mg, 0.25 mmol, 1 equiv.), copper(II) acetate monohydrate (2.5 mg, 5 mol%), copper metal (ca. 0.8 mg, 5 mol %), potassium acetate (122.5 mg, 1.25 mmol, 5 equiv.), 3-aminobenzoic acid (103 mg, 0.75 mmol, 3 equiv.), methanol (2.5% v/v, 4.0 mL), MW condition: 80 W, 95 °C; pressure up to 9.2 bar. **Reaction time:** 55 min. **Work up.** Purification was done by flash column chromatography on reversed-phase C-18 material using gradient of acetone in water 5%, 10%, 20%, then 40%). **Appearance:** blue powder. **Yield:** 40 mg (36%); **m.p.** > 300 °C. **Solubility:** The compound is soluble in acetone, ethanol, DMSO and water. **Analytical data:** ¹H-NMR (DMSO-*d*₆, 500 MHz) δ (ppm) = 2.25 (s, 3H, CH₃); 7.22-7.24 (m, 1H, 5'-H); 7.32 (d, *J* = 7.62 Hz, 1H, 2'-H); 7.39 (s, 1H, 3-H); 7.69 (d, *J* = 7.52 Hz, 1H, 4'-H); 7.74 (d, *J* = 2.11 Hz, 1H, 6'-H); 7.81-7.83 (m, 2H, 6-H, 7-H); 8.25-8.29 (m, 2H, 5-H, 8-H); 12.32 (s,

Experimental Part

1H, 4-NH); (1-NH₂ not detectable). ¹³C-NMR (DMSO, 126 MHz) δ (ppm) = 18.77 (-CH₃), 108.00, 109.14 (C-4a, C-9a), 123.44, 124.17, 124.51 (C-3), 125.55; 126.00 (C-5), 126.09 (C-8), 128.44, 132.74 (C-6), 132.86 (C-7), 134.06, 134.12 (C-8a, C-10a), 137.51 (C-2), 138.09, 142.78, 143.28 (C-4), 147.11 (C-1), 168.33 (-COOH), 181.60, 181.93 (C-9, C-10). Purity by HPLC-UV (220-650 nm): 96%. HRMS (ESI-TOF) *m/z*: [M-H]⁻ Calcd. for C₂₂H₁₅N₂O₄ 371.1037, Found 371.1039.

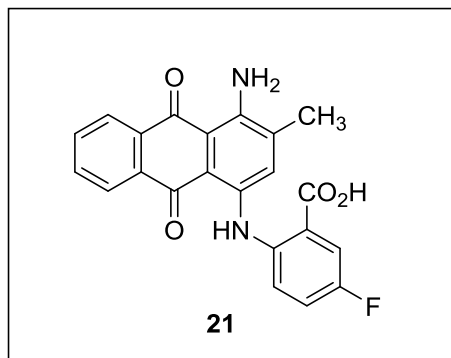
1-Amino-4-(4-carboxyphenylamino)-2-methylantracene-9,10-dione (20)



The compound was synthesized according to general procedure (II). 1-Amino-4-bromo-2-methylantracene-9,10-dione (1) (79 mg, 0.25 mmol, 1 equiv.), copper(II) acetate monohydrate (2.5 mg, 5 mol%), copper metal (ca. 0.8 mg, 5 mol%), potassium acetate (122.5 mg, 1.25 mmol, 5 equiv.), 4-aminobenzoic acid (103 mg, 0.75 mmol, 3 equiv.), methanol (2.5% v/v, 4.0 mL), MW condition: 80 W, 95 °C; pressure up to 9.2 bar. **Reaction time:** 65 min. **Work up.** Purification was done by flash column chromatography on reversed-phase C18 material using gradient of acetone in water 5%, 10%, 20%, then 40%). **Appearance:** blue powder. **Yield:** 45 mg (40%); **m.p.** > 300 °C. **Solubility:** The compound is soluble in acetone, ethanol, DMSO and water. **Analytical data:** ¹H-NMR (DMSO-*d*₆, 600 MHz) δ (ppm) = 2.29 (s, 3H, CH₃); 7.36 (d, *J* = 8.15 Hz, 2H, 2'-H, 6'-H); 7.63 (s, 1H, 3-H); 7.82-7.86 (m, 2H, 6-H, 7-H); 7.93 (d, *J* = 8.11 Hz, 2H, 3'-H, 5'-H); 8.23-8.27 (m, 2H, 5-H, 8-H); 12.07 (s, 1H, 4-NH); (1-NH₂ not detectable). ¹³C-NMR (DMSO, 126 MHz) δ (ppm) = 18.93 (-CH₃), 108.75, 112.08 (C-4a, C-9a), 120.78, 125.97 (C-3), 126.46, 126.53 (C-5, C-8), 131.55, 133.36 (C-6), 133.79 (C-7), 134.07, 134.42 (C-8a, C-10a), 137.46 (C-2), 139.62, 148.06 (C-1), 167.37 (-COOH), 181.32, 182.21 (C-9, C-10). Purity by

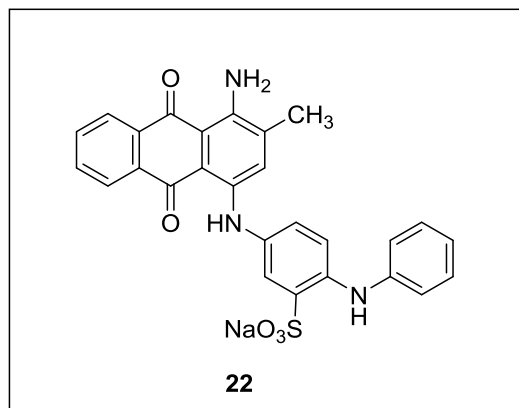
HPLC-UV (200-700 nm): 99%. **HRMS (ESI-TOF) m/z :** $[M-H]^-$ Calcd. for $C_{22}H_{15}N_2O_4$ 371.1037, Found 371.1033.

1-Amino-4-(2-carboxy-4-fluorophenylamino)-2-methylantracene-9,10-dione (21)²⁴⁰



The compound was synthesized according to general procedure (II). 1-Amino-4-bromo-2-methylantracene-9,10-dione (1) (79 mg, 0.25 mmol, 1 equiv.), copper(II) acetate monohydrate (2.5 mg, 5 mol%), copper metal (ca. 0.8 mg, 5 mol%), potassium acetate (122.5 mg, 1.25 mmol, 5 equiv.), 2-amino-5-fluorobenzoic acid (116 mg, 0.75 mmol, 3 equiv.), methanol (2.5% v/v, 4.0 mL), MW condition: 75 W, 95 °C; pressure up to 9.5 bar. **Reaction time:** 70 min. **Work up.** Purification was done by column chromatography on normal silica gel using methanol/dichloromethane (20:80), followed by flash column chromatography on reversed phase silica gel using a gradient of acetone in water (5%, 20%, then 40%). **Appearance:** blue powder. **Yield:** 52 mg (44%); **m.p.** > 300 °C. **Solubility:** The compound is soluble in water, acetone and DMSO, but insoluble in dichloromethane. **Analytical data:** ¹H-NMR (DMSO-*d*₆, 500 MHz) δ (ppm) = 2.25 (s, 3H, CH₃); 7.05 (s, 1H, 3'-H); 7.21-7.23 (m, 1H, 4'-H); 7.47 (s, 1H, 3-H); 7.57 (d, *J* = 4.56 Hz, 1H, 5'-H); 7.79 (d, *J* = 5.99 Hz, 2H, 6-H, 7-H); 8.22-8.24 (m, 2H, 5-H, 8-H); (4-NH or 1-NH₂ not detectable). ¹³C-NMR (DMSO, 126 MHz) δ (ppm) = 18.77 (-CH₃), 108.87, 112.22 (C-4a, C-9a), 122.00, 123.20 (C-3), 125.96, 126.54(C-5), 126.57 (C-8), 132.62, 132.74 (C-6, C-7), 134.03, 134.19 (C-8a, C-10a), 135.52 (C-2), 139.47 (C-4), 147.24 (C-1), 169.19 (-COOH), 182.42, 184.88 (C-9, C-10). Purity by **HPLC-UV (220-700 nm):** 95%. **HRMS (ESI-TOF) m/z :** $[M-H]^-$ Calcd. for $C_{22}H_{14}FN_2O$ 389.0938, Found 389.0943.

1-Amino-2-methyl-4-(4-phenylamino-3-sulfophenylamino)anthracene-9,10-dione (22)⁶⁴

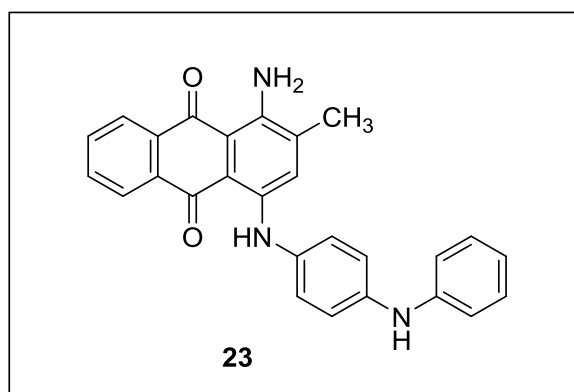


The compound was synthesized according to general procedure (II). 1-Amino-4-bromo-2-methylantracene-9,10-dione (1) (79 mg, 0.25 mmol, 1 equiv.), copper(II) acetate monohydrate (2.5 mg, 5

Experimental Part

mol %), copper metal (ca. 0.8 mg, 5 mol%), potassium acetate (122.5 mg, 1.25 mmol, 5 equiv.), 4-aminodiphenylamine-2-sulfonic Acid (99 mg, 0.375 mmol, 1.5 equiv.), methanol (2.5% v/v, 4.0 mL), MW condition: 80 W, 93 °C; pressure 8 bar. **Reaction time:** 40 min. **Work up.** Purification was done by flash column chromatography on reversed-phase C18 material using gradient of acetone in water 5%, 10%, 20%, then 40%). **Appearance:** blue powder. **Yield:** 63 mg (42%); **m.p.** > 300 °C. **Solubility:** The compound is soluble in acetone, water and DMSO, but insoluble in dichloromethane. **Analytical data:** ¹H-NMR (DMSO-*d*₆, 600 MHz) δ (ppm) = 2.25 (s, 3H, CH₃); 6.91 (t, *J* = 7.32 Hz, 1H, 4''-H); 7.11 (d, *J* = 7.90 Hz, 2H, 2''-H, 6''-H); 7.17 (dd, *J* = 2.74, 8.53 Hz, 1H, 6'-H); 7.28 (d, *J* = 6.26 Hz, 2H, 3''-H, 5''-H); 7.30 (s, 1H, 3-H); 7.33 (d, *J* = 8.52 Hz, 1H, 5'-H); 7.51 (d, *J* = 2.71 Hz, 1H, 2'-H); 7.80-7.83 (m, 2H, 6-H, 7-H); 8.26-8.28 (m, 2H, 5-H, 8-H); 8.51 (s, 1H, 3-H); 12.27 (s, 1H, 4-NH); (1-NH₂ not detectable). ¹³C-NMR (DMSO, 151 MHz) δ (ppm) = 18.82(-CH₃), 116.01, 118.34(C-4a, C-9a), 121.07, 124.00 (C-3), 124.36, 126.06, 126.17, 126.33, 126.38, 129.58, 132.79 (C-6), 132.83 (C-7), 134.09, 134.16 (C-8a, C-10a), 135.06 (C-2), 137.80 (C-4), 143.05, 143.76, 147.09 (C-1), 150.89, 164.16, 168.89, 181.28 (C-9), 181.93 (C-10). Purity by HPLC-UV (220-650 nm): 96%. HRMS (ESI-TOF) *m/z*: [M+H]⁺ Calcd. for C₂₇H₂₂N₃O₅S 500.1280, Found 500.1266.

1-Amino-2-methyl-4-(4-(phenylamino)phenylamino)anthracene-9,10-dione (23)



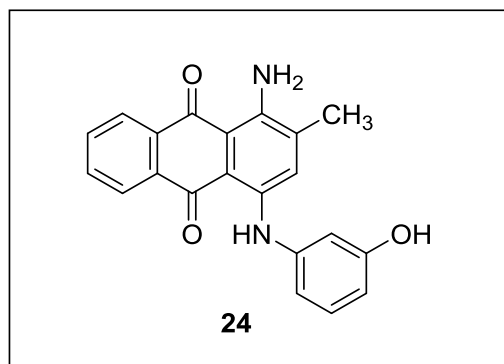
The compound was synthesized according to general procedure (II). 1-Amino-4-bromo-2-methylantracene-9,10-dione (1) (79 mg, 0.25 mmol, 1 equiv.), copper(II) acetate monohydrate (2.5 mg, 5 mol %), copper metal (ca. 0.8 mg, 5 mol%), potassium acetate (122.5 mg, 1.25 mmol, 5 equiv.), 4-aminodiphenylamine (69 mg, 0.375 mmol, 1.5 equiv.), methanol (2.5% v/v, 4.0 mL),

MW condition: 80 W, 93 °C; pressure up to 9.4 bar. **Reaction time:** 35 min. **Work up.** Purification was done by column chromatography on normal silica gel using methanol/dichloromethane (5:95). **Appearance:** blue powder. **Yield:** 50 mg (48%). **Solubility:** The compound is soluble in acetone, dichloromethane and DMSO, but insoluble in water. **Analytical data:** ¹H-NMR (DMSO-*d*₆, 600 MHz) δ (ppm) = 2.26 (s, 3H, CH₃); 6.87 (t, *J* = 7.30

Experimental Part

Hz, 1H, 2'-H or 6'-H); 7.06 (d, $J = 7.82$ Hz, 2H, 3'-H, 5'-H); 7.18 (dd, $J = 2.52, 8.64$ Hz, 1H, 2'-H or 6'-H); 7.25 (dd, $J = 7.27, 8.56$ Hz, 2H, 3''-H, 5''-H); 7.30 (d, $J = 8.75$ Hz, 1H, 4''-H); 7.36 (s, 1H, 2''-H or 6''-H); 7.41 (d, $J = 2.46$ Hz, 1H, 2''-H or 6''-H); 7.68 (s, 1H, 3-H); 7.81-7.83 (m, 2H, 6-H, 7-H); 8.25-8.28 (m, 2H, 5-H, 8-H); 12.12 (s, 1H, 4-NH); (1-NH₂ not detectable). ¹³C-NMR (DMSO, 151 MHz) δ (ppm) = 18.65 (-CH₃), 107.98, 109.32 (C-4a, C-9a), 117.91, 120.28, 120.56, 123.68 (C-3), 124.38, 124.48, 125.30, 125.95 (C-5), 126.11 (C-8), 129.20, 132.77 (C-6), 132.94 (C-7), 133.19 (C-8a), 133.94 (C-10a), 134.08 (C-2), 137.22 (C-4), 137.62, 142.51, 143.41, 147.16 (C-1), 181.70, 181.95 (C-9, C-10). Purity by HPLC-UV (220-700 nm): 85%.

1-Amino-4(3-hydroxyphenylamino)-2-methylantracene-9,10-dione (24)

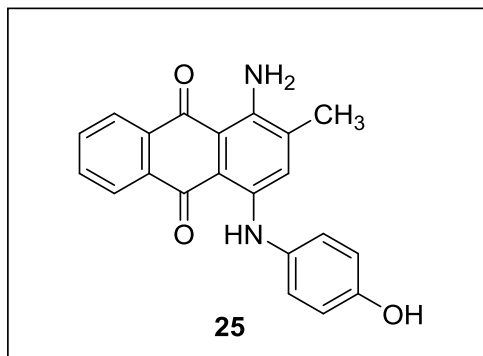


The compound was synthesized according to general procedure (II). 1-Amino-4-bromo-2-methylantracene-9,10-dione (**1**) (79 mg, 0.25 mmol, 1 equiv.), copper(II) acetate monohydrate (2.5 mg, 5 mol %), copper metal (ca. 0.8 mg, 5 mol%), potassium acetate (122.5 mg, 1.25 mmol, 5 equiv.), 3-aminophenol (58 mg, 0.375 mmol, 1.5 equiv.), methanol (2.5% v/v, 4.0 mL). MW

condition: 80 W, 95 °C; pressure up to 9. **Reaction time:** 70 min. **Work up.** Purification was done by column chromatography on normal silica gel using ethyl acetate/cyclohexane (30:70). **Appearance:** blue powder. **Yield:** 37 mg (43%); **m.p.** 285-286 °C. **Solubility:** The compound is soluble in dichloromethane, acetone and DMSO, but insoluble in water. **Analytical data:** ¹H-NMR (DMSO-*d*₆, 500 MHz) δ (ppm) = 2.26 (s, 3H, -CH₃); 6.59 (dd, $J = 1.98, 8.29$ Hz, 1H, 2'-H); 6.68 (t, $J = 2.22$ Hz, 1H, 4'-H); 6.72 (dd, $J = 1.98, 7.64$ Hz, 1H, 6'-H); 7.20 (t, $J = 8.01$ Hz, 1H, 5'-H); 7.46 (s, 1H, 3-H); 7.80-7.84 (m, 2H, 6-H, 7-H); 8.24-8.28 (m, 2H, 5-H, 8-H); 9.57 (s, 1H, 3'-OH); 12.18 (s, 1H, 4-NH); (1-NH₂ not detectable). ¹³C-NMR (DMSO, 126 MHz) δ (ppm) = 18.68 (-CH₃), 108.02, 109.54 (C-4a, C-9a), 109.82, 111.72, 113.79, 124.83 (C-3),

125.98 (C-5), 126.09 (C-8), 130.50, 132.78 (C-6), 132.97 (C-7), 133.94, 134.08 (C-8a, C-10a), 137.39, 140.41 (C-4), 142.02 (C-2), 147.15 (C-1), 158.59, 181.86 (C-9), 181.98 (C-10). Purity by **HPLC-UV (200-700 nm)**: 93%. **HRMS (ESI-TOF) m/z** : $[M-H]^-$ Calcd. for $C_{21}H_{15}N_2O_3$ 343,1088, Found 343,1087.

1-Amino-4(4-hydroxyphenylamino)-2-methylantracene-9,10-dione (25)



The compound was synthesized according to general procedure (II). 1-Amino-4-bromo-2-methylantracene-9,10-dione (**1**) (79 mg, 0.25 mmol, 1 equiv.), copper(II) acetate monohydrate (2.5 mg, 5 mol%), copper metal (ca. 0.8 mg, 5 mol%), potassium acetate (122.5 mg, 1.25 mmol, 5 equiv.), 4-aminophenol (58 mg, 0.375 mmol, 1.5 equiv.), methanol (2.5% v/v, 4.0 mL), MW

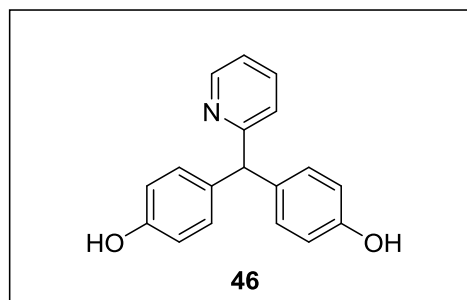
condition: 75 W, 95 °C; pressure up to 9.5 bar. **Reaction time**: 45 min. **Work up**. Purification was done by column chromatography on normal silica gel using methanol/dichloromethane (5:95), followed by ethyl acetate/cyclohexane (30:70). **Appearance**: blue powder. **Yield**: 39 mg (45%); **m.p.** 225-226 °C. **Solubility**: The compound is soluble in dichloromethane, acetone and DMSO, but insoluble in water. **Analytical data**: 1H -NMR (DMSO- d_6 , 500 MHz) δ (ppm) = 2.22 (s, 3H, -CH₃); 6.84 (d, J = 8.65 Hz, 2H, 3'-H, 5'-H); 7.12 (d, J = 8.70 Hz, 2H, 2'-H, 6'-H); 7.21 (s, 1H, 3-H), 7.79-7.82 (m, 2H, 6-H, 7-H); 8.24-8.28 (m, 2H, 5-H, 8-H); 9.49 (s, 1H, -OH); 12.22 (s, 1H, 4-NH); (1-NH₂ not detectable). ^{13}C -NMR (DMSO, 126 MHz) δ (ppm) = 18.70 (-CH₃), 107.84, 108.24 (C-4a, C-9a), 116.35, 124.16 (C-3), 125.89, 126.08 (C-5), 126.30 (C-8), 130.03, 132.67, 134.11, 137.72, 144.20 (C-2), 146.90 (C-1), 155.30, 181.00 (C-9), 181.78 (C-10). **Purity by HPLC-UV (200-700 nm)**: 91%.

7.5 5.5. Chemistry of bisacodyl-derived compounds

Bisacodyl (4,4'-diacetoxy-diphenyl)-(pyridyl-2)-methane which is a commercially available drug, was either subjected to complete hydrolysis of the di-acetyl ester groups affording the diphenol derivative (**46**), or the removal of one acetyl group formed the monohydroxylated derivative (**47**).

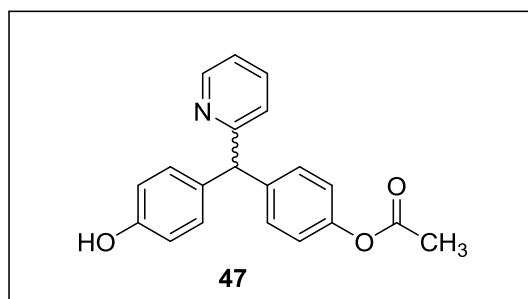
Bis-(*p*-hydroxyphenyl)pyridyl-2-methane (46)

Experimental Part



According to the reported procedure, a suspension of (pyridin-2-ylmethylene)bis-(4,1-phenylene) diacetate (5 g, 13.84 mmol) in 55 mL of a solution of KOH containing 10% of EtOH was stirred overnight at rt. After the completion of the reaction, the volatile solvent was removed and the solid residue was dissolved in EtOAc (100 mL). The mixture was treated with dilute aqueous HCl solution (2 M) until a pH value of 1-2 was reached, then treated with a saturated aqueous solution of Na₂CO₃ until the pH turned to ca. 8-9. The collected organic extracts were successively washed with brine (3 × 50 mL), three more times with water and then dried over MgSO₄. The residue after solvent removal was purified using column chromatography on silica gel using ethyl acetate/dichloromethane (25:75) to yield the title compound. **Reaction time:** 15 h. **Appearance:** white powder. **Yield:** 3.5 g (93%); **m.p.** 258-260 °C. **Solubility:** The compound is soluble in acetone, ethyl acetate and methanol, but insoluble in water. **Analytical data:** ¹H-NMR (DMSO-d₆, 600 MHz) δ (ppm) = 5.40 (s, 1H, -CH); 6.66 (d, *J* = 8.52 Hz, 4H, 3-H, 3'-H, 5-H, 5'-H); 6.94 (d, *J* = 8.53 Hz, 4H, 2-H, 2'-H, 6-H, 6'-H); 7.15 (d, *J* = 7.86 Hz, 1H, 3-H_{py}); 7.18 (dd, *J* = 5.15, 6.97 Hz, 1H, 4-H_{py}); 7.67 (td, *J* = 1.87, 7.68 Hz, 1H, 5-H_{py}); 8.48 (d, *J* = 4.03 Hz, 1H, 6-H_{py}); 9.23 (br s, 2H, -OH). ¹³C-NMR (DMSO, 151 MHz) δ (ppm) = 56.95(-CH), 115.07, 121.43 (5-C_{py}), 123.42 (3-C_{py}), 129.97, 133.94, 136.64(4-C_{py}), 149.126 (6-C_{py}), 155.75, 163.74. **LC-MS:** (*m/z*): positive mode 278 [M]⁺. Purity by **HPLC-UV (220-400 nm)**-ESI-MS: 98%. **HRMS (ESI-TOF) *m/z*:** [M-H]⁻ Calcd. for C₁₈H₁₄NO₂ 276.1030, Found 276.1056.

4-((4-Hydroxyphenyl)(pyridin-2-yl)methyl)phenyl acetate (47)



The title compound was prepared according to the method reported by Marie *et al.* with some modifications. (Pyridin-2-ylmethylene)bis-(4,1-phenylene) diacetate (1000 mg, 2.76 mmol; 1 equiv.) was suspended in a 30 mL mixture of (THF : MeOH 14 : 1). The mixture was treated LiOH·H₂O (150.5 mg, 3.59 mmol; 1.3 equiv.) in water (15 mL). After complete addition, the mixture was stirred at rt and the reaction was controlled by TLC. The solid residue obtained after evaporation of

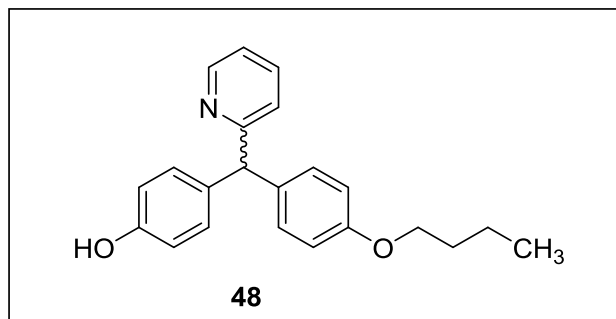
Experimental Part

solvents using a vacuum pump was diluted with water (50 mL). The aqueous mixture was extracted using EtOAc (3 × 50 mL), and then the organic layers were washed with brine (2 × 15 mL) and dried over anhydrous Na₂SO₄. Purification was done using column chromatography on silica gel using ethyl acetate/dichloromethane (5:95) to afford the pure product (**47**). **Reaction time:** 45 min. **Appearance:** white powder. **Yield:** 500 mg (57%); **m.p.** 150-152 °C. **Solubility:** The compound is freely soluble in acetone, methanol and dichloromethane, but insoluble in water. **Analytical data:** ¹H-NMR (DMSO-*d*₆, 600 MHz) δ (ppm) = 2.23 (s, 3H, -CH₃); 5.55 (s, 1H, -CH); 6.68 (d, *J* = 8.58 Hz, 2H, 3-H_{ArOH}, 5-H_{ArOH}); 7.00 (d, *J* = 3.13 Hz, 2H, 3-H_{Ar}, 5-H_{Ar}); 7.02 (d, *J* = 3.22 Hz, 2H, 2-H_{Ar}, 6-H_{Ar}); 7.19 (d, *J* = 8.61 Hz, 2H, 2-H_{ArOH}, 6-H_{ArOH}); 7.21-7.23 (m, 2H, 3-H_{Py}, 4-H_{Py}); 7.71 (td, *J* = 1.91, 7.70 Hz, 1H, 5-H_{Py}); 8.51-8.52 (m, 1H, 6-H_{Py}); 9.26 (s, 1H, -OH). ¹³C-NMR (DMSO, 151 MHz) δ (ppm) = 20.98 (-CH₃), 56.85 (-CH), 115.24, 121.56 (5-C_{Py}), 121.71, 123.64 (3-C_{Py}), 130.02, 130.06, 133.26, 136.88 (4-C_{Py}), 141.28, 148.86 (6-C_{Py}), 149.29, 155.98, 162.95, 169.39 (-COOCH₃). **LC-MS:** (m/z): positive mode 319.9 [M]⁺. Purity by **HPLC-UV (220-400 nm)-ESI-MS:** 97%. **HRMS (ESI-TOF) m/z:** [M-H]⁻ Calcd. for C₂₀H₁₆NO₃ 318.1136, Found 318.1148.

5.5.1. General synthetic procedure (III) (**48-66**, **68**, **69**, **72**, **78a**, **80**, **81**, **83**, **85**, and **99**)

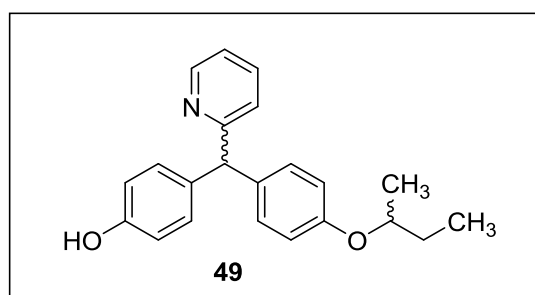
The phenolic (**46**, **50**, **55**, **79**, **82**, **78**, and **98**) or alcoholic (**71** and **84**) starting material (1 equiv.) was dissolved in DMF (5 mL), then the mixture thus obtained was cooled down to 0 °C, followed by the addition of NaH (60% in paraffin oil, 1.1 equiv. for each OH group) portionwise over 10 min. After stirring for an additional 30-45 min at the same temperature, the corresponding alkylating agent (1.1 equiv. for each OH group) was added dropwise. The reaction mixture was allowed to reach rt and was controlled by TLC. After the reaction was completed, the mixture was poured onto ice and extracted with EtOAc (3 × 25 mL). The organic layers were washed with brine (2 × 15 mL), dried over MgSO₄ and concentrated. Purification was done using column chromatography to give the pure compounds (**48-66** in case of starting material **46**; **68** in case of starting material **55**; **80** and **81** in case of starting material **79**; **83** in case of starting material **82**; **78a** in case of starting material **78**; **99** in case of starting material **98**; **72** in case of starting material **71**; and **85** in case of starting material **84**), some compounds needed further recrystallization.

5.5.2. Characterization of the bisacodyl-derived compounds

5.5.2.1. 4-((4-Butoxyphenyl)(pyridin-2-yl)methyl)phenol (**48**)

The compound was synthesized according to general procedure (III). Compound **46** (200 mg, 0.72 mmol, 1 equiv.), NaH (60% in paraffin oil, 63 mg, 1.6 mmol, 2.2 equiv.) and 1-bromobutane (0.15 mL, 219 mg, 1.6 mmol, 2.2 equiv.). **Reaction time:** 1 h. **Work up.** Purification was done by column

chromatography on silica gel using ethyl acetate/dichloromethane (5:95). **Appearance:** beige powder. **Yield:** 75 mg (31%); **m.p.** 145-146 °C. **Solubility:** The compound is freely soluble in acetone, methanol and ethyl acetate, but insoluble in water. **Analytical data:** ¹H-NMR (DMSO-*d*₆, 600 MHz) δ (ppm) = 0.90 (t, *J* = 7.39 Hz, 3H, -OCH₂-CH₂-CH₂-CH₃); 1.37-1.43 (m, -OCH₂-CH₂-CH₂-CH₃); 1.63-1.67 (m, 2H, -OCH₂-CH₂-CH₂-CH₃); 3.90 (t, *J* = 6.50 Hz, 2H, -OCH₂-CH₂-CH₂-CH₃); 5.45 (s, 1H, -CH); 6.65 (d, *J* = 8.54 Hz, 2H, 3-H_{ArOH}, 5-H_{ArOH}); 6.81 (d, *J* = 8.71 Hz, 2H, 3-H_{Ar}, 5-H_{Ar}); 6.95 (d, *J* = 8.53 Hz, 2H, 2-H_{ArOH}, 6-H_{ArOH}); 7.05 (d, *J* = 8.65 Hz, 2H, 2-H_{Ar}, 6-H_{Ar}); 7.16 (d, *J* = 7.84 Hz, 1H, 3-H_{Py}); 7.19 (dd, *J* = 4.89, 7.43 Hz, 1H, 4-H_{Py}); 7.69 (td, *J* = 1.87, 7.63 Hz, 1H, 5-H_{Py}); 8.49 (d, *J* = 4.60 Hz, 1H, 6-H_{Py}); 9.21 (s, 1H, -OH). ¹³C-NMR (DMSO, 151 MHz) δ (ppm) = 13.82 (-OCH₂-CH₂-CH₂-CH₃), 18.88 (-OCH₂-CH₂-CH₂-CH₃), 30.90(-OCH₂-CH₂-CH₂-CH₃), 56.80 (-CH), 67.15 (-OCH₂-CH₂-CH₂-CH₃), 114.20, 115.09, 121.50 (5-C_{Py}), 123.47 (3-C_{Py}), 129.97, 130.01, 133.76, 135.60, 136.70 (4-C_{Py}), 149.17 (6-C_{Py}), 155.78, 157.13, 163.49. **LC-MS:** (*m/z*): positive mode 333.9 [M]⁺. Purity by **HPLC-UV (220-400 nm)**-ESI-MS: 97%. **HRMS (ESI-TOF) *m/z*:** [M-H]⁻ Calcd. for C₂₂H₂₂NO₂ 332.1656, Found 332.1657.

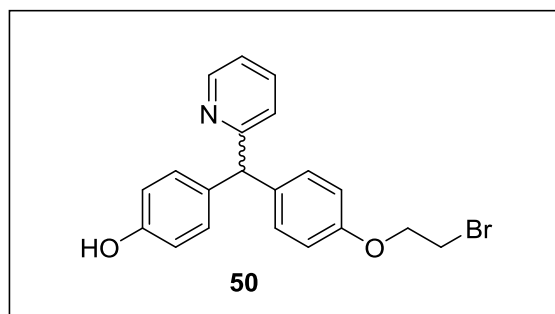
5.5.2.2. 4-((4-(Sec-butoxy)phenyl)(pyridin-2-yl)methyl)phenol (**49**)

The compound was synthesized according to general procedure (III). Compound **46** (1200 mg, 4.32 mmol, 1 equiv.), NaH (60% in paraffin oil, 380 mg, 9.5 mmol, 2.2 equiv.) and 2-bromobutane (1 mL,

Experimental Part

1302 mg, 9.5 mmol, 2.2 equiv.). **Reaction time:** 1.5 h. **Work up.** Purification was done by column chromatography on silica gel using ethyl acetate/dichloromethane (20:80), followed by crystallization with diethyl ether. **Appearance:** white powder. **Yield:** 640 mg (44%); **m.p.** 160-162 °C. **Solubility:** The compound is soluble in acetone and methanol, but insoluble in water. **Analytical data:** $^1\text{H-NMR}$ ($\text{DMSO-}d_6$, 600 MHz) δ (ppm) = 0.88 (t, $J = 7.43$ Hz, 3H, -CH(CH₃)-CH₂-CH₃); 1.16-1.18 (m, 3H, -CH(CH₃)-CH₂-CH₃); 1.49-1.63 (m, 2H, -CH(CH₃)-CH₂-CH₃); 4.26-4.31 (m, $J = 6.02$ Hz, 1H, -CH(CH₃)-CH₂-CH₃); 5.44 (s, 1H, -CH); 6.66 (d, $J = 8.53$ Hz, 2H, 3-H_{ArOH}, 5-H_{ArOH}); 6.80 (d, $J = 8.67$ Hz, 2H, 3-H_{Ar}, 5-H_{Ar}); 6.96 (d, $J = 8.59$ Hz, 2H, 2-H_{ArOH}, 6-H_{ArOH}); 7.04 (d, $J = 8.62$ Hz, 2H, 2-H_{Ar}, 6-H_{Ar}); 7.17-7.20 (m, 2H, 3-H_{Py}, 4-H_{Py}); 7.69 (td, $J = 1.89, 7.65$ Hz, 1H, 5-H_{Py}); 8.49-8.50 (m, 1H, 6-H_{Py}); 9.21 (s, 1H, -OH). $^{13}\text{C-NMR}$ (DMSO , 151 MHz) δ (ppm) = 9.71 (-CH-(CH₃)-CH₂-CH₃), 19.26 (-CH-(CH₃)-CH₂-CH₃), 28.74 (-CH-(CH₃)-CH₂-CH₃), 56.83 (-CH), 74.15 (-CH-(CH₃)-CH₂-CH₃), 115.10, 115.35, 121.51 (5-C_{Py}), 123.48 (3-C_{Py}), 129.98, 130.08, 133.77, 135.49, 136.71 (4-C_{Py}), 149.18 (6-C_{Py}), 155.79, 156.21, 163.51. **LC-MS:** (m/z): positive mode 333.9 [M]⁺. Purity by **HPLC-UV (220-400 nm)**-**ESI-MS:** 99%. **HRMS (ESI-TOF) m/z :** [M-H]⁻ Calcd. for C₂₂H₂₂NO₂ 332.1656, Found 332.1682.

5.5.2.3. 4-((4-(2-Bromoethoxy)phenyl)(pyridin-2-yl)methyl)phenol (50)

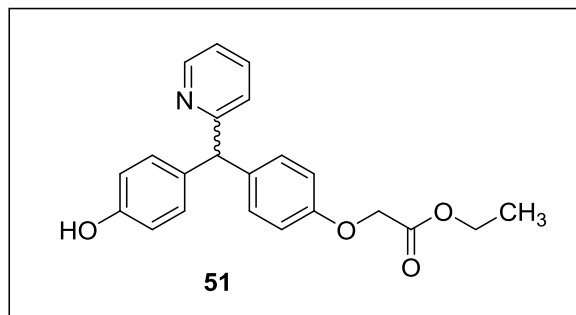


The compound was synthesized according to general procedure (III). Compound **46** (400 mg, 1.44 mmol, 1 equiv.), NaH (60% in paraffin oil, 127 mg, 3.2 mmol, 2.2 equiv.) and 1,2-dibromoethane (0.2 mL, 413 mg, 3.2 mmol, 2.2 equiv.). **Reaction time:** 2 h. **Work up.** Purification was done by column chromatography on silica gel using ethyl acetate/dichloromethane (5:95), followed by crystallization with ethyl acetate/cyclohexane (20:80). **Appearance:** yellow powder. **Yield:** 231 mg (42%); **m.p.** 155-157 °C. **Solubility:** The compound is soluble in acetone and methanol, but insoluble in water. **Analytical data:** $^1\text{H-NMR}$ ($\text{DMSO-}d_6$, 600 MHz) δ (ppm) = 3.76 (t, $J = 6.00$ Hz, 2H, -OCH₂-CH₂-Br); 4.26 (t, $J = 6.00$ Hz, 2H, -OCH₂-CH₂-Br); 5.47 (s, 1H, -CH); 6.66 (d, $J = 8.52$ Hz, 2H, 3-H_{ArOH}, 5-H_{ArOH}); 6.86 (d, $J = 8.68$ Hz, 2H, 3-H_{Ar}, 5-H_{Ar}); 6.96 (d, $J = 8.49$ Hz, 2H, 2-H_{ArOH}, 6-H_{ArOH}); 7.08 (d, $J = 8.63$ Hz, 2H, 2-H_{Ar}, 6-H_{Ar}); 7.17-7.20 (m, 2H, 3-H_{Py}, 4-H_{Py});

Experimental Part

7.69 (td, $J = 1.92, 7.70$ Hz, 1H, 5- H_{Py}); 8.49 (d, $J = 3.86$ Hz, 1H, 6- H_{Py}); 9.22 (s, 1H, -OH). ^{13}C -NMR (DMSO, 151 MHz) δ (ppm) = 31.66 (-OCH₂-CH₂-Br), 56.78 (-CH), 67.87 (-OCH₂-CH₂-Br), 114.47, 115.13, 121.56 (5- C_{Py}), 123.51 (3- C_{Py}), 129.99, 130.16, 133.69, 136.37 (4- C_{Py}), 136.75, 149.20 (6- C_{Py}), 155.82, 156.38, 163.40. LC-MS: (m/z): positive mode 383.9 [M]⁺. Purity by HPLC-UV (220-400 nm)-ESI-MS: 96%. HRMS (ESI-TOF) m/z : [M-H]⁻ Calcd. for C₂₀H₁₇BrNO₂ 382.0448, Found 382.0444.

5.5.2.4. Ethyl 2-(4-((4-hydroxyphenyl)(pyridin-2-yl)methyl)phenoxy)acetate (51)

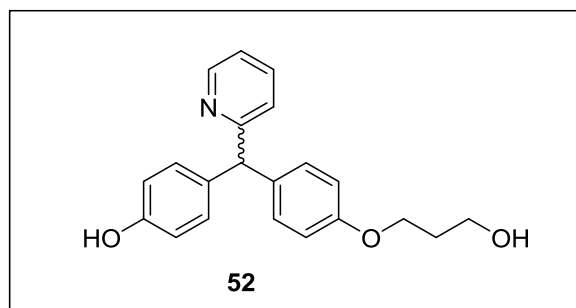


The compound was synthesized according to general procedure (III). Compound 46 (100 mg, 0.36 mmol, 1 equiv.), NaH (60% in paraffin oil, 16 mg, 0.396 mmol, 1.1 equiv.) and ethyl bromoacetate (0.04 mL, 66 mg, 0.396 mmol, 1.1 equiv.). **Reaction time:** 1 h. **Work up.**

Purification was done by column chromatography on silica gel using ethyl acetate/dichloromethane (10:90). **Appearance:** colorless oil. **Yield:** 60 mg (46%). **Solubility:** The compound is miscible with acetone and methanol, but immiscible with water. **Analytical data:** 1H -NMR (DMSO- d_6 , 500 MHz) δ (ppm) = 1.19 (t, $J = 7.11$ Hz, 3H, -OCH₂-CH₃); 4.14 (q, $J = 7.09$ Hz, 2H, OCH₂-CH₃); 4.70 (s, 2H, -OCH₂-CO); 5.46 (s, 1H, CH); 6.66 (d, $J = 8.52$ Hz, 2H, 3- H_{ArOH} , 5- H_{ArOH}); 6.82 (d, $J = 8.74$ Hz, 2H, 3- H_{Ar} , 5- H_{Ar}); 6.96 (d, $J = 8.53$ Hz, 2H, 2- H_{ArOH} , 6- H_{ArOH}); 7.07 (d, $J = 8.70$ Hz, 2H, 2- H_{Ar} , 6- H_{Ar}); 7.17-7.20 (m, 2H, 3- H_{Py} , 4- H_{Py}); 7.69 (td, $J = 1.90, 7.70$ Hz, 1H, 5- H_{Py}); 8.49-8.50 (m, 1H, 6- H_{Py}); 9.22 (s, 1H, OH). ^{13}C -NMR (DMSO, 126 MHz) δ (ppm) = 14.18 (-CH₃), 56.77 (-CH), 60.74 (-CH₂-CH₃), 64.84 (-OCH₂), 114.34, 115.14, 121.56 (5- C_{Py}), 123.51 (3- C_{Py}), 129.98, 130.06, 133.66, 136.55

(4-C_{Py}), 136.75, 149.21 (6-C_{Py}), 155.83, 156.09, 163.36, 168.91 (CO). **LC-MS:** (*m/z*): positive mode 364 [M]⁺. Purity by **HPLC-UV (220-400 nm)**-ESI-MS: 98%.

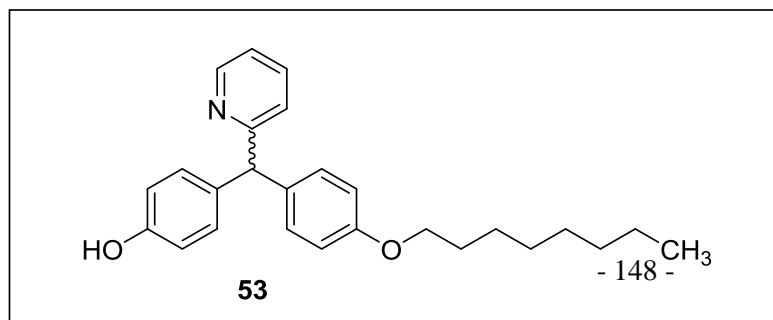
5.5.2.6. 4-((4-(3-Hydroxypropoxy)phenyl)(pyridin-2-yl)methyl)phenol (52)



The compound was synthesized according to general procedure (III). Compound **46** (800 mg, 2.9 mmol, 1 equiv.), NaH (60% in paraffin oil, 256 mg, 6.4 mmol, 2.2 equiv.) and 3-bromo-1-propanol (0.58 mL, 890 mg, 6.4 mmol, 2.2 equiv.). **Reaction time:** 2 h. **Work up.**

Purification was done by column chromatography on silica gel using ethyl acetate/dichloromethane (20:80). **Appearance:** yellow powder. **Yield:** 420 mg (43%); **m.p.** 100-102 °C. **Solubility:** The compound is soluble in acetone and methanol, but insoluble in water. **Analytical data:** ¹H-NMR (DMSO-*d*₆, 500 MHz) δ (ppm) = 1.79-1.84 (m, 2H, -OCH₂-CH₂-CH₂-OH); 3.50-3.54 (m, 2H, -OCH₂-CH₂-CH₂-OH); 3.97 (t, *J* = 6.38 Hz, 2H, -OCH₂-CH₂-CH₂-OH); 4.48 (t, *J* = 5.15 Hz, 1H, -OCH₂-CH₂-CH₂-OH); 5.45 (s, 1H, -CH); 6.66 (d, *J* = 8.54 Hz, 2H, 3-H_{ArOH}, 5-H_{ArOH}); 6.82 (d, *J* = 8.67 Hz, 2H, 3-H_{Ar}, 5-H_{Ar}); 6.95 (d, *J* = 8.46 Hz, 2H, 2-H_{ArOH}, 6-H_{ArOH}); 7.05 (d, *J* = 8.58 Hz, 2H, 2-H_{Ar}, 6-H_{Ar}); 7.15-7.20 (m, 2H, 3-H_{Py}, 4-H_{Py}); 7.69 (td, *J* = 1.87, 7.66 Hz, 1H, 5-H_{Py}); 8.49-8.50 (m, 1H, 6-H_{Py}); 9.19 (s, 1H, -OH). ¹³C-NMR (DMSO, 126 MHz) δ (ppm) = 32.30 (-OCH₂-CH₂-CH₂-OH), 56.81 (-CH), 57.47 (-OCH₂-CH₂-CH₂-OH), 64.63 (-OCH₂-CH₂-CH₂-OH), 114.22, 115.09, 121.49 (5-C_{Py}), 123.46 (3-C_{Py}), 129.96, 130.01, 133.77, 135.62, 136.68 (4-C_{Py}), 149.16 (6-C_{Py}), 155.77, 157.13, 163.50. **LC-MS:** (*m/z*): positive mode 335.9 [M]⁺. Purity by **HPLC-UV (220-400 nm)**-ESI-MS: 95%. **HRMS (ESI-TOF) m/z:** [M-H]⁻ Calcd. for C₂₁H₂₀NO₃ 334.1449, Found 334.1454.

5.5.2.7. 4-((4-(Octyloxy)phenyl)(pyridin-2-yl)methyl)phenol (53)

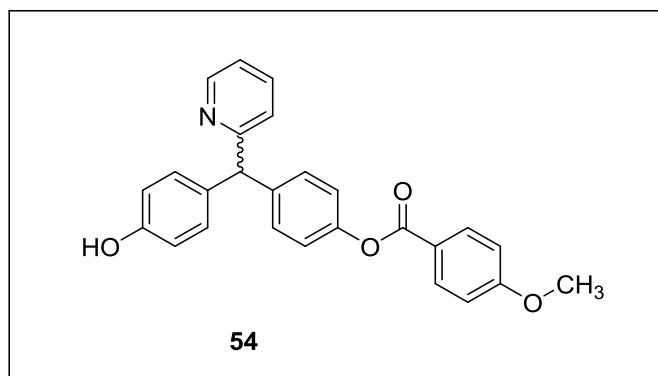


The compound was synthesized according to general procedure (III). Compound **46** (400 mg, 1.44 mmol, 1 equiv.), NaH (60% in

Experimental Part

paraffin oil, 127 mg, 3.2 mmol, 2.2 equiv.) and 1-bromooctane (0.4 mL, 425 mg, 3.2 mmol, 2.2 equiv.). **Reaction time:** 3 h. **Work up.** Purification was done by column chromatography on silica gel using ethyl acetate/dichloromethane (20:80). **Appearance:** white powder. **Yield:** 178 mg (32%); **m.p.** 112-114 °C. **Solubility:** The compound is soluble in acetone and methanol, but insoluble in water. **Analytical data:** $^1\text{H-NMR}$ (DMSO- d_6 , 600 MHz) δ (ppm) = 0.84 (t, J = 6.87 Hz, 3H, $-\text{OCH}_2-(\text{CH}_2)_5-\text{CH}_2-\text{CH}_3$); 1.24-1.30 (m, 8H, $-\text{OCH}_2-\text{CH}_2-\text{CH}_2-(\text{CH}_2)_4-\text{CH}_3$); 1.34-1.39 (m, $-\text{OCH}_2-\text{CH}_2-\text{CH}_2-(\text{CH}_2)_4-\text{CH}_3$); 1.63-1.68 (m, $-\text{OCH}_2-\text{CH}_2-\text{CH}_2-(\text{CH}_2)_4-\text{CH}_3$); 3.88 (t, J = 6.47 Hz, 2H, $-\text{OCH}_2-\text{CH}_2-\text{CH}_2-(\text{CH}_2)_4-\text{CH}_3$); 5.45 (s, 1H, $-\text{CH}$); 6.65 (d, J = 8.51 Hz, 2H, 3- H_{ArOH} , 5- H_{ArOH}); 6.81 (d, J = 8.66 Hz, 2H, 3- H_{Ar} , 5- H_{Ar}); 6.95 (d, J = 8.55 Hz, 2H, 2- H_{ArOH} , 6- H_{ArOH}); 7.04 (d, J = 8.68 Hz, 2H, 2- H_{Ar} , 6- H_{Ar}); 7.16-7.20 (m, 2H, 3- H_{Py} , 4- H_{Py}); 7.69 (td, J = 1.86, 7.68 Hz, 1H, 5- H_{Py}); 8.48-8.49 (m, 1H, 6- H_{Py}); 9.21 (s, 1H, $-\text{OH}$). $^{13}\text{C-NMR}$ (DMSO, 151 MHz) δ (ppm) = 14.09 ($-\text{OCH}_2-(\text{CH}_2)_5-\text{CH}_2-\text{CH}_3$), 22.21 ($-\text{OCH}_2-(\text{CH}_2)_5-\text{CH}_2-\text{CH}_3$), 25.68, 28.79, 28.85, 28.86, 31.37 ($-\text{OCH}_2-\text{CH}_2-\text{CH}_2-(\text{CH}_2)_4-\text{CH}_3$), 56.81 ($-\text{CH}$), 67.46 ($-\text{OCH}_2-(\text{CH}_2)_5-\text{CH}_2-\text{CH}_3$), 114.21, 115.10, 121.51 (5- C_{Py}), 123.47 (3- C_{Py}), 129.97, 130.02, 130.02, 133.77, 135.60, 136.70 (4- C_{Py}), 149.18 (6- C_{Py}), 155.78, 157.14, 163.50. **LC-MS:** (m/z): positive mode 390.4 $[\text{M}]^+$. Purity by **HPLC-UV (254 nm)-ESI-MS:** 97%.

5.5.2.8. 4-((4-Hydroxyphenyl)(pyridin-2-yl)methyl)phenyl 4-methoxybenzoate (54)

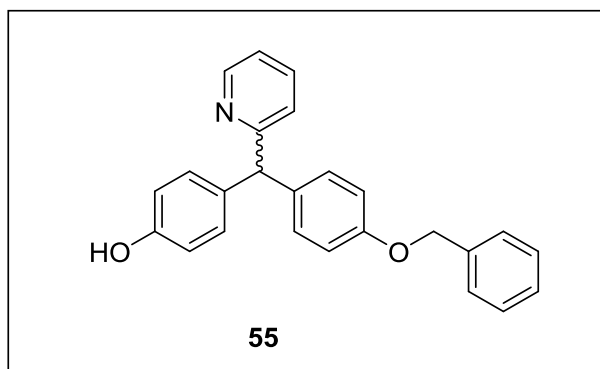


The compound was synthesized according to general procedure (III). Compound **46** (400 mg, 1.44 mmol, 1 equiv.), NaH (60% in paraffin oil, 127 mg, 3.2 mmol, 2.2 equiv.) and 4-methoxybenzoyl chloride (0.4 mL, 546 mg, 3.2 mmol, 2.2 equiv.).

Reaction time: 3 h. **Work up.** Purification was done by column chromatography on silica gel using ethyl acetate/dichloromethane (2:98). **Appearance:** beige powder. **Yield:** 165 mg (13%); **m.p.** 195-197 °C. **Solubility:** The compound is soluble in acetone and dichloromethane, but insoluble in water. **Analytical data:** $^1\text{H-NMR}$ (DMSO- d_6 , 600 MHz) δ (ppm) = 3.85 (s, 3H, $-\text{OCH}_3$); 5.59 (s, 1H, $-\text{CH}$); 6.70 (d, J = 8.53 Hz, 2H, 3- H_{ArOH} , 5- H_{ArOH}); 7.03 (d, J = 8.51 Hz, 2H, 2- H_{ArOH} , 6- H_{ArOH}); 7.10 (d, J = 8.87 Hz, 2H, 2H, 3- H_{ArOMe} , 5- H_{ArOMe}); 7.15 (d, J = 8.56 Hz, 2H,

2-H_{Ar}, 6-H_{Ar}); 7.21-7.25 (m, 4H, 3-H_{Ar}, 5-H_{Ar}, 3-H_{Py}, 4-H_{Py}); 7.73 (td, $J = 1.84, 7.69$ Hz, 1H, 5-H_{Py}); 8.05 (d, $J = 8.87$ Hz, 2H, 2-H_{ArOMe}, 6-H_{ArOMe}); 8.52-8.54 (m, 1H, 6-H_{Py}); 9.27 (s, 1H, -OH). ¹³C-NMR (DMSO, 151 MHz) δ (ppm) = 55.78 (-OCH₃), 56.85 (-CH), 114.41, 115.23, 121.14 (5-C_{Py}), 121.69, 123.64 (3-C_{Py}), 130.06, 132.09, 133.27, 136.87 (4-C_{Py}), 141.35, 149.04 (6-C_{Py}), 149.29, 155.96, 162.95, 163.85 (-CO), 164.37. LC-MS: (m/z): positive mode 412.2 [M]⁺. Purity by HPLC-UV (220-400 nm)-ESI-MS: 99%. HRMS (ESI-TOF) m/z : [M-H]⁻ Calcd. for C₂₆H₂₀NO₄ 410.1398, Found 410.1415.

5.5.2.9. 4-((4-(Benzyloxy)phenyl)(pyridin-2-yl)methyl)phenol (55)

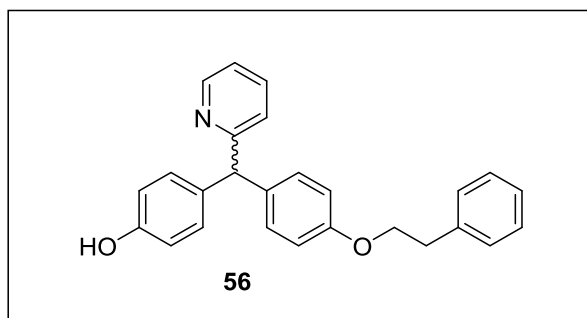


The compound was synthesized according to general procedure (III). Compound **46** (800 mg, 2.9 mmol, 1 equiv.), NaH (60% in paraffin oil, 256 mg, 6.4 mmol, 2.2 equiv.) and benzyl bromide (0.76 mL, 1095 mg, 6.4 mmol, 2.2 equiv.). **Reaction time:** 1 h. **Work up.** Purification was done by column chromatography on silica gel using ethyl acetate/dichloromethane (8:92). **Appearance:** yellow powder. **Yield:** 420 mg (20%); **m.p.** 160-161 °C. **Solubility:** The compound is soluble in acetone and methanol, but insoluble in water. **Analytical data:** ¹H-NMR (DMSO-*d*₆, 600 MHz) δ (ppm) = 5.04 (s, 2H, -CH₂); 5.46 (s, 1H, -CH); 6.66 (d, $J = 8.58$ Hz, 2H, 3-H_{ArOH}, 5-H_{ArOH}); 6.91 (d, $J = 8.76$ Hz, 2H, 2-H_{Ar}, 6-H_{Ar}); 6.96 (d, $J = 8.53$ Hz, 2H, 2-H_{ArOH}, 6-H_{ArOH}); 7.07 (d, $J = 8.68$ Hz, 2H, 3-H_{Ar}, 5-H_{Ar}); 7.16-7.20 (m, 2H, 3-H_{Py}, 4-H_{Py}); 7.30 (m, 1H, 4-H_{Ph}); 7.36 (m, $J = 7.52$ Hz, 2H, 3-H_{Ph}, 5-H_{Ph}); 7.41 (d, $J = 7.37$ Hz, 2H, 2-H_{Ph}, 6-H_{Ph}); 7.69 (td, $J = 1.87, 7.68$ Hz, 1H, 5-H_{Py}); 8.49-8.50 (m, 1H, 6-H_{Py}); 9.22 (s, 1H, -OH). ¹³C-NMR (DMSO, 151 MHz) δ (ppm) = 56.81 (-CH), 69.33 (-CH₂), 114.59, 115.13, 121.54 (5-C_{Py}), 123.50 (3-C_{Py}), 127.78, 127.92, 128.56, 130.00, 130.08, 133.74, 136.04 (4-C_{Py}),

Experimental Part

136.74, 137.34, 149.20 (6-C_{Py}), 155.82, 156.84, 163.46. **LC-MS:** (*m/z*): positive mode 368.1 [M]⁺. Purity by **HPLC-UV (220-400 nm)-ESI-MS:** 97%. **HRMS (ESI-TOF) *m/z*:** [M-H]⁻ Calcd. for C₂₅H₂₀NO₂ 366.1500, Found 366.1498.

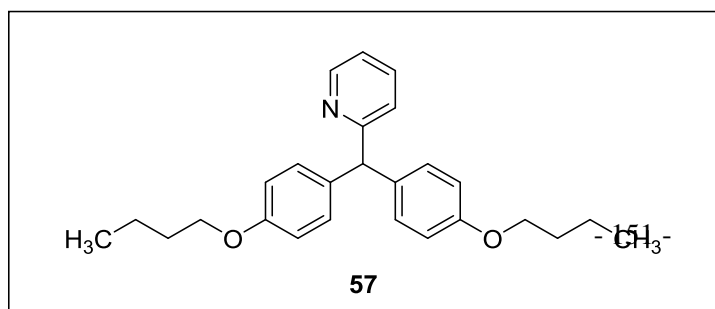
5.5.2.10. 4-((4-Phenethoxyphenyl)(pyridin-2-yl)methyl)phenol (**56**)



The compound was synthesized according to general procedure (**III**). Compound **46** (1200 mg, 4.32 mmol, 1 equiv.), NaH (60% in paraffin oil, 380 mg, 9.5 mmol, 2.2 equiv.) and (2-bromoethyl)benzene (0.3 mL, 407 mg, 9.5 mmol, 2.2 equiv.). **Reaction time:** 1 h. **Work up.** Purification was done by column

chromatography on silica gel using ethyl acetate/dichloromethane (20:80). **Appearance:** white powder. **Yield:** 155 mg (9%); **m.p.** 135-136 °C. **Solubility:** The compound is soluble in acetone and methanol, but insoluble in water. **Analytical data:** ¹H-NMR (DMSO-*d*₆, 600 MHz) δ (ppm) = 2.99 (t, *J* = 6.84 Hz, 2H, -OCH₂-CH₂-Ph); 4.12 (t, *J* = 6.85 Hz, 2H, -OCH₂-CH₂-Ph); 5.45 (s, 1H, -CH); 6.66 (d, *J* = 8.60 Hz, 2H, 3-H_{ArOH}, 5-H_{ArOH}); 6.83 (d, *J* = 8.79 Hz, 2H, 3-H_{Ar}, 5-H_{Ar}); 6.95 (d, *J* = 8.50 Hz, 2H, 2-H_{ArOH}, 6-H_{ArOH}); 7.05 (d, *J* = 8.70 Hz, 2H, 2-H_{Ar}, 6-H_{Ar}); 7.16 (d, *J* = 7.86 Hz, 1H, CH_{Ph}); 7.17-7.21 (m, 2H, 3-H_{Py}, 4-H_{Py}); 7.27-7.31 (m, 4H, CH_{Ph}); 7.68 (td, *J* = 1.88, 7.67 Hz, 1H, 5-H_{Py}); 8.48-8.50 (m, 1H, 6-H_{Py}); 9.21 (s, 1H, -OH). ¹³C-NMR (DMSO, 151 MHz) δ (ppm) = 35.43 (-OCH₂-CH₂-Ph), 57.12 (-CH), 68.53 (-OCH₂-CH₂-Ph), 114.59, 115.43, 121.83 (5-C_{Py}), 123.80 (3-C_{Py}), 126.69, 128.74, 129.37, 130.30, 130.39, 134.07, 136.13 (4-C_{Py}), 137.02, 138.87, 149.50 (6-C_{Py}), 156.12, 157.19, 163.80. **LC-MS:** (*m/z*): positive mode 382.2 [M]⁺. Purity by **HPLC-UV (220-400 nm)-ESI-MS:** 95%. **HRMS (ESI-TOF) *m/z*:** [M-H]⁻ Calcd. for C₂₆H₂₂NO₂ 380.1656, Found 380.1653.

5.5.2.11. Bis(*p*-butoxyphenyl)pyridyl-2-methane (**57**)

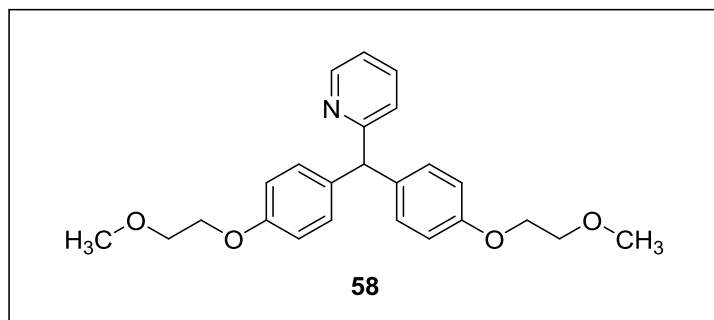


The compound was synthesized according to general procedure (**III**). Compound **46** (434 mg, 1.56 mmol, 1

Experimental Part

equiv.), NaH (60% in paraffin oil, 137 mg, 3.4 mmol, 2.2 equiv.) and 1-bromobutane (0.4 mL, 466 mg, 3.4 mmol, 2.2 equiv.). **Reaction time:** 2 h. **Work up.** Purification was done by column chromatography on silica gel using ethyl acetate/dichloromethane (2:98). **Appearance:** yellow oil. **Yield:** 574 (94%). **Solubility:** The compound is miscible with acetone, methanol and ethyl acetate, but immiscible with water. **Analytical data:** $^1\text{H-NMR}$ (DMSO- d_6 , 600 MHz) δ (ppm) = 0.90 (t, $J = 7.43$ Hz, 6H, 2(-OCH₂-CH₂-CH₂-CH₃)); 1.37-1.43 (m, 2(-OCH₂-CH₂-CH₂-CH₃)); 1.62-1.67 (m, 2(-OCH₂-CH₂-CH₂-CH₃)); 3.90 (t, $J = 6.46$ Hz, 4H, 2(-OCH₂-CH₂-CH₂-CH₃)); 5.51 (s, 1H, -CH); 6.82 (d, $J = 8.70$ Hz, 4H, 3-H, 3'-H, 5-H, 5'-H); 7.06 (d, $J = 8.63$ Hz, 4H, 2-H, 2'-H, 6-H, 6'-H); 7.18-7.21 (m, 2H, 3-H_{Py}, 4-H_{Py}); 7.69 (td, $J = 1.89, 7.68$ Hz, 1H, 5-H_{Py}); 8.50 (d, $J = 5.49$ Hz, 1H, 6-H_{Py}). $^{13}\text{C-NMR}$ (DMSO, 151 MHz) δ (ppm) = 13.80 (-OCH₂-CH₂-CH₂-CH₃), 18.87 (-OCH₂-CH₂-CH₂-CH₃), 30.90 (-OCH₂-CH₂-CH₂-CH₃), 56.67(-CH), 67.15 (-OCH₂-CH₂-CH₂-CH₃), 114.23, 121.56 (5-C_{Py}), 123.51 (3-C_{Py}), 130.01, 135.40, 136.74, 149.21 (6-C_{Py}), 157.18, 163.26. **LC-MS:** (m/z): positive mode 390.1 [M]⁺. Purity by **HPLC-UV (220-400 nm)**-**ESI-MS:** 95%. **HRMS (ESI-TOF) m/z :** [M+H]⁺ Calcd. for C₂₆H₃₂NO₂ 390.2428, Found 390.2397.

5.5.2.12. Bis-(*p*-(2-methoxyethoxy)phenyl)pyridyl-2-methane (58)

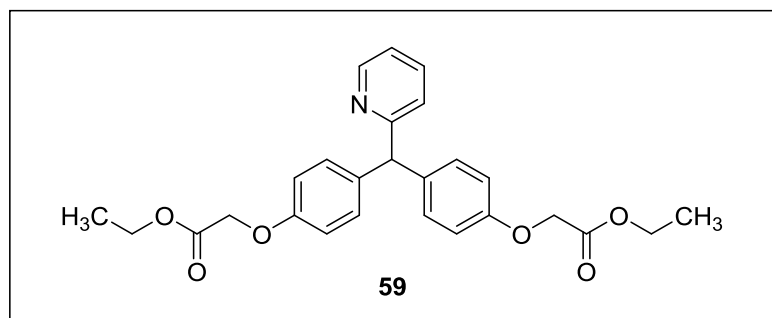


The compound was synthesized according to general procedure (III). Compound **46** (400 mg, 1.44 mmol, 1 equiv.), NaH (60% in paraffin oil, 127 mg, 3.2 mmol, 2.2 equiv.) and 1-bromo-2-methoxyethane (0.2 mL, 306 mg, 3.2 mmol, 2.2 equiv.).

Reaction time: 4 h. **Work up.** Purification was done by column chromatography on silica gel using ethyl acetate/dichloromethane (2:98). **Appearance:** yellow oil. **Yield:** 447 mg (79%). **Solubility:** The compound is miscible with acetone and methanol, but immiscible with water. **Analytical data:** $^1\text{H-NMR}$ (DMSO- d_6 , 600 MHz) δ (ppm) = 3.28 (s, 6H, 2(-OCH₃)); 3.61-3.62. (m, 4H, 2(-OCH₂-CH₂-OCH₃)); 4.02-4.03 (m, 4H, 2(-OCH₂-CH₂-OCH₃)); 5.52 (s, 1H, -CH); 6.84 (d, $J = 8.74$ Hz, 4H, 3-H, 3'-H, 5-H, 5'-H); 7.07 (d, $J = 8.71$ Hz, 4H, 2-H, 2'-H, 6-H, 6'-H); 7.18-7.21 (m, 2H, 3-H_{Py}, 4-H_{Py}); 7.70 (td, $J = 1.88, 7.66$ Hz, 1H, 5-H_{Py}); 8.50-8.51 (m, 1H, 6-H_{Py}).

$^{13}\text{C-NMR}$ (DMSO, 151 MHz) δ (ppm) = 56.63 (-CH), 58.29 (-OCH₂-CH₂-OCH₃), 66.96 (-OCH₂-CH₂-OCH₃), 70.54 (-OCH₂-CH₂-OCH₃), 114.29, 121.61 (5-C_{Py}), 123.55 (3-C_{Py}), 130.06, 135.63, 136.79 (4-C_{Py}), 149.25 (6-C_{Py}), 156.99, 163.21. **LC-MS:** (*m/z*): positive mode 394.2 [M]⁺. Purity by **HPLC-UV (220-400 nm)**-ESI-MS: 96%. **HRMS (ESI-TOF)** *m/z*: [M+H]⁺ Calcd. for C₂₄H₂₈NO₄ 394.2013, Found 394.1983.

5.5.2.13. Diethyl 2,2'-(4,4'-(pyridin-2-ylmethylene)-bis-(4,1-phenylene))-bis-(oxy)diacetate (59)²¹⁴

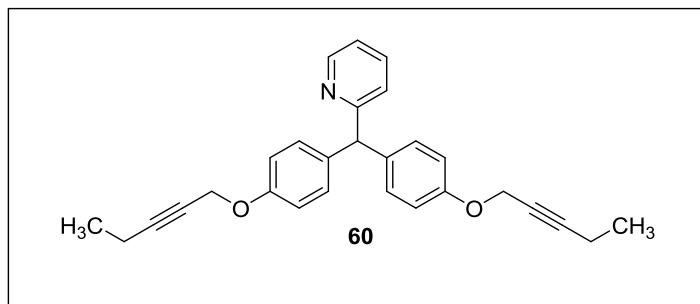


The compound was synthesized according to general procedure (III). Compound **46** (1200 mg, 4.32 mmol, 1 equiv.), NaH (60% in paraffin oil, 380 mg, 9.5 mmol, 2.2 equiv.) and ethyl bromoacetate (1.1 mL, 1587 mg, 9.5 mmol, 2.2

equiv.). **Reaction time:** 2 h. **Work up.** Purification was done by column chromatography on silica gel using ethyl acetate/dichloromethane (2:98). **Appearance:** light brown powder. **Yield:** 1490 mg (77%); **m.p.** 75-77 °C. **Solubility:** The compound is soluble in acetone and ethyl acetate, but insoluble in water. **Analytical data:** $^1\text{H-NMR}$ (DMSO-*d*₆, 600 MHz) δ (ppm) = 1.19 (t, *J* = 7.09 Hz, 6H, 2(-CH₂-CH₃)); 4.14 (q, *J* = 7.10 Hz, 4H, 2(-CH₂-CH₃)); 4.70 (s, 4H, 2(-OCH₂)); 5.54 (s, 1H, -CH); 6.83 (d, *J* = 8.77 Hz, 4H, 3-H, 3'-H, 5-H, 5'-H); 7.09 (d, *J* = 8.72 Hz, 4H, 2-H, 2'-H, 6-H, 6'-H); 7.20-7.22 (m, 2H, 3-H_{Py}, 4-H_{Py}); 7.71 (td, *J* = 1.88, 7.70 Hz, 1H, 5-H_{Py}); 8.50-8.51 (m, 1H, 6-H_{Py}). $^{13}\text{C-NMR}$ (DMSO, 151 MHz) δ (ppm) = 14.19 (-CH₃), 56.53 (-CH), 60.74 (-CH₂-CH₃), 64.81 (-OCH₂), 114.40, 121.69(5-C_{Py}), 123.60 (3-C_{Py}), 130.07, 136.21 (4-C_{Py}), 136.89, 149.26 (6-C_{Py}), 156.16, 168.89 (CO). **LC-MS:** (*m/z*): positive mode 450 [M]⁺.

Purity by HPLC-UV (220-400 nm)-ESI-MS: 95%. HRMS (ESI-TOF) m/z : $[M+H]^+$ Calcd. for $C_{26}H_{28}NO_6$ 450.1911, Found 450.1871.

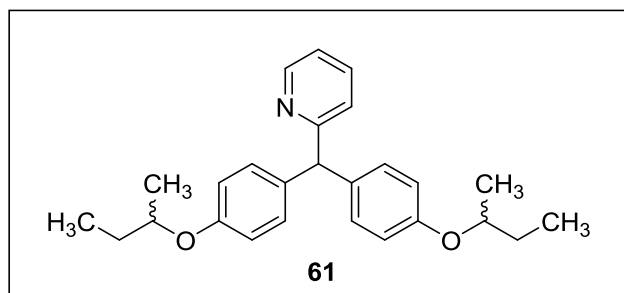
5.5.2.14. Bis-(*p*-(pent-2-yn-1-yloxy)phenyl)pyridyl-2-methane (60)



The compound was synthesized according to general procedure (III). Compound **46** (800 mg, 2.9 mmol, 1 equiv.), NaH (60% in paraffin oil, 256 mg, 6.4 mmol, 2.2 equiv.) and 1-bromo-2-pentyne (0.76 mL, 953.8 mg, 6.4

mmol, 2.2 equiv.). **Reaction time:** 3 h. **Work up.** Purification was done by column chromatography on silica gel using ethyl acetate/dichloromethane (3:97). **Appearance:** dark yellow oil. **Yield:** 750 mg (66%). **Solubility:** The compound is miscible with acetone and methanol, but immiscible with water. **Analytical data:** 1H -NMR (DMSO- d_6 , 600 MHz) δ (ppm) = 1.03 (t, J = 7.48 Hz, 6H, 2(-CH₂-CH₃)); 2.19 (qt, J = 2.10, 7.48 Hz, 4H, 2(-CH₂-CH₃)); 4.68 (t, J = 2.21 Hz, 4H, 2(-CH₂-C)); 5.53 (s, 1H, -CH); 6.87 (d, J = 8.71 Hz, 4H, 3-H, 3'-H, 5-H, 5'-H); 7.10 (d, J = 8.68 Hz, 4H, 2-H, 2'-H, 6-H, 6'-H); 7.20-7.21 (m, 2H, 3-H_{Py}, 4-H_{Py}); 7.70 (td, J = 1.86, 7.69 Hz, 1H, 5-H_{Py}); 8.50-8.51 (m, 1H, 6-H_{Py}). ^{13}C -NMR (DMSO, 151 MHz) δ (ppm) = 11.83, 13.66, 56.01, 56.63, 75.20, 89.04, 114.62, 121.65 (5-C_{Py}), 123.57 (3-C_{Py}), 130.00, 136.03, 136.82 (4-C_{Py}), 149.26 (6-C_{Py}), 156.01, 163.06. **LC-MS:** (m/z): positive mode 410.4 $[M]^+$. Purity by HPLC-UV (220-400 nm)-ESI-MS: 99%. HRMS (ESI-TOF) m/z : $[M+H]^+$ Calcd. for $C_{28}H_{28}NO_2$ 410.2115, Found 410.2085.

5.5.2.15. Bis-(*p*-(sec-butoxy)phenyl)pyridyl-2-methane (61)

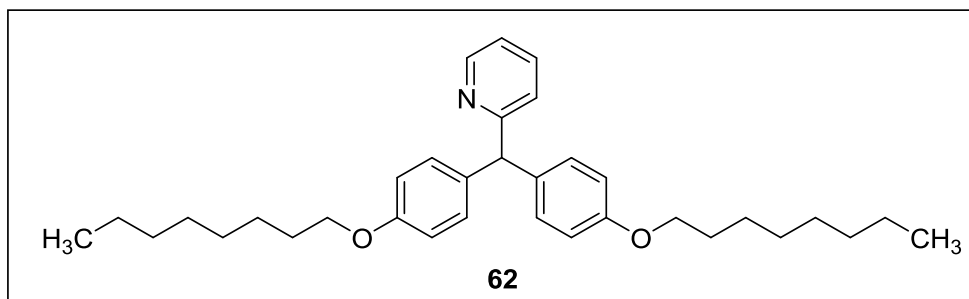


The compound was synthesized according to 5.5.2.2. **Reaction time:** 1.5 h. **Work up.** Purification was done by column chromatography on silica gel using ethyl acetate/dichloromethane (2:98). **Appearance:** yellow oil. **Yield:** 520 mg (31%). **Solubility:**

The compound is miscible with acetone and methanol, but immiscible with water. **Analytical**

data: $^1\text{H-NMR}$ ($\text{DMSO-}d_6$, 600 MHz) δ (ppm) = 0.88 (t, J = 7.43 Hz, 6H, 2(-CH-(CH₃)-CH₂-CH₃)); 1.18 (d, J = 6.04 Hz, 6H, 2(-CH-(CH₃)-CH₂-CH₃)); 1.49-1.64 (m, 4H, 2(-CH-(CH₃)-CH₂-CH₃)); 4.27-4.30 (m, 2H, 2(-CH-(CH₃)-CH₂-CH₃)); 5.49 (s, 1H, -CH); 6.81 (d, J = 8.75 Hz, 4H, 3-H, 3'-H, 5-H, 5'-H); 7.06 (d, J = 8.65 Hz, 4H, 2-H, 2'-H, 6-H, 6'-H); 7.19-7.21 (m, 2H, 3-H_{Py}, 4-H_{Py}); 7.70 (td, J = 1.87, 7.68 Hz, 1H, 5-H_{Py}); 8.50-8.51 (m, 1H, 6-H_{Py}). $^{13}\text{C-NMR}$ (DMSO , 151 MHz) δ (ppm) = 9.69 (-CH-(CH₃)-CH₂-CH₃), 19.24 (-CH-(CH₃)-CH₂-CH₃), 28.73 (-CH-(CH₃)-CH₂-CH₃), 56.69 (-CH), 74.15 (-CH-(CH₃)-CH₂-CH₃), 115.39, 121.57 (5-C_{Py}), 123.53 (3-C_{Py}), 130.08, 135.29, 136.77 (4-C_{Py}), 149.22 (6-C_{Py}), 156.27, 163.28. **LC-MS:** (m/z): positive mode 390 [M]⁺. Purity by **HPLC-UV (220-400 nm)-ESI-MS:** 96%. **HRMS (ESI-TOF) m/z :** [M+H]⁺ Calcd. for C₂₆H₃₂NO₂ 390.2428, Found 390.2358.

5.5.2.16. Bis(*p*-(octyloxy)phenyl)pyridyl-2-methane (62)



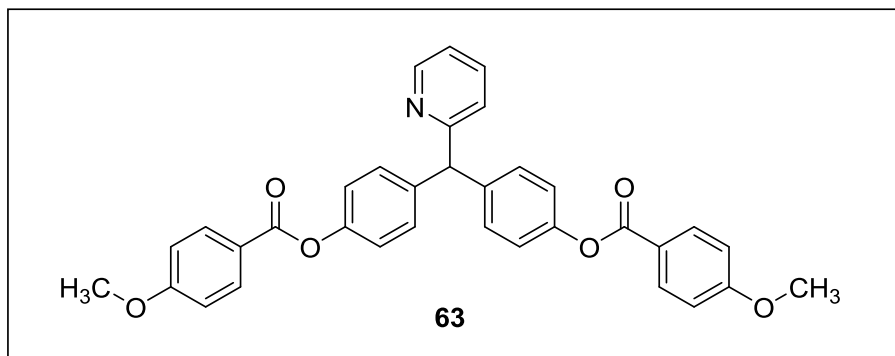
The compound was synthesized according to **5.5.2.7. Reaction time:** 3 h. **Work up.** Purification

was done by column chromatography on silica gel using ethyl acetate/dichloromethane (1:99). **Appearance:** yellow oil. **Yield:** 400 mg (55%). **Solubility:** The compound is soluble in acetone and dichloromethane, but insoluble in water. **Analytical data:** $^1\text{H-NMR}$ ($\text{DMSO-}d_6$, 500 MHz) δ (ppm) = 0.83-0.85 (m, 6H, 2(-OCH₂-(CH₂)₅-CH₂-CH₃)); 1.24-1.30 (m, 16H, 2(-OCH₂-CH₂-CH₂-(CH₂)₄-CH₃)); 1.34-1.40 (m, 4H, 2(-OCH₂-CH₂-CH₂-(CH₂)₄-CH₃)); 1.63-1.69 (m, 4H, 2(-OCH₂-CH₂-CH₂-(CH₂)₄-CH₃)); 3.89 (t, J = 6.50 Hz, 4H, 2(-OCH₂-CH₂-CH₂-(CH₂)₄-CH₃)); 5.50 (s, 1H, -CH); 6.81 (d, J = 8.70 Hz, 4H, 3-H, 3'-H, 5-H, 5'-H); 7.06 (d, J = 8.25 Hz, 4H, 2-H, 2'-H, 6-H, 6'-H); 7.17-7.21 (m, 2H, 3-H_{Py}, 4-H_{Py}); 7.69 (td, J = 1.89, 7.68 Hz, 1H, 5-H_{Py}); 8.49-8.50 (m, 1H, 6-H_{Py}). $^{13}\text{C-NMR}$ (DMSO , 151 MHz) δ (ppm) = 14.05 (-OCH₂-(CH₂)₅-CH₂-CH₃), 22.18 (-OCH₂-(CH₂)₅-CH₂-CH₃), 25.65, 28.76, 28.83, 28.84, 31.34 (-OCH₂-CH₂-CH₂-(CH₂)₄-CH₃), 56.69 (-CH), 67.47 (-OCH₂-(CH₂)₅-CH₂-CH₃), 114.25, 121.55 (5-C_{Py}), 123.49 (3-C_{Py}),

Experimental Part

130.00, 135.40, 136.72 (4-C_{Py}), 149.20 (6-C_{Py}), 157.18, 163.26. **LC-MS:** (*m/z*): positive mode 502.3 [M]⁺. Purity by **HPLC-UV (220-400 nm)-ESI-MS:** 96%. **HRMS (ESI-TOF) *m/z*:** [M+H]⁺ Calcd. for C₃₄H₄₈NO 502.3680, Found 502.3701.

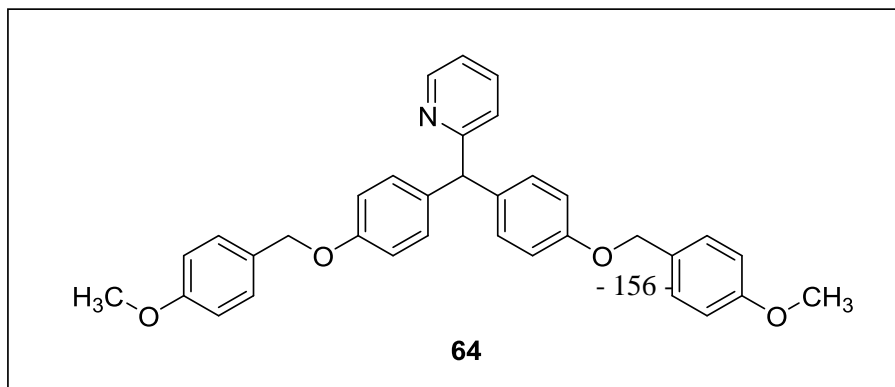
5.5.2.17. (Pyridin-2-ylmethylene)-bis-(4,1-phenylene)-bis-(4-methoxybenzoate) (63)



The compound was synthesized according to **5.5.2.8. Reaction time:** 3 h. **Work up.** Purification was done by column chromatography on silica gel using ethyl

acetate/petroleum ether (15:85), followed by crystallization with diethyl ether. **Appearance:** white powder. **Yield:** 267 mg (68%); **m.p.** 170-172 °C. **Solubility:** The compound is soluble in acetone and dichloromethane, but insoluble in water. **Analytical data:** ¹H-NMR (DMSO-*d*₆, 600 MHz) δ (ppm) = 3.86 (s, 6H, 2(-OCH₃)); 5.79 (s, 1H, -CH); 7.11 (d, *J* = 8.89 Hz, 4H, 3-H_{ArOMe}, 3'-H_{ArOMe}, 5-H_{ArOMe}, 5'-H_{ArOMe}); 7.20 (d, *J* = 8.61 Hz, 4H, 2-H, 2'-H, 6-H, 6'-H); 7.27 (m, 1H, 3-H_{Py}); 7.32-7.34 (m, 5H, 3-H_{Ar}, 3'-H_{Ar}, 5-H_{Ar}, 5'-H_{Ar}, 4-H_{Py}); 7.77 (td, *J* = 1.86, 7.69 Hz, 1H, 5-H_{Py}); 8.06 (d, *J* = 8.90 Hz, 4H, 2-H_{ArOMe}, 2'-H_{ArOMe}, 6-H_{ArOMe}, 6'-H_{ArOMe}); 8.58-8.59 (m, *J* = 0.91, 1.82, 4.78 Hz, 1H, 6-H_{Py}). ¹³C-NMR (DMSO, 151 MHz) δ (ppm) = 55.77 (-OCH₃), 56.73 (-CH), 114.41, 121.10 (5-C_{Py}), 121.89, 121.96, 123.86 (3-C_{Py}), 130.14, 132.09, 137.09 (4-C_{Py}), 140.64, 149.26 (6-C_{Py}), 149.46, 162.20, 163.86 (-CO), 164.34. **LC-MS:** (*m/z*): positive mode 546.2 [M]⁺. Purity by **HPLC-UV (220-400 nm)-ESI-MS:** 100%. **HRMS (ESI-TOF) *m/z*:** [M+H]⁺ Calcd. for C₃₄H₂₈NO₆ 546.1911, Found 546.1877.

5.5.2.18. Bis-(*p*-((4-methoxybenzyl)oxy)phenyl)pyridyl-2-methane (64)

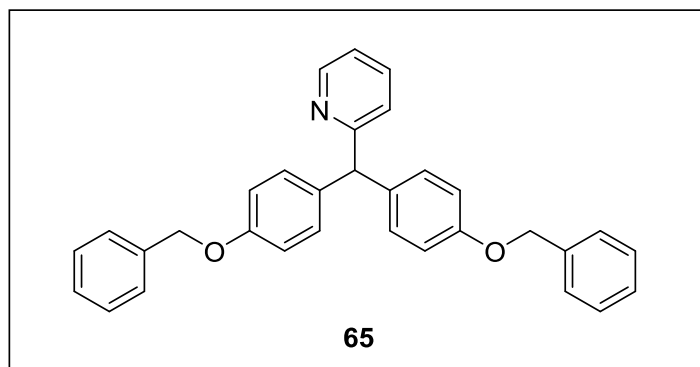


The compound was synthesized according to general procedure (III). Compound **46** (800 mg,

Experimental Part

2.9 mmol, 1 equiv.), NaH (60% in paraffin oil, 256 mg, 6.4 mmol, 2.2 equiv.) and 4-methoxybenzyl chloride (0.9 mL, 1002 mg, 6.4 mmol, 2.2 equiv.). **Reaction time:** 2 h. **Work up.** Purification was done by column chromatography on silica gel using ethyl acetate/dichloromethane (1:99). **Appearance:** white powder. **Yield:** 440 mg (29%); **m.p.** 122-124 °C. **Solubility:** The compound is soluble in acetone and methanol, but insoluble in water. **Analytical data:** $^1\text{H-NMR}$ (DMSO- d_6 , 600 MHz) δ (ppm) = 3.73 (s, 6H, 2(-OCH₃)); 4.95 (s, 4H, 2(-CH₂)); 5.52 (s, 1H, -CH); 6.90 (d, J = 8.79 Hz, 4H, 3-H_{ArOMe}, 3'-H_{ArOMe}, 5-H_{ArOMe}, 5'-H_{ArOMe}); 6.92 (d, J = 8.70 Hz, 4H, 2-H, 2'-H, 6-H, 6'-H); 7.07 (d, J = 8.71 Hz, 4H, 2-H_{ArOMe}, 2'-H_{ArOMe}, 6-H_{ArOMe}, 6'-H_{ArOMe}); 7.18-7.21 (m, 2H, 3-H_{Py}, 4-H_{Py}); 7.34 (d, J = 8.66 Hz, 4H, 3-H_{Ar}, 3'-H_{Ar}, 5-H_{Ar}, 5'-H_{Ar}); 7.70 (td, J = 1.86, 7.68 Hz, 1H, 5-H_{Py}); 8.50-8.51 (m, 1H, 6-H_{Py}). $^{13}\text{C-NMR}$ (DMSO, 151 MHz) δ (ppm) = 55.22 (-OCH₃), 56.65 (-CH), 69.06 (-CH₂), 113.93, 114.62, 121.59 (5-C_{Py}), 123.53 (3-C_{Py}), 129.15, 129.54, 130.02, 135.66, 136.78 (4-C_{Py}), 149.24 (6-C_{Py}), 156.92, 159.08, 163.18. **LC-MS:** (m/z): positive mode 518.3 [M]⁺. Purity by **HPLC-UV (254 nm)-ESI-MS:** 99%. **HRMS (ESI-TOF) m/z :** [M+H]⁺ Calcd. for C₃₄H₃₂NO₄ 518.2326, Found 518.2312.

5.5.2.19. Bis-(*p*-(benzyloxy)phenyl)pyridyl-2-methane (65)

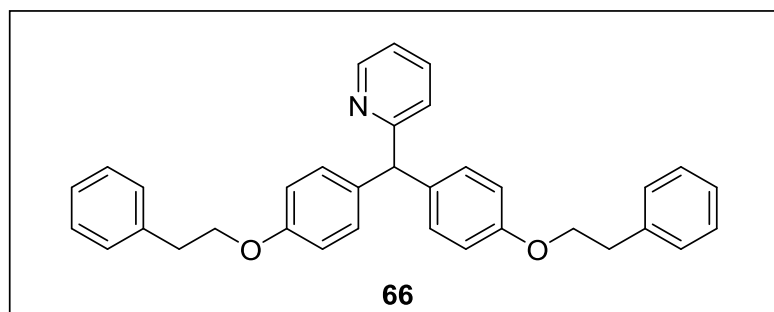


The compound was synthesized according to **5.5.2.9**. **Reaction time:** 1 h. **Work up.** Purification was done by column chromatography on silica gel using ethyl acetate/dichloromethane (2:98), followed by crystallization with diethyl ether. **Appearance:** white

powder. **Yield:** 517 mg (39%); **m.p.** 113-115 °C. **Solubility:** The compound is soluble in acetone and methanol, but insoluble in water. **Analytical data:** $^1\text{H-NMR}$ (DMSO- d_6 , 500 MHz) δ (ppm) = 5.52 (s, 4H, 2(-CH₂)); 5.52 (s, 1H, -CH); 6.92 (d, J = 8.68 Hz, 4H, 3-H_{Ar}, 3'-H_{Ar}, 5-H_{Ar}, 5'-H_{Ar}); 7.09 (d, J = 8.61 Hz, 4H, 2-H_{Ar}, 2'-H_{Ar}, 6-H_{Ar}, 6'-H_{Ar}); 7.19-7.21 (m, 2H, 3-H_{Py}, 4-H_{Py}); 7.29-7.32 (m, 2H, 4-H_{Ph}, 4'-H_{Ph}); 7.35-7.38 (m, J = 7.52 Hz, 4H, 2-H_{Ph}, 2'-H_{Ph}, 6-H_{Ph}, 6'-H_{Ph}); 7.41 (d, J = 6.96 Hz, 4H, 3-H_{Ph}, 3'-H_{Ph}, 5-H_{Ph}, 5'-H_{Ph}); 7.70 (td, J = 1.87, 7.68 Hz, 1H, 5-H_{Py}); 8.50-8.51 (m, 1H, 6-H_{Py}). $^{13}\text{C-NMR}$ (DMSO, 151 MHz) δ (ppm) = 56.64 (-CH), 69.32 (-CH₂), 114.62, 121.58

(5-C_{Py}), 123.52 (3-C_{Py}), 127.73, 127.88, 128.52, 130.04, 135.77, 136.77 (4-C_{Py}), 137.29, 149.22 (6-C_{Py}), 156.88, 163.12. **LC-MS:** (*m/z*): positive mode 458.3 [M]⁺. Purity by **HPLC-UV (220-400 nm)-ESI-MS:** 96%. **HRMS (ESI-TOF) *m/z*:** [M+H]⁺ Calcd. for C₃₂H₂₈NO₂ 458.2115, Found 458.2079.

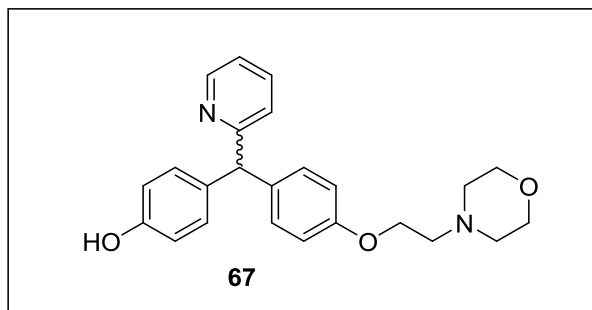
5.5.2.20. Bis-(*p*-phenethoxyphenyl)pyridyl-2-methane (66)



The compound was synthesized according to **5.5.2.10. Reaction time:** 1 h. **Work up.** Purification was done by column chromatography on silica gel using ethyl acetate/dichloromethane (3:97). **Appearance:** colorless oil.

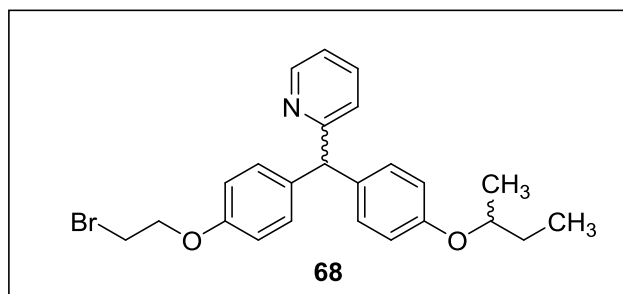
Yield: 700 mg (33%). **Solubility:** The compound is miscible with acetone and methanol, but immiscible with water. **Analytical data:** ¹H-NMR (Methanol-*d*₄, 600 MHz) δ (ppm) = 3.08 (t, *J* = 6.85 Hz, 4H, 2(-OCH₂-CH₂-Ph)); 4.19 (t, *J* = 6.87 Hz, 4H, 2((-OCH₂-CH₂-Ph)); 5.60 (s, 1H, -CH); 6.87 (d, *J* = 8.71 Hz, 4H, 3-H, 3'-H, 5-H, 5'-H); 7.02 (d, *J* = 8.72 Hz, 4H, 2-H, 2'-H, 6-H, 6'-H); 7.16 (d, *J* = 7.92 Hz, 1H, CH_{Ph}); 7.22-7.24 (m, 2H, 3-H_{Py}, 4-H_{Py}); 7.28-7.35 (m, 9H, CH_{Ph}); 7.78 (td, *J* = 1.84, 7.74 Hz, 1H, 5-H_{Py}); 8.48 (d, *J* = 4.30 Hz, 1H, 6-H_{Py}). ¹³C-NMR (151 MHz, MeOD) δ (ppm) = 37.06 (-OCH₂-CH₂-Ph), 58.90 (-CH), 70.18 (-OCH₂-CH₂-Ph), 115.83, 123.33 (5-C_{Py}), 125.73 (3-C_{Py}), 127.66, 129.70, 130.31, 131.61, 136.54 (4-C_{Py}), 138.94, 140.17, 149.93 (6-C_{Py}), 159.31, 165.36. **LC-MS:** (*m/z*): positive mode 486.3 [M]⁺. Purity by **HPLC-UV (220-400 nm)-ESI-MS:** 97%. **HRMS (ESI-TOF) *m/z*:** [M+H]⁺ Calcd. for C₃₄H₃₂NO₂ 486.2428, Found 486.2398.

5.5.2.21. 4-((4-(2-Morpholinoethoxy)phenyl)(pyridin-2-yl)methyl)phenol (67)



The compound was synthesized from compound **50** (192 mg, 0.5 mmol, 1 equiv.), anhydrous K_2CO_3 (138 mg, 1 mmol, 2 equiv.), morpholine (0.09 mL, 1 mmol, 1 equiv.) and acetonitrile (20 mL) at 60 °C. **Reaction time:** 13 h. **Work up.** Purification was done by column

chromatography on silica gel using ethyl acetate/petroleum ether (30:70). **Appearance:** beige powder. **Yield:** 105 mg (54%); **m.p.** 140-142 °C. **Solubility:** The compound is soluble in acetone and methanol, but insoluble in water. **Analytical data:** 1H -NMR (DMSO- d_6 , 500 MHz) δ (ppm) = 2.43-2.45 (m, 4H, $-N(CH_2)_2-(CH_2)_2-O$); 2.65 (t, $J = 5.75$ Hz, 2H, $-OCH_2-CH_2N-$); 3.54-3.56 (m, 4H, $-N(CH_2)_2-(CH_2)_2-O$); 4.02 (t, $J = 5.75$ Hz, 2H, $-OCH_2-CH_2N-$); 5.45 (s, 1H, $-CH$); 6.66 (d, $J = 8.58$ Hz, 2H, 3- H_{ArOH} , 5- H_{ArOH}); 6.83 (d, $J = 8.75$ Hz, 2H, 3- H_{ArOH} , 5- H_{Ar}); 6.95 (d, $J = 8.64$ Hz, 2H, 2- H_{ArOH} , 6- H_{ArOH}); 7.06 (d, $J = 8.78$ Hz, 2H, 2- H_{Ar} , 6- H_{Ar}); 7.16-7.20 (m, 2H, 3- H_{Py} , 4- H_{Py}); 7.69 (td, $J = 1.88, 7.69$ Hz, 1H, 5- H_{Py}); 8.48-8.50 (m, 1H, 6- H_{Py}); 9.19 (s, 1H, $-OH$). ^{13}C -NMR (DMSO, 126 MHz) δ (ppm) = 26.47 ($-OCH_2-CH_2N-$), 53.74 ($-N(CH_2)_2-(CH_2)_2-O$), 56.79 ($-CH$), 57.17 ($-OCH_2-CH_2N-$), 65.41, 66.30 ($-N(CH_2)_2-(CH_2)_2-O$), 114.27, 115.08, 121.48(5- C_{Py}), 123.45(3- C_{Py}), 129.94, 130.01, 133.73, 135.79, 136.67(4- C_{Py}), 149.15(6- C_{Py}), 155.77, 156.89, 163.45. **LC-MS:** (m/z): positive mode 391.2 $[M]^+$. Purity by **HPLC-UV (220-400 nm)**-ESI-MS: 99%. **HRMS (ESI-TOF) m/z :** $[M-H]^-$ Calcd. for $C_{24}H_{25}N_2O_3$ 389.1871, Found 389.1886.

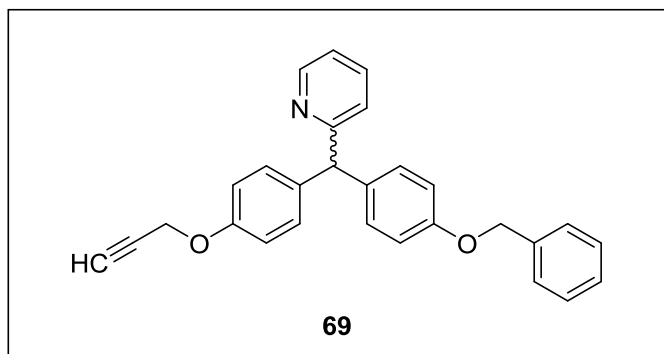
5.5.2.22. 2-((4-(2-Bromoethoxy)phenyl)(4-(*sec*-butoxy)phenyl)methyl)pyridine (68)

The compound was synthesized according to general procedure (III). Compound **50** (400 mg, 1.2 mmol, 1 equiv.), NaH (60% in paraffin oil, 52 mg, 1.3 mmol, 1.1 equiv.) and 1,2-dibromoethane (0.1 mL, 244 mg, 1.3 mmol 1.1 equiv.). **Reaction time:** 2 h. **Work**

up. Purification was done by column chromatography on silica gel using ethyl acetate/dichloromethane (5:95). **Appearance:** light brown oil. **Yield:** 150 mg (28%). **Solubility:** The compound is soluble in acetone and methanol, but insoluble in water. **Analytical data:** 1H -

NMR (Methanol-*d*₄, 600 MHz) δ (ppm) = 0.99 (t, J = 7.45 Hz, 3H, (-CH(CH₃)-CH₂-CH₃)); 1.27 (d, J = 6.05 Hz, 3H, (-CH(CH₃)-CH₂-CH₃)); 1.59-1.76 (m, 2H, (-CH(CH₃)-CH₂-CH₃)); 3.69 (t, J = 5.77 Hz, 2H, -OCH₂-CH₂Br); 4.30 (t, J = 5.78 Hz, 2H, -OCH₂-CH₂Br); 4.34 (q, J = 6.03 Hz, 1H, -CH(CH₃)-CH₂-CH₃); 5.61 (s, 1H, -CH); 6.86 (d, J = 8.72 Hz, 2H, 3-H, 5-H), 6.90 (d, J = 8.74 Hz, 2H, 3'-H, 5'-H); 7.02 (d, J = 8.64 Hz, 2H, 2-H, 6-H); 7.06 (d, J = 8.63 Hz, 2H, 2'-H, 6'-H); 7.17 (d, J = 7.93 Hz, 1H, 3-H_{Py}); 7.29 (ddd, J = 1.14, 4.94, 7.55 Hz, 1H, 4-H_{Py}); 7.77 (td, J = 1.85, 7.73 Hz, 1H, 5-H_{Py}); 8.49 (d, J = 4.09 Hz, 1H, 6-H_{Py}). **¹³C-NMR (MeOD, 151 MHz) δ (ppm)** = 10.36(-CH(CH₃)-CH₂-CH₃), 19.90(-CH(CH₃)-CH₂-CH₃), 30.55 (-OCH₂-CH₂Br), 30.82(-CH(CH₃)-CH₂-CH₃), 58.89 (-CH), 69.63 (-OCH₂-CH₂Br), 76.37 (-CH(CH₃)-CH₂-CH₃), 116.01, 117.15, 123.34 (5-C_{Py}), 125.70 (3-C_{Py}), 131.63, 131.73, 136.22 (4-C_{Py}), 137.20, 138.94, 149.96 (6-C_{Py}), 158.59, 158.72, 165.25. **LC-MS: (*m/z*):** positive mode 440.1 [M]⁺. Purity by **HPLC-UV (220-400 nm)-ESI-MS:** 97%. **HRMS (ESI-TOF) *m/z*:** [M+H]⁺ Calcd. for C₂₄H₂₇BrNO₂ 440.1220, Found 440.1167.

5.5.2.23. 2-((4-(Benzyloxy)phenyl)(4-(prop-2-ynoxy)phenyl)methyl)pyridine (69)



The compound was synthesized according to general procedure (III). Compound **55** (100 mg, 0.27 mmol, 1 equiv.), NaH (60% in paraffin oil, 12 mg, 0.297 mmol, 1.1 equiv.) and propargyl bromide (0.03 mL, 35 mg, 0.297 mmol, 1.1 equiv.). **Reaction time:** 1 h. **Work up.** Purification was

done by column chromatography on silica gel using ethyl acetate/dichloromethane (1:99). **Appearance:** brown oil. **Yield:** 30 mg (41%). **Solubility:** The compound is miscible with acetone and methanol, but immiscible with water. **Analytical data:** **¹H-NMR (DMSO-*d*₆, 600 MHz) δ (ppm)** = 3.51 (t, J = 2.38 Hz, 1H, -CH₂Ph); 4.73 (d, J = 2.40 Hz, 2H, -CH₂-C); 5.04 (s, 2H, -CH); 5.54 (s, 1H, -CH); 6.89 (d, J = 8.75 Hz, 2H); 6.92 (d, J = 8.74 Hz, 2H); 7.09-7.11 (m, 4H); 7.19-7.21 (m, 2H); 7.30 (t, J = 7.28 Hz, 1H); 7.37 (t, J = 7.53 Hz, 2H); 7.41 (d, J = 7.21 Hz, 2H); 7.70 (td, J = 1.91, 7.70 Hz, 1H, 5-H_{Py}); 8.50-8.51 (m, 1H, 6-H_{Py}). **¹³C-NMR (DMSO, 151 MHz) δ (ppm)** = 55.48, 56.61 (-CH), 69.31, 78.24, 79.49, 114.63, 114.66, 121.62 (5-C_{Py}), 123.55 (3-C_{Py}), 127.75, 127.90, 128.53, 130.02, 130.06, 135.70, 136.30(4-C_{Py}), 136.81, 137.29, 149.25(6-C_{Py}),

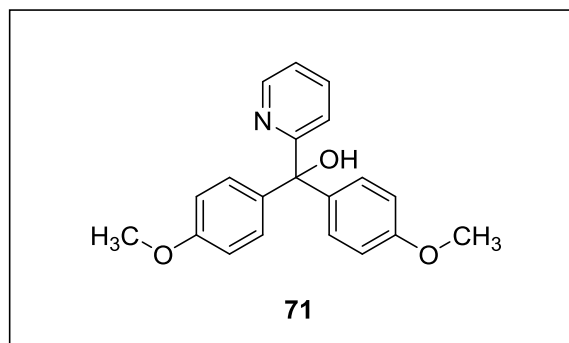
155.72, 156.90, 163.06. **LC-MS: (*m/z*):** positive mode 406.3 [M]⁺. Purity by **HPLC-UV (254 nm)-ESI-MS: 95%.****HRMS (ESI-TOF) *m/z*:** [M+H]⁺ Calcd. for C₂₈H₂₄NO₂ 406.1802, Found 406.1791.

5.5.3. General synthetic procedure (IV)

An ice-cooled suspension of the corresponding methoxy derivatives (1 equiv.) in dry DCM (15 mL) and a solution of BBr₃ in DCM (1M, 3.5 equiv.) was added dropwise. The mixture obtained was allowed to warm up to reach rt and stirred vigorously overnight. The resulting mixture was poured over a cold saturated aqueous solution NaHCO₃ and then extracted with EtOAc (2 × 25 mL), dried over MgSO₄, filtered, and concentrated in vacuum. The residue was chromatographed over column of silica gel to afford the corresponding pure products.

5.5.4. Characterization of compounds 71-74

5.5.4.1. Bis-(*p*-methoxyphenyl)(pyridin-2-yl)methanol (71)

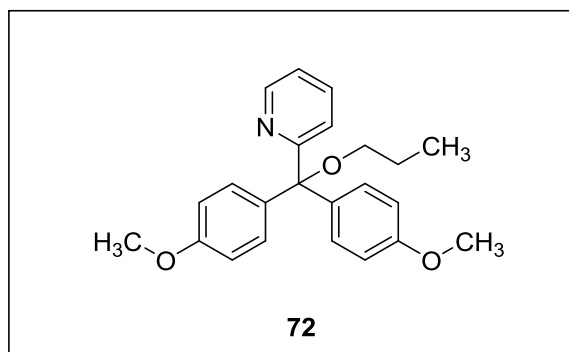


To an oven-dried 100 mL two-necked flask, ethyl 2-picolinate (0.7 mL, 756 mg, 5 mmol, 1 equiv.) was suspended in dry THF (20 mL) and then cooled using ice bath to 0 °C. 4-Methoxyphenylmagnesium bromide solution (0.25 M in THF, 40 mL, 2113 mg, 2 equiv.) in dry THF (30 mL) was added dropwise using a dropping

funnel and the resulting mixture was further stirred for 3 h at the same temperature under argon atmosphere. The reaction was quenched with saturated NH₄Cl solution (20 mL), and then extracted with ethyl acetate (3 × 50 mL) and the white precipitate which formed was stirred with ethyl acetate (2 × 15 mL). The organic extracts were combined, washed with brine (2 × 50 mL), dried over anhydrous MgSO₄, filtered and then concentrated in rotary evaporator till dryness. After the solvent was evaporated, purification of the crude material carried out with flash column chromatography using ethyl acetate/petroleum ether (25:75) to afford the pure product. **Appearance:** yellowish powder. **Yield:** 600 mg (37%); **m.p.** 88-89 °C. **Solubility:** The compound is soluble in acetone and methanol, but insoluble in water. **Analytical data:** ¹H-NMR

(DMSO-*d*₆, 500 MHz) δ (ppm) = 3.71 (s, 6H, 2(-OCH₃)); 6.28 (s, 1H, -OH); 6.81 (d, *J* = 8.88 Hz, 4H, 3-H, 3'-H, 5-H, 5'-H); 7.13 (d, *J* = 8.84 Hz, 4H, 2-H, 2'-H, 6-H, 6'-H); 7.24 (ddd, *J* = 1.14, 4.80, 7.48 Hz, 1H); 7.54 (dt, *J* = 1.06, 7.96 Hz, 1H); 7.77 (ddd, *J* = 1.85, 7.50, 7.98 Hz, 1H); 8.49-8.50 (m, 1H, 6-H_{Py}). ¹³C-NMR (DMSO, 126 MHz) δ (ppm) = 55.14 (-OCH₃), 80.08, 112.87, 121.47 (5-C_{Py}), 121.91 (3-C_{Py}), 129.11, 136.61 (4-C_{Py}), 139.56, 147.84 (6-C_{Py}), 158.03, 165.46.

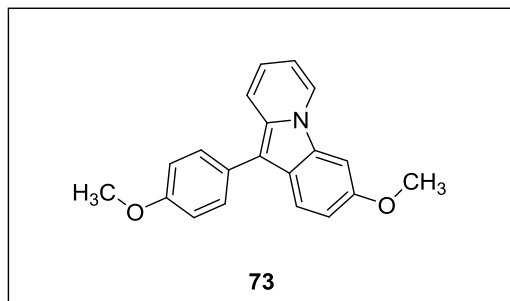
5.5.4.2. 2-(Bis-(*p*-methoxyphenyl)(propoxy)methyl)pyridine (72)



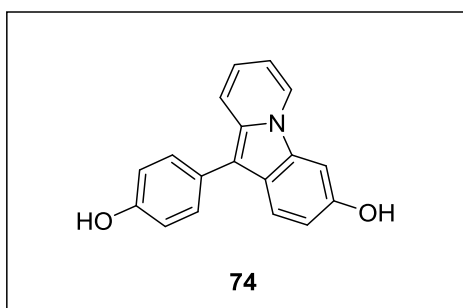
The compound was synthesized according to general procedure (III). Compound **71** (160 mg, 0.52 mmol, 1 equiv.), NaH (60% in paraffin oil, 23 mg, 0.57 mmol, 1.1 equiv.) and 1-bromopropane (0.02 mL, 33 mg, 0.57 mmol, 1.1 equiv.).

Reaction time: 1 h. **Work up.** Purification was done by column chromatography on silica gel

using ethyl acetate/petroleum ether (7:93). **Appearance:** pale yellow solid. **Yield:** 120 mg (64%); **m.p.** 100-102 °C. **Solubility:** The compound is soluble in acetone, ethyl acetate and methanol, but insoluble in water. **Analytical data:** ¹H-NMR (DMSO-*d*₆, 500 MHz) δ (ppm) = 0.88 (t, *J* = 7.40 Hz, 3H, -OCH₂-CH₂-CH₃); 1.53-1.60 (m, 2H, -OCH₂-CH₂-CH₃); 2.96 (t, *J* = 6.61 Hz, 2H, -OCH₂-CH₂-CH₃); 3.72 (s, 6H, 2(-OCH₃)); 6.84 (d, *J* = 8.90 Hz, 4H, 3-H, 3'-H, 5-H, 5'-H); 7.19 (m, 1H); 7.22 (d, *J* = 8.95 Hz, 4H, 2-H, 2'-H, 6-H, 6'-H); 7.70 (dt, *J* = 1.09, 8.03 Hz, 1H); 7.75-7.79 (m, *J* = 1.89, 7.42, 8.04 Hz, 1H); 8.46-8.48 (m, 1H, 6-H_{Py}). ¹³C-NMR (DMSO, 126 MHz) δ (ppm) = 10.89 (-OCH₂-CH₂-CH₃), 22.92 (-OCH₂-CH₂-CH₃), 55.12 (-OCH₃), 64.97 (-OCH₂-CH₂-CH₃), 85.67, 112.95, 120.80 (5-C_{Py}), 121.69 (3-C_{Py}), 130.09, 135.66, 136.70 (4-C_{Py}), 148.45 (6-C_{Py}), 158.11, 164.30.

5.5.4.3. 3-Methoxy-10-(4-methoxyphenyl)pyrido[1,2-*a*]indole (73)

The above compound was synthesized using an adapted reported procedure. Bis(4-methoxyphenyl)(pyridin-2-yl)methanol (**71**) (230 mg, 0.71 mmol, 1 equiv.) was placed in pressure tube and formic acid (3 mL) was added, then the mixture was heated at 120 °C. After cooling, neutralization of the remaining formic acid was accomplished with a saturated aqueous solution of NaHCO₃. The aqueous mixture was extracted with EtOAc (3 × 50 mL) and the combined organic layers were washed with brine (2 × 25 mL), dried over Na₂SO₄, filtered and then concentrated under vacuum. The pure compound was obtained after purification by column chromatography using ethyl acetate/petroleum ether (5:95) then crystallized with diethyl ether. **Reaction time:** 6 h. **Appearance:** pale yellow solid. **Yield:** 200 mg (93%); **m.p.** 156-158 °C. **Solubility:** The compound is soluble in acetone and ethyl acetate, but in soluble in water. **Analytical data:** ¹H-NMR (DMSO-*d*₆, 600 MHz) δ (ppm) = 3.81 (s, 3H); 3.89 (s, 3H); 6.56 (t, *J* = 6.24 Hz, 1H); 6.88-6.90 (m, 1H); 7.04-7.08 (m, 3H); 7.52 (d, *J* = 8.65 Hz, 2H); 7.56 (d, *J* = 9.34 Hz, 1H); 7.75 (d, *J* = 8.84 Hz, 1H); 7.83 (d, *J* = 2.26 Hz, 1H); 8.76 (d, *J* = 7.17 Hz, 1H). ¹³C-NMR (DMSO, 151 MHz) δ (ppm) = 55.28, 55.80, 94.25, 104.43, 108.26, 114.46, 114.67, 117.61, 119.51, 121.33, 121.98, 125.40, 127.11, 129.58, 129.62, 131.39, 154.95, 157.44.

5.5.4.4. 10-(4-Hydroxyphenyl)pyrido[1,2-*a*]indol-3-ol (74)

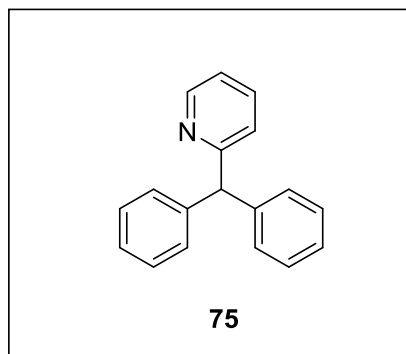
The compound was synthesized according to general procedure (IV). Compound **73** (190 mg, 0.62 mmol, 1 equiv.) and BBr₃ in DCM (1M, 2.17 mL, 2.17 mmol, 3.5 equiv.). **Reaction time:** 12 h. **Work up.** Purification was done by flash column chromatography on silica gel using ethyl acetate/dichloromethane (5:95). **Appearance:** greenish solid. **Yield:** 85 mg (50%); **m.p.** 94-96 °C. **Solubility:** The compound is soluble in acetone and ethyl acetate, but insoluble in water. **Analytical data:** ¹H-NMR (DMSO-*d*₆, 500 MHz) δ (ppm) = 6.46 (m, 1H); 6.80 (ddd, *J* = 1.07, 6.22, 9.35 Hz, 1H); 6.89 (d, *J* = 2.01 Hz, 1H); 6.91 (d, *J* = 2.03 Hz, 1H); 6.95 (dd, *J* = 2.14, 8.72 Hz, 1H); 7.38 (d, *J* = 2.05 Hz, 1H); 7.39

(d, $J = 2.02$ Hz, 1H); 7.47 (d, $J = 2.09$ Hz, 1H); 7.50 (dt, $J = 1.19, 9.27$ Hz, 1H); 7.66 (d, $J = 8.72$ Hz, 1H); 8.52 (d, $J = 7.23$ Hz, 1H); 9.34 (s, 2H). $^{13}\text{C-NMR}$ (DMSO, 151 MHz) δ (ppm) = 95.95, 104.81, 107.88, 114.60, 115.95, 117.72, 119.48, 120.67, 121.31, 125.15, 125.53, 129.57, 129.86, 130.79, 152.53, 155.47.

5.5.5. General synthetic procedure (V) (75-78)

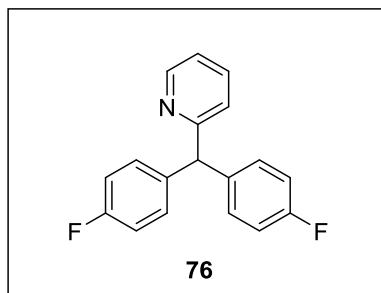
To a mixture of the starting material (5.8 equiv.) and sulfuric acid (8.7 equiv.) which cooled in an ice bath to 0 °C, 2-pyridinecarboxaldehyde (1 equiv.) was added via syringe dropwise over 10 min. The solution was allowed to reach room temperature (rt) and stirred overnight. The mixture was then poured onto crushed ice and extracted with EtOAc (50 mL). The aqueous layer containing the insoluble residue was neutralized with saturated solution of NaHCO_3 and was then extracted two times with 25 mL of EtOAc each. The combined EtOAc layers were washed with brine (2×25 mL), dried over anhydrous Na_2SO_4 , filtered and then concentrated under vacuum. The residual mixture was purified by column chromatography to afford the desired compounds.

5.5.5.1. 2-Benzhydrylpyridine (75)¹⁸⁴



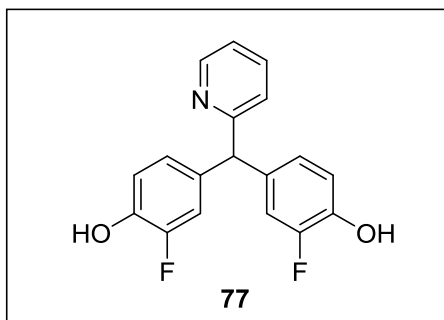
The compound was synthesized according to general procedure (V). 2-Pyridinecarboxaldehyde (0.2 mL, 214 mg, 2 mmol, 1 equiv.) and benzene (1 mL, 877 mg, 11.6 mmol, 5.8 equiv.) in sulfuric acid (0.93 mL, 1706.4 mg, 17.4 mmol, 8.7 equiv.). **Reaction time:** 13 h. **Work up.** Purification was done by column chromatography on silica gel using ethyl acetate/dichloromethane (5:95). **Appearance:** pale yellow

powder. **Yield:** 300 mg (61%); **m.p.** 62-64 °C. **Solubility:** The compound is soluble in acetone, ethyl acetate and methanol, but insoluble in water. **Analytical data:** $^1\text{H-NMR}$ (DMSO- d_6 , 500 MHz) δ (ppm) = 5.67 (s, 1H, -CH); 7.18-7.24 (m, 8H, CH_{Ph}); 7.27-7.30 (m, 4H, 2CH_{Ph} , 3- H_{Py} , 4- H_{Py}); 7.72 (td, $J = 1.51, 7.37$ Hz, 1H, 5- H_{Py}); 8.52-8.54 (m, 1H, 6- H_{Py}). $^{13}\text{C-NMR}$ (DMSO, 126 MHz) δ (ppm) = 58.21 (-CH), 121.74 (5- C_{Py}), 123.73 (3- C_{Py}), 126.37, 128.35, 129.15, 136.83 (4- C_{Py}), 143.13, 149.29 (6- C_{Py}), 162.51. **LC-MS:** (m/z): positive mode 245.9 $[\text{M}]^+$. Purity by **HPLC-UV (220-400 nm)-ESI-MS:** 96%. **HRMS (ESI-TOF) m/z :** $[\text{M}+\text{H}]^+$ Calcd. for $\text{C}_{18}\text{H}_{16}\text{N}$ 246.1277, Found 246.1275.

5.5.5.2. 2-(Bis-(*p*-fluorophenyl)methyl)pyridine (76)

The compound was synthesized according to general procedure (V). 2-Pyridinecarboxaldehyde (0.2 mL, 214 mg, 2 mmol, 1 equiv.) and fluorobenzene (1.1 mL, 1114.8 mg, 11.6 mmol, 5.8 equiv.) in sulfuric acid (0.93 mL, 1706.4 mg, 17.4 mmol, 8.7 equiv.). **Reaction time:** 13 h. **Work up.** Purification was done by column chromatography on silica gel using ethyl acetate/petroleum ether (15:85). **Appearance:** colorless oil. **Yield:** 140 mg (25%). **Solubility:** The compound is miscible with acetone, ethyl acetate and methanol, but immiscible with water. **¹H-NMR (DMSO-*d*₆, 500 MHz) δ (ppm)** = 5.71 (s, 1H, -CH); 7.09-7.13 (m, 4H, CH_{Ph}); 7.22-7.28 (m, 6H, 4CH_{Ph}, 3-H_{Py}, 4-H_{Py}); 7.74 (td, *J* = 1.89, 7.68 Hz, 1H, 5-H_{Py}); 8.53-8.55 (m, 1H, 6-H_{Py}). **¹³C-NMR (DMSO, 126 MHz) δ (ppm)** = 56.18 (-CH), 115.03, 115.20, 121.92 (5-C_{Py}), 123.76 (3-C_{Py}), 130.84, 130.90, 137.07 (4-C_{Py}), 139.25, 139.27, 149.41 (6-C_{Py}), 159.95, 161.88, 162.10. **LC-MS:** (*m/z*): positive mode 282 [M]⁺. Purity by **HPLC-UV (220-400 nm)-ESI-MS:** 97%. **HRMS (ESI-TOF) *m/z*:** [M+H]⁺ Calcd. for C₁₈H₁₄F₂N 282.1089, Found 282.1083.

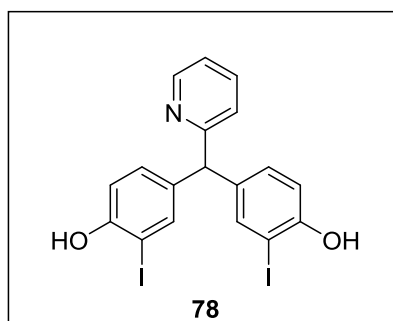
5.5.5.3. 4,4'-(Pyridin-2-ylmethylene)-bis-(2-fluorophenol) (77)



The compound was synthesized according to general procedure (V). 2-Pyridinecarboxaldehyde (0.2 mL, 214 mg, 2 mmol, 1 equiv.) and 2-fluorophenol (1 mL, 1300.4 mg, 11.6 mmol, 5.8 equiv.) in sulfuric acid (0.93 mL, 1706.4 mg, 17.4 mmol, 8.7 equiv.). **Reaction time:** 9 h. **Work up.** The purification was done by column chromatography on silica gel using ethyl acetate/dichloromethane (5:95). **Appearance:** yellow powder. **Yield:** 370 mg (60%); **m.p.** 246-248 °C. **Solubility:** The compound is soluble in acetone and methanol, but insoluble in water. **Analytical data:** **¹H-NMR (DMSO-*d*₆, 500 MHz) δ (ppm)** = 5.46 (s, 1H, -CH); 6.79 (dd, *J* = 2.08, 8.39 Hz, 2H, 5-H, 4'-H); 6.84-6.87 (m, 2H, 3-H, 5'-H); 6.92 (dd, *J* = 2.07, 12.64 Hz, 2H, 6-H, 6'-H); 7.20-7.23 (m, 2H, 3-H_{Py}, 4-H_{Py}); 7.71 (td, *J* = 1.88, 7.67 Hz, 1H, 5-H_{Py}); 8.5-8.53 (m, 1H, 6-H_{Py}); 9.66 (br s, 2H, -OH). **¹³C-NMR (DMSO, 126 MHz) δ (ppm)** = 55.92(-CH), 116.41, 116.56, 117.61, 117.63, 121.81(5-C_{Py}), 123.59(3-C_{Py}), 125.00, 125.03, 134.62, 134.66, 136.95(4-C_{Py}), 143.26, 143.36, 149.32(6-C_{Py}),

149.85, 151.77, 162.45. **LC-MS: (m/z):** positive mode 314 [M]⁺. Purity by **HPLC-UV (254 nm)-ESI-MS: 97%**. **HRMS (ESI-TOF) m/z:** [M-H]⁻ Calcd. for C₁₈H₁₂F₂NO₂ 312.0842, Found 312.0859.

5.5.5.4. 4,4'-(Pyridin-2-ylmethylene)bis(2-iodophenol) (78)

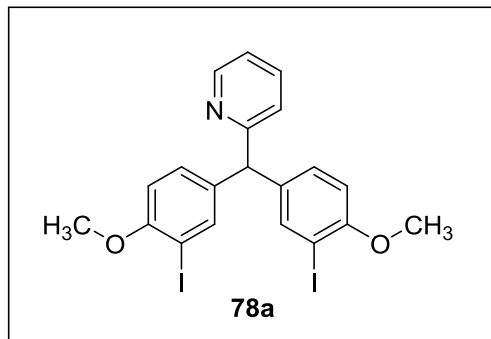


The compound was synthesized according to general procedure (V). 2-Pyridinecarboxaldehyde (0.2 mL, 214 mg, 2 mmol, 1 equiv.) and 2-iodophenol (2552.1 mg, 11.6 mmol, 5.8 equiv.) in sulfuric acid (0.93 mL, 1706.4 mg, 17.4 mmol, 8.7 equiv.) and DCM (5 mL). **Reaction time:** 14 h. **Work up.** The purification was done by column chromatography on silica gel using ethyl acetate/dichloromethane (5:95). **Appearance:** white

powder. **Yield:** 250 mg (24%); **m.p.** 186-187 °C. **Solubility:** The compound is soluble in acetone, ethyl acetate, dichloromethane and methanol, but insoluble in water. **Analytical data:** ¹H-NMR (DMSO-*d*₆, 500 MHz) δ (ppm) = 5.43 (s, 1H, -CH); 6.79 (d, *J* = 8.35 Hz, 2H; 3-H; 3'-H); 7.01 (dd, *J* = 2.23, 8.38 Hz, 2H, 5-H; 5'-H); 7.21-7.23 (m, 2H, 3-H_{Py}, 4-H_{Py}); 7.46 (d, *J* = 2.21 Hz, 2H, 6-H; 6'-H); 7.72 (td, *J* = 1.89, 7.65 Hz, 1H, 5-H_{Py}); 8.51-8.53 (m, 1H, 6-HPy). ¹³C-NMR (DMSO, 126 MHz) δ (ppm) = 84.46 (-CH), 114.87, 121.77 (5-C_{Py}), 123.59 (3-C_{Py}), 130.11, 135.92, 136.97 (4-C_{Py}), 138.87, 149.32 (6-C_{Py}), 155.16, 162.44. **LC-MS: (m/z):** positive mode 529.9 [M]⁺. Purity by **HPLC-UV (220-400 nm)-ESI-MS: 97%**. **HRMS (ESI-TOF) m/z:** [M-H]⁻ Calcd. for C₁₈H₁₂I₂NO₂ 527.8963, Found 527.8960.

5.5.5.5. 2-(Bis(3-iodo-4-methoxyphenyl)methyl)pyridine (78a)

Experimental Part

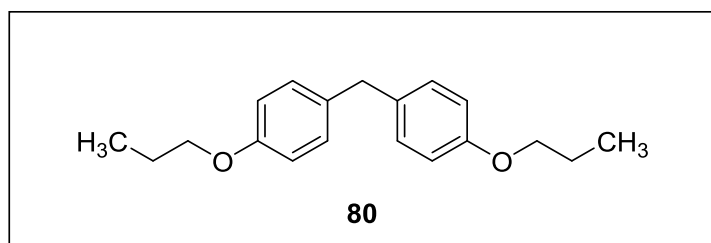


The compound was synthesized according to general procedure (III). Compound **78** (132 mg, 0.25 mmol), NaH (60% in paraffin oil, 22 mg, 0.55 mmol, 2.2 equiv.) and iodomethane (0.03 mL, 78 mg, 0.55 mmol, 2.2 equiv.). **Reaction time:** 30 min. **Work up.** Purification was done by column chromatography on silica gel using ethyl acetate/dichloromethane (7:93). **Appearance:**

white powder. **Yield:** 115 mg (83%); **m.p.** 68-70 °C. **Solubility:** The compound is soluble in acetone, dichloromethane and methanol, but insoluble in water. **Analytical data:** $^1\text{H-NMR}$ (DMSO- d_6 , 500 MHz) δ (ppm) = 3.77 (s, 6H, 2-OCH $_3$); 5.56 (s, 1H, -CH); 6.93 (d, J = 8.53 Hz, 2H, 3-H; 3'-H); 7.19 (dd, J = 2.21, 8.50 Hz, 2H, 5-H; 5'-H); 7.22-7.27 (m, 2H, 3-H_{Py}, 4-H_{Py}); 7.59 (d, J = 2.20 Hz, 2H, 6-H; 6'-H); 7.74 (td, J = 1.90, 7.70 Hz, 1H, 5-H_{Py}); 8.54-8.55 (m, 1H, 6-H_{Py}). $^{13}\text{C-NMR}$ (DMSO, 126 MHz) δ (ppm) = 54.85 (-OCH $_3$), 56.49 (-CH), 86.01, 111.57, 121.93 (5-C_{Py}), 123.73 (3-C_{Py}), 130.29, 137.11 (4-C_{Py}), 137.41, 139.16, 149.43 (6-C_{Py}), 156.43, 162.02. **LC-MS:** (m/z): positive mode 557.8 [M] $^+$. Purity by **HPLC-UV (220-400 nm)**-ESI-MS: 98%. **HRMS (ESI-TOF) m/z :** [M-H] $^-$ Calcd. for C $_{20}$ H $_{16}$ I $_2$ NO $_2$ 555.9276, Found 555.9265.

5.5.6. Characterization of the synthesized derivatives (**80**, **81**, **83**, **85**, **87** and **88**)

5.5.6.1. Bis-(*p*-propoxyphenyl)methane (**80**)

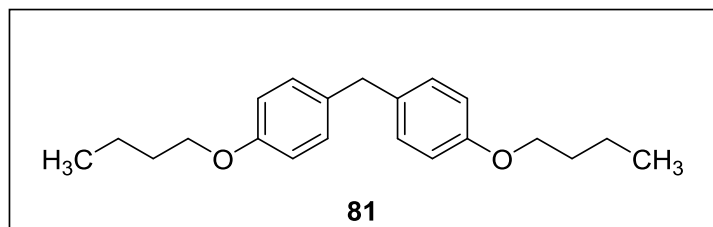


The compound was synthesized according to general procedure (III). 4,4'-methylenediphenol (**79**) (600 mg, 3 mmol, 1 equiv.), NaH (60% in paraffin oil, 264 mg, 6.6 mmol, 2.2

equiv.) and 1-bromopropane (0.6 mL, 811.8 mg, 6.6 mmol, 2.2 equiv.). **Reaction time:** 4 h. **Work up.** Purification was done by column chromatography on silica gel using ethyl acetate/dichloromethane (2:98). **Appearance:** yellow oil. **Yield:** 300 mg (35%). **Solubility:** The compound is miscible with acetone and methanol, but immiscible with water. **Analytical data:** $^1\text{H-NMR}$ (DMSO- d_6 , 600 MHz) δ (ppm) = 0.94 (t, J = 7.40 Hz, 6H, 2(-OCH $_2$ -CH $_2$ -CH $_3$)); 1.65-1.71 (m, 4H, 2(-OCH $_2$ -CH $_2$ -CH $_3$)); 3.77 (s, 2H, -CH $_2$); 3.85 (t, J = 6.52 Hz, 4H, 2(-OCH $_2$ -CH $_2$ -CH $_3$)); 6.81 (d, J = 8.55 Hz, 4H, 3-H, 3'-H, 5-H, 5'-H); 7.07 (d, J = 8.52 Hz, 4H, 2-H, 2'-H, 6-H,

6'-H). $^{13}\text{C-NMR}$ (DMSO, 151 MHz) δ (ppm) = 10.55 (-OCH₂-CH₂-CH₃), 22.22 (-OCH₂-CH₂-CH₃), 39.50 (-CH₂), 69.00 (-OCH₂-CH₂-CH₃), 114.47, 114.67, 129.64, 133.71, 157.04. **LC-MS:** (m/z): positive mode 285 [M]⁺. Purity by **HPLC-UV (220-400 nm)-ESI-MS:** 95%. **HRMS (ESI-TOF) m/z :** [M+H]⁺ Calcd. for C₁₉H₂₅O₂ 285.1849, Found 285.1853.

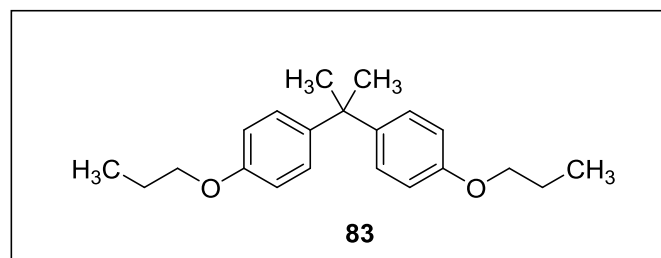
5.5.6.2. Bis-(4-butoxyphenyl)methane (**81**)²⁴⁷



The compound was synthesized according to general procedure (**III**). 4,4'-methylenediphenol (**79**) (1200 mg, 6 mmol, 1 equiv.), NaH (60% in paraffin oil, 528 mg, 13.2mmol, 2.2

equiv.) and 1-bromobutane (1.4 mL, 1808.7 mg, , 13.2 mmol, 2.2 equiv.). **Reaction time:** 3 h. **Work up.** Purification was done by column chromatography on silica gel using ethyl acetate/dichloromethane (3:97), followed by recrystallization from ethyl acetate/cyclohexane (20:80). **Appearance:** yellowish powder. **Yield:** 1200 mg (64%); **m.p.** 46-48 °C. **Solubility:** The compound is soluble in acetone and methanol, but insoluble in water. **Analytical data:** $^1\text{H-NMR}$ (DMSO-*d*₆, 600 MHz) δ (ppm) = 0.90 (t, J = 7.41 Hz, 6H, 2(-OCH₂-CH₂-CH₂-CH₃)); 1.37-1.43 (m, 4H, 2(-OCH₂-CH₂-CH₂-CH₃)); 1.62-1.67 (m, 4H, 2(-OCH₂-CH₂-CH₂-CH₃)); 3.76 (s, 2H, -CH₂); 3.89 (t, J = 6.49 Hz, 4H, 2(-OCH₂-CH₂-CH₂-CH₃)); 6.80 (d, J = 8.62 Hz, 4H, 3-H, 3'-H, 5-H, 5'-H); 7.07 (d, J = 8.60 Hz, 4H, 2-H, 2'-H, 6-H, 6'-H). $^{13}\text{C-NMR}$ (DMSO, 151 MHz) δ (ppm) = 13.84 (-OCH₂-CH₂-CH₂-CH₃), 18.89 (-OCH₂-CH₂-CH₂-CH₃), 39.50(-CH₂), 67.18(-OCH₂-CH₂-CH₂-CH₃), 114.47, 129.63, 133.71, 157.05. **LC-MS:** (m/z): positive mode 313.3 [M]⁺. Purity by **HPLC-UV (220-400 nm)-ESI-MS:** 99%. **HRMS (ESI-TOF) m/z :** [M+H]⁺ Calcd. for C₂₁H₂₉O₂ 313.2162, Found 313.2158.

5.5.6.3. 2,2-Bis-(*p*-propoxyphenyl)propane (**83**)



The compound was synthesized according to general procedure (**III**). 2,2-Bis-(4-hydroxyphenyl)propane (**82**) (685 mg, 3 mmol, 1 equiv.), NaH (60% in paraffin oil,

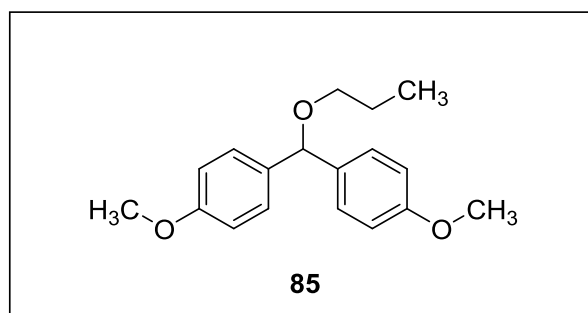
264 mg, 6.6 mmol, 2.2 equiv.) and 1-bromopropane (0.6 mL, 811.8 mg, 6.6 mmol, 2.2 equiv.).

Reaction time: 4 h. **Work up.** Purification was done by column chromatography on silica gel using ethyl acetate/petroleum ether (10:90). **Appearance:** colorless oil. **Yield:** 700 mg (75%).

Solubility: The compound is soluble in acetone and methanol, but insoluble in water. **Analytical**

data: $^1\text{H-NMR}$ (DMSO- d_6 , 600 MHz) δ (ppm) = 0.95 (t, $J = 7.39$ Hz, 6H, 2(-OCH₂-CH₂-CH₃); 1.56 (s, 6H, 2(-CH₃)); 1.66-1.71 (m, $J = 7.33$ Hz, 4H, 2(-OCH₂-CH₂-CH₃); 3.86 (t, $J = 6.50$ Hz, 4H, 2(-OCH₂-CH₂-CH₃); 6.79 (d, $J = 8.75$ Hz, 4H, 3-H, 3'-H, 5-H, 5'-H); 7.07 (d, $J = 8.78$ Hz, 4H, 2-H, 2'-H, 6-H, 6'-H). $^{13}\text{C-NMR}$ (DMSO, 151 MHz) δ (ppm) = 10.55 (-OCH₂-CH₂-CH₃), 22.21 (-OCH₂-CH₂-CH₃), 30.87 (-CH₃), 41.24 (-CH₃), 68.93 (-OCH₂-CH₂-CH₃), 113.89, 127.48, 142.55, 156.54. **LC-MS:** (m/z): positive mode 313.2 [M]⁺. Purity by **HPLC-UV (220-400 nm)**-**ESI-MS:** 98%. **HRMS (ESI-TOF) m/z :** [M+H]⁺ Calcd. for C₂₁H₂₉O₂ 313.2162, Found 313.2165.

5.5.6.4. 4,4'-(Propoxymethylene)-bis-(methoxybenzene) (85)



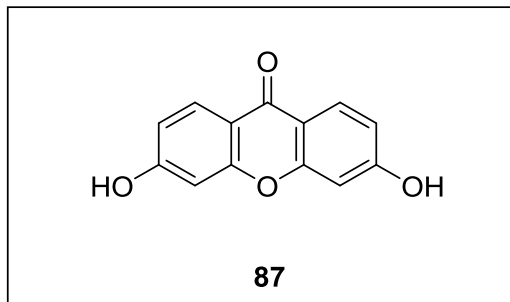
The compound was synthesized according to general procedure (III). Bis-(4-methoxyphenyl)methanol (**84**) (122 mg, 0.5 mmol, 1 equiv.), NaH (60% in paraffin oil, 22 mg, 0.55 mmol, 1.1 equiv.) and 1-bromopropane (0.05 mL, 68 mg, 0.55 mmol, 2.2 equiv.).

Reaction time: 3 h. **Work up.** Purification was done by column chromatography on silica gel using ethyl acetate/dichloromethane (2:98). **Appearance:** colorless oil. **Yield:** 75 mg (52%).

Solubility: The compound is soluble in acetone and methanol, but insoluble in water. **Analytical**

data: $^1\text{H-NMR}$ (DMSO- d_6 , 600 MHz) δ (ppm) = 0.87 (t, $J = 7.40$ Hz, 3H, -OCH₂-CH₂-CH₃); 1.51-1.56 (m, 2H, -OCH₂-CH₂-CH₃); 3.28 (t, $J = 6.52$ Hz, 2H, -OCH₂-CH₂-CH₃); 3.70 (s, 6H, 2(-OCH₃)); 5.28 (s, 1H, -CH); 6.86 (d, $J = 8.66$ Hz, 4H, 2-H, 2'-H, 6-H, 6'-H); 7.21 (d, $J = 8.62$ Hz, 4H, 3-H, 3'-H, 5-H, 5'-H). $^{13}\text{C-NMR}$ (DMSO, 151 MHz) δ (ppm) = 10.84 (-OCH₂-CH₂-CH₃), 22.76 (-OCH₂-CH₂-CH₃), 39.27 (-CH), 55.16 (-OCH₃), 69.78 (-OCH₂-CH₂-CH₃), 81.66, 113.74, 127.83, 135.29, 158.43.

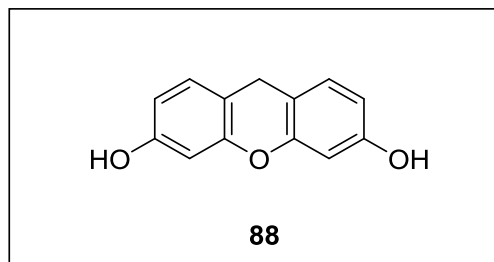
5.5.6.5. 3,6-Dihydroxy-9H-xanthen-9-one (87)



The synthetic procedure was achieved using a miniclave tube (Büchi AG, Uster, Switzerland). 2,2',4,4'-Tetrahydroxybenzophenone (**86**) (2000 mg, 8.12 mmol) was treated with water (12 mL) and then heated using an oil bath at 150 °C and the pressure inside was 3 bar during the reaction time. The vessel

was cooled to rt, and then the mixture was filtered using a vacuum pump. Pure product was obtained after crystallization with acetone : ethanol (2 : 1). **Reaction time:** 16 h. **Appearance:** light brown powder. **Yield:** 1200 mg (66%); **m.p.** > 300 °C. **Solubility:** The compound is soluble in acetone and ethyl acetate, but insoluble in water. **Analytical data:** ¹H-NMR (DMSO-*d*₆, 500 MHz) δ (ppm) = 6.81 (s, 2H); 6.85 (d, *J* = 8.62 Hz, 2H); 7.98 (d, *J* = 8.69 Hz, 2H); 10.77 (br s, 2H, -OH). ¹³C-NMR (DMSO, 126 MHz) δ (ppm) = 102.20, 113.77, 114.12, 127.87, 157.59, 163.47, 174.01 (CO). **LC-MS:** (*m/z*): positive mode 229.3 [M]⁺. Purity by **HPLC-UV (220-400 nm)**-ESI-MS: 99%. **HRMS (ESI-TOF)** *m/z*: [M-H]⁻ Calcd. for C₁₃H₇O₄ 227.0350, Found 227.0374.

5.5.6.6. 9H-xanthene-3,6-diol (**88**)



The corresponding product **87** (578 mg, 2.5 mmol) was suspended in 60 mL of dry THF and borane-tetrahydrofuran complex (1.0 M in THF) (10 mL) was added dropwise. The formed mixture was stirred vigorously at rt under argon atmosphere until a clear yellow solution was obtained. The excess solution was removed under reduced pressure and the sticky suspension was treated with 1.0 N HCl (15 mL) then filtered off. The residual material obtained was purified by flash column chromatography using ethyl acetate/dichloromethane (10:90) to afford the pure final product. **Reaction time:** 5 h. **Appearance:** orange yellow powder.

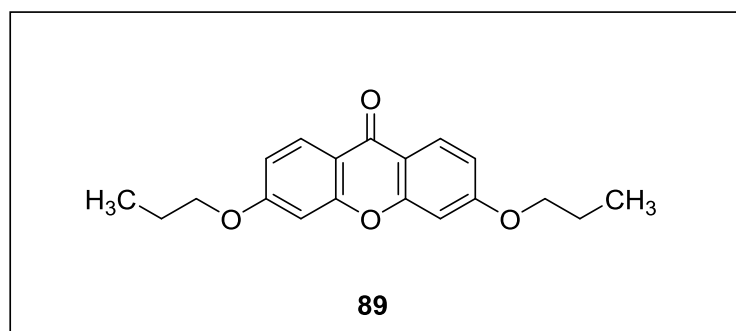
Yield: (95%); **m.p.** 215-217 °C. **Solubility:** The compound is soluble in acetone, ethyl acetate and methanol, but insoluble in water. **Analytical data:** ¹H-NMR (DMSO-*d*₆, 600 MHz) δ (ppm) = 3.77 (s, 2H, -CH₂); 6.40 (d, *J* = 2.38 Hz, 2H); 6.47 (dd, *J* = 2.44, 8.20 Hz, 2H); 6.98 (d, *J* = 8.10 Hz, 2H); 9.41 (br s, 2H, -OH). ¹³C-NMR (DMSO, 151 MHz) δ (ppm) = 25.73 (-CH₂), 102.77, 110.87, 110.97, 129.72, 151.85, 156.94. **LC-MS:** (*m/z*): positive mode 215.2 [M]⁺. Purity

by HPLC-UV (220-400 nm)-ESI-MS: 95%. HRMS (ESI-TOF) m/z : $[M-H]^-$ Calcd. for $C_{13}H_9O_3$ 213.0557, Found 213.0577.

5.5.7. General synthetic procedure (VI) used for the synthesized compounds 89, 90 and 95

Intermediates **87** and **88** or methyl 3-formyl-4-hydroxybenzoate (**94**) (1 equiv.) and anhydrous K_2CO_3 (5 equiv.) were suspended in the appropriate solvent (25 mL), the corresponding alkylating agent (15 equiv.) was added dropwise via syringe. The reaction mixture was refluxed until the starting material was consumed. The reaction mixture was cooled to rt and the solvent was removed under reduced pressure. The residue was taken up with water (25 mL) and extracted with EtOAc (3×50 mL). The combined extracts were washed with brine (2×25 mL), dried over anhydrous $MgSO_4$, filtered and then concentrated under vacuum. The pure products were obtained via purification using column chromatography.

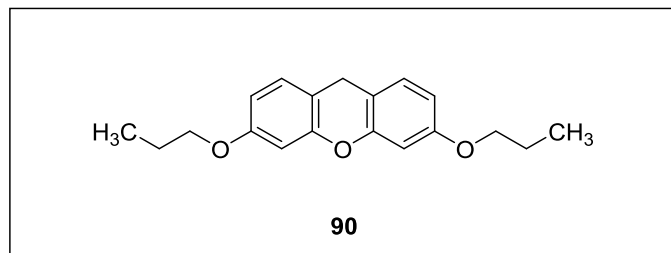
5.5.7.1. 3,6-Dipropoxy-9H-xanthen-9-one (**89**)



The compound was synthesized according to general procedure (VI). Compound **87** (228.2 mg, 1 mmol, 1 equiv.), anhydrous K_2CO_3 (691 mg, 5 mmol, 5 equiv.), 1-bromopropane (1.36 mL, 1884.9 mg, 15 mmol, 15 equiv.) and acetone (25 mL).

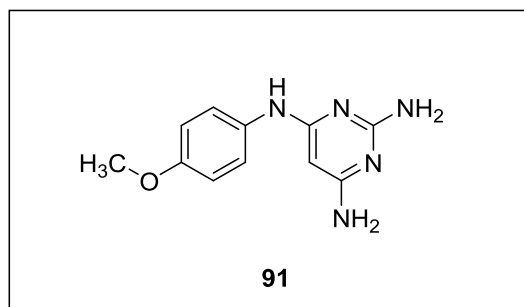
Reaction time: 16 h. **Work up.** Purification was done by column chromatography on silica gel using ethyl acetate/dichloromethane (2:98). **Appearance:** white powder. **Yield:** 110 mg (35%); **m.p.** 115-117 °C. **Solubility:** The compound is soluble in acetone and methanol, but insoluble in water. **Analytical data:** 1H -NMR (DMSO- d_6 , 500 MHz) δ (ppm) = 1.00 (t, $J = 7.41$ Hz, 6H, 2 (-OCH₂-CH₂-CH₃)); 1.74-1.81 (m, 4H, 2(-OCH₂-CH₂-CH₃)); 4.10 (t, $J = 6.51$ Hz, 4H, 2(-OCH₂-CH₂-CH₃)); 7.02 (dd, $J = 2.36, 8.80$ Hz, 2H); 7.05 (d, $J = 2.33$ Hz, 2H); 8.05 (d, $J = 8.81$ Hz, 2H). ^{13}C -NMR (DMSO, 126 MHz) δ (ppm) = 10.42 (-OCH₂-CH₂-CH₃), 21.93 (-OCH₂-CH₂-CH₃), 70.04 (-OCH₂-CH₂-CH₃), 101.11, 113.65, 115.00, 127.59, 157.62, 164.10, 174.13 (CO). **LC-MS:** (m/z): positive mode 313.1 $[M]^+$. Purity by HPLC-UV (220-400 nm)-ESI-MS: 99%. **HRMS (ESI-TOF) m/z :** $[M+H]^+$ Calcd. for $C_{19}H_{21}O_4$ 313.1434, Found 313.1439.

5.5.7.2. 3,6-Dipropoxy-9H-xanthene (90)



The compound was synthesized according to general procedure (VI). Compound **88** (53.6 mg, 0.25 mmol, 1 equiv.), anhydrous K_2CO_3 (172.7 mg, 1.25 mmol, 5 equiv.), 1-bromopropane (0.3 mL, 461.2 mg, 3.75

mmol, 15 equiv.) and acetonitrile (25 mL). **Reaction time:** 15 h. **Work up.** Purification was done by column chromatography on silica gel using ethyl acetate/petroleum ether (2:98). **Appearance:** white powder. **Yield:** 20 mg (27%); **m.p.** 83-84 °C. **Solubility:** The compound is soluble in acetone and methanol, but insoluble in water. **Analytical data:** 1H -NMR (DMSO- d_6 , 500 MHz) δ (ppm) = 0.96 (t, J = 7.39 Hz, 6H, 2(-OCH₂-CH₂-CH₃)); 1.69-1.73 (m, 4H, 2(-OCH₂-CH₂-CH₃)); 3.86 (s, 2H, -CH₂); 3.91 (t, J = 6.54 Hz, 4H, 2(-OCH₂-CH₂-CH₃)); 6.59 (d, J = 2.53 Hz, 2H); 6.63 (d, J = 2.53 Hz, 1H); 6.65 (d, J = 2.53 Hz, 1H); 7.11 (d, J = 8.38 Hz, 2H). ^{13}C -NMR (DMSO, 126 MHz) δ (ppm) = 10.48 (-OCH₂-CH₂-CH₃), 22.09 (-OCH₂-CH₂-CH₃), 25.67 (-CH₂), 69.26 (-OCH₂-CH₂-CH₃), 101.87, 110.35, 112.38, 114.46, 129.60, 129.80, 151.83, 158.36. **LC-MS:** (m/z): positive mode 299.3 [M]⁺. Purity by **HPLC-UV (220-400 nm)**-ESI-MS: 94%. **HRMS (ESI-TOF) m/z :** [M+H]⁺ Calcd. for C₁₉H₂₃O₃ 299.1642, Found 299.1648.

5.5.8. *N*⁴-(4-Methoxyphenyl)pyrimidine-2,4,6-triamine (91)

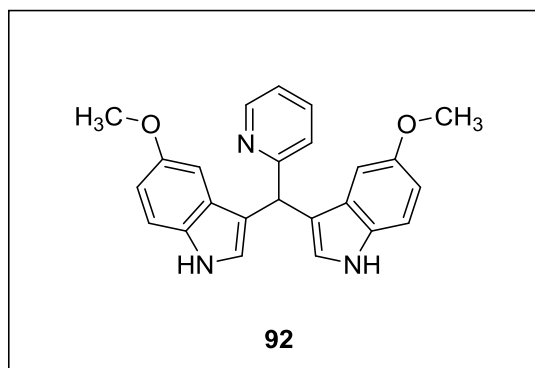
4-Methoxyaniline (264 mg, 2 mmol, 1 equiv.), was added to a suspension of 6-chloro-2,4-pyrimidinediamine (289 mg, 2 mmol, 1 equiv.) and DIPEA (0.4 mL, 284 mg, 2.2 mmol, 1.1 equiv.) in dioxane (25 mL). The reaction was refluxed under argon atmosphere and the formation of the compound

was monitored by TLC. After the reaction was completed, the formed mixture was then allowed to cool and the solvent was removed using a vacuum pump. The residue was diluted with water (50 mL) and extracted with EtOAc (2 × 50 mL). The collected organic layers were washed with brine (2 × 25 mL), dried over Na₂SO₄, filtered and then concentrated to dryness. The residual material was purified by flash column chromatography using methanol/dichloromethane (5:95) to afford the pure title compound. **Reaction time:** 24 h. **Appearance:** light green powder. **Yield:**

Experimental Part

120 mg (26%); **m.p.** 225-227 °C. **Solubility:** The compound is soluble in acetone and ethyl acetate, but insoluble in water. **Analytical data:** $^1\text{H-NMR}$ ($\text{DMSO-}d_6$, 600 MHz) δ (ppm) = 3.73 (s, 3H, $-\text{OCH}_3$); 5.19 (s, 1H, $-\text{H}_{\text{pyr}}$); 6.89 (d, $J = 8.90$ Hz, 2H, 3-H, 5-H); 7.07 (s, 2H, $-\text{NH}_2$); 7.16 (s, 2H, $-\text{NH}_2$); 7.35 (d, $J = 8.64$ Hz, 2H, 4-H, 6-H); 9.30 (s, 1H, $-\text{NH}$). $^{13}\text{C-NMR}$ (DMSO , 151 MHz) δ (ppm) = 55.75 ($-\text{OCH}_3$), 74.23, 114.59, 124.51, 132.20, 155.93, 156.37. **LC-MS:** (m/z): positive mode 231.9 $[\text{M}]^+$. Purity by **HPLC-UV (220-400 nm)**-**ESI-MS:** 99%. **HRMS (ESI-TOF) m/z :** $[\text{M}+\text{H}]^+$ Calcd. for $\text{C}_{11}\text{H}_{14}\text{N}_5\text{O}$ 232.1193, Found 232.1205.

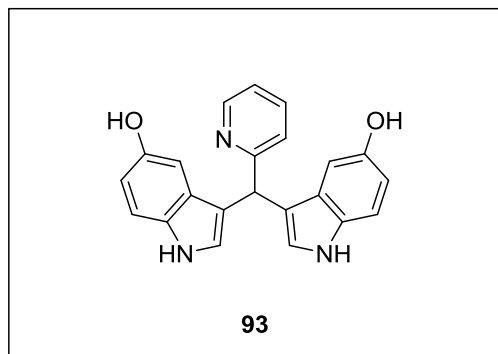
5.5.9. 3,3'-(Pyridin-2-ylmethylene)-bis-(5-methoxy-1H-indole) (92)



The compound was synthesized from 2-pyridinecarboxaldehyde (0.2 mL, 2 mmol, 1 equiv.), 5-methoxyindole (588 mg, 4 mmol, 2 equiv.) and sodium dodecyl sulfate (231 mg, 0.8 mmol, 0.4 equiv.) in water (20 mL). **Reaction time:** 17 h. **Work up.** Purification was done by column chromatography on silica gel using ethyl acetate/petroleum ether (60:40). **Appearance:** light brown powder. **Yield:** 500 (65%); **m.p.** 118-120 °C. **Solubility:** The compound is soluble in acetone and ethyl acetate, but insoluble in water. **Analytical data:** $^1\text{H-NMR}$ ($\text{DMSO-}d_6$, 500 MHz) δ (ppm) = 3.60 (s, 6H, 2($-\text{OCH}_3$)); 5.83 (s, 1H, $-\text{CH}$); 6.68 (dd, $J = 2.47, 8.74$ Hz, 2H, 2-H, 2'-H); 6.77 (d, $J = 2.51$ Hz, 2H, 6-H, 6'-H); 6.93 (d, $J = 2.39$ Hz, 2H, 4-H, 4'-H); 7.17 (ddd, $J = 1.14, 4.84, 7.43$ Hz, 1H, 3- H_{py}); 7.22 (d, $J = 8.73$ Hz, 2H, 7-H, 7'-H); 7.37-7.39 (m, 1H, 4- H_{py}); 7.67 (td, $J = 1.88, 7.64$ Hz, 1H, 5- H_{py}); 8.48-8.50 (m, 1H, 6- H_{py}); 10.65 (br s, 2H, 2($-\text{NH}$)). $^{13}\text{C-NMR}$ (DMSO , 126 MHz) δ (ppm) = 42.71 ($-\text{CH}$), 55.37 ($-\text{OCH}_3$), 101.34, 110.75, 112.09, 116.70, 121.27 (5- C_{py}), 122.61, 124.39 (3- C_{py}), 127.18, 131.76, 136.45 (4- C_{py}), 148.76 (6- C_{py}), 152.86, 164.20. **LC-MS:** (m/z): positive mode 384.2 $[\text{M}]^+$. Purity by

HPLC-UV (220-400 nm)-ESI-MS: 98%. **HRMS (ESI-TOF) m/z :** $[M-H]^-$ Calcd. for $C_{24}H_{20}N_3O_2$ 382.1561, Found 382.1574.

5.5.10. 3,3'-(Pyridin-2-ylmethylene)-bis-(1H-indol-5-ol) (93)

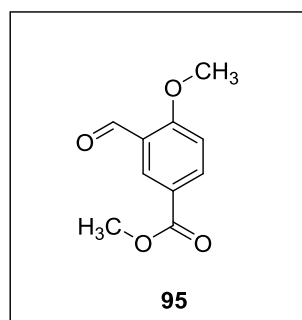


The compound was synthesized according to general procedure (IV). Compound **92** (191 mg, 0.5 mmol, 1 equiv.) and BBr_3 in DCM (1M, 1.8 ml, 1.75 mmol, 3.5 equiv.). **Reaction time:** 12 h. **Work up.** Purification was done by column chromatography on silica gel using ethyl acetate/petroleum ether (60:40). **Appearance:** brown powder. **Yield:** 150 mg (85%); **m.p.** 118-120 °C.

Solubility: The compound is soluble in acetone and ethyl acetate, but insoluble in water. **Analytical data:** 1H -NMR (DMSO- d_6 , 500 MHz) δ (ppm) = 5.65 (s, 1H, -CH); 6.53 (dd, J = 2.34, 8.60 Hz, 2H, 2-H, 2'-H); 6.61 (d, J = 2.36 Hz, 2H, 6-H, 6'-H); 6.74 (d, J = 2.26 Hz, 2H, 4-H, 4'-H); 7.11 (d, J = 8.56 Hz, 2H, 7-H, 7'-H); 7.17 (ddd, J = 1.16, 4.86, 7.50 Hz, 1H, 3- H_{Py}); 7.28-7.30 (m, 1H, 4- H_{Py}); 7.65 (td, J = 1.89, 7.68 Hz, 1H, 5- H_{Py}); 8.43 (s, 2H, 2-(OH)); 8.47-8.48 (m, 1H, 6- H_{Py}); 10.46 (d, J = 2.49 Hz, 2H, 2-(NH)). ^{13}C -NMR (DMSO, 126 MHz) δ (ppm) = 43.07 (-CH), 103.11, 111.30, 111.75, 116.07, 121.22, 122.43, 124.08, 127.48, 131.14, 136.34, 148.74, 150.09, 164.18. **LC-MS:** (m/z): positive mode 356.3 $[M]^+$. Purity by **HPLC-UV (220-400 nm)-ESI-MS:** 95%. **HRMS (ESI-TOF) m/z :** $[M-H]^-$ Calcd. for $C_{22}H_{16}N_3O_2$ 354.1248, Found 354.1247.

5.5.11. 5,5'-(4-(Benzyloxy)-1,3-phenylene)-bis-(3-ethyl-1,2,4-oxadiazole) (99)

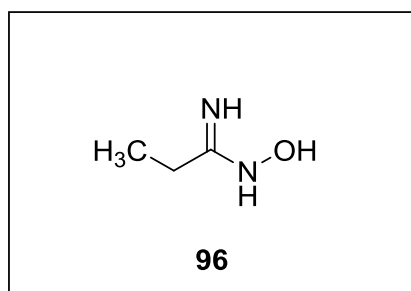
5.5.11.1. Methyl 3-formyl-4-methoxybenzoate (95)



The compound was synthesized according to general procedure (VI). Methyl 3-formyl-4-methoxybenzoate (**94**) (900.8 mg, 5 mmol, 1 equiv.), anhydrous K_2CO_3 (1382 mg, 10 mmol, 5 equiv.) and dimethyl sulfate (7.1 mL, 9460 mg, 75 mmol, 15 equiv.). **Reaction time:** 2 h. **Work up.** Purification was done by column chromatography on silica

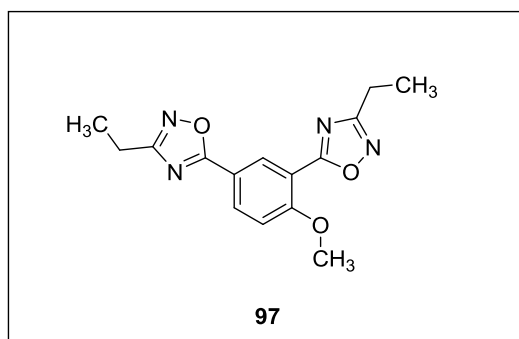
gel using ethyl acetate/dichloromethane (2:98). **Appearance:** white powder. **Yield:** 850 mg (88%). **Analytical data:** $^1\text{H-NMR}$ ($\text{DMSO-}d_6$, 600 MHz) δ (ppm) = 3.84 (s, 3H, $-\text{OCH}_3$); 3.99 (s, 3H, $-\text{COOCH}_3$); 7.35 (d, $J = 8.78$ Hz, 1H, 2-H); 8.19 (dd, $J = 2.37, 8.78$ Hz, 1H, 5-H); 8.23 (d, $J = 2.34$ Hz, 1H, 6-H); 10.33 (s, 1H, $-\text{CHO}$). $^{13}\text{C-NMR}$ (DMSO , 151 MHz) δ (ppm) = 52.31 ($-\text{COOCH}_3$), 56.73 ($-\text{OCH}_3$), 113.38, 122.10, 124.04, 129.38, 136.99, 164.72 ($-\text{COOCH}_3$), 165.37, 188.75 ($-\text{CHO}$).

5.3.11.2. Propionamidoxime (96)



A solution of propionitrile (1.7 mL, 1377 mg, 25 mmol) in MeOH (45 mL) was brought to reflux. $\text{NH}_2\text{-OH}$ (50% hydroxylamine by wt. in water, 0.99 ml, 1073.5 mg, 32.5 mmol, 1.3 equiv.) was added dropwise over 20 min via syringe. The resulting solution was refluxed overnight and then allowed to reach rt and evaporated. The residue was partially co-evaporated with toluene (3×25 mL) under reduced pressure. The desired compound was obtained as colorless viscous oil after drying over a high vacuum pump and used without any further purification.

5.5.11.3. 5,5'-(4-Methoxy-1,3-phenylene)-bis-(3-ethyl-1,2,4-oxadiazole) (97)

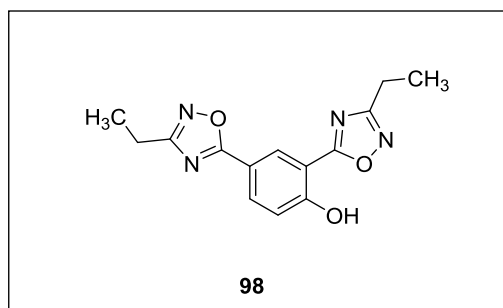


Using dean-stark apparatus, methyl 3-formyl-4-methoxybenzoate (**95**) (582.6 mg, 3 mmol, 1 equiv.), *N*-hydroxypropanimidamide (**96**) (528.6 mg, 6 mmol, 2 equiv.) and anhydrous K_2CO_3 (829.3 mg, 6 mmol, 2 equiv.) were suspended in toluene (100 mL). The mixture was refluxed at 150°C and was controlled by TLC. The mixture was cooled to rt and solvent was removed under reduced pressure. Water (50 mL) was added and the mixture was extracted with EtOAc (3×50 mL). The combined organic layers were washed with brine (2×20 mL) and then were dried over MgSO_4 , filtered, and concentrated under vacuum. Purification was done using column chromatography on silica gel using ethyl acetate/dichloromethane (5:95) to give the titled compound. **Reaction time:** 48 h. **Appearance:** white powder. **Yield:** 250 mg (28%); **m.p.** 105-

Experimental Part

107 °C. **Solubility:** The compound is soluble in acetone and ethyl acetate, but insoluble in water. **Analytical data:** $^1\text{H-NMR}$ ($\text{DMSO-}d_6$, 600 MHz) δ (ppm) = 1.27-1.31 (m, 6H, 2(-CH₂-CH₃); 2.77-2.83 (m, 4H, 2(-CH₂-CH₃); 4.04 (s, 3H, -OCH₃); 7.52 (d, J = 8.91 Hz, 1H); 8.32 (dd, J = 2.34, 8.84 Hz, 1H); 8.62 (d, J = 2.30 Hz, 1H). $^{13}\text{C-NMR}$ (DMSO , 151 MHz) δ (ppm) = 11.33 (-CH₃), 11.40 (-CH₃), 19.18 (-CH₂-CH₃), 19.25 (-CH₂-CH₃), 57.00 (-OCH₃), 113.58, 114.34, 116.33, 130.77, 133.82, 161.27, 171.40, 172.03, 173.30, 173.73. **LC-MS:** (m/z): positive mode 300.9 [M]⁺. Purity by **HPLC-UV (220-400 nm)-ESI-MS:** 98%. **HRMS (ESI-TOF) m/z :** [M+H]⁺ Calcd. for C₁₅H₁₇N₄O₃ 301.1295, Found 301.1305.

5.5.11.4. 2,4-Bis-(3-ethyl-1,2,4-oxadiazol-5-yl)phenol (98)

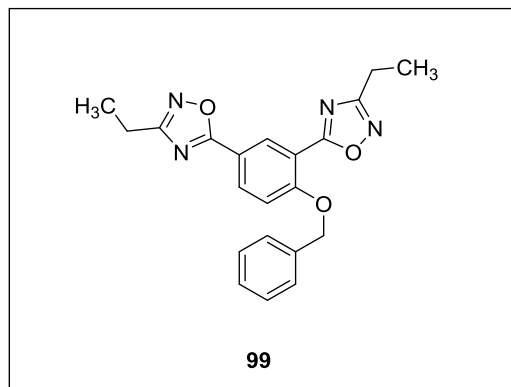


The compound was synthesized according to general procedure (IV). Compound **97** (200 mg, 0.66 mmol, 1 equiv.) and BBr₃ in DCM (1M, 2.3 ml, 2.31 mmol, 3.5 equiv.). **Reaction time:** 13 h. **Work up.** Purification was done by column chromatography on silica gel using ethyl acetate/dichloromethane (5:95).

Appearance: white powder. **Yield:** 130 mg (69%); **m.p.** 128-130 °C. **Solubility:** The compound is soluble in acetone, ethyl acetate and methanol, but insoluble in water. **Analytical data:** $^1\text{H-NMR}$ ($\text{DMSO-}d_6$, 500 MHz) δ (ppm) = 1.26-1.31 (m, 6H, 2(-CH₂-CH₃); 2.75-2.83 (m, 4H, 2(-CH₂-CH₃); 7.28 (d, J = 8.74 Hz, 1H); 8.15 (dd, J = 2.33, 8.77 Hz, 1H); 8.57 (d, J = 2.31 Hz, 1H); 11.59 (s, 1H, -OH). $^{13}\text{C-NMR}$ (DMSO , 126 MHz) δ (ppm) = 11.32 (-CH₃), 11.35 (-CH₃), 19.13 (-CH₂-CH₃), 19.23(-CH₂-CH₃), 111.43, 115.12, 118.73, 130.47, 133.45, 160.82, 171.10, 171.92, 173.52, 173.93. **LC-MS:** (m/z): positive mode 286.9 [M]⁺. Purity by **HPLC-UV (220-400 nm)-**

ESI-MS: 95%. **HRMS (ESI-TOF) m/z :** $[M-H]^-$ Calcd. for $C_{14}H_{13}N_4O_3$ 285.0993, Found 285.1020.

5.3.11.5. 5,5'-(4-(Benzyloxy)-1,3-phenylene)-bis-(3-ethyl-1,2,4-oxadiazole) (99)



The compound was synthesized according to general procedure (III). Compound **98** (100 mg, 0.35 mmol, 1 equiv.), NaH (60% in paraffin oil, 16 mg, 0.4 mmol, 1.1 equiv.) and benzyl bromide (0.05 mL, 68 mg, 0.4 mmol, 1.1 equiv.). **Reaction time:** 1 h. **Work up.** The purification was done by column chromatography on silica gel using ethyl acetate/dichloromethane (5:95).

Appearance: white powder. **Yield:** 85 mg (65%); **m.p.**

104-105 °C. **Solubility:** The compound is soluble in acetone, dichloromethane and methanol, but insoluble in water. **Analytical data:** 1H -NMR (DMSO- d_6 , 500 MHz) δ (ppm) = 1.27-1.32 (m, 6H, 2(-CH₂-CH₃)); 2.76-2.84 (m, 4H, 2(-CH₂-CH₃)); 5.45 (s, 2H, -OCH₂-Ph); 7.35 (m, 1H); 7.41 (m, 2H); 7.56 (m, 2H); 7.61 (d, J = 8.89 Hz, 1H); 8.31 (dd, J = 2.32, 8.87 Hz, 1H); 8.65 (d, J = 2.30 Hz, 1H). ^{13}C -NMR (DMSO, 126 MHz) δ (ppm) = 11.31 (-CH₃), 11.33 (-CH₃), 19.18 (-CH₂-CH₃), 19.25 (-CH₂-CH₃), 70.66 (-OCH₂-Ph), 113.99, 115.46, 116.60, 127.24, 128.09, 128.60, 130.83, 133.70, 136.10, 160.21, 171.41, 172.03, 173.27, 173.70. **LC-MS:** (m/z): positive mode 377.3 $[M]^+$. Purity by **HPLC-UV (220-400 nm)**-ESI-MS: 97%. **HRMS (ESI-TOF) m/z :** $[M-H]^-$ Calcd. for $C_{21}H_{19}N_4O_3$ 375,1463, Found 375,1452.

8 6. Abbreviation

Item	Abbreviation
5-BDBD	(5-(3-Bromophenyl)- 1,3-dihydro-2 <i>H</i> -benzofuro[3,2- <i>e</i>]-1,4-diazepin-2-one)
A-740003	<i>N</i> -(1-[[<i>Cyanoimino</i>](5-quinolinylamino)methyl]amino)-2,2-dimethylpropyl)-2-(3,4-dimethoxyphenyl)acetamide
AA	Amino acid
AB-25	Acid Blue 25
ADP	Adenosine 5'-diphosphate
AMP	Adenosine 5'-monophosphate
AQ	Anthraquinone
aq.	Aqueous
ATP	Adenosine 5'-triphosphate
ATP γ S	Adenosine 5'-O-(3-thio) triphosphate
BDNF	Brain-derived neurotrophic factor
BHPM	Bis-(<i>p</i> -hydroxyphenyl)-pyridyl-2-methane
Brine	Saturated solution of sodium chloride
BX430	Dibromo-4-isopropyl-phenyl)-3- (3-pyridyl)urea
cDNA	Complementary deoxyribonucleic acid
CNS	Central nervous system
Crysophanol	1,8-Dihydroxy-3-methylanthracenedione
Danthron	1,8-Dihydroxyanthraquinone
EC ₅₀	molar concentration of agonist that produces 50% of maximal effect
ECL	Extracellular loop
Emodin	1,3,8-Trihydroxy-6-methylanthraquinone
Equiv.	Equivalent
FDA	Food and Drug Administration
GABA	γ -Aminobutyric acid
GPCRs	G protein-coupled receptors
HEK	human embryonic kidney cells
HRMS	High-resolution mass spectral
HTS	High-throughput screening

Abbreviations

Item	Abbreviation
IC	Intracellular loop
IC ₅₀	molar concentration of antagonist that produces 50% of maximal effect
KN-62	1-[<i>N,O</i> -bis(5-isoquinolinesulfonyl)- <i>N</i> -methyl- <i>L</i> -tyrosyl]-4-phenylpiperazine
LC-MS	liquid chromatography-mass spectroscopy
LGICs	Ligand gated ion channels
MAOS	Microwave-assisted organic synthesis
MW	Microwave
NP-1815-PX	(5-[3-(5-Thioxo-4 <i>H</i> -[1,2,4]oxadiazol-3-yl)phenyl]-1 <i>H</i> -naphtho[1,2- <i>b</i>][1,4]diazepine-2,4(3 <i>H</i> ,5 <i>H</i>)-dione)
NSAIDs	Nonsteroidal anti-inflammatory drugs
PPADS	Pyridoxal-phosphate-6-azophenyl-2',4'-disulfonate
PSB-0702	1-Amino-4-[4-phenylamino-3-carboxyphenylamino]-9,10-dioxo-9,10-dihydroanthracene-2-sulfonate
PSB-0739	1-Amino-4-[4-phenylamino-3-sulfophenylamino]-9,10-dioxo-9,10-dihydroanthracene-2-sulfonate
PSB-12054	<i>N</i> -(benzyloxycarbonyl)phenoxazine
PSB-12062	<i>N</i> -(<i>p</i> -methylphenylsulfonyl)phenoxazine
Py	Pyridine
RB-2	Reactive Blue-2
Rhein	4,5-Dihydroxy-9,10-dioxoanthracene-2-carboxylic acid
RO-85	1-Methyl-3-phenyl-1 <i>H</i> -thieno[2,3- <i>c</i>]pyrazole-5-carboxylic acid [(<i>R</i>)-2-(4-acetyl-piperazin-1-yl)-1-methyl-ethyl]-amide
rt	Room temperature
SARs	Structure-activity relationships
TLC	Thin layer chromatography
TM	Transmembrane
TNP-ATP	2',3'- <i>O</i> -(2,4,6-trinitrophenyl)adenosine 5'-triphosphate
TRAMs	Triarylmethanes
UDP	Uridine diphosphate
UTP	Uridine -5'- triphosphate
VGICs	Voltage-gated ion channels
zfp2X4	Zebrafish P2X4 receptor

9 7. References

- (1) Burnstock, G. Discovery of purinergic signalling, the initial resistance and current explosion of interest. *Br. J. Pharmacol.* **2012**, *167*, 238–255.
- (2) Burnstock, G. Introduction: P2 receptors. *Curr. Top. Med. Chem.* **2004**, *4*, 793–803.
- (3) Vergani, A.; Tezza, S.; Fotino, C.; Visner, G.; Pileggi, A.; Chandraker, A.; Fiorina, P. The purinergic system in allotransplantation. *Am. J. Transplant.* **2014**, *14*, 507–514.
- (4) Drury, A. N.; Szent-Györgyi, A. The physiological activity of adenine compounds with especial reference to their action upon the mammalian heart. *J. Physiol.* **1929**, *68*, 213–237.
- (5) Buchtal, F.; Folokow, B. Close arterial injection of adenosine triphosphate and inorganic triphosphate into frog muscle. *Acta Physiol. Scand.* **1944**, *8*, 312–316.
- (6) Holton, B. F. A.; Holton, P. The capillary dilator substances in dry powders of spinal roots; a possible role of adenosine triphosphate in chemical transmission from nerve endings. *J. Physiol.* **1954**, *126*, 124–140.
- (7) Mary, S.; Medical, H. The liberation of adenosine triphosphate on antidromic stimulation of sensory nerves. *J. Physiol.* **1959**, *145*, 494–504.
- (8) Jo, Y.; Schlichter, R. Synaptic corelease of ATP and GABA in cultured spinal neurons. *Nat. Neurosci.* **1999**, *2*, 241–245.
- (9) Salgado, A. I.; Cunha, R. A.; Ribeiro, J. A. Facilitation by P2 receptor activation of acetylcholine release from rat motor nerve terminals: interaction with presynaptic nicotinic receptors. *Brain Res.* **2000**, *877*, 245–250.
- (10) Ergene, E.; Dunbar, J. C.; O’Leary, D. S.; Barraco, R. A. Activation of P2-purinoceptors in the nucleus tractus solitarius mediate depressor responses. *Neurosci Lett.* **1994**, *174*, 188–192.
- (11) Ziganshin, A. U.; Hoyle, C. H. V.; Burnstock, G. Ecto-enzymes and metabolism of extracellular ATP. *Drug Dev. Res.* **1994**, *32*, 134–146.

References

- (12) Zimmermann, H.; Mishra, S.; Shukla, V.; Langer, D.; Gampe, K.; Grimm, I.; Delic, J.; Braun, N. Ecto-nucleotidases, molecular properties and functional impact. *An. R. Acad. Nac. Farm.* **2007**, *73*, 537–566.
- (13) Burnstock, G. Physiology and pathophysiology of purinergic neurotransmission. *Physiol. Rev.* **2007**, *87*, 659–797.
- (14) Zeiser, R.; Robson, S. C.; Vaikunthanathan, T.; Dworak, M.; Burnstock, G. Unlocking the potential of purinergic signaling in transplantation. *Am. J. Transplant.* **2016**, *16*, 2781–2794.
- (15) Burnstock, G. Purinergic nerves. *Pharmacological Reviews*, **1972**, *24*, 509–581.
- (16) Burnstock, G. Purinergic receptors. *J. Theor. Biol.* **1976**, *62*, 491–503.
- (17) Abbracchio, M. P.; Burnstock, G. Purinoceptors: are there families of P2X and P2Y purinoceptors? *Pharmac. Ther.* **1994**, *64*, 445–475.
- (18) Webb, T. E.; Simon, J.; Krishek, B. J.; Bateson, A. N.; Smart, T. G.; King, B. F.; Burnstock, G.; Barnard, E. A. Cloning and functional expression of a brain G-protein-coupled ATP receptor. *Fed. Eur. Biochem. Soc.* **1993**, *324*, 219–225.
- (19) Brunschweiler, A.; Müller, C. E. P2 receptors activated by uracil nucleotides- an update. *Curr. Med. Chem.* **2006**, *13*, 289–312.
- (20) Borrmann, T.; Abdelrahman, A.; Volpini, R.; Lambertucci, C.; Alksnis, E.; Gorzalka, S.; Knospe, M.; Schiedel, A. C.; Cristalli, G.; Müller, C. E. Structure-activity relationships of adenine and deazaadenine derivatives as ligands for adenine receptors, a new purinergic receptor family. *J. Med. Chem.* **2009**, *52*, 5974–5989.
- (21) Bender, E.; Buist, A.; Jurzak, M.; Langlois, X.; Baggerman, G.; Verhasselt, P.; Ercken, M.; Guo, H. Q.; Wintmolders, C.; Van den Wyngaert, I.; Van Oers, I.; Schoofs, L.; Luyten, W. Characterization of an orphan G protein-coupled receptor localized in the dorsal root ganglia reveals adenine as a signaling molecule. *Proc. Natl. Acad. Sci. U. S. A.* **2002**, *99*, 8573–8578.
- (22) Burnstock, G. Purine and pyrimidine receptors. *Cell. Mol. Life Sci.* **2007**, *64*, 1471–1483.

References

- (23) Flower, D. R. Modelling G-protein-coupled receptors for drug design. *Biochim. Biophys.* **1999**, *1422*, 207–234.
- (24) Ferguson, S. S. Evolving concepts in G protein-coupled receptor endocytosis: the role in receptor desensitization and signaling. *Pharmacol Rev.* **2001**, *53*, 1–24.
- (25) Marinissen, M. J.; Gutkind, J. S. G-protein-coupled receptors and signaling networks: emerging paradigms. *Trends Pharmacol. Sci.* **2001**, *22*, 368–376.
- (26) Santos, R.; Ursu, O.; Gaulton, A.; Bento, A. P.; Donadi, R. S.; Bologa, C. G.; Karlsson, A.; Al-Lazikani, B.; Hersey, A.; Oprea, T. I.; Overington, J. P. A comprehensive map of molecular drug targets. *Nat. Rev. Drug Discov.* **2016**, *16*, 19–34.
- (27) Abbracchio, M. P.; Burnstock, G.; Boeynaems, J.; Eric, A.; Boyer, J. L.; Kennedy, C.; Knight, G. E.; Gachet, C.; Jacobson, K. A.; Weisman, G. A. International union of pharmacology LVIII: update on the P2Y G protein-coupled nucleotide receptors: from molecular mechanisms and pathophysiology to therapy. *Pharmacol. Rev.* **2012**, *58*, 281–341.
- (28) Burnstock, G.; Williams, M. P2 purinergic receptors: modulation of cell function and therapeutic potential. *J. Pharmacol. Exp. Ther.* **2000**, *295*, 862–869.
- (29) King, B. F.; Townsend-Nicholson, A. Nucleotide and nucleoside receptors. *Tocris Rev.* **2003**, *23*, (Published and distributed by Tocris Cookson, Bristol, UK).
- (30) Dubyak, G. R. Knock-out mice reveal tissue-specific roles of P2Y receptor subtypes in different epithelia. *Mol. Pharmacol.* **2003**, *63*, 773–776.
- (31) Burnstock, G. Purinergic signalling and disorders of the central nervous system. *Nat. Rev. Drug Discov.* **2008**, *7*, 575–590.
- (32) Bagal, S. K.; Brown, A. D.; Cox, P. J.; Omoto, K.; Owen, R. M.; Pryde, D. C.; Sidders, B.; Skerratt, S. E.; Stevens, E. B.; Storer, R. I.; Swain, N. A. Ion channels as therapeutic targets: a drug discovery perspective. *J. Med. Chem.* **2013**, *56*, 593–624.
- (33) Lemoine, D.; Jiang, R.; Taly, A.; Chataigneau, T.; Specht, A.; Grutter, T. Ligand-gated ion channels: new insights into neurological disorders and ligand recognition. *Chem. Rev.* **2012**, *112*, 6285–6318.

References

- (34) Compan, V.; Ulmann, L.; Stelmashenko, O.; Chemin, J.; Rassendren, F. P2X2 and P2X5 subunits define a new heteromeric receptor with P2X7-like properties. *J. Neurosci.* **2012**, *32*, 4284–4296.
- (35) Antonio, L. S.; Stewart, A. P.; Varanda, W. A.; Edwardson, J. M. Identification of P2X2/P2X4/P2X6 heterotrimeric receptors using atomic force microscopy (AFM) imaging. *FEBS Lett.* **2014**, *588*, 2125–2128.
- (36) North, R. A. Molecular physiology of P2X receptors. *Physiol. Rev.* **2002**, *82*, 1013–1067.
- (37) Jacobson, K. A.; Müller, C. E. Medicinal chemistry of adenosine , P2Y and P2X receptors. *Neuropharmacology* **2016**, *104*, 31–49.
- (38) Egan, T. M.; Samways, D. S.; Li, Z. Biophysics of P2X receptors. *Eur. J. Physiol.* **2006**, *452*, 501–512.
- (39) Brake, A. J.; Wagenbach, M. J.; Julius, D. New structural motif for ligand-gated ion channels defined by an ionotropic ATP receptor. *Nature* **1994**, *371*, 519–523.
- (40) Kaczmarek-Hájek, K.; Lörinczi, É.; Hausmann, R.; Nicke, A. Molecular and functional properties of P2X receptors-recent progress and persisting challenges. *Purinergic Signal.* **2012**, *8*, 375–417.
- (41) Ben, D. D.; Buccioni, M.; Lambertucci, C.; Marucci, G.; Thomas, A.; Volpini, R. Purinergic P2X receptors: structural models and analysis of ligand-target interaction. *Eur. J. Med. Chem.* **2015**, *89*, 561–580.
- (42) Jacobson, K. A.; Jarvis, M. F.; Williams, M. Purine and pyrimidine (P2) receptors as drug targets. *J. Med. Chem.* **2002**, *45*, 4057–4093.
- (43) Jacobson, K. A. P2X and P2Y receptors, *Tocris Reviews*, **2010**, *33*, 1-16.
- (44) Kawate, T.; Michel, J. C.; Birdsong, W. T.; Gouaux, E. Crystal structure of the ATP-gated P2X4 ion channel in the closed state. *Nature* **2009**, *460*, 592–598.
- (45) Hattori, M.; Gouaux, E. Molecular mechanism of ATP binding and ion channel activation in P2X receptors. *Nature* **2012**, *485*, 207–212.
- (46) Müller, C. E. Emerging structures and ligands for P2X3 and P2X4 receptors–towards

- novel treatments of neuropathic pain. *Purinergic Signal*. **2010**, 6, 145–148.
- (47) Chataigneau, T.; Lemoine, D.; Grutter, T. Exploring the ATP-binding site of P2X receptors. *Front. Cell. Neurosci.* **2013**, 7, 1–12.
- (48) Gonzales, E. B.; Kawate, T.; Gouaux, E. Pore architecture and ion sites in acid-sensing ion channels and P2X receptors. *Nature* **2009**, 460, 599–604.
- (49) Mansoor, S. E.; Lü, W.; Oosterheert, W.; Shekhar, M.; Tajkhorshid, E.; Gouaux, E. X-ray structures define human P2X3 receptor gating cycle and antagonist action. *Nature* **2016**, 538, 66–71.
- (50) Brandao-Burch, A.; Key, M. L.; Patel, J. J.; Arnett, T. R.; Orriss, I. R. The P2X7 receptor is an important regulator of extracellular ATP levels. *Front. Endocrinol.* **2012**, 3, 1–9.
- (51) Donnelly-Roberts, D. L.; Namovic, M. T.; Surber, B.; Vaidyanathan, S. X.; Perez-Medrano, A.; Wang, Y.; Carroll, W. A.; Jarvis, M. F. [3H]A-804598 ([3H]2-cyano-1-[(1S)-1-phenylethyl]-3-quinolin-5-ylguanidine) is a novel, potent, and selective antagonist radioligand for P2X7 receptors. *Neuropharmacology* **2009**, 56, 223–229.
- (52) Michel, A. D.; Chambers, L. J.; Walter, D. S. Negative and positive allosteric modulators of the P2X7 receptor. *Br. J. Pharmacol.* **2008**, 153, 737–750.
- (53) Bhattacharya, A.; Wang, Q.; Ao, H.; Shoblock, J. R.; Lord, B.; Aluisio, L.; Fraser, I.; Nepomuceno, D.; Neff, R. A.; Welty, N.; Lovenberg, T. W.; Bonaventure, P.; Wickenden, A. D.; Letavic, M. A. Pharmacological characterization of a novel centrally permeable P2X7 receptor antagonist: JNJ-47965567. *Br. J. Pharmacol.* **2013**, 170, 624–640.
- (54) Michel, A. D.; Clay, W. C.; Ng, S. W.; Roman, S.; Thompson, K.; Condreay, J. P.; Hall, M.; Holbrook, J.; Livermore, D.; Senger, S. Identification of regions of the P2X7 receptor that contribute to human and rat species differences in antagonist effects. *Br. J. Pharmacol.* **2008**, 155, 738–751.
- (55) Karasawa, A.; Kawate, T. Structural basis for subtype-specific inhibition of the P2X7 receptor. *Elife* **2016**, 5, 1–17.
- (56) Gever, J. R.; Cockayne, D. A.; Dillon, M. P.; Burnstock, G.; Ford, A. P. D. W. Pharmacology of P2X channels. *Eur. J. Physiol.* **2006**, 452, 513–537.

References

- (57) North, R. A.; Jarvis, M. F. P2X receptors as drug targets. *Mol. Pharmacol.* **2013**, *83*, 759–769.
- (58) Soto, F.; Lambrecht, G.; Nickel, P.; Stühmer, W.; Busch, A. E. Antagonistic properties of the suramin analogue NF023 at heterologously expressed P2X receptors. *Neuropharmacology* **1999**, *38*, 141–149.
- (59) Jacobson, K. A.; Kim, Y.; Wildman, S. S.; Mohanram, A.; Harden, T. K.; Boyer, L.; King, B. F.; Burnstock, G. A pyridoxine cyclic phosphate and its 6-azoaryl derivative selectively potentiate and antagonize activation of P2X1 receptors. *J. Med. Chem.* **1998**, *41*, 2201–2206.
- (60) Greenhouse, R.; Padilla, F.; Dillon, M. P.; Gever, J. R.; Ford, A. P. D. W. Discovery and synthesis of a novel and selective drug-like P2X1 antagonist. *Bioorg. Med. Chem. Lett.* **2005**, *15*, 3292–3295.
- (61) Hausmann, R.; Bodnar, M.; Woltersdorf, R.; Wang, H.; Fuchs, M.; Messemer, N.; Qin, Y.; Günther, J.; Riedel, T.; Grohmann, M.; Nieber, K.; Schmalzing, G.; Rubini, P.; Illes, P. ATP binding site mutagenesis reveals different subunit stoichiometry of functional P2X2/3 and P2X2/6 receptors. *J. Bio. Chem.* **2012**, *287*, 13930–13943.
- (62) Lorca, R. A.; Coddou, C.; Gazitu, M. C.; Bull, P.; Huidobro-toro, J. P. Extracellular histidine residues identify common structural determinants in the copper/zinc P2X2 receptor modulation. *J. Neurochem.* **2005**, *95*, 499–512.
- (63) Jacobson, K. A.; Kim, Y-C.; King, B. F. In search of selective P2 receptor ligands: interaction of dihydropyridine derivatives at recombinant rat P2X2 receptors. *J. Auton. Nerv. Syst.* **2015**, *81*, 152–157.
- (64) Baqi, Y.; Hausmann, R.; Rosefort, C.; Rettinger, J.; Schmalzing, G.; Müller, C. E. Discovery of potent competitive antagonists and positive modulators of the P2X2 receptor. *J. Med. Chem.* **2011**, *54*, 817–830.
- (65) Bo, X.; Kim, M.; Nori, S. L.; Schoepfer, R.; Burnstock, G.; North, R. A. Tissue distribution of P2X4 receptors studied with an ectodomain antibody. *Cell Tissue Res.* **2003**, *313*, 159–165.

References

- (66) Ulmann, L.; Hatcher, J. P.; Hughes, J. P.; Chaumont, S.; Green, P. J.; Conquet, F.; Buell, G. N.; Reeve, A. J.; Chessell, I. P.; Rassendren, F. Up-regulation of P2X4 receptors in spinal microglia after peripheral nerve injury mediates BDNF release and neuropathic pain. *J. Neurosci.* **2008**, *28*, 11263–11268.
- (67) Tsuda, M.; Shigemoto-Mogami, Y.; Koizumi, S.; Mizokoshi, A.; Kohsaka, S.; Salter, M. W.; Inoue, K. P2X4 receptors induced in spinal microglia gate tactile allodynia after nerve injury. *Nature* **2003**, *424*, 778–783.
- (68) Balázs, B.; Tamás Dankó, T.; Kovács, G.; Köles, L.; Hediger, M. A.; Zsembery, Á. Investigation of the inhibitory effects of the benzodiazepine derivative, 5-BDBD on P2X4 purinergic receptors by two complementary methods. *Cell. Physiol. Biochem.* **2013**, *32*, 11–24.
- (69) Abdelrahman, A.; Namasivayam, V.; Hinz, S.; Anke, C.; Köse, M.; Burton, M.; El-tayeb, A.; Gillard, M.; Ryck, M. De; Müller, C. E. Characterization of P2X4 receptor agonists and antagonists by calcium influx and radioligand binding studies. *Biochem. Pharmacol.* **2016**, *125*, 41-54.
- (70) Nagata, K.; Imai, T.; Yamashita, T.; Tsuda, M.; Tozaki-saitoh, H.; Inoue, K. Antidepressants inhibit P2X4 receptor function: a possible involvement in neuropathic pain relief. *Mol. Pain* **2009**, *5*, 1–12.
- (71) Sim, J. A.; North, R. A. Amitriptyline does not block the action of ATP at human P2X4 receptor. *Br. J. Pharmacol.* **2010**, *160*, 88–92.
- (72) Hernandez-olmos, V.; Abdelrahman, A.; El-tayeb, A.; Freudendahl, D.; Weinhausen, S.; Müller, C. E. N-substituted phenoxazine and acridone derivatives: structure–activity relationships of potent P2X4 receptor antagonists. *J. Med. Chem.* **2012**, *55*, 9576–9588.
- (73) Tian, M.; Abdelrahman, A.; Weinhausen, S.; Hinz, S.; Weyer, S.; Dosa, S.; El-Tayeb, A.; Müller, C. E. Carbamazepine derivatives with P2X4 receptor-blocking activity. *Bioorganic Med. Chem.* **2014**, *22*, 1077–1088.
- (74) Ase, A. R.; Honson, N. S.; Zaghdane, H.; Pfeifer, T. A.; Séguéla, P. Identification and characterization of a selective allosteric antagonist of human P2X4 receptor channels. *Mol. Pharmacol.* **2015**, *87*, 606–616.

References

- (75) Matsumura, Y.; Yamashita, T.; Sasaki, A.; Nakata, E.; Kohno, K. A novel P2X₄ receptor-selective antagonist produces anti-allodynic effect in a mouse model of herpetic pain. *Sci. Rep.* **2016**, 1–11.
- (76) Cello, G.; North, R. A.; Kawashima, E.; Buell, G.; Merlo-pith, E. Cloning of P2X₄ and P2X₅ receptors and the distribution and properties of an extended family of ATP-gated ion channels. *J. Neurosci.* **1996**, *16*, 2495–2507.
- (77) Le, K.; Archambault, V.; Se, P. Functional and biochemical evidence for heteromeric ATP-gated channels composed of P2X₁ and P2X₅ subunits. *J. Biol. Chem.* **1999**, *274*, 15415–15419.
- (78) Kotnis, S.; Bingham, B.; Vasilyev, D. V.; Miller, S. W.; Bai, Y.; Yeola, S.; Chanda, P. K.; Bowlby, M. R.; Kaftan, E. J.; Samad, T. A.; Whiteside, G. T. Genetic and functional analysis of human P2X₅ reveals a distinct pattern of exon 10 polymorphism with predominant expression of the nonfunctional receptor isoform. *Mol. Pharmacol.* **2010**, *77*, 953–960.
- (79) Banfi, C.; Ferrario, S.; Vincenti, O. De; Ceruti, S.; Fumagalli, M.; Mazzola, A.; Ambrosi, N. D.; Volontè, C.; Fratto, P.; Vitali, E.; Burnstock, G.; Beltrami, E.; Parolari, A.; Polvani, G.; Biglioli, P.; Tremoli, E.; Abbracchio, M. P. P₂ receptors in human heart: upregulation of P2X₆ in patients undergoing heart transplantation, interaction with tnfa and potential role in myocardial cell death. *J. Mol. Cell. Cardiol.* **2005**, *39*, 929–939.
- (80) Gargett, C. E.; Wiley, J. S. The isoquinoline derivative KN-62 a potent antagonist of the P_{2Z}-receptor of human lymphocytes. *Br. J. Pharmacol.* **1997**, *120*, 1483–1490.
- (81) Arulkumaran, N.; Unwin, R. J.; Tam, F. W. K. A potential therapeutic role for P2X₇ receptor (P2X_{7R}) antagonists in the treatment of inflammatory diseases. *Expert Opin. Investig. Drugs* **2011**, *20*, 897–915.
- (82) Ferrari, D.; Pizzirani, C.; Adinolfi, E.; Lemoli, R. M.; Curti, A.; Idzko, M.; Panther, E.; Di Virgilio, F. The P2X₇ receptor: a key player in IL-1 processing and release. *J. Immunol.* **2006**, *176*, 3877–3883.
- (83) Romagnoli, R.; Baraldi, P. G.; Cruz-lopez, O.; Lopez-cara, C.; Preti, D.; Borea, P. A.; Gessi, S. The P2X₇ receptor as a therapeutic target. *Expert Opin. Ther. Targets* **2008**, *12*,

- 647–662.
- (84) Guile, S. D.; Alcaraz, L.; Birkinshaw, T. N.; Bowers, K. C.; Ebden, M. R.; Furber, M.; Stocks, M. J. Antagonists of the P2X7 receptor. From lead identification to drug development. *J. Med. Chem.* **2009**, *52*, 3123–3141.
- (85) Humphreys, B. D.; Virginio, C.; Surprenant, A.; Rice, J.; Dubyak, G. R. Isoquinolines as antagonists of the P2X7 nucleotide receptor: high selectivity for the human versus rat receptor homologues. *Mol. Pharmacol.* **1998**, *32*, 22–32.
- (86) Donnelly-roberts, D. L.; Namovic, M. T.; Han, P.; Jarvis, M. F. Mammalian P2X7 receptor pharmacology: comparison of recombinant mouse, rat and human P2X7 receptors. *Br. J. Pharmacol.* **2009**, *157*, 1203–1214.
- (87) Honore, P.; Donnelly-Roberts, D.; Namovic, M. T.; Hsieh, G.; Zhu, C. Z.; Mikusa, J. P.; Hernandez, G.; Zhong, C.; Gauvin, D. M.; Chandran, P.; Harris, R.; Medrano, A. P.; Carroll, W.; Marsh, K.; Sullivan, J. P.; Faltynek, C. R.; Jarvis, M. F. A-740003 [*N*-(1-[[[(cyanoimino)(5-quinolinylamino)methyl]mino]-2,2-dimethylpropyl]-2-(3,4-dimethoxyphenyl)acetamide], a novel and selective P2X7 receptor antagonist, dose-dependently reduces neuropathic. *J. Pharmacol. Exp. Ther.* **2006**, *319*, 1376–1385.
- (88) Wilkinson, S. M.; Gunosewoyo, H.; Barron, M. L.; Boucher, A.; McDonnell, M.; Turner, P.; Morrison, D. E.; Bennett, M. R.; McGregor, I. S.; Rendina, L. M.; Kassiou, M. The first CNS-active carborane: a novel P2X7 receptor antagonist with antidepressant activity. *ACS Chem. Neurosci.* **2014**, *5*, 335–339.
- (89) Chen, C. C.; Akopian, A. N.; Sivilotti, L.; Colquhoun, D.; Burnstock, G.; Wood, J. N. A P2X purinoceptor expressed by a subset of sensory neurons. *Nature* **1995**, *377*, 428–431.
- (90) Virginio, C.; Robertson, G.; Surprenant, A.; North, R. A. Trinitrophenyl-substituted nucleotides are potent antagonists selective for P2X1, P2X3, and heteromeric P2X2/3 receptors. *Mol. Pharmacol.* **1998**, *53*, 969–973.
- (91) Dunn, P. M.; Zhong, Y.; Burnstock, G. P2X receptors in peripheral neurons. *Prog. Neurobiol.* **2001**, *65*, 107–134.
- (92) Bradbury, E. J.; Burnstock, G.; McMahon, S. B. The expression of P2X3 purinoreceptors

- in sensory neurons: effects of axotomy and glial-derived neurotrophic factor. *Mol. Cell. Neurosci.* **1998**, *12*, 256–268.
- (93) Dorn, G.; Patel, S.; Wotherspoon, G.; Hemmings-Mieszczak, M.; Barclay, J.; Natt, F. J.; Martin, P.; Bevan, S.; Fox, A.; Ganju, P.; Wishart, W.; Hall, J. siRNA relieves chronic neuropathic pain. *Nucleic Acids Res.* **2004**, *32*, 1–6.
- (94) Tsuda, M.; Koizumi, S.; Kita, A.; Shigemoto, Y.; Ueno, S.; Inoue, K. Mechanical allodynia caused by intraplantar injection of P2X receptor agonist in rats: involvement of heteromeric P2X2/3 receptor signaling in capsaicin-insensitive primary afferent neurons. *J. Neurosci.* **2000**, *20*, 1–5.
- (95) Lewis, C.; Neidhart, S.; Holy, C.; North, R. A.; Buell, G.; Surprenant, A. Coexpression of P2X2 and P2X3 receptor subunits can account for ATP-gated currents in sensory neurons. *Nature* **1995**, *377*, 432–435.
- (96) Burnstock, G. Purine-mediated signalling in pain and visceral perception. *Trends Pharmacol. Sci.* **2001**, *22*, 182–188.
- (97) Hausmann, R.; Bahrenberg, G.; Kuhlmann, D.; Schumacher, M.; Braam, U.; Bieler, D.; Schlusche, I.; Schmalzing, G. A hydrophobic residue in position 15 of the rP2X3 receptor slows desensitization and reveals properties beneficial for pharmacological analysis and high-throughput screening. *Neuropharmacology* **2014**, *79*, 603–615.
- (98) Hausmann, R.; Rettinger, J.; Gerevich, Z.; Meis, S.; Kassack, M. U.; Illes, P.; Lambrecht, G.; Schmalzing, G. The suramin analog 4,4',4'',4'''-(carbonylbis-(imino-5,1,3-benzenetriylbis-(carbonylimino)))tetra-kis-benzenesulfonic acid (NF110) potently blocks P2X3 receptors: subtype selectivity is determined by location of sulfonic acid groups *Mol. Pharmacol.* **2006**, *69*, 2058–2067.
- (99) Ballini, E.; Virginio, C.; Medhurst, S. J.; Summerfield, S. G.; Aldegheri, L. Characterization of three diaminopyrimidines as potent and selective antagonists of P2X3 and P2X2/3 receptors with in vivo efficacy in a pain model. *Br. J. Pharmacol.* **2011**, *163*, 1315–1325.
- (100) Jarvis, M. F.; Burgard, E. C.; Mcgaraughty, S.; Honore, P.; Lynch, K.; Brennan, T. J.; Subieta, A.; Biesen, T. Van; Cartmell, J.; Bianchi, B.; Niforatos, W.; Kage, K.; Yu, H.;

References

- Mikusa, J.; Wismer, C. T.; Zhu, C. Z.; Chu, K.; Lee, C.; Stewart, A. O.; Polakowski, J.; Cox, B. F.; Kowaluk, E.; Williams, M.; Sullivan, J.; Faltynek, C. A-317491, a novel potent and selective non-nucleotide antagonist of P2X3 and P2X2/3 receptors, reduces chronic inflammatory and neuropathic pain in the rat. *PNAS* **2002**, *99*, 17179–17184.
- (101) McGaraughty, S.; Wismer, C. T.; Zhu, C. Z.; Mikusa, J.; Honore, P.; Chu, K. L.; Lee, C.-H.; Faltynek, C. R.; Jarvis, M. F. Effects of A-317491, a novel and selective P2X3/P2X2/3 receptor antagonist, on neuropathic, inflammatory and chemogenic nociception following intrathecal and intraplantar administration. *Br. J. Pharmacol.* **2003**, *140*, 1381–1388.
- (102) Gum, R. J.; Wakefield, B.; Jarvis, M. F. P2X receptor antagonists for pain management: examination of binding and physicochemical properties. *Purinergic Signal.* **2012**, *8*, 41-56.
- (103) Ford, A. P. In pursuit of P2X3 antagonists: novel therapeutics for chronic pain and afferent sensitization. *Purinergic Signal.* **2012**, *8*, 3–26.
- (104) Gever, J. R.; Soto, R.; Henningsen, R. A.; Martin, R. S.; Hackos, D. H.; Panicker, S.; Rubas, W.; Oglesby, I. B.; Dillon, M. P.; Milla, M. E.; Burnstock, G.; Ford, A. P. D. W. AF-353, a novel, potent and orally bioavailable P2X3/P2X2/3 receptor antagonist. *Br. J. Pharmacol.* **2010**, *160*, 1387–1398.
- (105) Brotherton-pleiss, C. E.; Dillon, M. P.; Ford, A. P. D. W.; Gever, J. R.; Carter, D. S.; Gleason, S. K.; Lin, C. J.; Moore, A. G.; Thompson, A. W.; Villa, M.; Zhai, Y. Discovery and optimization of RO-85, a novel drug-like, potent, and selective P2X3 receptor antagonist. *Bioorg. Med. Chem. Lett.* **2010**, *20*, 1031–1036.
- (106) Saul, A.; Hausmann, R.; Kless, A.; Nicke, A. Heteromeric assembly of P2X subunits. *Front. Cell. Neurosci.* **2013**, *7*, 1–20.
- (107) Ford, A. P.; Udem, B. J. The therapeutic promise of ATP antagonism at P2X3 receptors in respiratory and urological disorders. *Front. Cell. Neurosci.* **2013**, *7*, 1–10.
- (108) Abdulqawi, R.; Dockry, R.; Holt, K.; Layton, G.; McCarthy, B. G.; Ford, A. P.; Smith, J. A. P2X3 receptor antagonist (AF-219) in refractory chronic cough: a randomised, double-blind, placebo-controlled phase 2 study. *Lancet* **2015**, *385*, 1198–1205.

References

- (109) Jung, K.; Moon, H. D.; Lee, G. E.; Lim, H.; Park, C.; Kim, Y. Structure-activity relationship studies of spinorphin as a potent and selective human P2X3 receptor antagonist. *J. Med. Chem.* **2007**, 4543–4547.
- (110) Yamamoto, Y.; Ono, H.; Ueda, A.; Shimamura, M.; Nishimura, K.; Hazato, T. Spinorphin as an endogenous inhibitor of enkephalin-degrading enzymes: roles in pain and inflammation. *Curr. Protein Pept. Sci.* **2002**, 3, 587–599.
- (111) Szántó, G.; Makó, A.; Vágó, I.; Hergert, T.; Bata, I.; Farkas, B.; Kolok, S.; Vastag, M. New P2X3 receptor antagonists. Part 2: Identification and SAR of quinazolinones. *Bioorganic Med. Chem. Lett.* **2016**, 26, 3905–3912.
- (112) Szántó, G.; Makó, A.; Bata, I.; Farkas, B.; Kolok, S.; Vastag, M.; Cselenyák, A. New P2X3 receptor antagonists. Part 1: Discovery and optimization of tricyclic compounds. *Bioorganic Med. Chem. Lett.* **2016**, 26, 3896–3904.
- (113) Takahashi, F.; Kinoshita, H.; Shimada, S. Pyrrolinone derivatives as a new class of P2X3 receptor antagonists . Part 1: Initial structure-activity relationship studies of a hit from a high throughput. *Bioorg. Med. Chem. Lett.* **2017**.
- (114) Rajagopal, M. R. Pain-basic considerations. *Indian J. Anaesth.* **2006**, 50, 331-334.
- (115) Williams, M.; Kowaluk, E. A.; Arneric, S. P. Emerging molecular approaches to pain therapy. *J. Med. Chem.* **1999**, 42, 1481-1500.
- (116) Woolf, C. J.; Ma, Q. Nociceptors-noxious stimulus detectors. *Neuron* **2007**, 55, 353–364.
- (117) Juhl, G. I.; Jensen, T. S.; Norholt, S. E.; Svensson, P. Central sensitization phenomena after third molar surgery: a quantitative sensory testing study. *Eur. J. Pain* **2008**, 12, 116–127.
- (118) Toth, C.; Lander, J.; Wiebe, S. The prevalence and impact of chronic pain with neuropathic pain symptoms in the general population. *Pain Med.* **2009**, 10, 918–929.
- (119) Colvin, L. A.; Dougherty, P. M. Peripheral neuropathic pain: signs, symptoms, mechanisms, and causes: are they linked? *Br. J. Anaesth.* **2014**, 114, 361–363.
- (120) Inoue, K. P2 receptors and chronic pain. *Purinergic Signal.* **2007**, 3, 135–144.

References

- (121) Donnelly-roberts, D.; Mcgaraughty, S.; Shieh, C.; Honore, P.; Jarvis, M. F. Painful purinergic receptors. *J. Pharmacol. Exp. Ther.* **2008**, *324*, 409–415.
- (122) Inoue, K.; Tsuda, M.; Koizumi, S. ATP receptors in pain sensation: involvement of spinal microglia and P2X4 receptors. *Purinergic Signal.* **2005**, *1*, 95–100.
- (123) Jarvis, M. F.; Kowaluk, E. A. Pharmacological characterization of P2X3 homomeric and heteromeric channels in nociceptive signaling and behavior. *Drug Dev. Res.* **2001**, *52*, 220–231.
- (124) Pankewitz, F.; Zöllmer, A.; Gräser, Y.; Hilker, M. Anthraquinones as defensive compounds in eggs of galerucini leaf beetles: biosynthesis by the beetles? *Arch. Insect Biochem. Physiol.* **2007**, *66*, 98–108.
- (125) Chien, S. C.; Wu, Y. C.; Chen, Z. W.; Yang, W. C. Naturally occurring anthraquinones: chemistry and therapeutic potential in autoimmune diabetes. *Evidence-based Complement. Altern. Med.* **2015**, *2015*, 1-13.
- (126) Caro, Y.; Anamale, L.; Fouillaud, M.; Laurent, P.; Petit, T.; Dufosse, L. Natural hydroxyanthraquinoid pigments as potent food grade colorants: an overview. *Nat. Products Bioprospect.* **2012**, *2*, 174–193.
- (127) Laurent, A. Ueber verschiedene verbindungen des anthracen's. *Justus Liebigs Ann. Chem.* **1840**, *34*, 287–296.
- (128) Graebe, C.; Liebermann, C. Ueber alizarin und anthracen. *Berichte der Dtsch. Chem. Gesellschaft* **1868**, *1*, 49–51.
- (129) Russell, W. J. Address to the chemical section. In *Chemical News and Journal of Industrial Science.*; Crookers, W., Ed.; Henry Gillman, Boy court, Ludgate Hill, E.C.: London, 1873; pp. 148–153.
- (130) Phillips, M. The chemistry of anthraquinone. *Chem. Rev.* **1929**, *6*, 157–174.
- (131) Fouillaud, M.; Venkatachalam, M.; Girard-Valenciennes, E.; Caro, Y.; Dufossé, L. Anthraquinones and derivatives from marine-derived fungi: structural diversity and selected biological activities. *Mar. Drugs* **2016**, *14*, 1-64.

References

- (132) Yusuf, M.; Shabbir, M.; Mohammad, F. Natural colorants: historical, processing and sustainable prospects. *Nat. Products Bioprospect.* **2017**, *7*, 123–145.
- (133) Aspland, J. R. Textile dyeing and coloration; *AATCC* **1997**, 1-410.
- (134) Zollinger, H. Color chemistry: syntheses, properties, and application of organic dyes and pigments; 3rd ed.; VCH Publishers, Inc.: New York, 1991.
- (135) Pearson, J. C.; Weaver, M. A.; Fleischer, J. C.; King, G. A. Copolymerizable methine and anthraquinone compounds and articles containing them. U.S. Patent 8501890 B2, 2013.
- (136) Motallebi, S.; Maghsoodi, S. Anthraquinone dye-containing material, composition including the same, camera including the same, and associated methods. U.S. Patent 20010149128 A1, 2011.
- (137) Huang, Q.; Lu, G.; Shen, H. M.; Chung, M. C. M.; Choon, N. O. Anti-cancer properties of anthraquinones from rhubarb. *Med. Res. Rev.* **2007**, *27*, 609–630.
- (138) Barnard, D. L.; Fairbairn, D. W.; O'Neill, K. L.; Gage, T. L.; Sidwell, R. W. Anti-human cytomegalovirus activity and toxicity of sulfonated anthraquinones and anthraquinone derivatives. *Antiviral Res.* **1995**, *28*, 317–329.
- (139) Wuthi-udomlert, M.; Kupittayanant, P.; Gritsanapan, W. In vitro evaluation of antifungal activity of anthraquinone derivatives of senna alata. *J Heal. Res* **2010**, *24*, 117–122.
- (140) Khan, N.; Karodi, R.; Siddiqui, A.; Thube, S.; Rub, R. Development of anti-acne gel formulation of anthraquinones rich fraction from rubia cordifolia (rubiaceae). *Int. J. Appl. Res. Nat. Prod.* **2011**, *4*, 28–36.
- (141) Fairbairn, J. W. The anthraquinone laxatives. *Pharmacol. Int. J. Exp. Clin. Pharmacol.* **1976**, *14*, 1–105.
- (142) Van Gorkom, B. A.; De Vries, E. G.; Karrenbeld, A.; Kleibeuker, J. H. Review article: anthranoid laxatives and their potential carcinogenic effects. *Aliment. Pharmacol. Ther.* **1999**, *13*, 443–452.
- (143) Gan, K. H.; Teng, C. H.; Lin, H.-C.; Chen, K. T.; Chen, Y. C.; Hsu, M. F.; Wang, J. P.; Teng, C. M.; Lin, C. N. Antiplatelet effect and selective binding to cyclooxygenase by

References

- molecular docking analysis of 3-alkylaminopropoxy-9,10-anthraquinone derivatives. *Biol. Pharm. Bull.* **2008**, *31*, 1547–1551.
- (144) Seo, E. J.; Ngoc, T. M.; Lee, S.-M.; Kim, Y. S.; Jung, Y. S. Chrysophanol-8-*O*-glucoside, an anthraquinone derivative in rhubarb, has antiplatelet and anticoagulant activities. *J. Pharmacol. Sci.* **2012**, *118*, 245–254.
- (145) Baqi, Y.; Atzler, K.; Köse, M.; Glänzel, M.; Müller, C. E. High-affinity, non-nucleotide-derived competitive antagonists of platelet P2Y₁₂ receptors. *J. Med. Chem.* **2009**, *52*, 3784–3793.
- (146) Jackson, T. C.; Verrier, J. D.; Kochanek, P. M. Anthraquinone-2-sulfonic acid (AQ2S) is a novel neurotherapeutic agent. *Cell Death Dis.* **2013**, *4*, e451.
- (147) Cirillo, C.; Capasso, R. Constipation and botanical medicines: an overview. *Phyther. Res.* **2015**, *29*, 1488–1493.
- (148) DiMarco, A.; Gaetini, M.; Dorigotti, L.; Soldatti, M.; Bellini, O. Studi sperimentali sull'attività antineoplastica del nuovo antibiotico daunomicina. *Tumori* **1963**, *49*, 203–217.
- (149) Dong, X.; Fu, J.; Yin, X.; Cao, S.; Li, X.; Lin, L.; Ni, J. Emodin: a review of its pharmacology, toxicity and pharmacokinetics. *Phyther. Res.* **2016**, 1207–1218.
- (150) Teich, L.; Daub, S.; Kru, V.; Nissler, L.; Gebhardt, R.; Eger, K. Synthesis and biological evaluation of new derivatives of emodin. *Bioorg. Med. Chem.* **2004**, *12*, 5961–5971.
- (151) Gewirtz, D. A. A critical evaluation of the mechanisms of action proposed for the antitumor effects of the anthracycline antibiotics adriamycin and daunorubicin. *Biochem. Pharmacol.* **1999**, *57*, 727–741.
- (152) Arcamone, F.; Cassinelli, G.; Fantini, G.; Grein, A.; Orezzi, P.; Pol, C.; Spalla, C. Adriamycin, 14-hydroxydaunomycin, a new antitumor antibiotic from *S. peucetius* var. *caesius*. *Biotechnol. Bioeng.* **1969**, *6*, 1101–1110.
- (153) Harris, F.; Pierpoint, L. Mitoxantrone, more than just another topoisomerase II poison. *Med. Res. Rev.* **2012**, *29*, 1292–1327.

References

- (154) Lawford, D. J.; White, R. G. "Daunomycin", a new antibiotic of the rhodomycin group. *Nature* **1964**, *201*, 706–607.
- (155) Tacar, O.; Sriamornsak, P.; Dass, C. R. Doxorubicin: an update on anticancer molecular action, toxicity and novel drug delivery systems. *J. Pharm. Pharmacol.* **2013**, *65*, 157–170.
- (156) Minotti, G. Anthracyclines: molecular advances and pharmacologic developments in antitumor activity and cardiotoxicity. *Pharmacol. Rev.* **2004**, *56*, 185–229.
- (157) Malik, E. M.; Müller, C. E. Anthraquinones as pharmacological tools and drugs. *Med. Res. Rev.* **2016**, *36*, 705–748.
- (158) Martinelli, B. F.; Vacchi, L.; Rovaris, M.; Capra, R.; Comi, G. Mitoxantrone for multiple sclerosis. *Cochrane Database Syst. Rev.* **2013**, 1–38.
- (159) Yu, C.; Qi, D.; Sun, J.-F.; Li, P.; Fan, H. Y. Rhein prevents endotoxin-induced acute kidney injury by inhibiting NF- κ B activities. *Sci. Rep.* **2015**, *5*, 11822.
- (160) Nguyen, M.; Dougados, M.; Berdah, L.; Amor, B. Diacerhein in the treatment of osteoarthritis of the hip. *Arthritis Rheum.* **1994**, *37*, 529–536.
- (161) U.S Department of Health and Human Services. Report on carcinogens, 4th ed.; **2016**.
- (162) Bennett, M.; Cresswell, H. Factors influencing constipation in advanced cancer patients: a prospective study of opioid dose, dantron dose and physical functioning. *Palliat. Med.* **2003**, *17*, 418–422.
- (163) Denizli, A.; Pişkin, E. Dye-ligand affinity systems. *J Biochem Biophys Methods.* **2001**, *49*, 391–416.
- (164) Glänzel, M.; Bültmann, R.; Starke, K.; Frahm, A. W. Constitutional isomers of reactive blue 2 - selective P2Y-receptor antagonists? *Eur. J. Med. Chem.* **2003**, *38*, 303–312.
- (165) Baqi, Y.; Müller, C. E. Rapid and efficient microwave-assisted copper(0)-catalyzed ullmann coupling reaction: general access to anilinoanthraquinone derivatives. *Org. Lett.* **2007**, *9*, 1271–1274.
- (166) Baqi, Y.; Müller, C. E. Synthesis of alkyl- and aryl-amino-substituted anthraquinone

- derivatives by microwave-assisted copper(0)-catalyzed ullmann coupling reactions. *Nat. Protoc.* **2010**, *5*, 945–953.
- (167) Weyler, S.; Baqi, Y.; Hillmann, P.; Kaulich, M.; Hunder, A. M.; Müller, I. A.; Müller, C. E. Combinatorial synthesis of anilinoanthraquinone derivatives and evaluation as non-nucleotide-derived P2Y₂ receptor antagonists. *Bioorg. Med. Chem. Lett.* **2008**, *18*, 223–227.
- (168) Baqi, Y.; Lee, S.-Y.; Iqbal, J.; Ripphausen, P.; Lehr, A.; Scheiff, A. B.; Zimmermann, H.; Bajorath, J.; Müller, C. E. Development of potent and selective inhibitors of ecto-5'-nucleotidase based on an anthraquinone scaffold. *J. Med. Chem.* **2010**, *53*, 2076–2086.
- (169) Baqi, Y.; Müller, C. E. Convergent synthesis of the potent P2Y receptor antagonist MG 50-3-1 based on a regioselective Ullmann coupling reaction. *Molecules* **2012**, *17*, 2599–2615.
- (170) Baqi, Y. Anthraquinones as a privileged scaffold in drug discovery targeting nucleotide-binding proteins. *Drug Discov Today* **2016**, *12*, 1571-1577.
- (171) Henkelmann, J.; Hoch, H.; Kahl, T.; Kilpper, G.; Maier, W. Preparation of 1-nitroanthraquinone-2-carboxylic acids. U.S. Patent CA2001989 A1, 1990.
- (172) Malik, E. M.; Baqi, Y.; Müller, C. E. Syntheses of 2-substituted 1-amino-4-bromoanthraquinones (bromaminic acid analogues) – precursors for dyes and drugs. *Beilstein J. Org. Chem.* **2015**, *11*, 2326–2333.
- (173) Hoffmann, K.; Baqi, Y.; Morena, M. S.; Glänzel, M.; Müller, C. E.; von Kügelgen, I. Interaction of new, very potent non-nucleotide antagonists with Arg256 of the human platelet P2Y₁₂ receptor. *J. Pharmacol. Exp. Ther.* **2009**, *331*, 648–655.
- (174) Giguere, R. J.; Bray, T. L.; Duncan, S. M. Application of commercial microwave ovens to organic synthesis. *Tetrahedron Lett.* **1986**, *27*, 4945–4948.
- (175) Mehta, B.; Bhardwaj, S. Microwave induced synthesis of anthraquinone derivatives a solvent free path. *Rasayan J. Chem.* **2009**, *2*, 659–661.
- (176) Hoz, A. De.; Díaz-Ortiz, Á.; Moreno, A. Microwaves in organic synthesis . thermal and non-thermal microwave effects *Chem. Soc. Rev.* **2005**, *34*, 164–178.

References

- (177) Larhed, M.; Hallberg, A. Chemistry: a new technique in drug discovery. *Drug Discov. Today* **2001**, *6*, 406–416.
- (178) Roberts, B. A.; Strauss, C. R. Toward rapid, “green”, predictable microwave-assisted synthesis. *Acc. Chem. Res.* **2005**, *38*, 653–661.
- (179) Ullmann, F.; Bielecki, J. Ueber synthesen in der biphenylreihe. *Berichte der Dtsch. Chem. Gesellschaft* **1901**, *34*, 2174–2185.
- (180) Ullmann, F. Ueber eine neue darstellungsweise von phenyläthersalicylsäure. *Berichte der Dtsch. Chem. Gesellschaft* **1904**, *37*, 853–854.
- (181) Sperotto, E.; van Klink, G. P. M.; van Koten, G.; de Vries, J. G. The mechanism of the modified ullmann reaction. *Dalt. Trans.* **2010**, *39*, 10338.
- (182) Goldberg, I. Ueber phenylirungen bei gegenwart von kupfer als katalysator. *Berichte der Dtsch. Chem. Gesellschaft* **1906**, *39*, 1691–1692.
- (183) Hassan, J.; Penalva, V.; Lavenot, L.; Gozzi, C.; Lemaire, M. Catalytic alternative of the Ullmann reaction. *Tetrahedron* **1998**, *54*, 13793–13804.
- (184) Kim, J. H.; Grebies, S.; Boultadakis-Arapinis, M.; Daniliuc, C.; Glorius, F. Rh(I)/NHC*-catalyzed site- and enantioselective functionalization of $c(sp^3)$ -H bonds toward chiral triarylmethanes. *ACS Catal.*, **2016**, *6*, 7652–7656.
- (185) Parai, M. K.; Panda, G.; Chaturvedi, V.; Manju, Y. K.; Sinha, S. Thiophene containing triarylmethanes as antitubercular agents. *Bioorg. Med. Chem. Lett.* **2008**, *18*, 289–292.
- (186) Mibu, N.; Yokomizo, K.; Uyeda, M.; Sumoto, K. Synthesis and antiviral activities of some 4,4'- and 2, 2'-dihydroxytriphenylmethanes. *Chem. Pharm. Bull.* **2005**, *53*, 30–33.
- (187) Jaratjaroonphong, J.; Sathalalai, S.; Techasauvapak, P.; Reutrakul, V. Iodine catalyzed friedel–crafts alkylation of electron-rich arenes with aldehydes: efficient synthesis of triarylmethanes and diarylalkanes. *Tetrahedron Lett.* **2009**, *50*, 6012–6015.
- (188) Muthyala, R. A synthetic study on the preparation of triarylmethanes. *Dyes Pigm.* **1994**, *25*, 303–324.
- (189) Gessner, T.; Mayer, U. Triarylmethane and diarylmethane dyes. *Ullmann's Encycl. Ind.*

- Chem.* **2012**, *37*, 425–478.
- (190) Angus, D. S.; Baker, R. S. U.; Bonin, A. M.; Callen, D.; Clark, A. M. Comparative of two triarylmethane food dyes in salmonella, and drosophila. *Fd Cosmet. Toxicol.* **1981**, *19*, 419–424.
- (191) Kienzle-Horn, S.; Vix, J.; Schuijt, C.; Piel, H.; Jordan, C. C.; Kamm, M. A. Efficacy and safety of bisacodyl in the acute treatment of constipation: a double-blind, randomized, placebo-controlled study. *Aliment. Pharmacol. Ther.* **2006**, *23*, 1479–1488.
- (192) Hawes, R. H.; Lowry, A.; Deziel, D. A consensus document on bowel preparation before colonoscopy: prepared by a task force from the american society of colon and rectal surgeons (ASCRS), the american society for gastrointestinal endoscopy (ASGE), and the society of american gastrointestinal and endoscopic surgeons (SAGES). *Gastrointest. Endosc.* **2006**, *63*, 894–909.
- (193) Zeniou, M.; Fève, M.; Mameri, S.; Dong, J.; Salomé1, C.; Chen1, W.; El-Habr, E. A.; Bousson, F.; Sy, M.; Obszynski, J.; Boh, A.; Villa, P.; Kahn, S. A.; Didier, B.; Bagnard, D.; Junier, M.; Chneiweiss, H.; Haiech, J.; Hibert, M.; Kilhoffer, M. Chemical library screening and structure-function relationship studies identify bisacodyl as a potent and selective cytotoxic agent towards quiescent human glioblastoma tumor stem-like cells. *PLoS One* **2015**, 1–35.
- (194) Li, H.; Liu, A.; Zhao, Z.; Xu, Y.; Lin, J.; Jou, D.; Li, C. Fragment-based drug design and drug repositioning using multiple ligand simultaneous docking (MLSD): identifying celecoxib and template compounds as novel inhibitors of signal transducer and activator of transcription 3 (STAT3). *J. Med. Chem.* **2011**, *54*, 5592–5596.
- (195) Spanier, C. Identification and characterization of novel ligands for purinergic P2X receptors. Dr. rer. nat. thesis, Rheinische Friedrich-Wilhelms-Universität Bonn, Germany, **2016**.
- (196) Tsang, A.; Von Korff, M.; Lee, S.; Alonso, J.; Karam, E.; Angermeyer, M. C.; Borges, G. L. G.; Bromet, E. J.; de Girolamo, G.; de Graaf, R.; Gureje, O.; Lepine, J. P.; Haro, J. M.; Levinson, D.; Oakley Browne, M. A.; Posada-Villa, J.; Seedat, S.; Watanabe, M. Common chronic pain conditions in developed and developing countries: gender and age differences

- and comorbidity with depression-anxiety disorders. *J. Pain* **2008**, *9*, 883–891.
- (197) Watkins, L. R.; Maier, S. F. Glia: a novel drug discovery target for clinical pain. *Nat. Rev. Drug Discov.* **2003**, *2*, 973–985.
- (198) Volpini, R.; Mishra, R. C.; Kachare, D. D.; Ben, D. D.; Lambertucci, C.; Antonini, I.; Vittori, S.; Marucci, G.; Sokolova, E.; Nistri, A.; Cristalli, G. Adenine-based acyclic nucleotides as novel P2X3 receptor ligands. *J. Med. Chem.* **2009**, *52*, 4596–4603.
- (199) Ukponmwan, D. O.; Greenhalgh, M.; Peters, A. T. Physical characteristics of synthesized 1-amino-4-(arylamino)anthraquinone 2-ether dyes for synthetic-polymer fibers. *J. Chem. Eng. Data* **1984**, *29*, 483–484.
- (200) Malik, E. M.; Rashed, M.; Wingen, L.; Baqi, Y.; Müller, C. E. Ullmann reactions of 1-amino-4-bromoanthraquinones bearing various 2-substituents furnishing novel dyes. *Dye. Pigment.* **2016**, *131*, 33–40.
- (201) Harris, R. M.; Marriott, G. J.; Smith, J. C. The effect of alkyl groups on the properties of anthraquinone and fluorescein dyes. *J. Chem. Soc.* **1936**, 1838–1844.
- (202) Baqi, Y.; Weyler, S.; Iqbal, J.; Zimmermann, H.; Müller, C. E. Structure-activity relationships of anthraquinone derivatives derived from bromaminic acid as inhibitors of ectonucleoside triphosphate diphosphohydrolases (E-NTPDases). *Purinergic Signal.* **2009**, 91–106.
- (203) Baqi, Y.; Müller, C. E. Convergent synthesis of the potent P2Y receptor antagonist MG 50-3-1 based on a regioselective Ullmann coupling reaction. *Molecules* **2012**, *17*, 2599–2615.
- (204) Burnett, J. F.; Zahler, R. E. Aromatic nucleophilic substitution reactions. *Chem Rev* **1951**, *49*, 273–412.
- (205) Tuong, T. D.; Hida, M. Mechanism of the Ullmann condensation. I. kinetic and thermodynamic studies. *Bull Chem Soc Jpn* **1970**, *43*, 1763–1768.
- (206) Malik, E. M. Synthetic access to novel anthraquinone derivatives, biological evaluation, and analysis of structure-activity relationships at P2Y receptors. Dr. rer. nat. thesis, Rheinische Friedrich-Wilhelms-Universität Bonn, Germany, **2015**.

References

- (207) Arai, S.; Hida, M.; Yamagishi, T.; Ototake, S. The Ullmann condensation reaction of haloanthraquinone derivatives with amines in aprotic solvents II. the presence of induction period in the condensation with 2-aminoethanol. *Bull Chem Soc Jpn* **1977**, *50*, 2982–2985.
- (208) Arai, S.; Hashimoto, Y.; Yamagishi, T.; Hida, M. The Ullmann condensation reaction of haloanthraquinone derivatives with amines in aprotic solvents. VI. The combination of Cu(I) and hydroxo or alkoxo Cu(II) as effective catalyst system. *Bull Chem Soc Jpn* **1989**, *62*, 3143–3149.
- (209) Gragerov, I. P.; Kasukhin, L. F. Mechanism of the Ullmann reaction. II. Effects of the medium, the additives and the substituents. *Bull Chem Soc Jpn* **1971**, *44*, 765–771.
- (210) Mereyala, H. B.; Sambaru, K. Synthesis of triphenylmethane derivative : bisacodyl. *Indian J. Chem.* **2005**, *44*, 615–617.
- (211) Junhui, Z.; Hongyu, L.; Jinling, L.; Shende, J. A preparation method of bisacodyl. CN101973932 B, 2012.
- (212) Seelye, D. E.; Plummer, E. L. Process of preparation of tetrafluoro 2,3-dihydrobenzofurans. U.S. Patent 4730062 A, 1988.
- (213) Feve, M.; Zenyou-Mayer, M.; Haiech, J.; Chneiwiss, H.; Kilhoffer, M.; Mameri, S.; Hibert, M. Bisacodyl and analogues as drugs for treating cancer. PCT Int. Appl., WO2012168885 A2, 2014.
- (214) Nath, B.; Kalita, D.; Baruah, J. B. Zwitterionic metal carboxylate complexes: in solid state. *Solid State Sci.* **2012**, *14*, 880–884.
- (215) Breslin, H. J.; Chatterjee, S.; Diebold, J. L.; Dorsey, B. D.; Dunn, D.; Gingrich, D. E.; Hostetler, G. A.; Hudkins, R. L.; Hunter, R.; Josef, K.; Lisko, J.; Mesaros, E. F.; Milkiewicz, K. L.; Ott, G. R.; Sundar, B. G.; Theroff, J. P.; Thieu, T.; Tripathy, R.; Underiner, T. L.; Weinberg, L.; Wells, G. J.; Zifcsak, G. A. Preparation of pyrrolotriazines as inhibitors of ALK and JAK2 kinases for treating proliferative diseases. PCT Int. Appl., WO2010071885 A1, 2010.
- (216) Karthikeyan, I.; Sekar, G. Iron-catalyzed C-H bond functionalization for the exclusive synthesis of pyrido[1,2-*a*]indoles or triarylmethanols. *Eur. J. Org. Chem.* **2014**, *2014*,

- 8055–8063.
- (217) Karthikeyan, I.; Arunprasath, D.; Sekar, G. An efficient synthesis of pyrido[1,2-*a*]indoles through aza-nazarov type cyclization. *Chem. Commun.* **2015**, *51*, 1701–1704.
- (218) Jones, C. D.; Winter, M. A.; Hirsch, K. S.; Stamm, N.; Taylor, H. M.; Holden, H. E.; Davenport, J. D.; Krumkalns, E. V.; Suhrt, R. G. Estrogen synthetase inhibitors. 2.¹ comparison of the in vitro aromatase inhibitory activity for a variety of nitrogen heterocycles substituted with diarylmethane or diarylmet hanol groups. *J. Med. Chem.* **1990**, *33*, 416–429.
- (219) Greene, M. A.; Yonova, I. M.; Williams, F. J.; Jarvo, E. R. Traceless directing group for stereospecific nickel-catalyzed alkyl-alkyl cross-coupling reactions. *Org. Lett.* **2012**, *14*, 4293–4296.
- (220) Kenmoku, S.; Urano, Y.; Kanda, K.; Kojima, H. Rational design of novel photoinduced electron transfer type fluorescent probes for sodium cation. *Tetrahedron* **2004**, *60*, 11067–11073.
- (221) Altieri, A.; Alvino, A.; Ohnmacht, S.; Ortaggi, G.; Neidle, S.; Nocioni, D.; Franceschin, M.; Bianco, A. Xanthene and xanthone derivatives as G-quadruplex stabilizing ligands. *Molecules* **2013**, *18*, 13446–13470.
- (222) Lane, F. Reduction of organic compounds with diborane. *Chem. Rev.* **1976**, *76*, 773–799.
- (223) Koh, J. J.; Zou, H.; Lin, S.; Lin, H.; Soh, R. T.; Lim F. H.; Koh, W.L.; Li, J.; Lakshminarayanan R.; Verma, C.; Tan, D. T.; Cao, D.; Beuerman, R. W.; Liu, S. Nonpeptidic amphiphilic xanthone derivatives: structure-activity relationship and membrane-targeting properties. *J. Med. Chem.* **2016**, *59*, 171–193.
- (224) O'brien, D. E.; Baiocchi, F.; Robins, R. K.; Cheng, C. C. Pyrimidines. IX. 4- and 5-(Substituted-anilino)pyrimidines. *J. Med. Chem.* **1962**, *5*, 1085–1103.
- (225) Carceller, G. E.; Salas, S. J.; Soliva, S. R.; Medina, M. E. F.; Martí, V. J. Preparation of diaminopyrimidines as modulators of histamine H4 receptor activity, PCT Int. Appl., WO2007031529 A1, 2007.
- (226) Sonar, S. S.; Sadaphal, S. A.; Kategoanekar, A. H.; Pokalwar, R. U.; Shingate, B. B.;

- Shingare, M. S. Alum catalyzed simple and efficient synthesis of bis(indolyl) methanes by ultrasound approach. *Bull. Korean Chem. Soc* **2009**, *30*, 825–828.
- (227) Praveen, C.; Dheenkumar, P.; Muralidharan, D.; Perumal, P. T. Synthesis, antimicrobial and antioxidant evaluation of quinolines and bis(indolyl)methanes. *Bioorg. Med. Chem. Lett.* **2010**, *20*, 7292–7296.
- (228) Kamal, A.; Khan, M. N. A.; Reddy, K. S.; Srikanth, Y. V. V; Ahmed, S. K.; Kumar, K. P.; Murthy, U. S. N. An efficient synthesis of bis(indolyl)methanes and evaluation of their antimicrobial activities. *J. Enzyme Inhib. Med. Chem.* **2009**, *24*, 559–565.
- (229) Balu Pawar, Vinod Shinde, A. C. n-Dodecylbenzene sulfonic acid (DBSA) as a novel brønsted acid catalyst for the synthesis of bis(indolyl)methanes and bis(4-hydroxycoumarin-3-yl) methanes in water. *Green Sustain. Chem.* **2013**, *3*, 56–60.
- (230) Ganguly, N. C.; Mondal, P.; Barik, S. K. Iodine in aqueous micellar environment: a mild effective ecofriendly catalytic system for expedient synthesis of bis(indolyl)methanes and 3-substituted indolyl ketones. *Green Chem. Lett. Rev.* **2012**, *5*, 73–81.
- (231) Mathvink, R. J.; Barritta, A. M.; Candelore, M. R.; Cascieri, M. A.; Deng, L.; Tota, L.; Strader, C. D.; Wyvratt, M. J.; Fisher, M. H.; Weber, A. E. Potent, selective human β_3 adrenergic receptor agonists containing a substituted indoline-5-sulfonamide pharmacophore. *Bioorg. Med. Chem. Lett.* **1999**, *9*, 1869–1874.
- (232) Rostamizadeh, S.; Reza, H.; Aryan, R.; Mohammad, A. Clean one-pot synthesis of 1, 2, 4-oxadiazoles under solvent-free conditions using microwave irradiation and potassium fluoride as catalyst and solid support. *Tetrahedron* **2010**, *66*, 494–497.
- (233) Polyák, M.; Varga, G.; Szilágyi, B.; Juhász, L.; Docsa, T.; Gergely, P.; Begum, J.; Hayes, J. M.; Somsák, L. Synthesis, enzyme kinetics and computational evaluation of *N*-(β -D-glucopyranosyl) oxadiazolecarboxamides as glycogen phosphorylase inhibitors. *Bioorg. Med. Chem.* **2013**, *21*, 5738–5747.
- (234) Bora, R. O.; Bashir Dar, B.; Pradhan, V.; Farooqui M. [1, 2, 4]-Oxadiazoles: synthesis and biological applications. *Mini-Reviews Med. Chem.* **2013**, 1–15.
- (235) Vörös, A.; Mucsi, Z.; Baán, Z.; Timári, G.; Hermeecz, I.; Mizsey, P.; Finta, Z. An

- experimental and theoretical study of reaction mechanisms between nitriles and hydroxylamine. *Org. Biomol. Chem.* **2014**, *12*, 8036–8047.
- (236) Zotti, G.; Schiavon, G.; Zecchin, S.; Morin, J.; Leclerc, M. Electrochemical, conductive, and magnetic properties of 2,7-carbazole-based conjugated polymers. *Macromolecules* **2002**, *35*, 2122–2128.
- (237) Du, Z. T.; Lu, J.; Yu, H. R.; Xu, Y.; Li, A. P. A facile demethylation of ortho substituted aryl methyl ethers promoted by $AlCl_3$. *J. Chem. Res.* **2010**, *34*, 222–227.
- (238) Thanigaimalai, P.; Konno, S.; Yamamoto, T.; Koiwai, Y.; Taguchi, A.; Takayama, K.; Yakushiji, F.; Akaji, K.; Chen, S.; Tavakolian, A. N.; Schön, A.; Freire, E.; Hayashi, Y. Development of potent dipeptide-type SARS-CoV 3CL protease inhibitors with novel P3 scaffolds: Design, synthesis, biological evaluation, and docking studies. *Eur. J. Med. Chem.* **2013**, *68*, 372–384.
- (239) Fylaktakidou, K. C.; Litinas, K. E.; Varella, E. A.; Nicolaidis, D. N. Recent developments in the chemistry and in the biological applications of amidoximes. *Curr. Pharm. Des.* **2008**, *14*, 1001–1047.
- (240) Rafehi, M.; Malik, E. M.; Neumann, A.; Abdelrahman, A.; Hanck, T.; Namasivayam, V.; Müller, C. E.; Baqi, Y. Development of potent and selective antagonists for the UTP-activated $P2Y_4$ receptor. *J. Med. Chem.* **2017**, *60*, 3020–3038.
- (241) Hillmann, P.; Ko, G.; Spinrath, A.; Raulf, A.; Ku, I. Von; Wolff, S. C.; Nicholas, R. a; Kostenis, E.; Ho, H.; Müller, C. E. Key determinants of nucleotide-activated G protein-coupled $P2Y$ receptor function revealed by chemical and pharmacological experiments, mutagenesis and homology modeling key determinants of nucleotide-activated G protein-coupled $P2Y_2$ receptor function. *J. Med. Chem.* **2009**, *52*, 2762–2775.
- (242) Rafehi, M. Development of tools and ligands for the uracil nucleotide-activated g protein-coupled $P2Y$ receptors. Dr. rer. nat. thesis, Rheinische Friedrich-Wilhelms-Universität Bonn, Germany, **2017**.
- (243) Wolber, G.; Langer, T. Ligandscout: 3-D pharmacophores derived from protein-bound ligands and their use as virtual screening filters. *J. Chem. Inf. Model.* **2005**, *45*, 160–169.

References

- (244) Hawkins, P. C. D.; Nicholls, A. Conformer generation with OMEGA: learning from the data set and the analysis of failures. *J. Chem. Inf. Model.* **2012**, *52*, 2919–2936.
- (245) Wolber, G.; Dornhofer, A. A.; Langer, T. Efficient overlay of small organic molecules using 3D pharmacophores. *J. Comput. Aided. Mol. Des.* **2006**, *20*, 773–788.
- (246) Vuorinen, A.; Engeli, R.; Meyer, A.; Bachmann, F.; Griesser, U. J.; Schuster, D.; Odermatt, A. Ligand-based pharmacophore modeling and virtual screening for the discovery of novel 17 β -hydroxysteroid dehydrogenase 2 inhibitors. *J. Med. Chem.* **2014**, *57*, 5995–6007.
- (247) Sanmartín, C.; Echeverría, M.; Mendivíl, B.; Cordeu, L.; Cubedo, E.; Foncillas, G. J.; Font, M.; Palop, A. J. Synthesis and biological evaluation of new symmetrical derivatives as cytotoxic agents and apoptosis inducers. *Bioorg. Med. Chem.* **2005**, *13*, 2031–2044.

Acknowledgement

Throughout the process of earning my doctoral degree, I was blessed to find the support of many outstanding individuals. First and foremost I would like to express my deep and sincere gratitude to my mentor and supervisor Prof. Dr. Christa E. Müller. This thesis would not have been possible without her invaluable dedication and kindness. Thank you very much for giving me the opportunity to be part of your research group, for inspiring me, for your thought provoking discussion, for your continuous support and your exceptional patience.

I would like to thank Priv.-Doz. Dr. Anke Schiedel for her kindness and for being the second examiner of my PhD thesis.

I would like also to thank Dr. Ali El-Tayeb for his sincere dedication, scientific discussion, technical assistance and guidance. I really appreciate that he always made himself available all time for discussion and giving valuable suggestions.

I would like to say thank you to my current office mates Dr. Sanyong Lee, Salahuddin Mirza, for their support, and for nice atmosphere in the office. Special thanks also to my previous office mates Dr. Enas Malik and Dr. Thanigaimali Pillaiyer for the nice time we spent together and for the great moments we shared.

I extend my sincere thanks to my friends and colleagues Dr. Ahmed Aglan, Dr. Mohamed Ghonim, Dr. Nader Boshta, Dr. Ahmed Elgokha, and Dr. Anais Barré, for their continuing encouragement and support.

I would like to thank Dr. Aliaa Abdelrahman, Dr. Muhammad Rafehi, and Isaac Attah for assistance with testing the biological activity of the compounds, Dr. Vigneshwaran Namasivayam for helping with the pharmacophore modeling experiments, Marion Schneider for assistance with LC-MS spectra measurement and Sabine Terhart-Krabbe and Annette Reiner for their help with the NMR analysis; thank you for your training, kind help and friendship. I learned a lot from you over these past four years.

I am sincerely grateful to Dr. Ralf Mayer, Dr. Marcus Hubert, Dr. Meryem Köse, and Horst Schmidt for their unlimited support and guidance during my work in the 'Analyseausgabe'. I also

would like to thank my mentor Prof. Dr. Gerd Bendas for his kindness and commitment throughout the time I spent with the Bonn International Graduate School of Drug Sciences (BIGS-DrugS).

I thank from my heart all members of the Institute of Pharmaceutical Chemistry I, Bonn University for their kind support and assistance I have been given over the years.

I wish to express my deep thanks and appreciation to the Egyptian Ministry of Higher Education for sponsoring my PhD scholarship and for providing all the essential aids for fulfilment of the study to completion. I also wish to thank all my colleagues in the Department of Pharmaceutical Chemistry, Faculty of Pharmacy, Al-Azhar University, Cairo, Egypt.

Finally I would like to thank my parents and family, for their love and support although it would be hard to express my gratitude towards them without writing another hundred pages.

Special thanks to my incredible wife Nancy and lovely daughter Layan for their unlimited support, continuous encouragement, love and patience during the four years of this work. Thank you for always being here.

Mahmoud Rashed